Offprinted from the *Transactions of The Faraday Society*,
No. 480, Vol. 58, Part 12, December, 1962

KINETIC THEORY OF PSEUDO-CAPACITANCE AND ELECTRODE REACTIONS AT APPRECIABLE SURFACE COVERAGE

Kinetic Theory of Pseudo-Capacitance and Electrode Reactions at Appreciable Surface Coverage

By B. E. Conway and E. Gileadi

Dept. of Chemistry, University of Ottawa, Ottawa, Canada

Received 30*th March*, 1962

The kinetics of consecutive electrochemical reactions are examined for cases where surface coverage by intermediates is sufficient to influence the free energies of activation. The treatment is applied particularly to reaction sequences, e.g., those in electrochemical oxygen evolution, in which more than two consecutive reactions are involved and hence for cases where the electrode surface may be significantly covered by more than one adsorbed intermediate. The surface induction model of Boudart is used to provide a basis for the linear variation of heat of adsorption of a given species with coverage by both species in the electrochemical reactions. The role of *a priori* heterogeneity of adsorption sites is also considered. The kinetic limiting cases are deduced and shown to be different from those for two-step reactions such as hydrogen evolution in important general ways, and are also different from those obtained for limitingly low or high coverage conditions.

The consequences of coverage-dependent activation energies are examined in relation to the pseudo-capacitance associated with adsorbed intermediates and new general cases are distinguished, and in particular the extent of potential-dependence of the pseudo-capacitance is evaluated for various conditions. The conclusions are applied to the comparison of Tafel and e.m.f. decay slopes and it is shown that previous experimental data for the H-recombination process at platinum can uniquely correspond to appreciable coverage conditions leading to potential-independent capacity and identity of Tafel and decay slopes; similar behaviour is found at the nickel-oxide electrode for the oxygen evolution reaction.

Early deductions [1-3] of criteria for distinction of rate-controlling mechanisms in electrode reactions have been based on the assumption of either limitingly low or limitingly high coverage of the electrode surface by adsorbed reaction intermediates and the potential dependence of the coverage is usually considered. The fact that coverages by intermediates (e.g., adsorbed H in the hydrogen evolution reaction) were in some cases neither unity nor very small was already recognized experimentally by the Russian workers [4] some years ago and an isotherm involving a heat of adsorption linearly dependent upon coverage was formulated.[5] Experimentally, various more recent studies [6, 7] have shown that at certain electrodes the fractional coverage θ by adsorbed H in the hydrogen evolution reaction is between 0·1 and 0·9 and potential dependent; similar results were found by Conway and Bourgault [8, 9] for the coverage of oxide electrodes by adsorbed oxygen-containing species and the role of surface-coverage dependent zero-point energies in determining isotopic relative rates of the H_2—D_2 production reactions has been treated by Conway.[10] Parsons [11] has demonstrated the importance of coverage effects, and the type of adsorption isotherm involved, in determining the dependence of electrochemical exchange currents on heat of adsorption of H at metals [12, 13] and, in a recent paper, Thomas [14] has shown that linear Tafel plots can arise for intermediate coverage conditions ($0{\cdot}2<\theta<0{\cdot}8$) where a coverage-dependent heat of activation predominantly determines the kinetics of steps involving adsorption and desorption of radicals on the electrode surface.

It is the purpose of the present paper to examine the potential dependence of the pseudo-capacitance associated with adsorbed species when heats of activation

for steps in electrochemical reactions are dependent on coverage by the species and to investigate the kinetic consequences of these conditions when reactions of greater complexity than the hydrogen evolution reaction (e.g., anodic oxygen evolution) are involved, and take place through more than two steps. It will be shown that several conclusions of a general nature can be deduced for consecutive electrochemical reaction sequences.

SURFACE COVERAGE EFFECTS AND THE FREE ENERGY OF ACTIVATION

For the hydrogen evolution reaction, proceeding, for example, by the pathways

$$H^+ + M + e \rightarrow MH \qquad \text{I}$$

$$MH + H^+ + e \rightarrow M + H_2 \qquad \text{II}$$

or

$$MH + HM \rightarrow 2M + H_2 \qquad \text{III}$$

the velocity of I can be written as

$$v_1 = k_1 C_{H^+}(1-\theta_H) \exp\left[-(\Delta G_1^{\ddagger} + \alpha r\theta)/RT\right] \exp\left[-\beta VF/RT\right] \qquad (1)$$

and for its reverse

$$v_{-1} = k_{-1}\theta_H \exp\left[-\{\Delta G_{-1}^{\ddagger} - (1-\alpha)r\theta/RT\}\right] \exp\left[(1-\beta)VF/RT\right] \qquad (2)$$

where the heat of adsorption ΔH_θ of H per g atom, has been assumed [4, 11, 14] to be given by a linear function of coverage θ as

$$\Delta H_\theta = \Delta H^c - r\theta_H \qquad (3)$$

where r is a coefficient determining the variation of heat ΔH° of adsorption * with coverage, ΔH_0 is the initial heat of adsorption, α and β are symmetry factors and V is the metal-solution potential difference. For significant surface coverage by H atoms, the variation of the pre-exponential term in θ can be neglected with respect to the variation of the exponential term in θ (cf. ref. 11, 14). The latter term will then predominantly determine v_1 and v_{-1}, and lead to the same Tafel slopes (cf. ref. 14) for rate-determining II or III as those deduced, viz., 2·3 ($2RT/3F$) and 2·3 $RT/2F$, respectively, assuming Langmuir low coverage conditions. This arises since, when reaction I is assumed fast and in quasi-equilibrium, the coverage θ is a linear function of potential (cf. ref. 14)

$$\Delta G_{-1}^{\ddagger} - \Delta G_1^{\ddagger} = r\theta + VF + K_1 \qquad (4)$$

where K_1 is a constant at constant temperature and composition of the solution, and the $r\theta$ terms in the rate equations for II and III can then be substituted accordingly.

In a radical desorption step such as II or III, in which molecule production occurs, conditions corresponding to activated adsorption of the H_2 have been shown [14] to lead to a Tafel slope of 2·3 RT/F for II or III, not previously deduced for these mechanisms under the conditions assumed.†

We have summarized the previously published treatment in order to develop it further below for consecutive reactions in which more than two steps are involved, since new problems arise when (*a*) there is more than one intermediate adsorbed and (*b*) when two adsorbed intermediates are in equilibrium in a pre-rate-determining step.

* Heats and free energies of adsorption are used in the following treatment equivalently, assuming (cf. ref. (11)) that the change of non-configurational entropy of adsorption with coverage is negligible. It is realized, however, that the rate at which these quantities vary with coverage may, under certain conditions, be different.

† Such a slope for the " recombination " mechanism has, however, been deduced for (*a*) first order recombination [11] or (*b*) slow diffusion of H atoms to recombination sites.[15]

CONSECUTIVE ANODIC REACTIONS

(i) REACTION SCHEMES

We consider a typical [8] anodic series of consecutive electrochemical reactions involving more than two steps such as:

$$\begin{aligned} M+OH^- &\rightarrow MOH+e && IV \\ MOH+OH^- &\rightarrow MO+H_2O+e && V \\ MO+MO &\rightarrow 2M+O_2 && VI \end{aligned} \qquad \text{Scheme A}$$

or

$$\begin{aligned} M+OH^- &\rightarrow MOH+e && IV \\ MOH+MOH &\rightarrow MO+H_2O+M && VII \\ MO+MO &\rightarrow 2M+O_2 && VI \end{aligned} \qquad \text{Scheme B}$$

involved in oxygen evolution. Other more complex sequences have been formulated [1, 8] such as

$$\begin{aligned} M+OH^- &\rightarrow MOH+e && IV \\ MOH+OH^- &\rightarrow MO+H_2O+e && V \\ MO+OH^- &\rightarrow MHO_2+e && VIII \\ MHO_2+MOH &\rightarrow 2M+H_2O+O_2 && IX \end{aligned} \qquad \text{Scheme C}$$

M may be the metal or a surface already covered with a thin film of metal oxide.[17, 18] The oxygen-containing species may originate from H_2O or from OH^- without changing the formal kinetic representation of the reaction sequence.

(ii) MODELS FOR VARIATION OF HEAT OF ADSORPTION WITH COVERAGE

In the above sequence of reactions, the heat of adsorption of intermediates will, in principle, be a function of the coverage by all the adsorbed intermediates involved. In order to formulate kinetic equations, it is necessary to obtain a relation analogous to eqn. (3) applicable to, say, at least two intermediates. The form of such an equation will depend on the model chosen [19] to represent the fall of energy of adsorption with coverage. The models which lead to the linear fall of heat of adsorption with coverage indicated, for example, in terms of Temkin's discussion [5] by the observed potential-independent pseudo-capacitance associated with adsorbed H at platinum [4] and O or OH at nickel oxide [8, 9] under some conditions, are as follows: (*a*) a distribution of sites having a range of energies of adsorption varying linearly with coverage. For a surface on which two intermediates are adsorbed, we must assume in this model that the sites which are more active for adsorption of one species are also more active for the other, although the variation of heat of adsorption of one species with coverage, i.e., its r value, may not necessarily be quite identical with that for other species. The alternative model (*b*) is one in which "induced heterogeneity", in the sense of Boudart,[19] is the origin of a linear fall of heat of adsorption with coverage, and is associated with the effect of the adsorbed dipole double-layer on the work function of the metal, which in turn determines in part [20] the energy of chemisorption.

In terms of model (*a*), we may anticipate that the heat of adsorption of a given species A varies with the *total* coverage θ_T in a manner given approximately by

$$\Delta H_A = \Delta H_A^\circ - r_A\theta_T \qquad (5)$$

and for B

$$\Delta H_B = \Delta H_B^\circ - r_B\theta_T \qquad (6)$$

since the sites remaining beyond the *total* coverage θ_T determine, through the respective r values, the energy of adsorption which A or B will experience when adsorbed under such conditions.

Model (*b*) is regarded [19] as the most satisfactory one which can account for the linearly falling heats of adsorption with coverage (cf. ref. 23) observed, for example, in the chemisorption of N [21] and O [22] at metals. In the case of combined adsorption of N and H at iron,[23] *a priori* heterogeneity of adsorption sites has been shown [19] to be quite incapable of explaining the observed adsorption behaviour of N in the presence of H. It may be noted that the latter work [23, 19] indicates that the r values for variation of heats of adsorption of N and H with coverage are different. This is clearly relevant to the problem to be discussed here, where more than one electrochemical intermediate may be chemisorbed in a complex reaction sequence.

A third model in which two-dimensional interactions determine the fall of heat of absorption ΔH with coverage θ, cannot lead to a linear variation of ΔH with θ. Dipole-dipole repulsion leads to a repulsive energy term in $\theta^{\frac{3}{2}}$, ion-ion interaction at the surface to a term in $\theta^{\frac{1}{2}}$ and London dispersion forces to an attractive term proportional approximately to θ^3. Two-dimensional interactions are generally regarded [19, 24] as being too small to explain the observed fall of ΔH with θ in H, O or N chemisorption in the range of intermediate coverages (e.g. $0{\cdot}1<\theta<0{\cdot}9$) to be considered here. We hence adopt the induced heterogeneity model [19] as the most reasonable for considering a linear fall of heat of adsorption with coverage and apply it to the case of two (or more) chemisorbed species. The equations analogous to (3), (5) and (6) for species A and B, may then be written as

$$\Delta H_A = \Delta H_A^\circ - r_A\theta_A - r_B\theta_B \tag{7}$$

$$\Delta H_B = \Delta H_B^\circ - r_A\theta_A - r_B\theta_B \tag{8}$$

since the variation of heat of adsorption of the species A or B will depend, to a first approximation, on the sum of two terms involving the respective dipole double-layer surface potential contributions from *both* species A and B, i.e., the term in $r_A\theta_A$ will involve the dipole moment of A and that in $r_B\theta_B$ the moment of B. It is important to note that the *same* terms determine the variation of heat of adsorption of both A and B with coverage by A and B, and we shall represent the terms $r_A\theta_A + r_B\theta_B$ by $f(\theta)$.

(iii) KINETIC EQUATIONS FOR THE OXYGEN EVOLUTION REACTION

This is a reaction where more than one intermediate may be adsorbed simultaneously. By analogy with the formulation given in eqn. (1) and (2) and previously [11, 14] we now write the rate of reaction IV (schemes A, B or C), using equations similar to (7) and (8) referring to coverage θ of the electrode by " MOH " and " MO " species, as

$$v_4 = k_4 C_{OH^-}(1-\theta_T)\exp\left[-\{\Delta G_4^{\ddagger} + \alpha f(\theta)\}/RT\right]\exp(\beta VF/RT), \tag{9}$$

where we shall write in general in the above and following equations $k_n \exp[-\Delta G_n^{\ddagger}/RT]$ as the rate constant for a reaction " n " at zero coverage. The rate of the back reaction in IV is given by

$$v_{-4} = k_{-4}\theta_{MOH}\exp\left[-\{\Delta G_{-4}^{\ddagger} - (1-\alpha)f(\theta)\}/RT\right]\exp\left[-(1-\beta)VF/RT\right]. \tag{10}$$

Reaction V is a radical-ion recombination with charge transfer (cf. $MH + H^+ + e \rightarrow M + H_2$) but in distinction to the corresponding hydrogen producing process shown

in the brackets, does not involve desorption of the immediate product. The rate equation for V is then

$$v_5 = k_5\theta_{MOH}C_{OH^-}\exp\left[-\{\Delta G_5^{\ddagger}+\gamma f(\theta)-(1-\gamma)f(\theta)-\beta VF\}/RT\right] \quad (11)$$

$$= k_5'\theta_{MOH}C_{OH^-}\exp(\beta VF/RT) \text{ for } \gamma = \beta = 0{\cdot}5^* \quad (11a)$$

since the effects of coverage by MOH and MO species on the activation energy for V are equal if $\gamma = 0{\cdot}5$. When V is rate-determining and the pre-exponential terms in coverage are of the order of magnitude $0{\cdot}2 < \theta_{MOH} < 0{\cdot}8$ (cf. 11, 14) IV can be regarded as in quasi-equilibrium, so that

$$f(\theta) = VF + K_4 \quad (12)$$

where K_4 is a constant at constant composition of the solution. In this case θ_{MO} will be negligible with respect to θ_{MOH} and hence

$$f(\theta) \simeq r_{MOH}\theta_{MOH} \simeq r_{MOH}\theta_T,$$

where θ_T is now the total coverage by radicals on the surface. The coverage by OH radicals will vary linearly with potential (eqn. (12)), except at very low or very high coverage when Langmuir behaviour will hold.[1, 8, 9] The Tafel slope for V will be $b = 2{\cdot}3 \times 2RT/F$ with $\beta = 0{\cdot}5$, which is identical with the result for the Langmuir case at $\theta_{MOH} = 1$. It will be noted that reaction V, with coverage-dependent free energy of activation, does not lead to a slope of $RT/(1+\beta)F$ (i.e., $2RT/3F$ with $\beta = 0{\cdot}5$) as in the Langmuir case or for radical-ion desorption to form a gaseous product (as in the atom-ion desorption path in hydrogen evolution).

When the MOH species are removed by a formal "recombination" type of process (actually an H transfer process) such as VII not involving charge transfer, the rate equation is

$$v_7 = k_7\theta_{MOH}^2\exp\left[-\{\Delta G_7^{\ddagger}-2\gamma f(\theta)+(1-\gamma)f(\theta)\}/RT\right]. \quad (13)$$

Substituting $f(\theta)$ from eqn. (12) and neglecting the variation of the pre-exponential term with θ gives

$$v_7 = k_7'\exp(2VF/RT) \quad \text{and} \quad b = 2{\cdot}3\,2RT/F \qquad (\gamma = 0{\cdot}5),$$

i.e., the same result as for V under comparable conditions. We note that a first order heterogeneous chemical step such as occurs in electrochemical decarboxylation,[25] e.g. the steps

$$HCOO\cdot \rightarrow H\cdot + CO_2$$

or

$$CF_3COO\cdot \rightarrow CO_2 + CF_3\cdot$$

following discharge of the corresponding ions, will not involve exponential terms in $f(\theta)$ since they cancel out, so that the rate of such steps at intermediate coverages will be practically independent of potential (a slight dependence may be observed since the rate of these reactions is proportional to the surface concentration of the appropriate radical, and hence to the coverage, and the latter is a linear function of potential (according to eqn. (12)) and the Tafel slope will tend to infinity). Under Langmuir conditions, the velocities of these reactions, when rate-controlling, will involve terms in $\exp(VF/RT)$ arising from quasi-equilibrium in the previous ion-discharge step, so that their Tafel slopes would be $dV/d\ln i = RT/F$.

* The assumption that $\gamma = \beta$ is justified since field effects on the potential energy diagram will originate quantitatively in the same way as effects of varying energy of adsorption of reactants and products, because both effects involve the same pair of potential energy curves.

TERMINAL DESORPTION STEPS

For the oxygen evolution process, at least two steps must occur prior to the final reaction producing oxygen molecules. If the final step is recombination of MO entities, and is rate-determining, both MOH and MO species can cover the surface significantly depending on the magnitude of the chemical or electrochemical equilibrium constants for reactions VII and V, respectively. The f(θ) can then involve significant terms in both θ_{MOH} and θ_{MO}, determined by

$$\theta_{MO}/\theta_{MOH} = K_5 \exp(VF/RT) \tag{14}$$

for reaction V and by

$$\theta_{MO}/\theta^2_{MOH} = K_7 \exp[f(\theta)/RT] = K'_7 \exp(VF/RT) \tag{15}$$

for reaction VII. The rate equation for the final step VI (e.g. in schemes A or B) is

$$v_6 = k_6\theta^2_{MO} \exp[-\{\Delta G^{\ddagger}_6 - 2f(\theta)\}/RT] \tag{16}$$

for non-activated adsorption of O_2 (cf. ref. 14) and

$$v_6 = k_6\theta^2_{MO} \exp[-\{\Delta G^{\ddagger}_6 - 2\delta f(\theta)\}/RT] \tag{16a}$$

for activated adsorption of O_2, where δ is a symmetry factor (probably different from β or γ) for the energy barrier associated with activated chemisorption of oxygen. In the case of reaction VI, we can only regard the pre-exponential term in θ_{MO} as relatively invariant with potential compared with the term exp $[2f(\theta)/RT]$ if θ_{MO} is comparable with θ_{MOH}, that is, if the equilibrium constants in eqn. (14) and (15) are not very much less than unity. This is probably the case for the species involved in the oxygen evolution reaction, since the MO bond energy would be expected to be greater than the energy of binding of the monovalent species OH to the surface M.

From eqn. (16) and (12), and (16*a*) and (12), the Tafel slopes for reaction VI are then

$$dV/d\ln i = RT/2F \quad \text{or} \quad RT/2\delta F, \text{ respectively.} \tag{17}$$

The corresponding slope for the terminal step under Langmuir conditions (θ_{MOH} and $\theta_{MO} \ll 1$) is $RT/4F$.

Under conditions where K_5 or K_7 are $\ll 1$ (and at low anodic potentials), θ_{MO} can be much less than θ_{MOH}; if the total coverage (i.e., that now principally due to MOH entities) is still appreciable and of the order 0·5, eqn. (16) and (16*a*) still hold except that the potential dependence of θ_{MO} must be taken into account, i.e., eqn. (16) becomes

$$v_6 = k_6K_5\theta^2_{MOH} \exp(2VF/RT) \exp[-\{\Delta G^{\ddagger}_6 - 2f(\theta)\}/RT]$$

and with eqn. (12) and θ^2_{MOH} of the order 0·5, the Tafel slope for reaction VI is $RT/4F$; similarly using eqn. (16*a*), the slope is $RT/2F(1+\delta)$ or $RT/3F$ if $\delta = 0{\cdot}5$. The same results for the Tafel slopes follow if reaction VII is the equilibrium step preceding rate-determining VI. In general, θ_{MO} will always become appreciable or predominant at higher anodic potentials and the results first deduced (eqn. (17)) will apply.

We have hitherto examined the kinetics for steps in a sequence of three reactions. In a scheme such as C, the kinetics for IV and V will be the same as we have discussed above. The kinetic equation for reaction VIII rate-controlling will be

$$v_8 = k_8\theta_{MO}C_{OH^-} \exp[-\{\Delta G^{\ddagger}_8 - \gamma f(\theta) + (1-\gamma)f(\theta) - \beta VF\}/RT] \tag{18}$$

where f(θ) involves θ_{MO}, θ_{MOH} and θ_{MHO_2}. Again the same f(θ) will be related to VF by eqn. (12) with IV in equilibrium giving the Tafel slope for reaction VIII as $dV/d\ln i = 2RT/F$ ($\beta = \gamma = 0{\cdot}5$). Similarly the recombination step IX in scheme C will give

$$v_9 = k_9\theta_{MOH}\theta_{MHO_2} \exp\left[-\{\Delta G_9^{\ddagger} - 2\delta f(\theta)\}/RT\right] \quad (19)$$

or

$$v_9 = k_9\theta_{MOH}\theta_{MHO_2} \exp\left[-\{\Delta G_9^{\ddagger} - 2f(\theta)\}/RT\right] \quad (20)$$

for activated and non-activated adsorption of O_2, respectively, as when reaction VI is rate-determining. The Tafel slopes are then $RT/2\delta F$ or $RT/2F$ as for reaction VIII, with the same assumptions made above (and previously [14]) about the magnitude of the pre-exponential θ terms.

GENERALIZATIONS

It is clear from the above discussion of steps in the oxygen evolution reaction, that some important general conclusions may be drawn regarding the kinetic consequences of considering coverage dependent activation energies in a complex sequence of reactions. In the Langmuir case, Tafel slopes diminish down a sequence of consecutive reactions following a primary ion discharge step. Thus, for successive steps involving an " electrochemical mechanism " the Naperian Tafel slopes will be $RT/(n+\beta)F$ where n is an integer >1 while formal bimolecular " chemical " recombination steps will have a slope of RT/mF where m is an integer >2 and increases down the reaction sequence, e.g., VII gives $RT/2F$, and VI or IX give $RT/4F$.

In the present case, where coverage-dependent activation energies are introduced, it is clear that normally no slopes less than $RT/2F$ will arise and the values are less diagnostic of mechanism than are the corresponding slopes for low coverage conditions. It will also be seen that the " recombination " slope of $RT/2F$ arises only in the case of a *terminal* recombination step in a series of consecutive reactions, and intermediate recombination (or bimolecular rearrangement) steps are not associated with this slope or corresponding values of the form RT/mF. Also the slope $RT/2F$ arises under Temkin conditions if the terminal step is a recombination irrespective of how many previous steps are involved, while the corresponding Langmuir slope can be RT/mF where m is an integer only equal to two for a recombination step immediately following the initial change transfer step, as in the hydrogen evolution case. The conditions $\theta_{MO} \ll 1$ when $\theta_{MOH} \sim 0{\cdot}5$ leading to the lower slopes $RT/4F$ or $RT/2F(1+\delta)$, are actually unlikely in anodic oxygen evolution since, on chemical grounds as pointed out above, K_5 or K_7 will not be expected to be $\ll 1$ and in addition the potential V in eqn. (14) and (15) will normally be well above the potential of zero charge of most metals at rates of oxygen evolution which can be conveniently measured (i.e., at current densities $> 10^{-7}$ A cm^{-2}).

The results deduced above are also independent of the exact form of f(θ), since f(θ) can always be expressed in terms of VF and constants in an equation of the form of (12) for quasi-equilibrium in the ion-discharge step (when a subsequent step is rate-controlling), and the *same* f(θ) always arises in the argument of the exponential involving the free energy of activation in the rate equation for the rate-controlling step. These general conclusions only apply, of course, to intermediate coverage conditions. At very low or quite high coverage, limiting Langmuir conditions apply with the Tafel slopes as previously deduced,[1, 2, 8, 9] based on direct potential-dependence of the concentrations of all adsorbed intermediates in pre-exponential terms in the rate-equations for the steps prior to the rate-determining step. Although

we have made the above deductions for steps in the oxygen evolution reaction, it is clear that the conclusions are general for any reaction involving several steps and more than one adsorbed intermediate.

KINETIC THEORY OF PSEUDO-CAPACITANCE

The significance of the direction of potential dependence of adsorption pseudo-capacitance in oxygen evolution has been discussed in an earlier paper [9] in relation to extent of surface coverage of the electrode by intermediates, and to the type of isotherm applying to the adsorption of the electromotively active intermediate. During publication of the latter work Bockris and Kita [26] have presented a general mathematical treatment of transients for cases of potential-dependent pseudo-capacitance based implicitly on the Langmuir isotherm. In the latter treatment, no conditions are considered which could lead to a pseudo-capacitance independent of potential over any significant range of electrode potentials, however, such potential-independent pseudo-capacitance is experimentally observed over an appreciable range of potentials for the oxygen evolution process at the nickel electrode [8 9] and is implicit in the e.m.f. decay at a platinized-platinum hydrogen cathode where the e.m.f. decay slope in log [time] has the *same* numerical slope $2.3RT/2F$ as that of the Tafel relationship [28] viz., $-2.3RT/2F$. Were the H-pseudo-capacitance in the platinum case potential-dependent, the e.m.f. decay slope would be either greater or smaller than $2.3RT/2F$ depending on the sign of the coefficient of the potential term in the argument of the exponential relating capacitance to potential.

The steady-state* kinetic treatment or a treatment in which equilibrium in pre-rate-determining steps is considered leads, as shown elsewhere,[26 27] to an exponential dependence of the coverage of adsorbed intermediates on potential, and hence to a potential-dependent pseudo-capacitance associated with these intermediates. In the Langmuir case,[26 27] this pseudo-capacity has a maximum value at a certain potential determined by the relative values of the rate constants involved and the concentration of reacting ions, and varies symmetrically about this potential, falling to practically zero within about ± 0.12 V of the potential of the maximum, so that the actual electrode capacity is then simply the ionic double-layer capacity. The value of the maximum capacity [26] C_{max} is $k'F/4RT$ where k is the charge associated with the formation of a monolayer of the intermediates. For 10^{15} univalent radicals per cm^2, $C_{max} \simeq 1600\ \mu$F cm^{-2} [26].

The direct observation* of a potential-independent pseudo-capacitance for adsorbed H over an appreciable range of potentials at platinum electrodes was, in fact, originally discussed [5] in terms of an isotherm involving a free energy of adsorption linearly dependent on coverage. While, in principle, such an isotherm leads in the limiting case to a potential independent contribution to the overall pseudo-capacitance, a result which really arises from the conditions assumed to derive eqn (12), we now show that, in general the pseudo-capacitance can never be completely independent of potential and the extent of the potential dependence and the magnitude of the capacity maximum depends on the values of the coefficients of the θ terms in eqn (7) and (8).

* The normal requirement for validity of a steady-state treatment for deducing concentrations of intermediates is that the concentrations of the intermediates are small and hence do not change significantly during the reaction. This condition does not however apply to electrochemical reactions under constant current and potential conditions since the reaction is forced to be in a steady state irrespective of the concentrations of the various intermediates involved. The steady state treatment can hence legitimately be used for calculating the coverage by intermediates and the associated pseudo-capacity.

EXTENT OF POTENTIAL-DEPENDENCE OF THE PSEUDO-CAPACITY IN RELATION TO VALUES OF r

We write eqn. (9) for conditions where the adsorption pseudo-capacitance is due only to MOH species; i.e. when reaction V is the slow step for $k_5 \ll k_4$, k_{-4} and k_6, and VI is not in equilibrium. The surface is then significantly covered only by MOH species (and the solvent) and f(θ) becomes simply $r_{OH}\theta_{OH}$ which we shall designate as $r_1\theta$ for brevity.

If IV is in quasi-equilibrium

$$k_4(1-\theta)C_{OH^-}\exp(\beta VF/RT)\exp(-\alpha r_1\theta/RT) = k_{-4}\theta\exp[-(1-\beta)VF/RT]\exp[(1-\alpha)r_1\theta/RT], \quad (21)$$

then

$$V = \frac{RT}{F}\ln[\theta/1-\theta] + r_1\theta/F + K', \quad (22)$$

where K' is a constant at constant concentration and temperature. The pseudo-capacity for MOH is then given by

$$\frac{k'}{C} = \frac{dV}{d\theta} = \frac{RT}{F}\frac{d\ln[\theta/1-\theta]}{d\theta} + r_1/F, \quad (23)$$

which involves a " Langmuir " term in $\theta/1-\theta$ in addition to a " Temkin " term in r_1.* For the purpose only of defining the terms for limiting cases, we see that eqn. (23) gives

$$\frac{k'}{C} = \frac{r_1}{F} \text{ (which we shall call } k'/C_T), \quad (24a)$$

when

$$\frac{r_1}{F} \gg \frac{RT}{F}\frac{d\ln[\theta/1-\theta]}{d\theta}$$

and

$$\frac{k'}{C} = \frac{RT}{F}\frac{d\ln[\theta/1-\theta]}{d\theta} = \frac{RT}{F}\left(\frac{1}{\theta}+\frac{1}{1-\theta}\right) \quad (24b)$$

(which we shall call k'/C_L) if

$$\frac{r_1}{F} \ll \frac{RT}{F}\frac{d\ln[\theta/1-\theta]}{d\theta} \quad (25)$$

where we have called the capacities C-" Temkin " for (24a) and C-" Langmuir " for (24b). It is clear that eqn. (23) can be written in the form:

$$\frac{1}{C} = \frac{1}{C_T}+\frac{1}{C_L} \quad (26)$$

so that

$$C = \frac{C_TC_L}{C_T+C_L}. \quad (27)$$

* It is important to note here that, while in the rate equations terms in θ and $1-\theta$ can be legitimately neglected when $0{\cdot}2 < \theta < 0{\cdot}8$ and an exponential term in f(θ) is important, in the pseudo-capacity eqn. (23) the term $d\ln[\theta/1-\theta]/d\theta$ can normally not be neglected in comparison with r_1/F.

Thus, the two pseudo-capacity contributions evidently combine effectively in series to determine the overall pseudo-capacity, i.e., when one is much larger than the other, the smaller capacity will determine the overall capacity. In terms of potential-dependent coverage, this implies that when two terms involve the coverage as in eqn. (22), the actual coverage will be determined by the term predicting the lower coverage at a given potential.

The potential dependence of C for various values of r_1 may be evaluated in the general case by calculating C as a function of θ and θ as a function of V using eqn. (22) and (23). We note that $K_4 \ll 1$, otherwise θ_{MOH} will be near unity even at low anodic overpotentials. We take log $K_4 = -2$ as an example (choice of other values of K_4 will only shift the scale of values of V and will not change the form of the dependence of θ or C on V) and r_1 having values of 0, 5, 10 and 20 kcal mole^{-1} (these

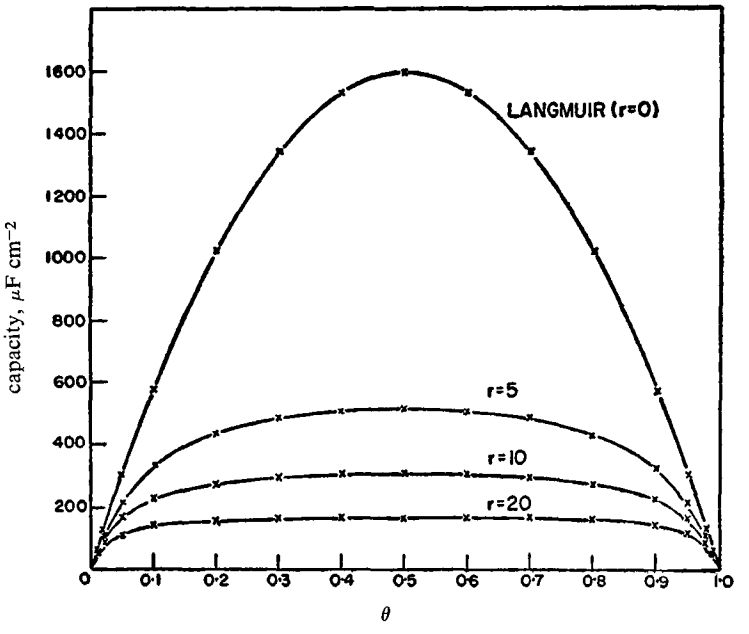

FIG. 1.—Variation of the overall adsorption pseudo-capacity with coverage θ.

figures are chosen to be approximately within the observed range of the mean variation of heats of adsorption of various species with coverage where approximately linear relations between θ and heat of adsorption arise for $0{\cdot}1 < \theta < 0{\cdot}9$). The calculated values of C * as a function of θ and V are shown in fig. 1 and 2, respectively, and the Langmuir case, corresponding to $r_1 = 0$, is shown for comparison. These cases will apply to *any* univalent species predominantly covering the surface for the values of k' and r_1 chosen. It will be noted that for the Langmuir case: (*a*) C is never potential-independent except as it tends to zero and (*b*) the pseudo-capacitance will only have measurable values over a narrow potential range of some 240 mV.

* In these calculations the same constants are used for the evaluation of k' as discussed above. Their exact values are not of importance here as we are only interested in the relative *variation* of C with θ or V. Comparison with experimental data will require an assignment of the surface concentration corresponding to $\theta = 1$ and the charge transferred per radical adsorbed as well as the real/apparent area ratio for the electrode surface.

Introduction of a finite value of r_1 produces a range of C values which are less potential dependent than in the Langmuir case but never strictly potential-independent. However, when $r = 10$ or 20 kcal mole^{-1}, C is sensibly constant over 350 and 700 mV, respectively, as we have previously deduced qualitatively by a quasi-thermodynamic argument.[9] This is the kind of behaviour that is observed experimentally in some cases [8, 9, 20] but potential-dependent pseudo-capacity is found under other conditions, e.g., for the hydrogen evolution reaction at nickel in alkaline solution,[7] and with the nickel oxide electrode.[8, 9] When a potential independent pseudo-capacity contribution is involved (" Temkin " conditions; r finite) it will be noted that the maximum pseudo-capacity is substantially lower than the $C_{max.}$ calculated

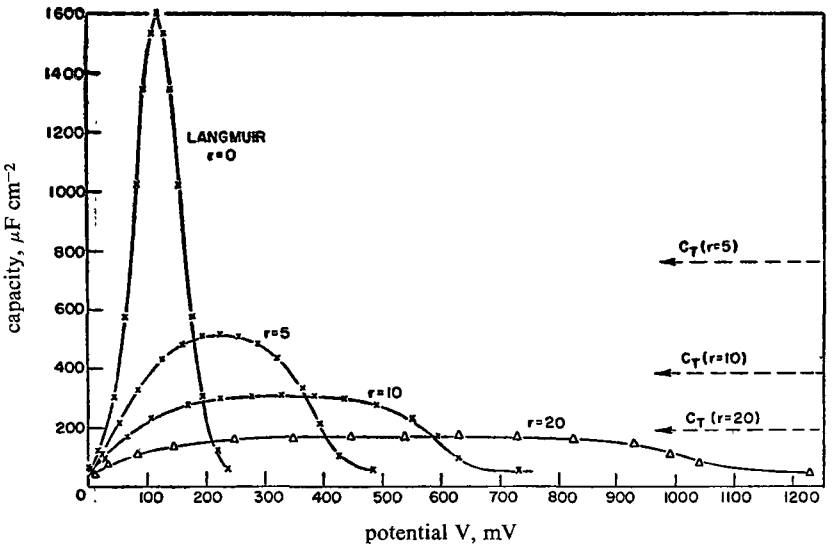

FIG. 2.—Variation of the overall pseudo-capacity with potential V.

(1600 μF cm^{-2}) for the " Langmuir " case. However, for values of r even as high as 20 kcal mole^{-1}, the maximum capacity should be readily distinguishable, over a wide range of potential or coverage, from the ionic double-layer capacity, which normally does not exceed about 100 μF cm^{-2} at potentials anodic to the potential of zero charge.[29] In all cases at very high potentials $C \rightarrow C_{d.l.}$, i.e., the measured capacity will tend to the ionic double-layer capacity. The " Langmuir " case (eqn. (24*b*)) is evidently a special case of eqn. (22) and in most cases will not correspond to experimental conditions, since heats of adsorption are rarely independent of coverage. Even if r is as low as 1 kcal mole^{-1}, $C_{max.}$ will be significantly less (actually 1100 μF cm^{-2}) than 1600 μF cm^{-2} and the range of the potential dependence of C will be substantially larger than that for the " Langmuir " case. Some values of $C_{max.}$ and C_T as a function of r have been plotted in fig. 3; C_T can have values greater than $C_{L,max.}$ for low r, but combined with C_L (eqn. 26) must lead to values of overall C *less* than $C_{L,max.}$. The above conclusions are general and will refer to any single adsorbed species which arises from a Faradaic process in an electrochemical reaction, using the appropriate value of r. We now examine a more general case for more than one adsorbed species at the surface.

GENERAL CASE.—Pseudo-capacity associated with more than one adsorbed species.

The general reaction scheme

$$M+A^- \rightleftarrows MA+e \quad \text{(fast)} \qquad \text{(X)}$$

$$MA \rightleftarrows MB \quad \text{(fast)} \qquad \text{(XI)}$$

$$2MB \rightarrow B_2 \quad \text{(slow)} \qquad \text{(XII)}$$

is considered with XII rate controlling so that θ_A and θ_B may both be significant. The heats of adsorption of A and B are assumed to be given by eqn. (7) and (8) involving $f(\theta)$. For X and XI at equilibrium (cf. eqn. (12))

$$f(\theta) = VF + K_{10} \tag{28}$$

and

$$\theta_B/\theta_A = k_{11}/k_{-11} = K_{11}. \tag{29}$$

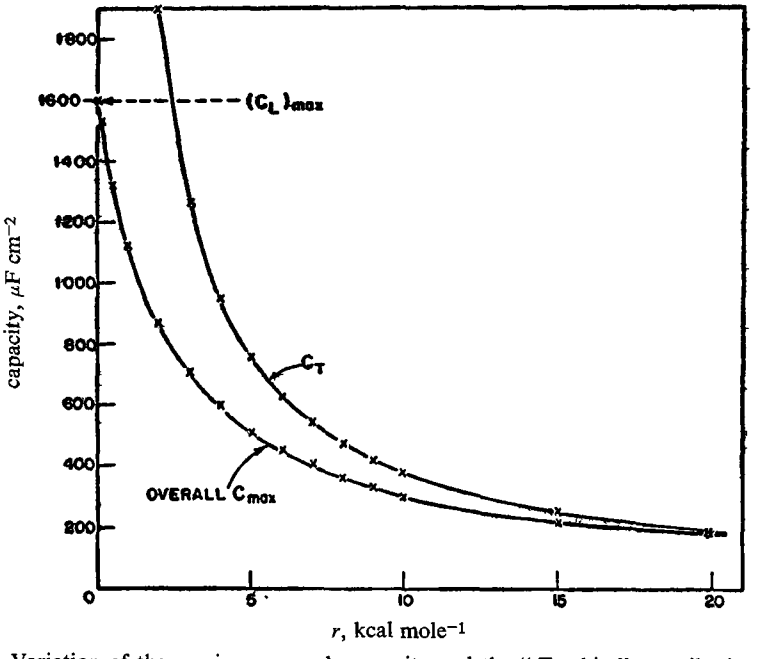

FIG. 3.—Variation of the maximum pseudo-capacity and the "Temkin" contribution with values of r_1.

The latter ratio is independent of total coverage and potential, so that

$$f(\theta) = r_A\theta_A + r_B\theta_B = r_A\theta_A + K_{11}r_B\theta_A = K'_{11}\theta_A, \tag{30}$$

where $K'_{11} = r_A + K_{11}r_B$.

Now

$$C = \frac{k'd\theta_T}{dV} = k'd[\theta_A+\theta_B]/dV \tag{31}$$

but

$$\theta_A+\theta_B = \theta_A+K_{11}\theta_A = (1+K_{11})\theta_A. \tag{32}$$

Now from eqn. (30) and an eqn. similar to (12) referring to reaction X

$$d\theta_A/dV = F/[r_A+K_{11}r_B] \tag{34}$$

so that, from eqn. (31) and (32)

$$C = k'(1+K_{11})\mathrm{d}\theta_A/\mathrm{d}V = k'\left(\frac{1+K_{11}}{r_A+K_{11}r_B}\right)F = k'F/r', \tag{35}$$

where we have defined

$$r' = (r_A+K_{11}r_B)/(1+K_{11}).$$

It is thus seen that when more than one intermediate is adsorbed, a constant pseudo-capacity contribution is still obtained and, moreover, the apparent value of the rate of change of heat of adsorption with coverage is simply a weighted average of the values for the two individual species.

Normally the ratio θ_B/θ_A will depend on potential, either: (*a*) due to a change in the number of adsorbed species caused by an act of the given step (e.g. $2MA \rightarrow MB$,* viz., $2MOH \rightarrow MO + H_2O$ [reaction VII]) with the previous charge transfer step in electrochemical equilibrium; or (*b*) when there is a direct potential-dependence of the equilibrium constant for XI (i.e., for a reaction such as $MA + A^- \rightarrow e + MB$; cf. reaction V). In either case θ_A and θ_B will only be comparable † over a small range of electrode potentials (which may or may not be accessible practically in an experiment) so that we can treat the problem generally by assuming $\theta_A \gg \theta_B$ or $\theta_A \ll \theta_B$ so that $f(\theta) \simeq r_A\theta_A$ or $r_B\theta_B$.

The total Temkin pseudo-capacity contribution given by eqn. (35) will combine with the Langmuir term as in eqn. (26) and 23) to give the overall pseudo-capacity which will then have a potential dependence similar to that deduced above depending now on the value of r' in eqn. (35).

OPEN-CIRCUIT DECAY OF E.M.F. AND REACTION MECHANISMS

We have discussed how a pseudo-capacitance can be sensibly potential independent over an appreciable range of potentials when the free energy of activation is dependent on coverage and how the Langmuir treatment leads only to an exponential dependence of θ on V except as $C \rightarrow C_{d.l.}$ when $\theta \rightarrow 0$ or 1. An important kinetic case is that of the recombination controlled cathodic hydrogen producing reaction at platinized platinum. Here the Tafel slope is $-RT/2F$ and is normally deduced by assuming that the step

$$H^+ + e + M \rightarrow MH_{ads.} \qquad \text{III}$$

is in quasi-equilibrium at low coverage by $MH_{ads.}$ (high coverage leads to a recombination-controlled limiting current observed experimentally [30]) so that

$$\theta_H = K \exp(-VF/RT) \tag{38}$$

where K is a constant at constant electrolyte composition. The recombination rate is then proportional to $[\exp(-VF/RT)]^2$ giving the characteristic Tafel slope of $RT/2F$. On the basis of these assumptions, the pseudo-capacity associated with adsorbed H is

$$C_H = -k'(\mathrm{d}\theta_H/\mathrm{d}V) = K(k'F/RT)\exp(-VF/RT) \tag{39}$$

† Thus, if XI were of the form $2MA \rightleftarrows MB$, rather than $MA \rightleftarrows MB$

$$k_{11}\theta_A^2 \exp[(3\gamma-1)f(\theta)/RT] = k_{-11}\theta_B \exp[-(2-3\gamma)f(\theta)/RT] \tag{37}$$

and with (28), $\theta_B/\theta_A^2 = k_{11}\exp(VF/RT)$. If $\theta_A = \theta_B$ at a given value of V, $\theta_A \ll \theta_B$ or $\theta_B \ll \theta_A$ within $\pm 0{\cdot}06$ V of that potential so that in practice the total coverage will be largely determined by that of one species or the other over a wide potential range. The same conclusions would follow if XI were of the form $MA + A^- \rightarrow MB + e$.

and for the e.m.f. decay process, with self-discharge of the pseudo-capacity, the kinetic equation is

$$-C_H(dV/dt) = i_0 \exp[-2VF/RT] \tag{40}$$

for continuing recombination as the rate-controlling process in self-discharge on open-circuit.

Thus

$$-Kk'(F/RT)\exp[-VF/RT](dV/dt) = i_0 \exp[-2VF/RT],$$

or

$$-\exp[VF/RT]dV = (i_0RT/Kk'F)dt. \tag{41}$$

After integrating, this gives the e.m.f. decay slope as

$$dV/d\ln(t+\phi) = -RT/F,$$

where ϕ is the usual integration constant.[8]

The experimental e.m.f. decay slope (28) is close to $RT/2F$, i.e., numerically identical with the Tafel slope. This can only arise if the capacity is potential *independent*, i.e., if the rate of the recombination step is given (14) approximately by the equation for intermediate coverage by H, viz.,

$$v_3 = k_3 \exp[-(\Delta G_3^{\ddagger} - 2r\theta)/RT],$$

so that with eqn. (4)

$$dV/d\ln i = -RT/2F$$

as at low coverages. We must hence conclude that the reaction at platinum [28] occurs on a surface appreciably covered by adsorbed H, with r significant, as is slso evident from the directly observed galvanostatic discharge transients.[4] The observation of the identity of Tafel and decay slopes in this case can be regarded as a direct proof of the validity of the assumption [14] of coverage dependent activation energies. Similarly, for the oxygen evolution process at the nickel oxide electrode, we have given direct proof that the Tafel and decay slopes are identical only if the pseudo-capacitance (which in that case can be obtained directly [8, 9]) is independent of potential. When, on the other hand, it is found to be potential dependent, the observed Tafel and decay slopes differ in the expected direction.[9] MacDonald and Conway [18] have experimentally found similar effects at the gold anode for low coverage conditions in the oxygen evolution reaction.

It could be argued that the identity of Tafel and decay slopes at platinum [28] is simply the result of limitingly low or limitingly high coverage conditions where the Langmuir pseudo-capacity ($r = 0$) tends to zero. This possibility can be discounted in the platinum case since observed fractional coverages by H do not tend to zero and in fact are quite substantial,[4] nor are they unity since otherwise the characteristic recombination limiting current [30] would be observed, which is not actually found until much higher current densities than those from which the e.m.f. decay has been followed.[28]

ELECTRODE POTENTIAL AND COVERAGE

The dependence of θ on V for the Langmuir case can be obtained from the equation given previously [26] and for the combined Langmuir-Temkin case from eqn. (22) or (27) assuming the same arbitrary values for K_4 and C_{OH^-} taken previously.

In the Langmuir case ($f(\theta) = 0$), θ varies with potential as shown in fig. 4. An approximately linear region occurs over a range of about 60 mV. As r_1 becomes greater, the linear region of the plot of θ against V increases, but at high or low

potentials a short non-linear region arises from the non-exponential term in θ in the rate equations. The coverage is essentially linear with V over 450 mV when r_1 is 10 kcal mole^{-1}. The dotted lines in fig. 4 show what the θ(V) behaviour would be if only the exponential term in θ in eqn. (22) determined the dependence of θ on V. Obviously this must lead to a completely linear dependence of θ on V as shown. This is a fictitious case, since in reality at very low or very high θ, the $\theta/1-\theta$ term will always be important and give the curving-off region of the lines at each extremity.

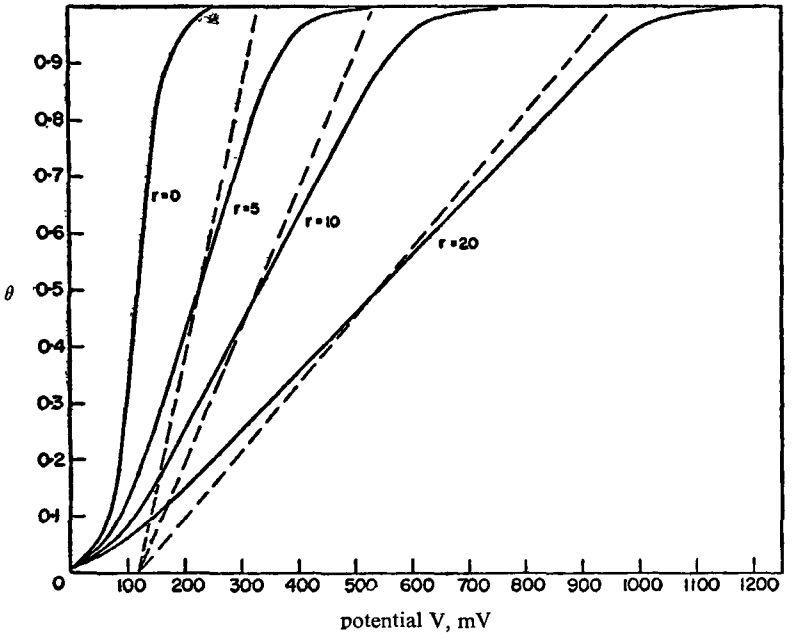

FIG. 4.—Variation of coverage θ with potential V for Langmuir ($r_1 = 0$) and Langmuir+Temkin conditions (indicated r_1 values).

It is of interest, however, that in the range where θ is linear with V (for appreciable values of r_1), the actual values of θ at any given potential are significantly different from those calculated from the exponential (Temkin) term in θ alone. For example, when $r = 10$ kcal, the pre-exponential term in θ never becomes negligible compared with the exponential one, so far as the relationship between θ and V is concerned. Nevertheless, an almost linear variation of θ with V (constant capacity) is still obtained, since the deviation of the pre-exponential term from a linear $\theta - V$ relationship is negligible with respect to the value of θ arising from the exponential term, except at very high or very low θ.

APPENDIX

KINETIC EQUATIONS ARISING FOR *a priori* HETEROGENEITY

Here we consider briefly the consequences of assuming that the variation of heat of adsorption with coverage is due to an intrinsic heterogeneity of the surface. If there is no specificity of surface sites for two or more adsorbed intermediates at a total coverage θ_T

(which will be the case if they are chemically similar, as in the oxygen evolution reaction considered above), we can write in general for intermediates A and B

$$\Delta H_A = \Delta H_A^\circ - r_A\theta_T; \quad \Delta H_B = \Delta H_B^\circ - r_B\theta_T \tag{1A}$$

since the energy of adsorption of a given species will depend on the sites remaining just beyond the total coverage θ_T and the r values define the distribution (assumed linear) of energies of adsorption with total coverage. It is not necessary that $r_A = r_B$, since the variation of the energy of chemisorption of the species A and B with coverage probably depends on the electronegativity difference between the sites and each of the species adsorbed. In many cases it will, however, be legitimate to regard $r_A \simeq r_B$ particularly, as in the oxygen evolution case for O and OH species, where the species are chemically similar. When there is complete specificity of sites for the two or more species, the surface behaves essentially as a mixture of two types of surface with independent properties for each of the species so that

$$\Delta H_A = \Delta H_A^\circ - r_A\theta_A; \quad \Delta H_B = \Delta H_B^\circ - r_A\theta_B.$$

It is unlikely that this applies to most electrochemical reactions including the oxygen evolution reaction.

We may proceed in a similar way to that adopted in the main part of the paper by considering steps in the oxygen evolution reaction assuming that the primary discharge step IV is in quasi-equilibrium followed by rate-determining V or VII. We obtain

$$r_{OH}\theta_T = VF + K_4 \tag{2A}$$

as in eqn. (12), and for rate-determining V,

$$v_5 = k_5\theta_{MOH}C_{OH^-}\exp\left[-\{\Delta G_5^\ddagger - \gamma r_{OH}\theta_T - \beta VF + (1-\gamma)r_O\theta_T\}/RT\right],$$

which gives the Tafel slope for V for intermediate coverage by MOH as

$$\frac{dV}{d\ln i} = \frac{2RT}{F}\frac{r_{OH}}{2r_{OH}-r_O} \text{ when } \gamma = 0{\cdot}5 = \beta$$

which obviously gives a slope of $2RT/F$ when $r_{OH} = r_O$. Similarly, for rate-determining VII, which does not involve a direct potential term in the rate equation, we obtain the same result

$$\frac{dV}{d\ln i} = \frac{2RT}{F}\frac{r_{OH}}{2r_{OH}-r_O} = \frac{2RT}{F} \text{ when } r_{OH} = r_O.$$

These equations give the same limiting result when $r_{OH} = r_O$ as the general treatment in terms of $f(\theta)$ for the induction model given in the main part of the paper. We may note also, as with $f(\theta)$, that the exact form of the function of θ_T in equation 1A is immaterial as it will always be eliminated when equation 2A is used to substitute for this function of θ_T in the rate equations in terms of VF. Any arbitrariness in assuming a *linear* function in θ_T in equation 1A is hence not of importance in the general deduction of kinetic current-potential equations and Tafel slopes.

It is readily seen that a terminal recombination step with desorption, such as VI, will give

$$\frac{dV}{d\ln i} = \frac{RT}{2F}\frac{r_{OH}}{r_O} = \frac{RT}{2F} \text{ when } r_{OH} = r_O$$

for non-activated adsorption (*cf.* ref. 14) of the O species from O_2. The results derived on the basis of *a priori* heterogeneity, when the r values for various intermediates are identical, will in general be the same as those deduced on the induction model. However, since the r values need not, in principle, be quite identical, the heterogeneity model allows of the possibility of some variation of Tafel slopes from the above limiting values derived assuming equal r values.

Grateful acknowledgement is made to the Defence Research Board, Department of National Defence, for support of this and related work on Grant No. 5480-12. One of us (E. G.) is indebted to the National Research Council for an award of a scholarship.

1 Bockris, *J. Chem. Physics*, 1956, **24**, 817.
2 Bockris, *Modern Aspects of Electrochemistry* (Academic Press, New York, 1954), vol. 1, chap. IV.
3 Bockris and Potter, *J. Electrochem. Soc.*, 1952, **99**, 169.
4 Frumkin and Slygin, *Acta physicochim.*, 1935, **3**, 791. Slygin and Ershler, *Acta physicochim.*, 1939, **11**, 45. Frumkin, Dolin and Ershler, *Acta physicochim.*, 1940, **13**, 779.
5 Temkin, *Zh. Fiz. Khim.*, 1941, **15**, 296.
6 Devanathan, Bockris and Mehl, *J. Electroanal. Chem.*, 1959/60, **1**, 143.
7 Devanathan and Servaratram, *Trans. Faraday Soc.*, 1960, **56**, 1820.
8 Conway and Bourgault, *Can. J. Chem.*, 1959, **37**, 292; 1960, **38**, 1557; 1962, **40**, 1690.
9 Conway and Bourgault, *Trans. Faraday Soc.*, 1962, **58**, 593.
10 Conway, *Proc. Roy. Soc. A*, 1960, **256**, 128.
11 Parsons, *Trans. Faraday Soc.*, 1958, **54**, 1053.
12 Conway and Bockris, *J. Chem. Physics*, 1957, **26**, 532.
13 Conway, Beatty and de Maine, *Electrochim. Acta*, 1962, **7**, 39. See also Conway, *Phil. Trans. Roy. Soc. Canada*, 1960, **54**, (III), 19.
14 Thomas, *Trans. Faraday Soc.*, 1961, **57**, 1603.
15 Bockris, Pentland and Sheldon, *J. Electrochem. Soc.*, 1957, **104**, 182.
16 Laidler, *J. Physic. Chem.*, 1949, **53**, 712.
17 Breiter, *Advances in Electrochemistry and Electrochemical Engineering*, ed. Delahay and Tobias (Interscience, New York, 1961), vol. I, p. 123.
18 Macdonald and Conway, *Proc. Roy. Soc. A*, 1962, in press.
19 Boudart, *J. Amer. Chem. Soc.*, 1952, **72**, 3566. See also de Boer, *Chemisorption*, ed. Garner (Butterworths, London, 1957), p. 57.
20 Dowden, *J. Chem. Soc.*, 1950, 242.
21 Bosworth, *Trans. Roy. Soc. N.S.W.*, 1946, **79**, 166.
22 Bosworth, *Trans.Roy. Soc. N.S.W.*, 1946, **79**, 53. Bosworth and Rideal, *Physica*, 1937, **4**, 925.
23 de Boer, *Electron Emission and Adsorption Phenomena* (Cambridge, Univ. Press, 1935).
24 Halsey and Taylor, *J. Chem. Physics*, 1947, **15**, 624.
25 Conway and Dzieciuch, *Can. J. Chem.*, in press. See also *Nature*, 1961, **189**, 914; *Proc. Chem. Soc.*, 1962, 121.
26 Bockris and Kita, *J. Electrochem. Soc.*, 1961, **108**, 676.
27 Eucken and Weblus, *Z. Elektrochem.*, 1951, **55**, 114.
28 Butler and Armstrong, *Trans. Faraday Soc.*, 1933, **29**, 1261.
29 Grahame, *Chem. Rev.*, 1947, **41**, 441.
30 Azzam and Bockris, *Trans. Faraday Soc.*, 1952, **48**, 145.

PRINTED IN GREAT BRITAIN AT
THE UNIVERSITY PRESS
ABERDEEN

ELECTROCHEMISTRY OF THE NICKEL OXIDE ELECTRODE

PART IV. ELECTROCHEMICAL KINETIC STUDIES OF REVERSIBLE POTENTIALS AS A FUNCTION OF DEGREE OF OXIDATION

B. E. CONWAY AND E GILEADI

Department of Chemistry, University of Ottawa, Ottawa, Ontario

Received May 22, 1962

ABSTRACT

Electrochemical kinetic studies have been carried out at the nickel oxide electrode showing that the reversible potential for the Ni^{II}–Ni^{III} system is independent of the state of oxidation of the bulk oxide in the electrode over a wide range of degrees of oxidation The properties of the electrode are shown to be determined by the state of a surface phase, which is completely charged when the bulk oxide material in the electrode has been charged to 10% of its total charge capacity Experiments on sparingly charged electrodes have proved that charging of the bulk oxide does not commence significantly until the electrode is charged to about 1 5% Consecutive electrochemical reactions possibly involved in the charging process are discussed

INTRODUCTION

The real reversible potential of the nickel oxide (Ni^{II}–Ni^{III}) electrode has been the subject of controversy for some years and previously reported values are misleading since they have not been based on well-defined equilibrium conditions or a well-defined state of the system Determination of the reversible potential is complicated by the self-discharge processes which occur at the electrode in the oxidized form and also by the fact that the electrode may exist in a range of chemical states corresponding to the extent of conversion of Ni^{2+} to Ni^{3+} (and possibly Ni^{4+} under certain conditions) in the hydrated oxide

In an earlier paper (1), the true reversible potential of partially charged nickel oxide electrodes at a single controlled state of oxidation "$NiO_{1\ 25}$" was examined as a function of potassium hydroxide and water activities in aqueous alkali solutions, and distinguished from the mixed potential assumed in previous work (2, also 12, 13) to be the reversible potential A polarization decay method was employed (1, 3, 4) in which the reversible potential was approached both from the anodic and the cathodic directions

In the present phase of our work, the same method has now been applied to the study of the potential of partially charged nickel oxide electrodes as a function of the degree of charge, at constant electrolyte composition This method was found to be applicable only over a limited range of degree of oxidation of the electrode ("$NiO_{1\ 10}$"–"$NiO_{1\ 30}$") owing to problems of extrapolation to the reversible potential to be discussed below. Stationary potentials, taken at very long times on open circuit, were therefore also measured as a function of the degree of charge over a much wider range of degree of oxidation ("$NiO_{1\ 025}$"–"$NiO_{1\ 50}$")

The role of the surface and bulk phases in determining the measured potential was deduced It will be shown that three well-defined regions in the charging process can be distinguished experimentally. In the first, the surface phase alone is being charged, in the intermediate region, the Faradaic current is used to charge both phases, until the surface phase is fully charged, after which oxidation of the bulk is the main Faradaic process (Most of the charging process occurs at a potential anodic to the reversible oxygen electrode, so that oxygen evolution must occur to a certain extent as a parallel process in all three regions described above It does not, however, become appreciable until most of the bulk material has been charged)

EXPERIMENTAL

(1) Electrodes

Nickel hydroxide electrodes were prepared in sintered-nickel plaques by methods described in detail previously (1, 3, 5) Each electrode was charged and discharged three times before use, at a 5-hour charging rate, in order to stabilize its electrochemical behavior (3, 4)

(2) Solutions

All solutions and reagents were prepared as described previously (1, 3), and most experiments were carried out in 1 *N* aqueous KOH at 25° C Some comparative runs were carried out in 7 2 *N* KOH

(3) Reversible Potentials

The reversible potential of the Ni^{II}–Ni^{III} system was obtained by extrapolating anodic and cathodic e m f decay lines, plotted logarithmically in time, to the potential of their intersection, as described in a previous paper (1).

The "discharged" electrodes still contained a small amount of the higher oxide of nickel, which at the apparent end of discharging is evidently inaccessible, probably due to insulation by the less conducting $Ni(OH)_2$ (6) The electrodes were reduced completely by prolonged cathodic polarization until a total of 3 F/equivalent had been passed The electrodes were then transferred to another cell containing freshly prepared electrolyte and reference electrodes, and left on open circuit overnight with purified oxygen bubbling through the cell

The following sequence of operations was then performed at a current corresponding to a 2-hour charging rate, i e at 143 ma g^{-1} of active material calculated as $Ni(OH)_2$ (cf ref 1)

(*a*) The electrode was charged for 24 minutes to an extent of oxidation of 20% ($NiO_{1.10}$) based on the oxidation change $Ni^{II} \rightarrow Ni^{III}$ in the oxide The current was then interrupted and open-circuit decay of potential followed for about an hour

(*b*) Charging was then continued for 24 minutes, followed immediately by discharge for the same length of time The current was then interrupted and buildup (i e recovery of potential on open circuit to more anodic values) was followed for an hour, the degree of charge again being 20%, as in (*a*)

Anodic and cathodic open-circuit decay and recovery of potential were followed in a similar manner at the 40%, 60% and 80% charged electrodes, corresponding to formal degrees of oxidation of $NiO_{1.20}$ $NiO_{1.30}$, $NiO_{1.40}$ respectively Charging and discharging curves for one of these experiments are shown in Fig 1 Similar charging and discharging cycles were carried out to obtain data for electrodes in 25%, 50%, and 75% degrees of oxidation (see Table I)

TABLE I

Degree of charge (%)	KOH concn (*N*)	Anodic decay slope		Cathodic buildup slope	E_{rev}†	Number of experiments
		Initial, b_1 (mv)	Lower, b_2 (mv)	b_3 (mv)	(mv)	
20	1	−12 7	−18 2	+11 0	423	1
25	1	− 9 5±0 6	−18 3±3 5	+13 1±2 1	424±4	5
40	1	−12 0	−15 2	+ 9 0	427	1
50	1	−10 8±1 5	−19 8±5 0	+10 9±1 6	423±5	9
60	1	−35 3	−17 8	+11 4	*	1
75	1	−32±13	−22±2 3	+ 9 4±1 2	*	5
80	1	−60	−21 0	+14 3	*	1
"Overcharge"	1	−45±2 6	—	—	*	6

*See comment in text with regard to these degrees of oxidation
†The reversible potentials are given vs that of a Hg/HgO reference electrode in the same solution

(4) Stationary Potentials

In this series of experiments, the electrodes were charged to a given degree of oxidation, and decay of e m f on open circuit was followed by means of a high impedance recorder for about a week, at which time the e m f varied at a rate of 1 mv/day or less

(5) Sparingly Charged Electrodes

A series of experiments was conducted on electrodes charged to a very small extent (0 33% to 5% of total charge capacity)

RESULTS

Plots of decay of e m f after anodic and cathodic polarization vs log $(t+\theta)$ are shown in Fig 2 The significance of this type of plot, of e m f decay slopes, and of the parameter θ have been discussed previously (1, 3, 4, 7, 8)

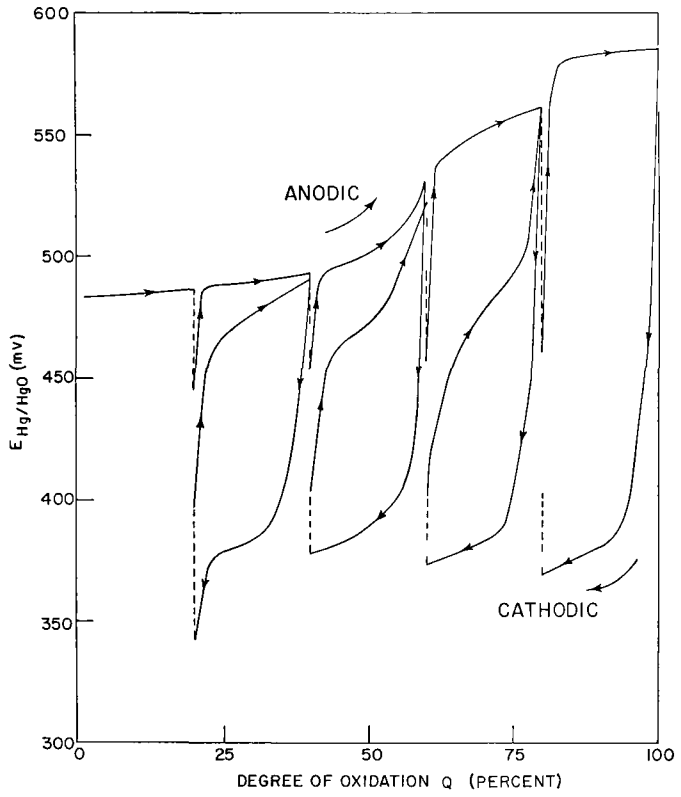

FIG 1 Anodic and cathodic polarization curves for the nickel oxide electrode in 1 *N* KOH, 2 hour charging rate Vertical broken lines correspond to open circuit e m f decay or recovery Solid lines correspond to changes of potential associated with changes of degree of charge between successive open-circuit measurements

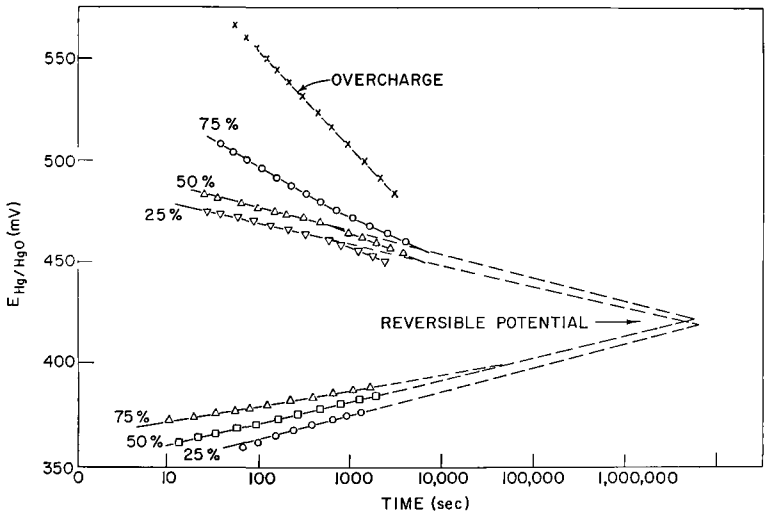

FIG 2 Decay and recovery of e m f of the nickel oxide electrode in log [time] at various degrees of charge after anodic and cathodic polarization, respectively (data for 1 *N* KOH) compare ref 1

All e m f decay lines from anodic polarization are seen to have two distinct regions For electrodes charged to 50% ("$NiO_{1.25}$") or less, an initial low slope (about -10 mv) is followed by a higher slope (about -20 mv) When the electrode is charged to 75%, a high initial slope (about -32 mv) is followed by the same slope (-20 mv) mentioned above, in the lower-potential region Electromotive force recovery lines from cathodic polarization have a slope of about $+11$ mv, independent of degree of charge Results for a typical individual experiment are given in Fig 2 and some slight increase of recovery slope is apparent as the charge is reduced, however, this trend does not appear to be very significant statistically (e g see Table I).

In Table I, the reversible potentials for the Ni^{II}–Ni^{III} system, obtained by extrapolating cathodic and (initial) anodic e m f decay lines (1), are given for different degrees of charge (between 20% and 50% formal degree of oxidation) of the electrode at 25° C, together with other kinetic parameters An important result obtained here is that the reversible potential is seen to be *independent* of formal degree of charge over the above range of charge Similar conclusions were arrived at from two comparative runs in 7 2 *N* KOH

For reasons to be discussed, it is not possible to obtain the true reversible potentials by extrapolation of cathodic and anodic e m f decay lines above degrees of oxidation of about 50% In order, however, to study further the potentials of the nickel oxide electrode, the "stationary" or quasi equilibrium potentials were examined at higher states of oxidation

In Table II, the 'stationary" potentials measured after 4×10^5 and 6×10^5 seconds on

TABLE II

Stationary potentials of the nickel oxide electrode in 1 *N* KOH 25° C

Degree of charge (%)	Potential reached after 4×10^5 sec (mv, Hg/HgO)	Potential reached after 6×10^5 sec (mv, Hg/HgO)
Overcharge	426 5	422 6
50	426 5	424 0
20	420 4	417 2
10	422 6	419 9
7	406 0	404 8
5	401 5	399 3

open circuit are given for various degrees of charge of the electrode between 5% and 100% (overcharged electrode) These results were obtained by reducing the electrode completely, polarizing it anodically to the appropriate degree of charge and then leaving it on open circuit for 6×10^5 seconds or longer It is seen that the "stationary potential measured after a long period of standing on open circuit is still independent of the degree of charge above 10% extent of oxidation ("$NiO_{1.05}$"), and in this respect exhibits a behavior similar to that of the true reversible potentials

Results of experiments on sparingly charged electrodes (0 33% to 5% degree of oxidation) are shown in Fig 3, where the e m f time relation is plotted for decay on open circuit after anodic charging for various degrees of charge It is seen that the decay process changes qualitatively once quite low degrees of charge are reached These results can, for the purpose of interpretation, be best represented graphically as plots of the degree of charge, Q, held by the electrode vs the time required for the electrode potential to decay to a given value (Fig 4) or in terms of the charge held vs the potential reached after a given time (Fig 5) These plots are equivalent to taking cuts at a given value

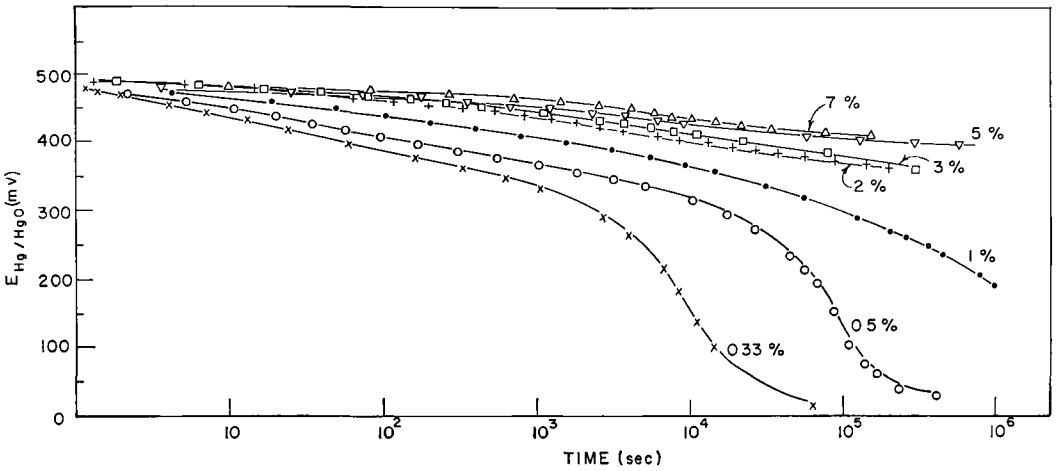

FIG 3 Plots of e m f decay at sparingly charged electrodes, for various degrees of charge

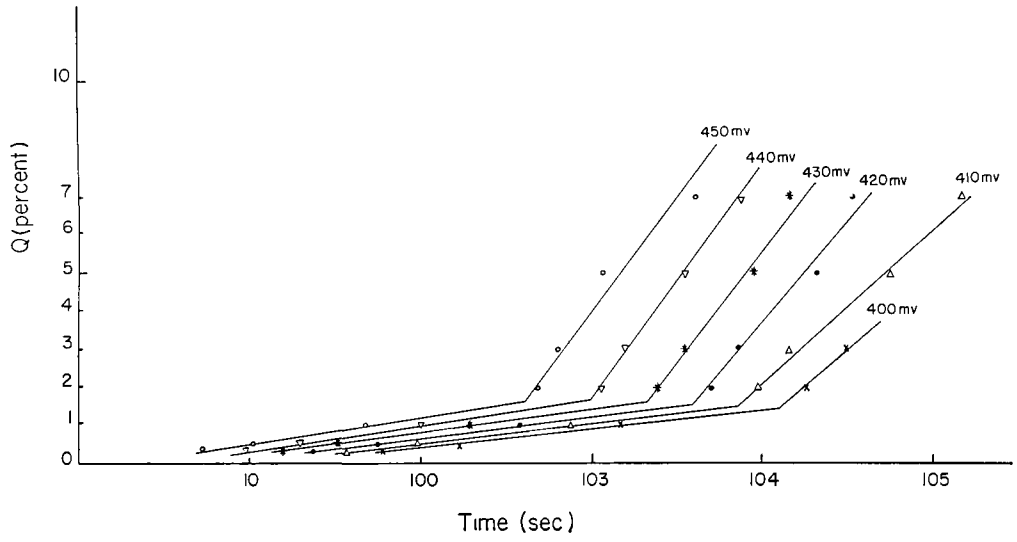

FIG 4 The length of time necessary for the electrode to reach a certain potential on open circuit vs the degree of charge of the electrode (Lines show inflection at common degree of charge $Q = 1\,6 \pm 0\,1\%$)

of the abscissa or ordinate in Fig 3

It is seen from both these derived plots that two linear regions are observed for each of the two families of lines, which intersect at a degree of charge of ca $1\,5 \pm 0\,1\%$ This observation leads to the important conclusion that electrodes charged to $1\,5\%$ or less are in a fundamentally different state than electrodes charged to a greater extent of oxidation This point is further demonstrated by examining the decay slopes listed in Table III below It was shown previously (1) that the initial low slope (ca -10 mv) is characteristic of the oxidation of the bulk nickel oxide In the present work, this slope was only observed for electrodes charged to 2% or more Below the latter extent of charge, no oxidation of the bulk material appears to occur, and the potential on open circuit drops much more rapidly

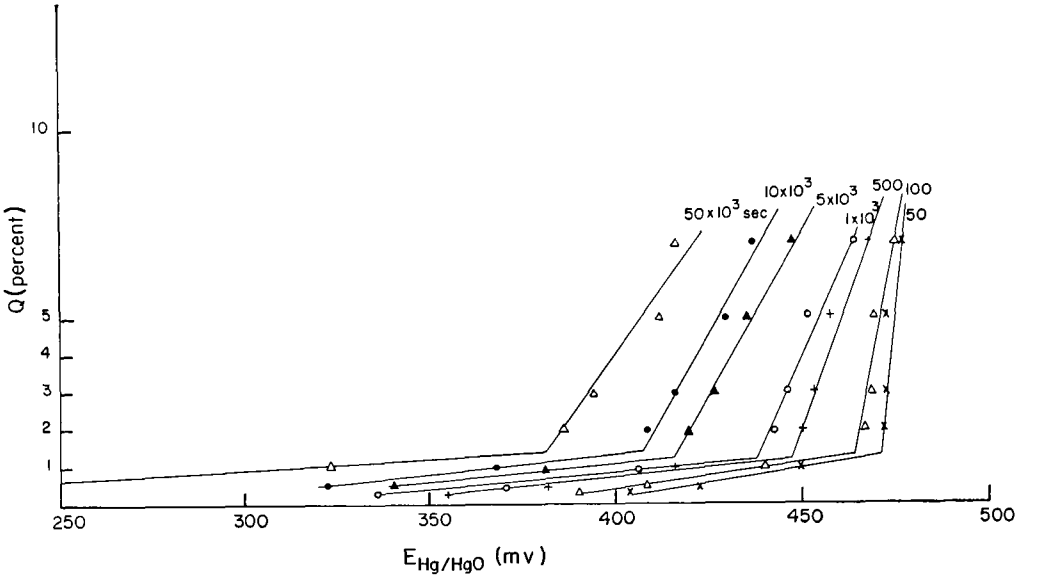

FIG 5 The potential reached after a given length of time on open circuit vs the degree of charge (Lines show inflection at common degree of charge $Q = 1.35 \pm 0.1\%$)

TABLE III

E m f and e m f -decay behavior at sparingly charged electrodes

Degree of charge (%)	Decay slopes (as in Table I)		E m f I (mv) at time of last measurement	Time of last measurement (10^5 sec) after interruption of polarization	$\Delta V/\Delta t$ for the last day (mv/day)
	b_1 (mv)	b (mv)			
7	—	—	404 8	6	0 2
5	−12 3	−23 2	398 3	7	0 8
3	−15 5	−34 1	366 5	2 8	5
2	−12 6	−34 2	356 1	6	2
1	−34 3	>100	188 6	9 5	8
½	−40	>100	41	4 1	1
¼	−48	>300	18	0 7	1

DISCUSSION

The reversible potential for the Ni^{II}–Ni^{III} system in the electrochemically formed nickel oxide has been shown to be independent of the degree of charge of the electrode Between 20% and 50% degree of charge, it was measured by extrapolating anodic and cathodic e m f decay lines, plotted logarithmically in time, as described earlier (1). Values of the reversible potential could only be obtained over a limited range of degrees of oxidation (20–50% of total charge) since at a higher degree of charge the initial low anodic slope, characteristic of the oxidation of the bulk material (1), was not observed (see Fig 2), and at a very low degree of charge, cathodic e m f recovery lines were irregular and difficult to reproduce

It is of interest to discuss why the reversible potential cannot be obtained by extrapolation of anodic and cathodic polarization decay lines above a degree of charge of about 50% In Fig 2 it is evident that the e m f. decay line, e g for 75% degree of charge, shows two linear regions in "concave" relationship to one another as also found for the

"overcharged" electrode (3), whereas (1) at lower degrees of charge, a "convex" relation is observed between two linear regions We have previously shown (1, 3) how such relations arise, respectively, from two processes in an overall mechanism which are consecutive, so that one or the other becomes rate determining, depending on the potential range, or the two processes are parallel and the faster determines the kinetics Above 50% degree of charge (for example, with the 75% charged electrode), it is clear that the former type of process is operative, as it is in oxygen evolution at overcharged nickel oxide electrodes (3), moreover, the Tafel slopes are similar to those obtained for the oxygen evolution process at the overcharged electrode We cannot hence identify the initial process as involving the Ni^{II}–Ni^{III} oxidation reaction as we have done for the 50% charged electrode (1) and so cannot obtain the true reversible potential by the extrapolation procedure under these conditions We can have, in effect, two pathways for the anodic reaction which could be written, for example, as

$$M + OH^- \rightarrow MOH + e \quad (I)$$

$$MOH + OH^- \rightarrow MO + H_2O + e \quad (II)$$

(A) oxide oxidation in bulk of material

(B) O_2 evolution by further steps (cf refs 1 3 15)

e g

$$MO + MOH \rightarrow MHO_2 \quad (III)$$

$$MHO_2 + MOH \rightarrow O_2 + H_2O + M \quad (IV)$$

or

$$MO + OH^- \rightarrow MHO_2 + e \quad (V)$$

$$MHO_2 + MOH \rightarrow O_2 + H_2O + M \quad (IV)$$

or

$$2MO \rightarrow O_2 \quad (VI)$$

At the higher degrees of charge ($> \simeq 50\%$), the pathway is evidently one involving *consecutive* rate-determining steps and is therefore probably associated with the scheme (I), (II) with pathway (B) to oxygen evolution with, for example, (II) or (VI) (cf ref 16) rate determining

At low degrees of charge 50% or less, the course of the e m f decay corresponds to alternative reactions, one or the other of which becomes predominant as the potential changes, as we have discussed previously (1) The pathway is thus probably (I), (II), and (A) at short times after decay (higher anodic potentials) and (I), (II), and (B) to oxygen evolution at longer times when the pathway which is faster at lower anodic potentials dominates the kinetics of the decay process

The above discussion is intended only as a qualitative, plausible explanation of the effects associated with the e m f decay behavior, as a function of charge and we have discussed in detail elsewhere (1, 3, 16) the evidence for assignment of some of the mechanisms involved in the oxygen evolution process in the scheme shown above

In order to supplement the above data on true reversible potentials, steady or quasi-equilibrium potentials were measured over a wider range of degrees of oxidation (5–100%) The significance of these potentials as kinetically determined mixed potentials

has been discussed previously (1) They cannot be related directly to the reversible potential of the system at different degrees of charge, since the exchange current for the nickel II → III oxidation process may strictly depend on the degree of charge Nevertheless, the constancy of these potentials over a large range of formal degree of oxidation of the electrode ("$NiO_{1.05}$" to "$NiO_{1.50}$"), combined with the fact that the true reversible potential has been shown above to be independent of degree of charge in the range where it is directly accessible, makes it most probable that the reversible potential is, in fact, constant over the whole range of degrees of oxidation where the steady potential is found to be constant This is contrary to conclusions reported by Lukovtsev and Temerin (9) (using electrodes with a graphite matrix), who claimed that the apparent reversible potential of this system follows a Nernst-type equation with a slope of 0.050 v The observed variation of actual potential during charging and discharging, on which the latter conclusion was based, may be due to a concentration polarization in the solid phase (6, 9), or a change in effective current density due to a change in available surface area, and not due to a variation of the true reversible potential of the system, as claimed by Lukovtsev and Temerin

Our present findings are not in conflict with the equation

$$E = a + b_2' \log \left(\frac{q_{ox} - q_{red}}{q_{red}} \right),$$

discussed by Lukovtsev and Temerin and examined and evaluated by Conway and Bourgault (4), since that equation refers to the variation of electrode potential with degree of oxidation of the *surface* phase in the overcharge region, and in fact the potential of the electrode was shown (1) to involve a term corresponding to uptake of adsorbed KOH

For electrodes charged to less than 10%, the open circuit steady potential was found to depend on the degree of charge to a large extent Electrodes charged to 1% or less behaved quite differently from those charged to a greater extent The results suggest that up to a degree of charge $Q = 1.5 \pm 0.1\%$ (i.e., the average value of Q at the points of intersection of the lines in Figs. 4 and 5) only a surface phase is being charged Above that, and up to a degree of oxidation of about 10%, both surface and bulk phases are being charged When the electrode has been charged to 10% of its total charge capacity, it appears that the surface phase is completely charged, and any further charging can then only affect the bulk material

The variation of the observed true reversible, and stationary or quasi-equilibrium potentials as a function of charge in 1 *M* KOH is shown in Fig. 6 The electrochemical behavior of the electrode is evidently determined by the *surface* phase, since the reversible (or steady) potential is independent of the degree of charge so long as the surface phase is apparently completely charged, i.e., above 10% formal degree of oxidation The theoretical Nernst plot for a one-electron transfer process (in terms of formal degrees of charge) which would be observed for ideal solid-solution behavior, with the bulk material potential determining, is shown in Fig. 6 for comparison

The independence of reversible (or steady) potential demonstrated, above a degree of oxidation of 10%, could formally arise for either of the following reasons (*a*) If the electrode were a two-phase mixture of lower and higher oxide, the potential would be independent of apparent degree of oxidation so long as both oxides were present (*b*) If the potential were determined by a surface phase of constant composition, superimposed on a bulk phase of varying degree of oxidation but not potential determining, the observed potential would be independent of composition of the bulk

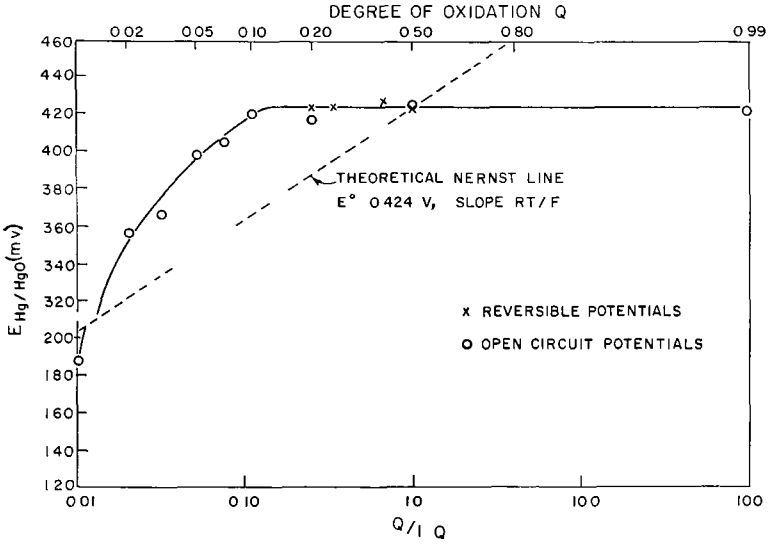

FIG 6 True reversible potentials and quasi equilibrium 'stationary potentials of the nickel oxide as a function of degree of oxidation One electron theoretical Nernst slope is shown for comparison

The latter situation, (*b*), is consistent with our previous kinetic conclusions (1) on the mechanism of charging of the bulk material via a surface phase, and our observation of a large adsorption pseudocapacitance associated with the (overcharged) nickel oxide electrode The former possibility, (*a*), is rendered unlikely by the X-ray diffraction pattern of nickel oxide at various degrees of charge (10, 11) where it was shown that there was a continuous variation of the pattern consistent with a complete range of solid solutions of Ni II and III oxide states The observed variation of potential between 2% and 10% degree of oxidation confirms the view that a two-phase mixture cannot be present and potential determining, since such a mixture should give a constant potential except at a state of complete oxidation or complete reduction We must hence conclude that the surface phase is potential determining, and that above a degree of oxidation of 10% of the whole material in the oxide electrode, a more or less constant potential is reached

We may conclude by summarizing the reasons why previous assignments of reversible potentials (2, 12, 13) are of limited validity

(*a*) In most cases, kinetically determined mixed potentials were involved which differ from the true reversible values by 0–30 mv depending on concentration of KOH

(*b*) The species (14), e g "NiO_2", to which the potentials were assumed to refer have not been identified or characterized and their existence is doubtful (such species may correspond only to the surface phase at the overcharged electrode)

(*c*) The phase to which the potentials refer is evidently not the bulk phase oxide but the electrochemically active surface phase

(*d*) Potentials attained during charging or discharging of the electrode differ substantially and neither can be identified with a thermodynamically significant reversible potential

ACKNOWLEDGMENTS

We are indebted to the Defence Research Board, Department of National Defence, for support of this work on Grant No 5480-12 One of us, E G , is indebted to the National Research Council for the award of a scholarship for the year 1962–63

REFERENCES

1 P L Bourgault and B E Conway Can J Chem **38**, 1557 (1960)
2 F Kornfeil Proceedings of the 127th U S Army Battery Research and Development Conference 1958
3 B E Conway and P L Bourgault Can J Chem **37**, 292 (1959)
4 B E Conway and P L Bourgault Trans Faraday Soc **58**, 593 (1962)
5 E J Casey, P L Bourgault, and P E Lake Can J Technol **34**, 95 (1956)
6 B V Ershler and E M Kuchinskii Zhur Fiz Khim **20** 539 (1946)
7 G Armstrong and J A V Butler Trans Faraday Soc **29**, 1261 (1933)
8 H B Morley and F E W Wetmore Can J Chem **34** 359 (1956)
9 P D Lukovtsev and V I Temkin Akad Nauk S S S R, Otdel Khim Nauk, 494 (1953)
10 O Glemser and J Einerhand Z anorg Chem **261**, 26 (1950), Z Elektrochem **54**, 302 (1950) G W D Briggs and W F K Wynne Jones Trans Faraday Soc **52**, 1272 (1956)
11 W Feitknecht, H R Christen, and H Studer Z anorg u allgem Chem **283**, 88 (1956)
12 F Folkerts Z Elektrochem **13**, 414 (1907) **14** 17, 285 (1908)
13 J Zednik Z Elektrochem **11**, 809 (1905) **12**, 463 (1906), **13**, 752 (1907).
14 W M Latimer Oxidation potentials 2nd ed Prentice Hall 1952
15 J O M Bockris J Chem Phys **24** 817 (1956)
16 B E Conway and P L Bourgault Can J Chem **40**, 1690 (1962)

The Theory of Current Distribution and Potential Profile at an Electrode of Significant Ohmic Resistance

B.E. Conway[1], E. Gileadi and H.C. Oswin[2]

[1]Department of Chemistry, University of Ottawa

and

[2] Leesona Moos Laboratories, Jamaica, New York.

ABSTRACT = The problem of current distribution at an electrode of linear geometry having a significant ohmic resistance is examined for conditions where the ohmic potential drop along the electrode material is of the same order of magnitude as the metal-solution potential difference. This problem is of practical significance in primary and secondary cells at high current drains and in certain types of fuel cell electrodes. The current distribution and metal-solution potential profiles are calculated as limiting cases of a general theory. The true and apparent current-potential relations are compared theoretically.

Manuscript received:

I. INTRODUCTION

In recent years, current distribution problems in electrolysis processes have become of renewed importance in certain applications involving high current drains in batteries, palladium hydrogen diffusion anodes operating at elevated temperatures and in anodic electrolytic machining. General problems of current density distribution were recognised in early work on electro-plating and throwing-power (1,2) and renewed interest in this and related kinds of problems has recently been apparent (3,4). In the above work, the inhomogeneous current density distribution is treated largely in terms of the finite resistance of the electrolyte. The corresponding problem, in which the electrode resistance is significant at high current drains, has not previously been examined, except in the case of thin film light modulators (5) where film resistance and solution conductance effects have been simultaneously considered as a special problem. Co-conduction effects longitudinally through the solution (6) and through the double-layer (7) parallel to a thin wire electrode have been considered for cases where the electrode resistance was not negligible compared with the electrolyte solution resistance. Such studies can lead to information about adsorption in the double-layer (7) and the electrode potential distribution in the case of a wire in a solution with contacts at each end to an external electric circuit (6).

In the present work, we examine the general theory of current-density and overpotential distribution for a thin wire or tubular electrode having significant ohmic resistance and immersed in an electrolyte with contact to the external circuit at one end; relations are also obtained for the true and apparent Tafel slope for an electrode process occurring at the wire under such conditions.

II. CALCULATION OF POTENTIAL AND CURRENT PROFILES

1. Model

We consider the model for a cylindrical electrode of length L radius r and specific resistance ρ, shown in Fig. 1. The electrode may be a thin wire or a thin tube, as in the case of palladium hydrogen diffusion anodes where significant electrode resistance can arise. An element of current di_x is regarded as passing across one element of area $2\pi r dx$ at a position x below the top of the electrode (taken as the level of immersion of the electrode in the electrolyte). The total current passing into, or out of, the electrode is written as I and the overvoltage which would determine the rate of the electrode reaction if ρ were negligible is expressed as V_o. The normal current density i passing in the absence of ohmic effects is related to the exchange current density by the Tafel equation in exponential form as

$$i = i_o \exp [\alpha V_o F/RT] = i_o \exp [V_o/b]$$

CAPTION TO FIGURE

Fig. 1. Schematic diagram of the model considered in the current distribution problem at a cylindrical electrode, showing some of the quantities involved in the treatment.

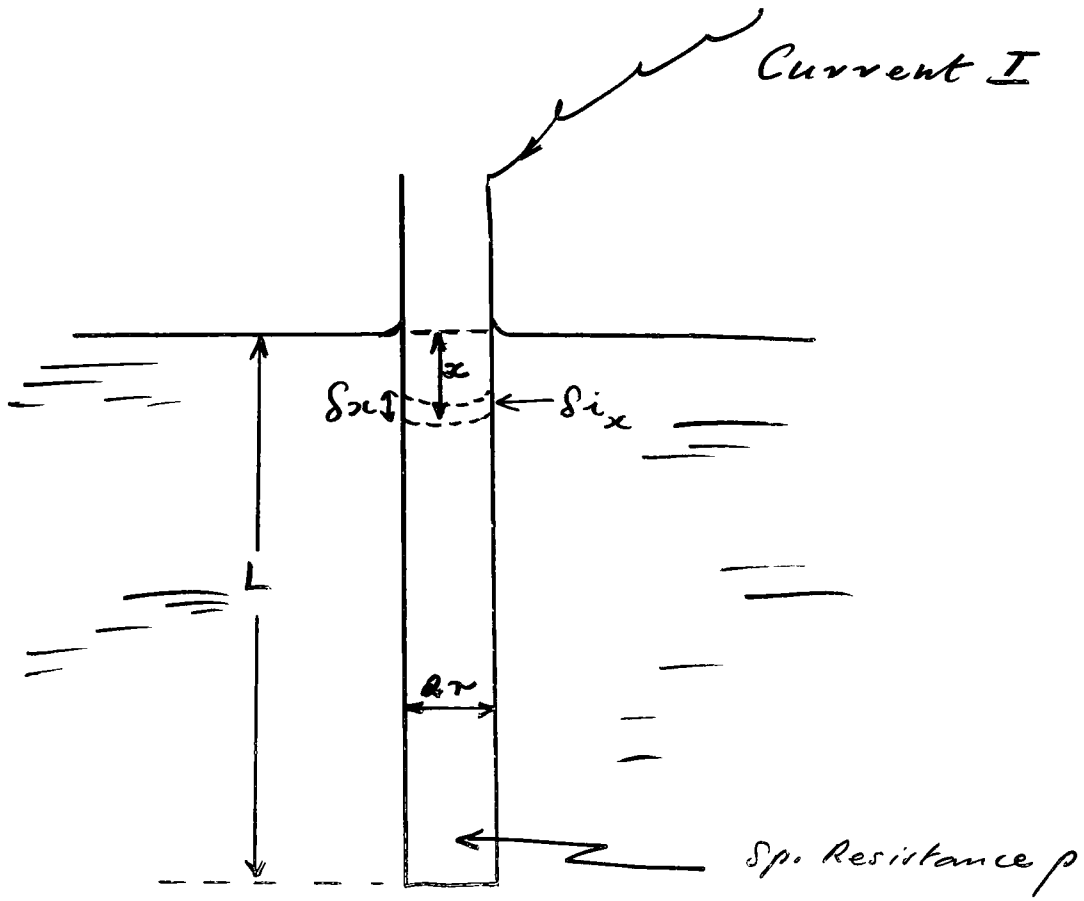

FIGURE 1

We assume the current density passing at any point x along the electrode is determined by the overvoltage V_o (arising from an impressed voltage, or from a galvanic potential difference in the case of a battery or fuel cell) less the ohmic drop ΔV_x existing at the position x down the electrode from the top. This potential drop will be determined by the current passing in the cylinder from the top to x and by the specific resistance of the electrode. The current passing will not be uniform and will decrease down the electrode. At any given point, the current density will be exponentially related to the overpotential and hence the metal-solution p.d. existing at that point, i.e. to $V_o - \Delta V_x$.

2 Formulation of equations

At x, the element of actual anodic* current passing across an area ds equal to $2\pi r.dx$ is

$$di_x = i_o \exp.[\alpha(V_o - \Delta V_x)F/RT].2\pi r.dx \qquad [1]$$

where i_o is the usual exchange current density for the electrode process concerned and α the transfer coefficient characteristic of the rate-determining process.

The potential drop ΔV_x in the conductor is a function of length but is not simply linearly related to it since the

* For convenience, we write the kinetic expression for an anodic reaction involving a one-electron transfer as in the H-ionisation case.

current in the conductor is not uniform but decreases down the cylinder. The quantity ΔV_x will hence increase with x but as some function x^n where $0 < n < 1$.

In the element of the electrode surface of area $2\pi r.dx$, at the position x, the potential drop dV down the element is given by

$$dV = i_x \rho \, dx/\pi r^2$$

where i_x is the total current in the conductor crossing a plane perpendicular to the electrode axis at a position x along the electrode determined by the sum of all current elements entering the electrode from x = L to the representative position x = x.

The total potential drop ΔV_x from the top of the electrode to x is then

$$\Delta V_x = \int_o^x dV = \frac{\rho}{\pi r^2} \int_o^x i_x.dx \qquad [2]^*$$

But i_x is already the integral of di_x over the length x = L to a position x which involves ΔV_x from equation [1], i.e.,

$$i_x = i_o \exp. \left[\frac{\alpha V_o F}{RT}\right].2\pi r \int_x^L \exp. - \left[\frac{\alpha \Delta V_x F}{RT}\right].dx \qquad [3]$$

---

* In this and other related equations, the term $\rho/\pi r^2$ will become $\rho/\pi(r^2-[r-a]^2)$ for the case of a tubular electrode of radius r and annular thickness a.

and ΔV_x in equation [3] is given by the integral equation [2] which itself involves i_x. The mathematical problem is thus a particularly complex one and an explicit solution is not obtainable without some simplification.

3. Linear Approximation

Equation [3] can be linearised under two conditions:

a) if the current densities along the electrode do not exceed approximately 3 i_o (the condition for linear current - potential behaviour in the basic rate expression), or

b) if $\Delta V_x < RT/\alpha F$; this latter condition only obtains at moderately low c.d. or fairly low ohmic resistance of the conductor such as is the case in most practical problems.

In either case, we could write approximately for the forward (anodic) current e.g. in H ionisation

$$i_x = i_o \exp\left[\frac{\alpha V_o F}{RT}\right] 2\pi r \int_x^L \left[1 - \frac{\alpha \Delta V_x F}{RT}\right] dx \qquad [4]$$

and the equation then becomes with [2] and $i = i_o \exp\left[\frac{\alpha V_o F}{RT}\right]$

$$i_x = 2\pi r i \int_x^L dx - 2\pi r i \int_x^L \frac{\alpha \Delta V_x F}{RT} dx \qquad [5]$$

which can be written

$$i_x = K_1 - K_2 x - K_3 \int_x^L \left[\int_o^x i_x dx\right] dx \qquad [6]$$

where K_1, K_2 and K_3 are constants, the significance of which follows by reference to equation [5]. We may write equation [6]

conveniently in differential form as

$$di_x/dx = - K_2 - K_3 \int_o^x i_x dx \qquad [7]$$

and

$$d^2i_x/dx^2 = - K_3 i_x = - \frac{2\rho i \alpha F}{rRT} i_x \qquad [8]$$

4. Evaluation of ΔV_x as a function of x and determination of the profile of i_x as a function of x.

The final second-order differential equation [8] is of the form:

$$d^2Y/dX^2 = - kY$$

and its solution is

$$Y = A \cos \sqrt{k}.X$$

so that

$$i_x = A \cos \left[\frac{2i\rho \alpha F}{rRT} \right]^{1/2} x \qquad [9]$$

where A is a constant.

When x = 0, at the top of the electrode, $i_x = I$, the total measured current corresponding to the overpotential V_o. Therefore

$$A = i_{x=o} = I$$

so that

$$i_x = I \cos \left[\frac{2i\rho\alpha F}{rRT}\right]^{1/2} x. \qquad [10]$$

from which the current density distribution can be obtained as a function of x as

$$\frac{1}{2\pi r}\frac{di_x}{dx} = \frac{di_x}{ds} = -I\left[\frac{2i\rho\alpha F}{rRT}\right]^{1/2} \cdot \sin\left[\frac{2i\rho\alpha F}{rRT}\right]^{1/2} x \qquad [11]$$

The evaluation of ΔV_x as f(x) then proceeds as follows: from [1], substituting for i_x (linear approximation)

$$\Delta V_x = \frac{I\rho}{\pi r^2}\int_0^x \cos\left[\frac{2i\rho\alpha F}{rRT}\right]^{1/2} x\,dx$$

$$= \left[\frac{\rho I^2 RT}{2\pi^2 r^3 i\alpha F}\right]^{1/2} \cdot \sin\left[\frac{2i\rho\alpha F}{rRT}\right]^{1/2} x \qquad [12]$$

In considering these distributions of i_x and ΔV_x, it must be recalled that i_x is the total current passing in the conductor from the bottom up to a position x, i.e. where the potential drop is ΔV_x measured from the top of the electrode. Hence, as ΔV_x increases down the electrode, the current density decreases, as expected and indicated by the negative sign in equation [11] compared with the positive one in equation [12]

III. CALCULATION OF THE APPARENT CURRENT-POTENTIAL RELATION

1) Conditions and Model

We now consider the relation between the apparent and real current-potential behaviour at an electrode of length L and specific resistance ρ, as defined in section II. The model is the same as that considered above but the electrode is regarded as divided into a large number n of segments Δx in length ($n\Delta x = L$) and Δi_j is taken as

the actual current passing from a representative j'th segment into the solution.

2) Formulation of Equations

For convenience in the mathematical development, we treat the problem now in terms of summations. From the definitions above, we may write

$$\sum_{j=1}^{n} \Delta i_j = I \qquad [13]$$

If the ohmic resistance of the electrode is not negligible, conditions will be as in the previous calculation (section II) and the current density will decrease down the electrode. Let it be assumed that each segment is small enough for the ohmic p.d. within it to be, to a first approximation, negligible and that the potential operative at the j'th segment depends on the potential V_o applied to the electrode less the ohmic potential drop down the j-1 preceding segments, as in the previous calculation. At the middle of the first segment the current passing is taken as

$$\Delta i_1 = i_o 2\pi r \Delta x \exp [V_o/b] \qquad [14]$$

At the corresponding position in the second segment, the potential operative in determining the current will be less than V_o by the ohmic potential drop in segment one, i.e.

$$\Delta i_1 = i_o 2\pi r \Delta x \exp \frac{1}{b} [V_o - \frac{\rho}{\pi r^2} \Delta x \, (I - \Delta i_1)]$$

$$= i_o 2\pi r \Delta x \exp \frac{V_o}{b} [1 - \frac{\rho}{\pi r^2} \frac{\Delta x}{V_o} (I - \Delta i_1)] \qquad [15]$$

Similarly

$$\Delta i_3 = i_o 2\pi r \Delta x \exp \frac{1}{b} \left[V_o - \frac{\rho}{\pi r^2} \Delta x \, (I - \Delta i_1) - \frac{\rho}{\pi r^2} \Delta x (I - \Delta i_1 - \Delta i_2) \right]$$

$$= i_o 2\pi r \Delta x \exp \frac{V_o}{b} \left[1 - \frac{\rho}{\pi r^2} \frac{\Delta x}{V_o} (2I - 2\Delta i_1 - \Delta i_2) \right] \qquad [16]$$

and

$$\Delta i_4 = i_o 2\pi r \Delta x \exp \frac{1}{b} \left[V_o - \frac{\rho}{\pi r^2} \Delta x (2I - 2\Delta i_1 - \Delta i_2) - \frac{\rho}{\pi r^2} \Delta x \, (I - \Delta i_1 - \Delta i_2 - \Delta i_3) \right]$$

$$= i_o 2\pi r \Delta x \exp \frac{V_o}{b} \left[1 - \frac{\rho}{\pi r^2} \frac{\Delta x}{V_o} (3I - 3\Delta i_1 - 2\Delta i_2 - \Delta i_3) \right] \qquad [17]$$

and, in general, for the current at the j'th element

$$\Delta i_j = i_o 2\pi r \Delta x \exp \frac{1}{b} \left[V_o - \frac{\rho}{\pi r^2} \Delta x \left\{ (j-1)I - (j-1)\Delta i_1 - (j-2)\Delta i_2 - (j-3)\Delta i_3 - (j-k)\Delta i_k \right\} \right]$$

$$= i_o 2\pi r \Delta x \exp \frac{V_o}{b} \exp - \left[\frac{\rho}{\pi r^2} \frac{\Delta x}{b} (j-1)I \right] . \exp \frac{\rho}{\pi r^2} \frac{\Delta x}{b} \left[\sum_{k=1}^{j-1} (j-k)\Delta i_k \right]$$

..... [18]

From [13], the total current is

$$I = \sum_{j=1}^{n} \Delta i_j$$

The latter summation cannot be evaluated analytically since it is a sum of exponentials having different arguments. However, if the variation of current density along the electrode is not too large, the procedures given below can be adopted as an approximation (and this corresponds to the linearisation approximation made in section II).

Here, let it be assumed that the arithmetic mean of the current over the n elements can be approximated by the geometric mean. That is

$$\frac{1}{n}\sum_{j=1}^{n}\Delta i_j = (\prod_{j}^{}\Delta i_j)^{1/n} \qquad [19]$$

and hence

$$I = n(\prod_{j}^{}\Delta i_j)^{1/n} \qquad [20]$$

Taking logarithms of the terms in equation [18] for Δi_j gives

$$\ln\Delta i_j = \ln(i_o 2\pi r\Delta x) + \frac{V_o}{b} + \frac{1}{b}\left[- \frac{\rho}{\pi r^2}\Delta x(j-1)I + \frac{\rho}{\pi r^2}\Delta x\sum_{k=1}^{j-1}(j-k)\Delta i_k\right] \qquad [21]$$

then since

$$\ln[\prod_{j}^{}\Delta i_j] = \sum_{j=1}^{n}\ln[\Delta i_j] \qquad [22]$$

we obtain

$$\sum_{1}^{n} \ln\Delta i_j = n\ln(i_o 2\pi r\Delta x) + \frac{nV_o}{b} - \frac{1}{b}\frac{\rho}{\pi r^2}\Delta x I \sum_{j=1}^{n}(j-1)$$

$$+ \frac{\rho}{\pi r^2}\frac{\Delta x}{b}\sum_{j=1}^{n}\sum_{k=1}^{j-1}(j-k)\Delta i_k \qquad [23]$$

or

$$\frac{1}{n}\sum_{j=1}^{n}\ln\Delta i_j = \ln(i_o 2\pi r\Delta x) + \frac{V_o}{b} - \frac{1}{nb}\frac{\rho}{\pi r^2}\Delta x I \frac{n(n-1)}{2}$$

$$+ \frac{\rho}{\pi r^2}\frac{\Delta x}{nb}\sum_{j=1}^{n}\sum_{k=1}^{j-1}(j-k)\Delta i_k \qquad [24]$$

Now

$$\ln(\frac{I}{n}) = \ln[\prod^{j}\Delta i_j]^{1/n} = \frac{1}{n}\sum_{j=1}^{n}\ln[\Delta i_j]$$

so that

$$\ln(I/n) = \text{r.h.s. of [24]}$$

or

$$\frac{I}{n} = i_o 2\pi r\Delta x \exp[\frac{V_o}{b}] \exp[-\frac{\rho I\Delta x}{\pi r^2 b}\frac{(n-1)}{2}] \exp[\frac{\rho\Delta x}{\pi r^2 nb}\sum_{j=1}^{n}\sum_{k=1}^{j-1}(j-k)\Delta i_k$$

..... [25]

If we make the simplification that n-1 = n since n can be made arbitrarily large, and with $n\Delta x = L$, we have

$$I = i_o 2\pi rL \exp[\frac{V_o}{b}] . \exp[\frac{\rho L}{\pi r^2} \cdot \frac{I}{2b}] \exp\left[\frac{\rho L}{\pi r^2} \cdot \frac{1}{n^2 b} \sum_{j=1}^{n} \sum_{k=1}^{j-1} (j-k)\Delta i_k\right] \quad [26]$$

Since the resistance of the whole electrode is given by $R = \rho L/\pi r^2$ and its total surface area is $S = 2\pi rL$, we can rewrite equation [26] as

$$I = i_o S \exp(V_o/b) \exp(-RI/2b) \exp\left[\frac{R}{n^2 b} \sum_{j=1}^{n} \sum_{k=1}^{j-1} (j-k)\Delta i_k\right] \quad [26a]$$

We shall now examine the physical significance of the various terms in equation [26a]. The equation

$$I/S = i_o \exp [V/b] \quad [27]$$

is obviously the value of I/S when $\rho = 0$, i.e. when no finite resistance of the electrode is considered. The term $i_o \exp [V_o/b]$ is the theoretically significant quantity since its value and, in particular, its variation with V_o are characteristic of the kinetics of the electrochemical reaction occurring at the electrode. In fact, it is the purpose of these calculations to relate this "ideal" current density to the mean overall value which would be experimentally measured, viz. I/S.

The second term in equation [26a], $\exp[-RI/2b]$, is effectively a correction factor which takes into account a linear

potential drop along the electrode due to its ohmic resistance; the last term on the r.h.s. of equation [26a] is a second order correction factor which takes into account the departure from linearity of this potential drop arising from the exponential variation of reaction resistance with electrode potential. The double sum in the last term can be represented in tabular form as shown below:

Terms in the double sum in Equation [26]

k	j	1	2	3	4	5 ------- j
1		0	Δi_1	$2\Delta i_1$	$3\Delta i_1$	$4\Delta i_1$.....$(j-1)\Delta i_1$
2		0	0	Δi_2	$2\Delta i_2$	$3\Delta i_2$.....$(j-2)\Delta i_2$
3		0	0	0	Δi_3	$2\Delta i_3$.....$(j-3)\Delta i_3$
4		0	0	0	0	Δi_4.....$(j-4)\Delta i_4$
5		0	0	0	0	0 .....$(j-5)\Delta i_5$
⋮						
k		0	0	0	0	0 .....$(j-k)\Delta i_k$

Since the term involving the summation in equation [26a] constitutes a second order correction, we may make the approximation

$$\Delta i_k = \Delta i_{k+1} = I/n \qquad [28]$$

so that the last term in equation [26a] becomes

$$\exp \frac{R}{b} \cdot \frac{1}{n^2} \sum_{j=1}^{n} \sum_{k=1}^{j-1} (j-k)\Delta i_k = \exp \frac{RI}{b} \cdot \frac{1}{n^3} \sum_{j=1}^{n} \sum_{k=1}^{j-1} (j-k)$$

It can be shown that

$$\lim_{n \to \infty} \left[\frac{1}{n^3} \sum_{j=1}^{n} \sum_{k=1}^{j-1} (j-k) \right] = 1/6 \qquad [29]$$

so that, combining equations [26a] and [29],

$$I/S = i \exp[-\frac{RI}{2b}] \exp[\frac{RI}{6b}] = i \exp [-\frac{RI}{3b}] \qquad [30]$$

or

$$i = (I/S)\exp[RI/3b] \qquad [31]$$

Equation [31] has been derived for convenience for an anodic process; it is obviously applicable generally for any electrode process since $I/b > 0$ in all cases.

Apparent Tafel Slope

The observed Tafel slope dV/dlnI will be related to the mechanistically significant Tafel slope dV/dlni through the equation

$$dV/d\ln i = (dV/d\ln I)(d\ln I/d\ln i) \qquad [32]$$

From equation [31]

$$(d\ln i/d\ln I) = 1 + \frac{R^{\prime}}{3b} \qquad [33]$$

Hence

$$dV/d\ln i = dV/d\ln I\ (1 + R^{\prime}/3b)^{-1} \qquad [34]$$

We note, therefore, that a finite electrode resistance will cause a decrease in the overall current density from that predicted by the corresponding Tafel equation; also the observed apparent Tafel slope will be larger than the real one (b, in equation 34) and will tend to increase with current density.

Since equation [34] was derived assuming that RI, although not negligible, was relatively small, the true Tafel slope can be obtained from a measured value of dV/dlnI and the known specific resistance of the electrode at a given total current I. The result can be further improved, if required, by a series of successive approximations. It is of interest to note also that the current-potential behaviour at electrodes at which a given reaction is proceeding with a high value of b will be relatively less affected by electrode resistance effects that that for reactions associated with low Tafel slopes.

The above calculations have been made in order that, at electrodes of significant resistance where internal ohmic potential drops are not negligible at high current densities,

the true, mechanistically significant, Tafel slopes can nevertheless be evaluated from the observed current-potential relation for high load conditions, and the current-density distribution can also be calculated.

References

1. Haring, H.E. and Blum, W. Trans. Amer. Electrochem. Soc., 44, 313 (1923).
2. Hoar, T.P. and Agar, J.N., Discussions Faraday Soc., 1, 162 (1947).
3. Tobias, C.W., Papers presented at the Electrochemical Society Meeting, Boston 1962 and at the C.I.T.C.E. meeting, Rome, 1962.
4. Wagner, C., J. Electrochem. Soc., 107, 445 (1960).
5. Zaromb, S., J. Electrochem. Soc., 109, 912 (1962).
6. Harvey, W.W., J. Electrochem. Soc., 109, 638 (1962).
7. Schmid, G.M. and Hackerman, N., J. Electrochem. Soc., 107, 647 (1960); 107, 142 (1960).

THE BEHAVIOUR OF ADSORBED INTERMEDIATES IN ELECTRODE REACTIONS

by

Eliezer Gileadi

A thesis submitted in partial fulfillment
of the requirements for the
degree of Doctor of Philosophy in
the Department of Chemistry, University of Ottawa, Canada.

December 1962.

E Gileadi

Eliezer Gileadi
Candidate

B.E. Conway
Professor of Chemistry
Research Supervisor.

PREFACE

In the development of the subject of the kinetics of electrode processes, studies of the double-layer and the adsorption of reactants, together with characterisation and interpretation of the current-potential relationships, have played a predominant role. Although such work has been supported by numerous theoretical approaches for many electrochemical processes, the principal contributions have been directed to applications to the hydrogen and oxygen evolution reactions.

The related problem of the behaviour of the chemisorbed intermediates in such gas-producing reactions has, on the whole, been studied in less detail. Thus, the basic theoretical problems have not hitherto been developed fully, although the importance of such studies was recognised early by Butler (1934), the Russian workers and others, and important experimental work has been contributed, e.g. on the behaviour of chemisorbed hydrogen and oxygen at electrodes, by workers of the German school, in particular Breiter, Knorr, and Vetter.

Previous experimental work in this Department on the electrochemistry of the nickel oxide electrode and on anodic decarboxylation, had demonstrated the need for further development of theoretical approaches for interpretation of

the kinetic and adsorption pseudocapacity behaviour which had been observed.

In the work described in the present thesis, particular attention has accordingly been focussed on three aspects of the behaviour of adsorbed reaction intermediates:

(a) the pseudocapacity associated with the potential dependence of coverage by intermediates;

(b) the isotherm for adsorption of such intermediates and

(c) the corresponding kinetics of reactions in which chemisorbed intermediates arise at intermediate values of the steady-state coverage θ, (i.e. for $0.2 < \theta < 0.8$).

Most of the original work described in this thesis is theoretical in nature, but supporting experimental studies have been made with the nickel oxide electrode and other applications have been made to the behaviour of the intermediates involved in the anodic electrochemical decarboxylation of formate ions in pure anhydrous formic acid.

The principal original contributions involve the deduction of the dependence of adsorption pseudocapacity on potential and coverage for Temkin isotherms involving different values of a parameter r determining the variation of the free energy of adsorption of intermediates with coverage. The consequences of using other isotherms involving electrostatic

interaction energy terms, which are non-linear in θ, have also been examined.

The degree to which the primary ion discharge step is not in "equilibrium", when a subsequent step is "rate-determining", is shown to be a factor of great importance when the pseudocapacity behaviour is deduced, particularly when the Temkin isotherm applies at intermediate coverage and the parameter r is appreciable. A more detailed summary of the original contributions is given in the section on "Claims to Original Research".

Most of the work described in this thesis has been either published or is in press, as indicated in the following list of papers:

1) Kinetic Theory of Pseudocapacitance and Electrode Reactions at Appreciable Surface Coverages, B.E. Conway and E. Gileadi, Trans. Faraday Soc., 58, 2493 (1962).

2) Electrochemistry of the Nickel Oxide Electrode. Part IV. Electrochemical Kinetic Studies of Reversible Potentials as a Function of Degree of Oxidation, B.E. Conway and E. Gileadi, Can. J. Chem., 40, 1933 (1962).

3) Calculation and Analysis of Adsorption Pseudo-capacity and Surface Coverage from E.M.F. Decay and Polarization Curves: Application to a Decarboxylation Reaction, B.E. Conway, E. Gileadi and M. Dzieciuch, Electrochim. Acta. Accepted for publication.

The work on non-equilibrium pseudocapacity is in course of publication and a further theoretical contribution on potential and current distribution at electrodes of finite ohmic resistance has been prepared and is submitted together with the other papers. This work is, however, not described in the thesis as the problems involved were very different from those considered in the main body of the work described.

ACKNOWLEDGEMENT

The author wishes to express his thanks to Professor B.E. Conway, under whose direction and constant supervision this work was done. Throughout the course of this research, as well as in the preparation of the manuscript, Professor Conway was always prepared to give freely of his time and advice whenever difficulties arose.

The author is also indebted to the Defence Research Board for financial support of this research project, and to the National Research Council for the award of a Studentship.

TABLE OF CONTENTS

LIST OF FIGURES

LIST OF TABLES

ABSTRACT

The role of adsorbed intermediates in electrode kinetics is examined in relation to the form of the adsorption isotherm applying to the system. The various models which may give rise to a linear variation of the free energy of adsorption with coverage (Temkin isotherm) are discussed. The Boudart "induced heterogeneity" model is adopted as the most plausible model. Kinetic equations are derived for complex reaction sequences involving three or more consecutive steps and two or more adsorbed intermediates (e.g. as in the oxygen evolution reaction) for conditions of intermediate coverage where a Temkin adsorption isotherm applies. The results are shown to be significantly different from those derived previously for limiting Langmuir conditions or for Temkin conditions when only two consecutive steps are involved (e.g. the hydrogen evolution reaction).

The variation of the adsorption pseudocapacity with coverage and potential is evaluated for the case of a single adsorbed intermediate, or for a case when two or more species are adsorbed simultaneously on the surface. It is shown that a Langmuir term and a Temkin term (depending on the pre-exponential and exponential terms in θ, respectively) combine in series to determine the total effective adsorption

pseudocapacity. Cases for which the free energy of adsorption is a linear function of $\theta^{1/2}$ or $\theta^{3/2}$ and a case when the assumption of quasi-equilibrium in the initial ion discharge step is not quite valid are examined quantitatively.

Methods are proposed for the determination of the parameter r (related to the rate of change of the free energy of adsorption with coverage) and the surface roughness factor f from the shape of the C-V plot obtained experimentally. These methods are applied to the observed pseudocapacity behaviour in the anodic decarboxylation of formate ions in pure anhydrous formic acid.

Surface effects in determining the reversible potential of the Ni^{II} - Ni^{III} couple in a nickel oxide electrode have been examined; it is shown experimentally that this potential is independent of the degree of oxidation of the bulk phase, and hence depends on the state of the surface phase only. Related adsorption pseudocapacity measurements at an "overcharged" nickel oxide electrode are also reported and three independent methods for the determination of C are shown to yield the same results, within experimental error.

CHAPTER I

INTRODUCTION

1. THE ORIGIN AND ROLE OF ADSORBED INTERMEDIATES IN ELECTRODE REACTIONS

Early investigations of the mechanism of cathodic hydrogen evolution (1,2,3,4) have revealed that the overall reaction involving transfer of two electrons does not occur in a single step. Two types of steps are regarded as occurring, one of which is the discharge of a proton at the electrode surface with formation of an adsorbed atom and the second, its desorption by one of several possible mechanisms. Since these early studies of the hydrogen evolution reaction (h.e.r.), the evaluation of the role of adsorbed intermediates has played a major part in discussions of the mechanisms of electrode reactions of various kinds, and in particular those leading to a gaseous product e.g. H_2, O_2, CO_2 and hydrocarbons. This is hardly surprising since the field of electrode kinetics constitutes an important part of the broader field of the kinetics of heterogeneous reactions, the rates of which are usually controlled by the concentrations and properties of species adsorbed at the relevant interface.

The discharge of an ion adsorbed at one of the regions of the ionic double-layer at an electrode and its further desolvation to form an adsorbed atom or radical at

the surface, may be considered the fundamental step in any electrode reaction producing a non-ionic product (we thus exclude from this discussion ionic electrochemical redox reactions). The adsorbed atom or radical may then migrate on the surface to a point where its energy will be the lowest (as can be the case in metal deposition (5)) or it may combine with a similar adsorbed species to form the final product e.g. $H_{(ads)} + H_{(ads)} = H_{2(gas)}$ in the case of the h.e.r., or form a second intermediate, e.g. $OH_{(ads)} + OH_{(ads)} \longrightarrow O_{(ads)} + H_2O$ in the case of the oxygen evolution reaction (6,7); alternatively, it may decompose in a unimolecular manner as in decarboxylation reactions, e.g. $CF_3COO_{(ads)} \longrightarrow CF_{3(ads)} + CO_{2(ads)}$ (8,9). It is evident that the rate of the initial discharge step, as well as that of the subsequent step(s) of removal of the adsorbed intermediate, will depend, apart from the usual activation energy terms, on the chemical potentials of all intermediates adsorbed at the surface of the electrode (in more complex electrode reactions, such as oxygen or nitrogen evolution (6,7,10,11), several kinds of intermediates may be adsorbed simultaneously at the interface), and these chemical potentials will themselves depend on the surface concentrations, the mobilities of species on the surface, the heats of adsorption and the kind of adsorption isotherm applicable to the system.

2. A DEFINITION OF ADSORPTION PSEUDOCAPACITANCE AND ITS PHYSICAL SIGNIFICANCE

A characteristic feature of electrode reactions, in comparison with heterogeneous reactions in general, is that formation of adsorbed intermediates usually requires the passage of electric charge across the interphase.* The charge q required is obviously proportional to the surface concentration of the adsorbed intermediate, or the partial coverage θ, which would arise by production of this intermediate on account of the passage of the charge q, i.e.

$$q = k'\theta \qquad [1]$$

where k' is a proportionality constant, determined by the charge required to form a complete monolayer of adsorbed intermediates of a given kind.

In order to show the origin of equations defining the electrochemical behaviour of adsorbed intermediates we shall consider as an example the h.s.r. proceeding through an initial discharge step in acid media represented by

$$H_3O^+ + e + M \longrightarrow MH + H_2O \qquad [A]$$

---

* Here we use the term "interphase" and distinguish it from the term "interface" which we define as the physical two-dimensional boundary of the metal-electrolyte system. The "interphase" is regarded as a three-dimensional region of intermediates, adsorbed ions and solvent molecules residing at the interface.

where M is an available site on the electrode surface, MH represents an adsorbed hydrogen atom and H_3O^+ the source of protons in solution*, followed either by the so-called "electrochemical" desorption step or the "catalytic" atom recombination desorption** which can be represented by

$$H_3O^+ + e + MH \longrightarrow M + H_2O + H_2 \qquad [B]$$

or

$$MH + MH \longrightarrow 2M + H_2 \qquad [C]$$

respectively. If we assume that the rate of the initial discharge step is relatively high, both in the forward and the reverse directions compared with that of either of the desorption steps [B] or [C], it is clear that the desorption step will then become rate-determining (r.d.) and the discharge step may be assumed to be in quasi-equilibrium.***

---

* We shall use the symbols H_3O^+ and OH^- to represent the source of protons and hydroxyl radicals in solution. Our argument will be basically the same whether the source of protons, say, is H_3O^+ or H_2O.

** Some authors (53) prefer to use the terms "ion-atom recombination" and "atom-atom" recombination", respectively, to describe these steps in the h.e.r.

*** The term "quasi-equilibrium" is used because a reaction cannot strictly be at equilibrium and yet proceed at a finite net rate in any one direction. It may be assumed, however, that the equilibrium is disturbed only to a negligible extent, so that the pre-rate-determining step can be treated as though it were at equilibrium. Cases where the quasi-equilibrium assumption is not applicable are examined in original calculations to be presented subsequently.

The rate of this step in the forward and reverse directions can be written (neglecting here the variation of the free energy of adsorption of intermediates with coverage, a factor which, however, will be examined in detail subsequently) as follows (cf. ref. 12):

$$\vec{i} = \vec{i}_o(1-\theta) \exp - \beta \eta F/RT \qquad [2]$$

$$\overleftarrow{i} = \overleftarrow{i}_o \, \theta \exp (1-\beta) \eta F/RT \qquad [3]$$

where $\vec{i}$ and $\overleftarrow{i}$ are the current densities associated with the forward and reverse directions of the reaction, β is a symmetry factor depending on the form of the energy barrier for charge transfer across the interphase (13,14,15,16), η is the overpotential, and other symbols have their usual significance. The currents $\vec{i}_o$ and $\overleftarrow{i}_o$ are related to the exchange current density i_o through the equation (cf. ref. 12)

$$i_o = \vec{i}_o (1-\theta^*) = \overleftarrow{i}_o \, \theta^* \qquad [4]$$

where θ^* is the coverage at the reversible potential ($\eta = 0$). Since the discharge step is assumed to be at quasi-equilibrium we can also write

$$\vec{i} = \overleftarrow{i} \qquad [5]$$

so that combining equations [2,3 and 5] we obtain

$$\frac{\theta}{1-\theta} = \frac{\vec{i}_o}{\overleftarrow{i}_o} \exp - \eta F/RT \qquad [6]$$

We note that the symmetry factor β cancels out when the forward and reverse currents are equated. This is a necessary requirement, of course, since β is a strictly kinetic parameter, depending on the shape of the energy barrier for charge transfer at the interphase and cannot therefore affect the equilibrium behaviour of a system.

We shall use equation [6], or its equivalent for an anodic process, again in the subsequent discussion. The only conclusion we wish to draw from it at present is that the fractional surface coverage θ by intermediates involved in the discharge step is an exponential function of the overpotential, whenever the rate-determining step in a series of consecutive reactions is preceded by a relatively fast charge transfer step at quasi-equilibrium. The definition of the "adsorption pseudocapacitance" then follows directly from these considerations, since, from equation [1] it is apparent that we can write a quantity

$$\frac{dq}{d\eta} = k' \frac{d\theta}{d\eta} = \pm C^{*} \qquad [7]$$

where C is recognised as a differential capacity, which may or may not itself be a function of potential, and is usually referred to as the "adsorption pseudocapacitance".

The differential capacity defined by equation [7]

---

* The plus or minus signs refer to anodic and cathodic processes, respectively.

originates physically from the dependence of extent of adsorption of intermediates at the electrode surface on potential, where these intermediates have arisen as a result of charge transfer across the metal-solution interphase. The value of C and its variation with overpotential will therefore be expected to depend on the type of adsorption isotherm obeyed by the system, as we shall discuss in detail below. While formally defined, and experimentally measured as a capacity, the adsorption pseudocapacity differs qualitatively from its electrical analogue (and the ionic double-layer capacity at an ideal polarized electrode) in that it arises on account of actual transfer of charge across the interphase (analoguous to a leakage current across a real electric capacitor) rather than from accumulation of charge on one side and the resulting induction of charges on the other side, to an extent dependent on potential difference across the capacitor.

Two other kinds of capacitances can arise at a metal-solution interphase: the ionic double-layer capacitance and the diffusional pseudocapacitance. The former has been treated in detail by Grahame (17) and by Parsons (18) and a mathematical treatment of the latter type of capacitance has been presented by Grahame (19) and by Ershler (20). In this thesis we shall restrict our discussion to the case of adsorption pseudo-

capacitance, assuming that our reactions are purely activation controlled so that no diffusion effects arise. The ionic double-layer capacitance will lie in parallel with the adsorption pseudocapacitance and the normally measured capacity will be the sum of these quantities. However, as shown below, we shall be mainly interested in a region of the overpotential where the adsorption pseudocapacity is appreciably larger than the ionic double-layer capacity, and any variations in the latter may therefore be assumed relatively negligible.

3. EXPERIMENTAL METHODS FOR THE DETERMINATION OF θ AND C

It is evident from the above discussion that the fractional surface coverage θ and the adsorption pseudo-capacitance C are directly related (equation 7). The experimental methods available to determine these quantities can therefore be classified into two groups: (i) those in which the coverage is determined experimentally as a function of overpotential, and the capacity is obtained by differentiation, and (ii) those in which the directly measured quantity is the capacity, and the coverage is obtained from it by integration with respect to potential. In the latter method, it is possible to evaluate only the change of coverage corresponding to a given change in potential, unless an integration constant (the absolute value of the coverage at

some reference potential) is known from an independent measurement.

In this section we shall discuss briefly the various experimental methods available for the determination of θ and C and, in the following section, some of the results recorded in the literature will be reviewed and their theoretical significance will be discussed.

(i) Determination of Coverage

(a) Slow Galvanostatic Charging Method

This method originated with Bowden and Rideal (15) and was developed by the Russian school of electrochemistry, in particular by Frumkin and co-workers (3,22). The procedure involves slow charging of a reversible hydrogen electrode by means of a small anodic current and determination of the number of coulombs required to ionize all the adsorbed hydrogen on the surface (the termination of this ionization process is indicated by a sudden rise of potential towards that corresponding to oxide formation and oxygen evolution). In the work of Frumkin et al. it was realized that if the charging process continued for more than about 10 m.sec., re-adsorption of hydrogen from the solution (normally containing molecular hydrogen dissolved to saturation) to the electrode surface might occur, resulting in a very high apparent surface concentration of hydrogen. To overcome this complication, they bubbled

hydrogen through the solution until the electrode reached its equilibrium potential (i.e. became reversible with respect to hydrogen) and then eliminated the dissolved hydrogen by bubbling nitrogen. In doing so, the potential of the electrode changed by some 0.1 V., but it was assumed to remain reversible with respect to hydrogen at a correspondingly reduced partial pressure.

This method can furnish results of qualitative value only, since the true variation of the surface coverage of the reversible hydrogen electrode with partial pressure of hydrogen is not known. Moreover, assuming (with Frumkin et. al.) that the electrode remains reversible with respect to hydrogen when nitrogen is passed through the solution, the observed change of potential of 0.1 volts would correspond to a change of partial pressure of hydrogen of about three orders of magnitude, so that re-adsorption may therefore not have been completely eliminated.

The major limitation of the slow charging method is that it cannot be applied to electrodes which are polarised cathodically and upon which hydrogen is being evolved. The solution close to such an electrode will always be saturated with hydrogen and re-adsorption could be appreciable. Additionally, if the anodic current density applied is quite small, so that the potential remains cathodic to the hydrogen

reversible potential for an appreciable length of time, some removal of adsorbed hydrogen atoms may continue through catalytic recombination on the surface, (similar to that occurring during steady state cathodic polarisation). This is not exactly compensated by the amount of re-adsorbed hydrogen (it is only at the reversible potential that these two processes occur at the same rate) and an error of unknown magnitude can therefore be introduced.

(b) Rapid Galvanostatic Charging Method

The rapid charging method was first suggested by Bowden in 1929 (23), further developed by Pearson and Butler in 1938 (24) and Breiter, Knorr and Völkl in 1955 (25). In general, this method is similar to the slow galvanostatic charging method, except that a much shorter (about 1 m.sec. or less) and much larger anodic pulse is used to ionize the adsorbed hydrogen atoms. This eliminates, to a large extent, errors arising from re-adsorption of hydrogen and continued hydrogen evolution on the electrode surface. It is not necessary in this method to bubble nitrogen through the solution and the uncertainty regarding the effective partial pressure of hydrogen with which the electrode is in equilibrium, as well as the dependence of θ on this quantity, is largely eliminated. Moreover, measurements can be extended to electrodes polarized cathodically, while the slow galvanostatic method

is only applicable to electrodes at the reversible potential, as discussed above.

Bowden (23) used an anodic pulse of intermediate length (about 1 sec) and measured the total number of coulombs required to change the potential of the electrode from that of the hydrogen reversible electrode to that corresponding to "oxygen evolution". While Bowden opened the way for a new and improved technique for the determination of surface coverage, his own experiments were of a rather crude and qualitative nature. In fact, the current densities used by Bowden were not high enough, so that the errors inherent in the slow galvanostatic charging method were only partially eliminated.

Pearson and Butler (24) used anodic current densities of the order of 1 Amp.cm.$^{-2}$ and their pulse duration was consequently reduced to about 0.1 msec. In this way the errors due to re-adsorption of hydrogen from solution were largely eliminated and the amount of adsorbed hydrogen lost on account of continuation of the cathodic process during the anodic pulse (while the potential was still negative to the hydrogen reversible potential) became negligible. These measurements may be considered the first quantitative determinations of the surface concentration of hydrogen atoms. The same technique was used by Hickling (26) in 1945 and his results were in

general agreement with those of Pearson and Butler.

In Fig. 1 is shown a typical potential (V)-time (t) curve obtained during anodic charging. Two arrests (regions where the change of potential with time is relatively slow) are observed, the first corresponding to ionization of hydrogen and the second to the formation of an oxide or adsorbed oxygen layer. The two arrests are separated by a region of much greater rate of change of potential with time, corresponding to change of charge in the ionic double-layer.

The rapid galvanostatic method was further developed and refined by Breiter, Knorr and Völkl (25) in 1955. These authors were the first to measure the amount of adsorbed hydrogen on electrodes which were polarized cathodically and upon which hydrogen evolution was occurring at a steady rate. In this method, a cathodic polarization was changed to an anodic polarization at a much higher current density by use of two separate polarizing circuits. The procedure involved switching the anodic current on, without switching the cathodic current off, and since the anodic circuit was set to pass a current larger by about two orders of magnitude than the cathodic circuit, a net anodic current was caused to pass.

The fast galvanostatic method of Breiter et al. (25) has been used by several workers (3, 27) for the determination of surface coverage by adsorbed intermediates on the platinum

Figure 1. Galvanostatic charging curve for Pt in 1N H_2SO_4. Anodic current density i_a = 0.61 Am. $cm.^{-2}$ (diagram taken from ref. 28).

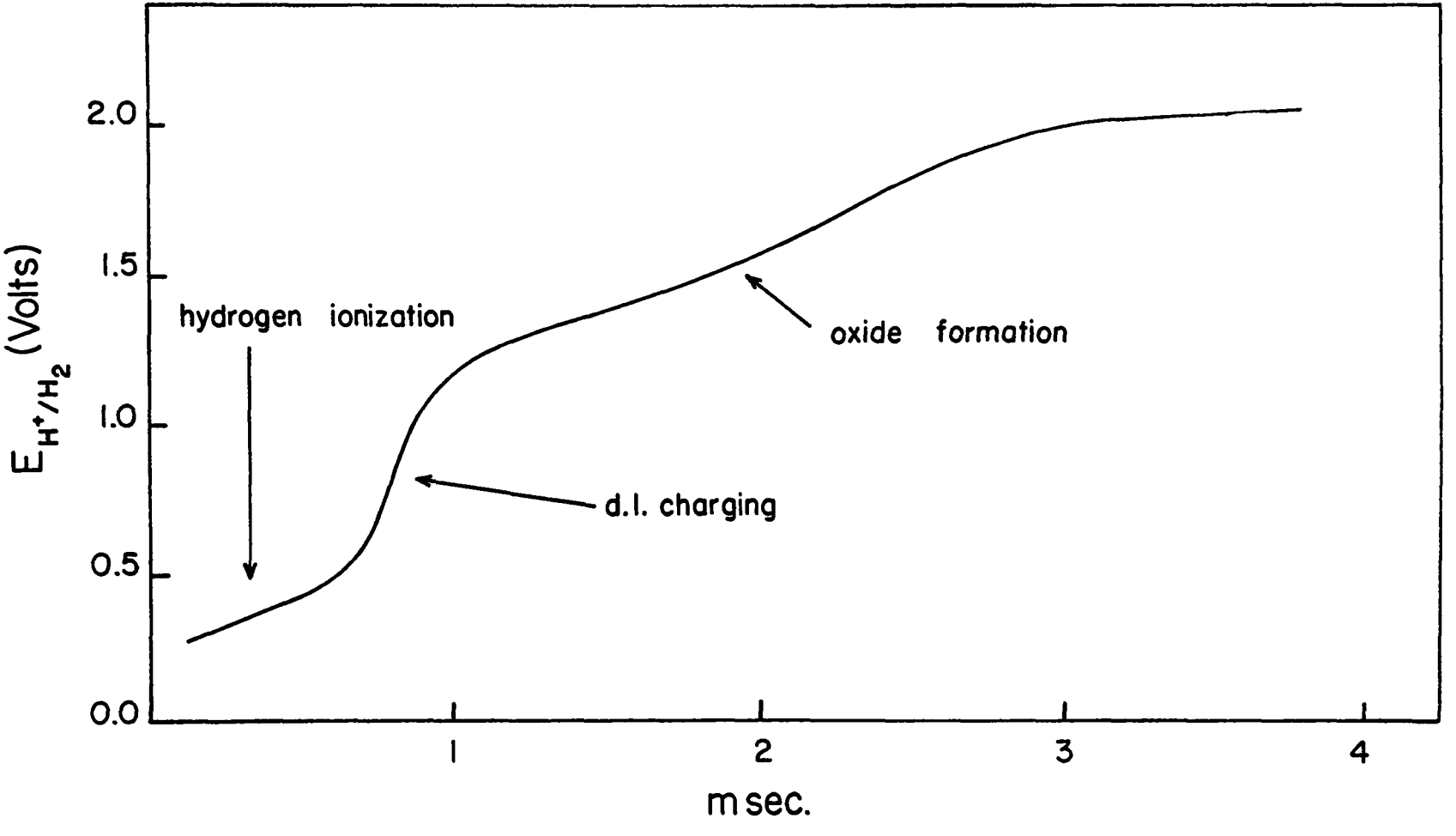
2.0
1.5
1.0
0.5
0.0
E_{H^+/H_2} (Volts)
hydrogen ionization
oxide formation
d.l. charging
1
2
3
4
m sec.

group metals. The exact method of determining the charge corresponding to the amount of adsorbed intermediates is illustrated in Fig. 2 taken from ref. (27). Breiter et al. (25) assumed that the second arrest in the charging curve was due to the formation of an oxide film one layer thick. From the charge corresponding to this arrest they calculated the real surface area of the electrode. This procedure is, however, not fully justified, as we shall show below. It provides, nevertheless, a reasonable approximation; when combined with results on the amount of adsorbed hydrogen on the surface obtained from the first arrest in the anodic charging curve, the method can lead to the evaluation of the fractional coverage θ_H of the surface with hydrogen atoms.

There are two factors which restrict the use of the rapid galvanostatic methods mainly to noble metal electrodes. If the surface of the electrode is covered to a very small extent ($\theta < 0.01$), the adsorption pseudocapacity will be small* and comparable with or less than the ionic double-layer capacity. In this case, the part of the anodic current used to change the charge in the ionic double-layer will be comparable with

---

* The dependence of adsorption pseudocapacity on coverage under various conditions is discussed in detail below in the section on original theoretical work.

Figure 2. Schematic representation of the method of calculating the amount of charge associated with adsorbed hydrogen by the fast charging method. Hydrogen ionization occurs for a length of time represented by AB', but the charge associated with adsorbed hydrogen is only that passed in the time AB, the remainder (BB') being used to change the potential of the ionic double-layer. The charge associated with formation of a surface oxide (or a film of adsorbed oxygen) is taken as that passed during the time DE.

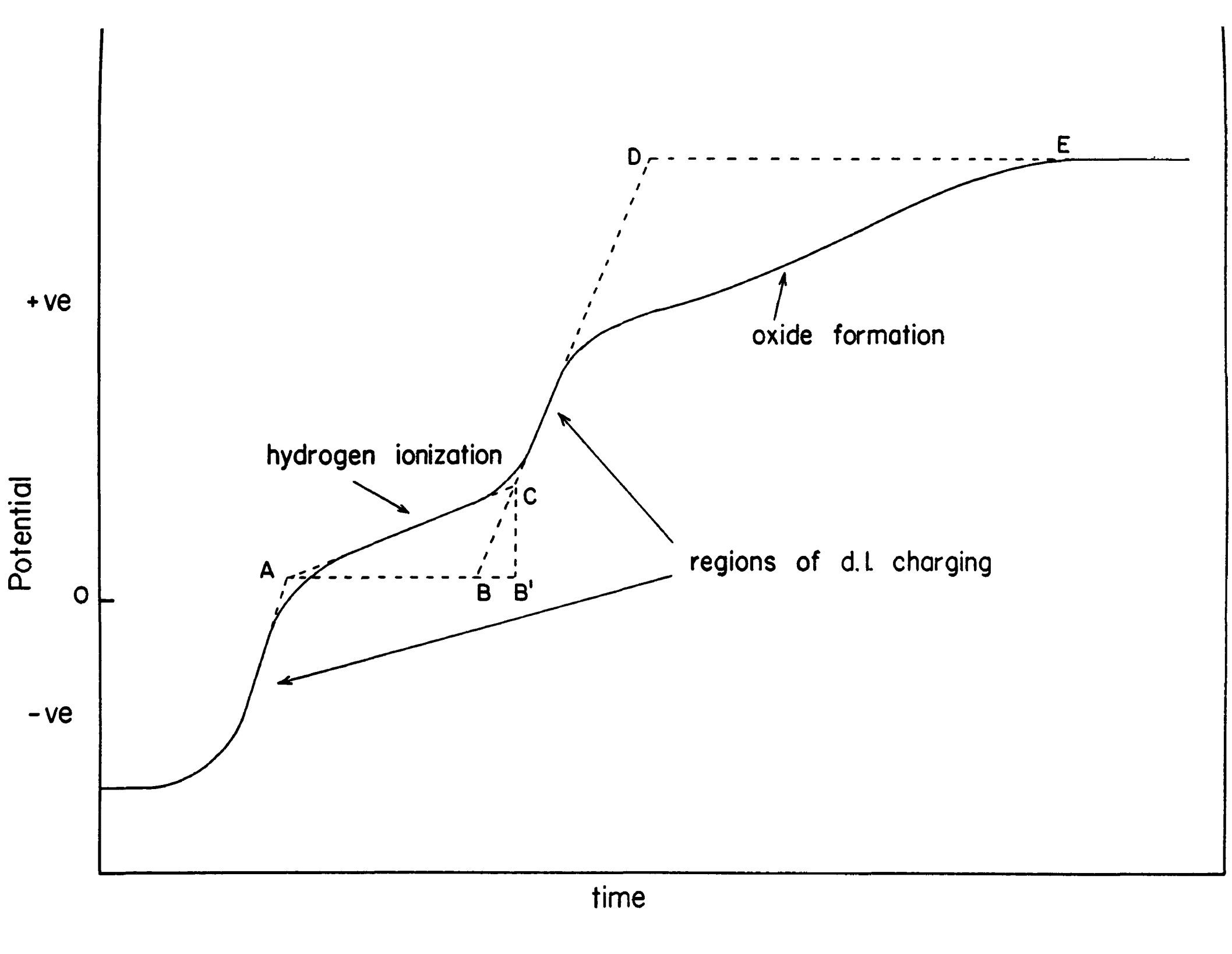
+ve
0
-ve
Potential
time
A
B
B'
C
D
E
hydrogen ionization
oxide formation
regions of d.l. charging

the part involved in removal of the adsorbed hydrogen atoms from the surface. The typical arrest in potential (Fig. 2) will then not be observed, and it will not generally be possible to calculate the amount of hydrogen adsorbed on the surface of the electrode.* At slightly higher coverages ($0.01 < \theta < 0.1$), or when the free energy of adsorption varies markedly with coverage, the adsorption pseudocapacity may be somewhat, but not very much, larger than the ionic double-layer capacity** (i.e. between approximately three and ten times greater). In this case, the part of the current used to charge the ionic double-layer capacity is not negligible, but a correction for the total charge taken up by this process during desorption of the hydrogen atoms from the surface can easily be made, as illustrated in Fig. 2.

The second, and more serious, limitation to the use of the rapid galvanostatic method arises on account of the particular form of the variation of potential with time during

---

* The usefulness of the fast galvanostatic charging method is not, in fact, restricted to a substantial extent by this effect, since the extent of surface coverage and its variation with potential is important mainly in the range where the coverage is appreciable. At very low values of θ (say $\theta < 0.01$), the effect of coverage on the reaction kinetics is trivial, and other phenomena caused by an adsorbed layer of hydrogen (e.g. metal embrittlement) are of little practical importance.

** See footnote on the previous page.

the anodic pulse and this time function is determined by the kind of metal used as the electrode. In Fig. 2 a typical rapid galvanostatic charging curve is given for a noble metal electrode, say platinum. In Fig. 3 is represented schematically the kind of relationship obtained at a silver or nickel electrode. On the noble metal the arrests due to ionization of adsorbed hydrogen and formation of an oxide layer (or adsorbed layer of oxygen on the surface) are well separated by an intermediate region where the charge in the ionic double-layer is changed and the potential rises rapidly with time. When a "less noble" metal is used as an electrode, the regions of potential over which the two anodic processes (hydrogen ionization and oxide film formation) take place tend to overlap to an increasing extent (Fig. 3) and the amount of charge specifically involved in the oxidation of the adsorbed hydrogen cannot be unambiguously determined.*

---

* An equivalent technique was used by Conway and Dzieciuch (8) to determine the surface concentration of adsorbed intermediates during steady anodic polarization in the formate decarboxylation reaction, by imposing a large cathodic current on the electrode. In their case, the applicability of the method depended on the fact that the arrest due to ionization of the intermediate was well separated on the potential axis from the arrest due to formation of an adsorbed layer of hydrogen atoms and subsequent hydrogen evolution.

Figure 3. Galvanostatic charging curve for Ag in 0.2N NaOH. Anodic current density i_a = 0.4 Amp. cm.$^{-2}$ following steady-state cathodic polarization at 1 x 10^{-3} Amp. cm.$^{-2}$ (diagram taken from ref. 28).

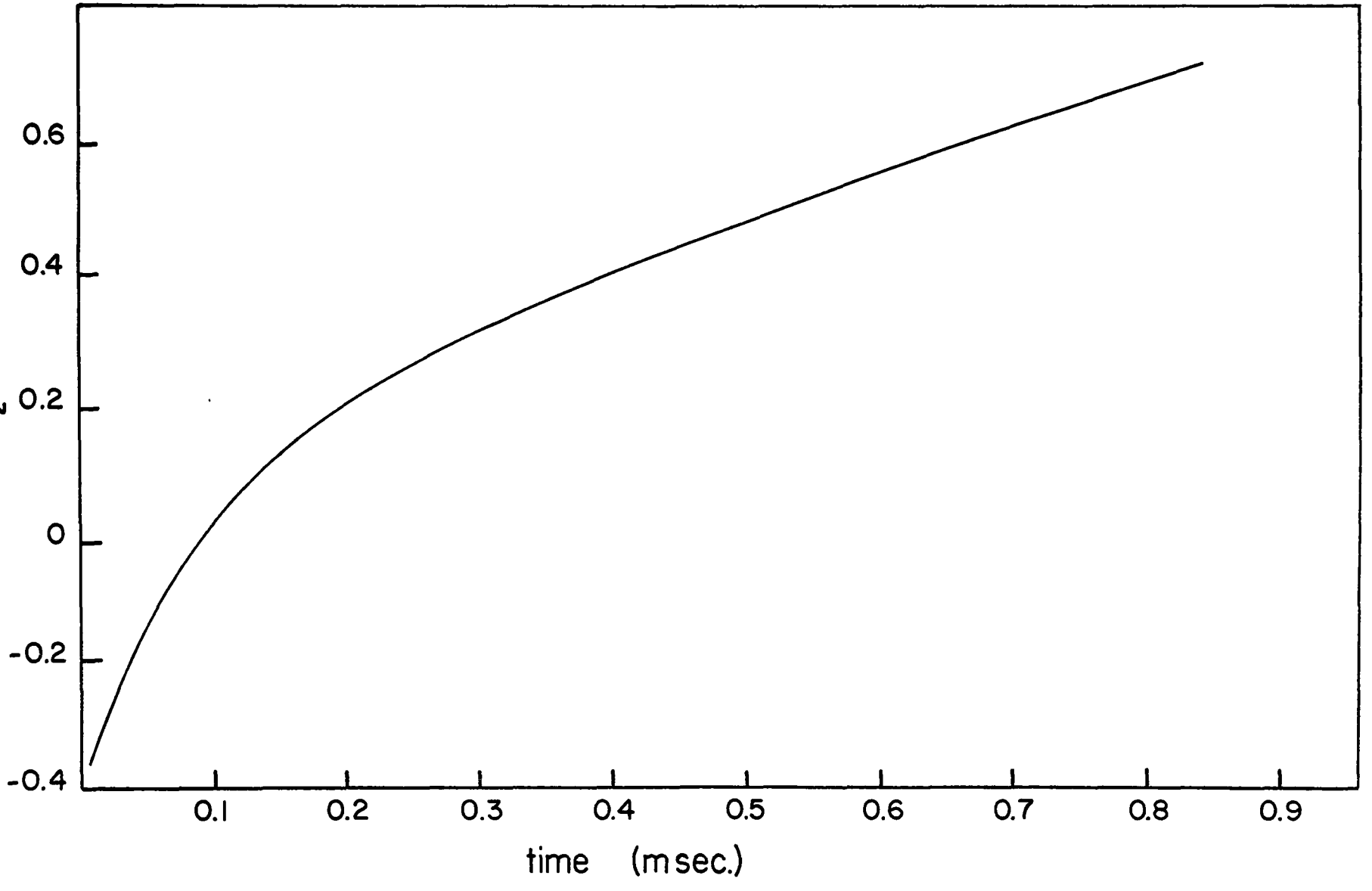
0.6
0.4
0.2
0
-0.2
-0.4
E_{H^+/H_2} (mV)
0.1
0.2
0.3
0.4
0.5
0.6
0.7
0.8
0.9
time (msec.)

An ingenious method, which overcomes the latter difficulty, was devised by Devanathan, Bockris and Mehl (28) and used by the same authors (28) and later by Devanathan and Selvaratnam (12) to determine the partial coverage of the surface of silver and nickel electrodes during steady cathodic polarization as a function of potential. This method will be discussed in the next section.

(c) The Double Charging Method

(a) Description of Method

The double charging method has been discussed in detail in several recent publications (12,31,28). Only a brief account of the underlying principles will be given here and the scope and limitations of the method will be discussed.

Let a large anodic galvanostatic pulse i_a be imposed on an electrode polarized cathodically at a given current density i_c, and let the ionic double-layer capacity of the electrode/C_V^{be} (the subscript indicates that this quantity will, in the general case, be a function of potential). Then

$$C_V\left(\frac{dV}{dt}\right) = i_a - i_F \qquad [8]$$

where i_F is the sum total of all anodic Faradaic currents given by

$$i_F = i_H + i_{an}(1 - \theta) \qquad [9]$$

and other terms are defined as follows: i_H is the current associated with dissolution of hydrogen per sq. cm. of real area of the electrode (whatever is the fraction of this area covered by hydrogen); i_{an} is the current associated with any other anodic process (e.g. oxide formation) per sq. cm. of <u>bare</u> real surface area of the electrode.

Combining equations [8] and [9] gives

$$C_V\left(\frac{dV}{dt}\right) = i_a - [i_H + i_{an}(1-\theta)] \qquad [10]$$

A second charging curve may now be taken, starting from a potential sufficiently anodic to the hydrogen reversible potential that surface coverage by hydrogen atoms under steady state conditions can be assumed negligible. The equation corresponding to [10] is then for this case

$$C_V\left(\frac{dV}{dt}\right) = i_a - i_{an} \qquad [11]$$

Subtracting equation [10] from equation [11] gives

$$C_V\left[\left(\frac{dV}{dt}\right)_2 - \left(\frac{dV}{dt}\right)_1\right] = i_H - i_{an}\theta \qquad [12]$$

where the subscripts 1,2 refer to values of dV/dt taken on the charging curves started from steady cathodic or anodic polarizations, respectively.

Schematic plots of the quantity given on the r.h.s. of equation [12] as a function of potential and time are given in Fig. 4 (a,b) which has been reproduced from ref. (28).

Figure 4. Current density obtained as the difference of the Faradaic current densities of charging process 1 and 2

a. as a function of potential

b. as a function of time required to reach the corresponding potential during a charging process of type 1.

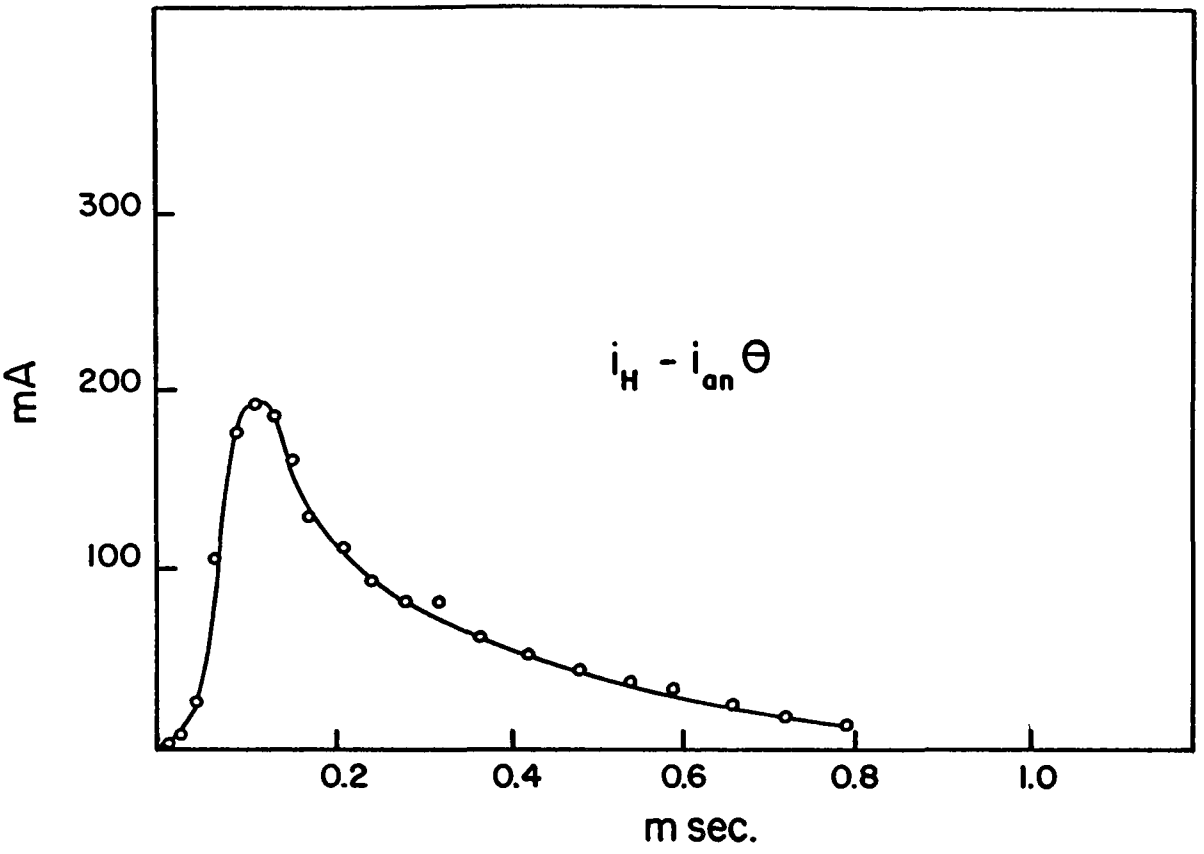
300
200
100
mA
$i_H - i_{an}\Theta$
0.2
0.4
0.6
0.8
1.0
m sec.

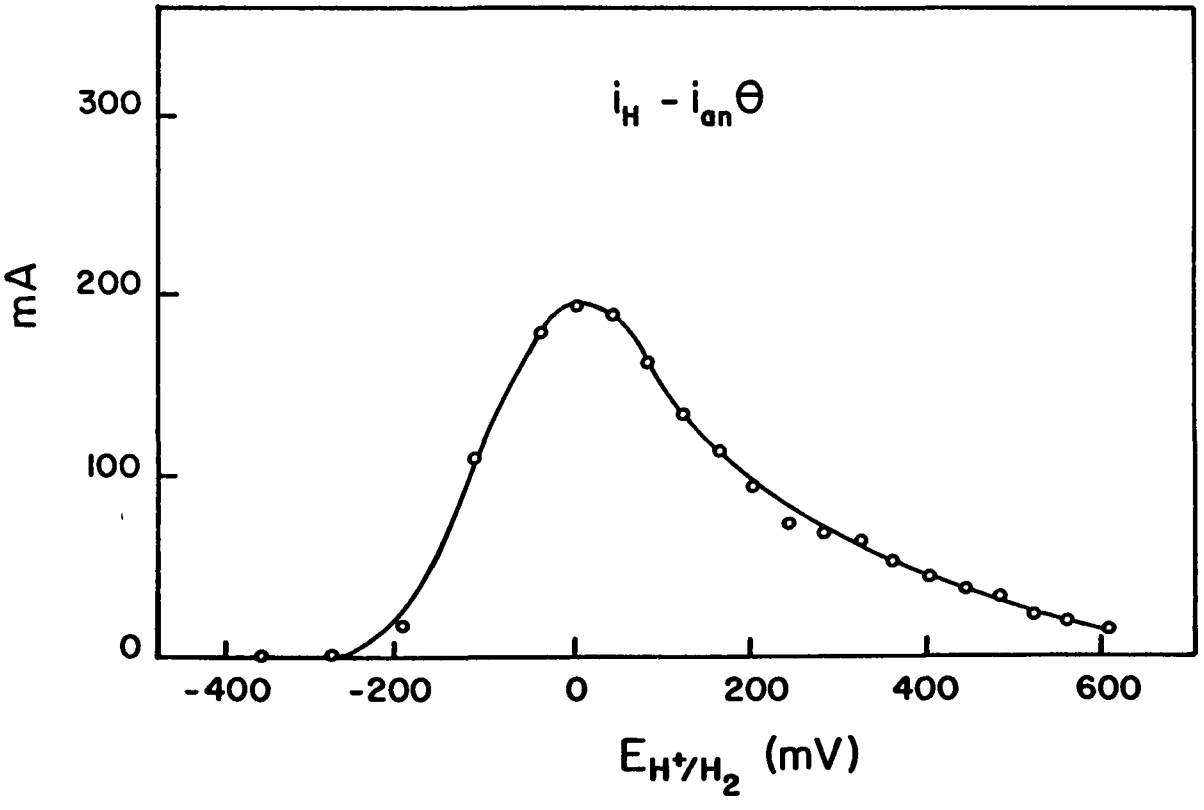
300
200
100
0
mA
$i_H - i_{an}\Theta$
-400
-200
0
200
400
600
E_{H^+/H_2} (mV)

The time corresponding to each potential on the first type of charging curve (starting from a cathodic polarization) was used to obtain Fig. 4b. The area under the curve in Fig. 4b is given by

$$\int_o^t (i_H - i_{an}\theta)\, dt = \int_o^t i_H \left(1 - \frac{i_{an}\theta}{i_H}\right) dt \qquad [13]$$

If it is assumed that

$$i_{an}\theta/i_H \ll 1 \qquad [14]$$

then equation [13] is reduced to the simple form

$$\int_o^t i_H\, dt = q_H \qquad [15]$$

and the amount of adsorbed hydrogen can be computed directly. The validity of this assumption (equation 14) will now be discussed.

At cathodic overpotentials both i_H and i_{an} are zero. As the potential becomes anodic to the hydrogen reversible potential, i_H increases first while i_{an} still remains negligible, but as the potential is made even more anodic, i_{an} becomes appreciable. At this point, however, θ has become negligibly small and the inequality in equation [14] still holds.

Additional proof of the validity of equation [14]

was given (28) as follows: From equation [14] we can write

$$\frac{i_{an}^{\theta}}{i_H} = \frac{i_{an}^{\theta}}{i_F - i_{an} + i_{an}^{\theta}} \quad ; \qquad [16]$$

substituting

$$A = i_F - i_{an} \qquad [17]$$

and dividing by i_{an}^{θ} we obtain

$$\frac{i_{an}^{\theta}}{i_H} = \frac{1}{1 + \frac{A}{i_{an}^{\theta}}} \qquad [18]$$

The argument then follows as above, since at low overpotentials i_{an} is very small and at higher anodic overpotentials θ becomes negligible, hence

$$\frac{A}{i_{an}^{\theta}} \gg 1 \qquad [19]$$

at all anodic overpotentials and

$$\frac{1}{1 + \frac{A}{i_{an}^{\theta}}} \doteq \frac{1}{A/i_{an}^{\theta}} \ll 1 \qquad [20]$$

so that the assumption made in equation [14] is valid. A numerical evaluation of the error introduced by neglecting the term i_{an}^{θ}/i_H with respect to unity was shown (28) to introduce a total error not exceeding 3% in the calculated value of θ.

(β) Limitation of the Double Charging Method

The various experimental errors involved in determining the surface coverage by the double charging method have been discussed by Devanathan et al. (21,28) in detail and numerical estimates of the maximum expected error were obtained. Apart from the uncertainty in relating surface charge to fractional surface coverage, which depends on the accuracy with which the real surface area of a solid electrode can be determined and on the validity of estimates of the number of surface sites per unit real surface area, the major source of error, according to the above authors, arises from the variation of the magnitude of the ionic double-layer capacity with potential (equation 12). In applying the double charging method for the determination of the coverage on silver and nickel, this capacity was taken to be a constant. If, in fact, the ionic double-layer capacity varied by as much as a factor of two as the anodic overpotential varied from zero to 0.6 volts, the calculated values of the coverage would be in error by some 25%. It may be noted that this uncertainty arises from lack of experimental data regarding the variation of the ionic double-layer capacity with potential at solid metals, and is not inherent in the experimental method proposed.

Another source of error in the method of Devanathan, Bockris and Mehl is of a rather more serious nature and seems

to have been overlooked by these authors. Considering the definition of the quantities involved on the r.h.s. of equation [9]

$$i_F = i_H + i_{an}(1-\theta) \qquad [9]$$

it is apparent that the current i_H as defined there must be proportional to fractional coverage θ, since it is the anodic current associated with the reaction

$$MH + H_2O \longrightarrow M + H_3O^+ + e \qquad [A]$$

Equations [9] to [18] could therefore conveniently be rewritten making use of the relationship

$$i_H = i_H^o \theta \qquad [21]$$

where i_H^o is now defined (more consistently)as the current associated with dissolution of hydrogen per sq. cm. of real area of the electrode completely covered ($\theta = 1$) by adsorbed hydrogen (cf. the definition following equation [9]). Using this definition, we obtain

$$C_V \left[\left(\frac{dV}{dt}\right)_2 - \left(\frac{dV}{dt}\right)_1\right] = (i_H^o - i_{an})\,\theta \qquad [12a]$$

and the area under the curve in Fig. 4b is given by

$$\int_o^t i_H^o \theta \left(1 - \frac{i_{an}}{i_H^o}\right) dt \qquad [13a]$$

We now consider the error introduced by assuming

$$i_{an}\theta/i_H = i_{an}/i_H^o \ll 1 \qquad [14a]$$

At relatively low anodic overpotentials, i_H^o is appreciable while i_{an} is still negligible. In this range, the above assumption (equation 14a) is justified. At higher anodic overpotentials i_{an} becomes appreciable, and since i_{an}/i_H^o is independent of θ, the error in the calculated value of θ will increase.

We conclude, therefore, that the double charging method can only be applicable to systems where i_{an} becomes appreciable only at high anodic overpotentials, where θ has reached negligible values (and therefore the term $[i_H^o - i_{an}]\,\theta$ is close to zero). This condition obtains at noble metals and may be a fair approximation at slightly less noble metals such as silver, but is intrinsicly inapplicable to baser metals, where the ionization of hydrogen and the formation of oxide layers occur over largely overlapping regions of electrode potential. Thus, for the type of metal for which the method was designed, it is seen that severe limitations still apply. However, the method constitutes a significant improvement over the fast galvanostatic charging method discussed above, in that the current used to change the charge in the ionic double-layer is at least taken into account and evaluated quantitatively. Fairly accurate determinations of the surface concentration of adsorbed hydrogen during steady

state cathodic polarization can be made at electrodes where the arrest due to hydrogen ionization and that due to oxide formation overlap slightly or are separated by only a small range of potential.

(d) Potentiostatic Methods for the Determination of θ

(a) The Method of Devanathan and Bockris (21)

In cases where the rapid galvanostatic method is applicable, it is possible to use a simple potentiostatic method, provided that a fast rise-time electronic potentiostat is available. In this method, the cathodic constant polarizing current is switched off and a constant anodic potential is switched in. The value of this applied fixed potential is chosen to lie between the two arrests in the corresponding galvanostatic charging curve, so that the only process which can take place is dissolution of hydrogen and a small change of charge in the double-layer. Integration of the current-time relationship at constant potential then gives the total charge associated with hydrogen adsorbed on the surface at the initial potential in the prior constant current cathodic polarization.

The above method offers no improvement over the rapid galvanostatic method and is more limited in scope than

the double charging method. It requires rather more complex equipment and is intrinsically less accurate than the two galvanostatic methods mentioned above, since no correction can be made for the current used to charge the ionic double-layer.

(β) The Method of Gerischer and Mehl

A better potentiostatic method for the determination of θ was discussed by Gerischer and Mehl in 1955 (29). Their method involves, in principle, switching on a cathodic potential and evaluation of the steady state coverage from the form of the current-time transient observed. A detailed mathematical treatment, including discussion of various limiting cases, has been given by the above authors (29) and will not be reproduced here. However, the qualitative form of the current transient can be deduced directly from the nature of the electrochemical processes involved.

Thus, we may consider the hydrogen evolution reaction proceeding through the step

$$M + H_3O^+ + e \longrightarrow MH + H_2O \qquad [A]$$

followed by

$$H_3O^+ + e + MH \longrightarrow M + H_2 + H_2O \qquad [B]$$

or

$$MH + MH \longrightarrow 2M + H_2 \qquad [C]$$

If we assume (with Gerischer and Mehl) that the adsorbed hydrogen obeys the Langmuir adsorption isotherm, it is obvious that the rates of the above reactions at a given potential are proportional to $(1 - \theta)$, θ and θ^2, respectively. Different cases will now be considered.

Case 1: Discharge rate-determining followed by electrochemical desorption. In this case the current will increase instantaneously to a value corresponding to the rate of reaction (A) at the fixed potential and the initial coverage.* The degree of coverage will increase with time and the overall current will also increase until a steady state is reached, since the decrease in rate of reaction (A) on account of the increase in θ is more than compensated by the increase in rate of reaction (B) which is also a charge transfer reaction.

Case 2: Discharge rate-determining followed by catalytic atom-atom recombination. The current will rise instaneously to the same value as in case 1, but will decrease subsequently towards a steady state value corresponding to the steady state coverage. The difference between case 1 and case 2 arises because the step following the rate-determining discharge reaction involves charge transfer in the first case only.

Case 3: Either of the alternative desorption steps is rate-determining

---

* In the original publication it was assumed that $\theta = 0$ at $t = 0$. This is not necessarily correct (2). The argument as presented here does not, however, depend on this assumption.

Again an initial large current will be observed, corresponding to the rate of the discharge reaction at the set potential and the initial degree of coverage θ (t=0). The current will then decrease with increasing θ until a steady state, controlled by the rate of the desorption step, will be reached.

The potentiostatic method of Gerischer and Mehl (29) offers obvious advantages over all other methods discussed so far, since it involves only cathodic polarization of the electrode studied, and complications due to parallel anodic reactions can thus be avoided, even on base metal electrodes.

A serious limitation of this method arises, however, from the fact that it is based on the assumption that the adsorbed intermediates in the reaction obey the Langmuir adsorption isotherm throughout the range of coverage ($0 < \theta < 1$). It is rather unlikely that this will be the case (4,10,30) in the range of intermediate values of coverage ($0.2 < \theta < 0.8$)* and the analysis of Gerischer and Mehl is therefore not generally valid.

---

* A different view on this point is held by Breiter (31) who finds that in certain cases the changes in enthalpy and "non configurational" entropy of adsorption compensate each other, so that the free energy of adsorption is practically independent of coverage and a Langmuir type adsorption isotherm is obeyed.

Furthermore, the rates of the reverse reactions (e.g. in the discharge step) have been neglected. This may be justified when discharge is rate-determining and measurements are taken at an appreciable overpotential, if molecular hydrogen is not in equilibrium with adsorbed H atoms on the surface. However, it is evident that if either desorption step is rate-determining, the initial discharge step will be more or less in quasi-equilibrium, and hydrogen ionization (the reverse of the discharge step) may proceed, in principle, at any rate. If the rate of this reverse reaction is neglected, it can be inferred from the representation of Gerischer and Mehl that rate-determining desorption by atom-atom or ion-atom mechanism must lead in both cases to a practically complete coverage. This is evidently not the case since as $\theta \rightarrow 1$ the Tafel slopes for catalytic and electrochemical desorption would tend to infinity and $RT/\beta F$ respectively, and the characteristic slopes of $RT/2F$ and $RT/(1+\beta)F$ would never be observed.

(γ) A Potentiostatic Step Method

A semi-empirical potentiostatic method for the determination of coverage has been devised by Gileadi and Conway, and its applicability to different systems is now being explored experimentally; the principles of this method will now be considered.

Let an electrode be polarized initially to a cathodic overpotential η_1 and let the steady rate of hydrogen evolution at this overpotential correspond to an initial current density i_1. Suppose now that the potential is set to a new value $\eta_2 = \eta_1 + \Delta\eta$ where $\Delta\eta$ is chosen to be relatively small (say $\Delta\eta < 20$ mV) and let the current corresponding to η_2 at a steady state be i_2. The current i during the transition period will be given by

$$i(t) = i_H(t) + i_{H_2}(t) \qquad [22]$$

where $i_H(t)$ is the time-dependent current used to change the degree of coverage of the electrode surface and $i_{H_2}(t)$ is the current used to evolve hydrogen. Integrating equation [22] we obtain

$$\int_o^t i(t)dt = \int_o^t i_H(t)dt + \int_o^t i_{H_2}(t)dt \qquad [23]$$

The quantity on the l.h.s. of equation [23] can be determined experimentally, and will be referred to as $\Delta q(exp)$. The first expression on the r.h.s. of equation [23] is the charge associated with the change in coverage as the potential is increased from η_1 to η_2, and will be denoted Δq_H. Hence

$$\Delta q(exp.) = \Delta q_H + \int_o^t i_{H_2}(t)dt \qquad [23a]$$

The integral in equation [23a] cannot be evaluated rigorously unless the variation of i_{H_2} with θ is known. However, if $\Delta\eta$ is taken small enough, then $\Delta\theta$ will also be small and the rate of hydrogen evolution during the transient will be approximately equal to its steady state rate at an overpotential η_2, i.e.

$$i_{H_2}(t) \doteq i_{H_2}(t \rightarrow \infty) = i_2 \qquad [24]$$

with this assumption, equation [23a] becomes

$$\Delta q(exp) = \Delta q_H + i_2 \Delta t \qquad [23b]$$

so that Δq_H can be easily evaluated. The accuracy of the method can be improved, if desired, by repeating the experiment using smaller values of $\Delta\eta$ and extrapolating the results to $\Delta\eta \rightarrow 0$.

We note that this method will be most satisfactorily applicable to systems where fast discharge is followed by slow, rate-determining desorption and the fractional coverage θ has an intermediate value, since in such cases $i_2 \Delta t \ll \Delta q_H$, and the error involved in using equation [24] will have a negligible effect on the value of Δq_H calculated from equation [23b]. In this sense it is complementary to the method of Gerischer and Mehl (29) which is most accurate at low values of the coverage, when the Langmuir isotherm is usually a satisfactory approximation (10). Normally the method would be used to obtain θ as a

function of potential over an appreciable range of potentials by making successive incremental potentiostatic measurements each with small changes of η .

(ii) Determination of Adsorption Pseudocapacity

(a) Measurements Involving Charging and Forced Decay Curves

The most straightforward method for the determination of the capacity at the metal solution interface is from the variation of potential with time during anodic or cathodic polarization at a constant current density, since we can write

$$C = \frac{dq}{dV} = \frac{d(it)}{dV} = i\left(\frac{dt}{dV}\right) \qquad [25]$$

This method was first applied successfully by Bowden and Rideal (33) for the determination of the ionic double-layer capacity at a mercury electrode and later by Barkley and Butler (34). Frumkin and co-workers (4,22) applied the method to the determination of adsorption pseudocapacitance at solid electrodes, and studied in detail its variation with potential and with the nature of the electrolyte.

The determination of capacity from galvanostatic charging and forced decay curves has become an important technique in modern electrochemical kinetics. It is important to remember, however, that equation [25] is only correct if

all/the measured current is used to charge or discharge the "capacitor" (or the "pseudocapacitor", i.e. to form or ionize adsorbed species on the surface). This implies that such measurements are not valid within, say, a value $2b_1$ of the potential at which a parallel Faradaic process (e.g. hydrogen evolution) takes place at a rate corresponding to the total current used, where b_1 is the Brigsian Tafel slope for the relevant Faradaic process.

(b) Measurements Involving Open-Circuit Decay Curves

(a) From Initial Decay Slopes

The study of open-circuit decay or build-up of potential after anodic or cathodic polarization, respectively, provides complementary information to that obtained by direct polarization methods. Thus, the potential recovery behaviour of platinized platinum has, for example, been studied and discussed by Armstrong and Butler (35). Further theoretical interpretations of the significance of results obtained in this manner have been given by Morley and Wetmore (36), Past and Jofa (37), Milner (38) and more recently by Conway and Bourgault (39) who considered how the decay behaviour depended on surface coverage by intermediates.

The determination of electrode capacity from initial rates of decay of overpotential on open-circuit after steady state polarization at a current density i_{in} has been discussed

by several authors (36,37,40). It is based on the assumption that the Faradaic process taking place during steady state polarization continues on open-circuit by a self-discharge process, which momentarily has the same rate as that corresponding to the initial steady state polarizing current density. Hence for e.m.f. decay following anodic polarization

$$-C(d\eta/dt)_{t=0} = i_{in} = i_o \exp(\eta_{in}/b_1) \qquad [26]$$

where i_o is the exchange current density, b_1 is here the Naperian Tafel slope and η_{in} is the initial (steady state) overpotential for the relevant anodic process. By conducting polarizations at various current densities, and hence at various values of the overpotential, the capacity can be obtained in this manner as a function of potential.

(β) From Analyses of the Whole Decay Curve

The analysis of open-circuit decay behaviour for the determination of the capacity of the electrode as a function of potential has been extended by Conway, Gileadi and Dzieciuch (9) to the whole of the e.m.f. decay curve (cf. 37) for cases when the current-potential relationship is known experimentally over the same range of potential. Thus, at any time t, during open-circuit decay, when the overpotential has reached a value η_t, the capacity corresponding to this potential can be calculated from an equation similar to

equation [26], namely

$$-C\,(d\eta/dt)_t = i_o \exp(\eta_t/b_1) \qquad [26a]$$

It is not necessary to assume that the mechanism of the reaction remains the same throughout the potential decay process, but we must regard whatever process is rate-determining during steady polarization at any overpotential η, as also rate-determining in the self-discharge process at the same overpotential during open-circuit decay. This is usually implicit in most previous discussions (35,36,37,39) of the mechanism of e.m.f. decay on open-circuit at non-ideally polarizable electrodes (17).*

It is seen that the capacity is obtained here by combining the current-potential relationship obtained on direct polarization with the potential-time relationship

---

* At an ideally polarizable electrode (in the sense defined by Grahame (17)), we cannot write an equation such as [26a] since, by definition, no Faradaic process occurs and there is no charge transfer across the double-layer. In this case, the open-circuit decay of potential must occur by a first order relaxation of the ionic space charge on the solution side, and the electron excess charge in the metal electrodes being polarised. When Faradaic process occur, the case is evidently quite different, and the experimental decay behaviour found at mercury (35) must not be confused with that which would occur at an ideally polarizable electrode made of the same metal.

observed during open-circuit decay (8,9,37). The method is best suited to systems where a transition region in the current-potential relationship is observed (8,9,27) (as in passivation), and the current is practically constant over an appreciable range of potential.*

(γ) From the Parameter ϕ in Semi-Logarithmic E.M.F. Decay Plots

Early studies (35) of open-circuit decay (or build-up) of potential after steady state polarization have shown that a linear relationship exists between the over-potential and log t (except at very short times), where t is measured from the time when polarization was terminated. Subsequently it was shown (7,36,39,41), that an equation of the form

$$\eta = a \pm b_2 \log (t + \phi) \qquad [27]$$

is obeyed experimentally down to $t \rightarrow 0$; in equation [27] a and b_2 are constant parameters of the relevant electrode reaction** and ϕ is an integration constant (see below) related

---

* However, if the system exhibits hysteresis in the current-potential plot (8,27), the relationship obtained on the decreasing potential and current part of the plot is to be used, or preferably, a potentiostatic study should be made of the current-potential relationship.

** The relation of the parameter b_2 to the Tafel slope $b_1 = d\eta/d \log i$ under various limiting conditions has been discussed elsewhere by Conway and Bourgault (39,41) and by Lukovtsev and Temerin (33).

to the polarizing current density and the capacity of the electrode (the plus and minus signs in equation [27] correspond to cathodic and anodic reactions, respectively). The quantity ϕ is obtained in practice from the observed η - log t behaviour by a trial and error method (7,41) with an accuracy of better than 10%. From ϕ, the capacity of the electrode is calculated as follows: starting from equation [26a], which is written for an anodic process, we have

$$-C\,(d\eta/dt) = i_o \exp(\eta_t/b_1) \qquad [26a]$$

Rearranging and integrating this equation gives

$$-\int \exp(-\eta_t/b_1)\, d\eta = \frac{i_o}{C}\int dt \qquad [28]$$

or

$$\exp(-\eta_t/b_1) = \frac{i_o}{b_1 C}(t + \phi) \qquad [29]$$

Now at $t = 0$, $\eta_t = \eta_{in}$, so that

$$\exp(-\eta_{in}/b_1) = \frac{i_o}{b_1 C}\phi \qquad [30]$$

The current i_{in} under steady state conditions prior to termination of the polarization is related to the overpotential η_{in} by a Tafel equation

$$i_{in} = i_o \exp(\eta_{in}/b_1) \qquad [31]$$

hence, from equation [30],

$$C = \frac{i_{in}}{b_1} \phi \qquad [32]$$

We note that knowledge of the true Tafel slope b_1 is required to evaluate the capacity from the experimental parameter ϕ. Only under certain conditions, as discussed by Conway and Bourgault (39) (i.e. when the capacity is independent of potential over the range studied) is it justified to take the open-circuit decay slope b_2, defined in equation [27], as equal to the Tafel slope b_1. Equation [32] cannot therefore be used to determine the capacity unless the Tafel slope is known from direct polarization measurements. However, if the open-circuit decay slope b_2 is used instead of b_1 in equation [32] and the capacity is found to be <u>independent</u> of potential, it may be safely assumed that $b_1 = b_2$ and the calculated values of the capacity* are then correct.

(c) <u>Direct Measurements by the A.C. Bridge Method</u>

The most accurate method for the determination of the capacity at a metal solution interface is the a.c. bridge method, where the capacitative and resistive parts of the

---

* Another method for the analysis of open-circuit decay lines by which the capacity can be evaluated, has been suggested by Bockris and Potter (42). This method seems to be rather more complex and no improvement in accuracy is obtained. It appears, however, that the method has never been applied to any experimental results.

electrode impedance are evaluated simultaneously. The method was initially devised to measure the ionic double-layer capacity (43,44,45) and developed to a high degree of precision by Grahame (17). It was later applied to the measurement of adsorption pseudocapacity arising in the hydrogen evolution reaction by Bucken and Weblus (46) and by Breiter (31,32). The theory of Faradaic admittance involved in the interpretation of the a.c. impedance behaviour has been developed by Ershler (20) and Grahame (19).

The intrinsic difficulty in interpreting the capacity measurements obtained by the a.c. bridge method arises from the fact that the measured capacity is usually found to be a function of the frequency of the a.c. signal used. The ionic double-layer capacity is evaluated fairly easily by extrapolating the results to infinite frequency (17). The adsorption pseudocapacity would be obtained by extrapolating to zero frequency (31,46); however, such a procedure is very difficult to achieve experimentally, owing to the problem of obtaining accurate capacity measurements at low frequencies and hence a satisfactory extrapolation to zero frequency. Furthermore, it will not generally be possible to apply the method to porous electrodes or to platinized platinum electrodes which have a roughness factor of the order of 10^3-10^4 and therefore may have a total adsorption pseudo-

capacity of up to several hundred Farads (4,7,39,41).

In spite of the limitations mentioned above, the a.c. bridge method seems to be the most promising one for the study of the detailed structure of the C vs. V curve; such determinations are of great importance as we show below, in determining the kind of adsorption isotherm which applies to the intermediates involved in the electrochemical reaction, thus it is possible to evaluate the extent of variation of the free energy of adsorption with coverage and the roughness factor (9).

(d) Indirect Measurements from the Volume of Gas Desorbed on Open-Circuit

The development of microvolumetric techniques by Conway and Bourgault (41) and later by Ruetschi (48) for the determination of minute quantities of gas evolved from electrodes, has made available an additional method for the determination of the adsorption pseudocapacity. This method is, however, only suitable for porous or highly irregular electrodes having a large real surface area (of the order of $10^4 cm^2$) since it is not possible to measure the amount of gas evolved from, say, a bright metal electrode having a a real surface area of 1 cm^2, even by the most refined technique.

This method was developed and used first by Conway and Bourgault (7) to determine the adsorption pseudocapacity on a fully charged nickel oxide porous electrode. The

electrode was polarized galvanostatically to a steady over-potential, and the change in potential and amount of gas desorbed on open-circuit were followed simultaneously by means of automatic recorders. Since the volume of oxygen desorbed is directly related to the change of coverage on the electrode surface, the adsorption pseudocapacity can be obtained from the slope of a plot of volume of oxygen evolved vs. the potential (7,41). Alternatively, the electrode can be polarized to different overpotentials and the total amount of gas desorbed on open-circuit following steady state polarization measured. The differences in the total volumes of gas evolved on open-circuit following steady state polarization to different current densities will then give the capacity as a function of potential.

The rate of oxygen evolution from charged nickel oxide electrodes following termination of anodic polarization was studied by Conway and Fourgault (7,41) while Ruetschi et al. (48) studied the total volume of oxygen evolved from lead oxide, silver oxide and nickel oxide electrodes and the volume of hydrogen evolved from a porous lead electrode. The latter authors did not use their results, however, to calculate the adsorption pseudocapacity of these electrodes, and explained the slopes of their curves of volume of gas evolved vs.

potential in terms of a different theory.*

We note that the experimentally measured quantity in the method at present under discussion is essentially the change of surface coverage with potential (and time) and the pseudocapacity is obtained from it by differentiating with respect to potential. We choose to discuss this method along with methods where the capacity is measured, rather than those where the coverage is measured, since only changes in coverage, corresponding to a given change in potential, can be obtained in this way. It is obvious that the coverage of the electrode after long times on open-circuit is not necessarily zero, and the absolute value of the coverage can hence only be obtained if the coverage corresponding to a particular value of the potential is known.

4. REVIEW OF THEORETICAL APPROACHES TO THE INTERPRETATION OF EXPERIMENTAL RESULTS IN PREVIOUS WORK

(1) Adsorption Isotherms

The rates of heterogeneous reactions, including electrode processes, depend on the rates of adsorption and desorption of reactants and/or products at the interface, and

---

* This theory was discussed in a paper submitted to the Journal of the Electrochemical Society in 1959, which, to the best of our knowledge, has not yet been published. The arguments in ref. (48), based on this theory will therefore not be discussed here.

hence on the kind of adsorption isotherm obeyed by the system. The isotherm most commonly used is the Langmuir (49) isotherm which can be written as

$$\frac{\theta}{1-\theta} = aP \qquad [33]$$

for the adsorption of noble gases on solids, or the physical adsorption of any other gas. The form more relevant to a number of electrode processes is

$$(\frac{\theta}{1-\theta})^2 = aP \qquad [33a]$$

which applies to the dissociative chemisorption of e.g. diatomic gases. The constant a is related to the standard free energy of adsorption, i.e. to the free energy change in a general dissociative adsorption reaction of the type

$$M + X_2(gas) \longrightarrow 2MX$$

as

$$a = \exp - \Delta G^{\circ}/RT \qquad [34]$$

and P is the partial pressure of the gas being adsorbed. The derivation of this equation relies implicitly on the assumption that the free energy of adsorption is strictly independent of the extent of coverage, in other words, the differential and integral free energies of adsorption are equal throughout the range of coverage. Such can only be the case (a) if the surface of the solid is completely homogeneous, and there are

no induced heterogeneity effects (i.e. the energy of interaction between sites on the surface and the species to be adsorbed is not affected by a surface dipole induced by species already adsorbed on the surface*; and (b) if lateral energies of interaction between adsorbed species are neglibible and (c) if the adsorbed species are immobile on the surface, yet equilibrium between the bulk phase and the interphase is maintained. It is evident therefore, that the Langmuir isotherm is only an approximation, which may or may not be satisfactory for describing the experimentally observed phenomena. The limitations of the Langmuir isotherm in the treatment of electrode reactions will be discussed below in detail.

We have shown above (equation [6]) that the potential dependence of coverage in a pre rate-determining cathodic discharge step at quasi-equilibrium could be obtained assuming Langmuir conditions, viz.

$$\frac{\theta}{1-\theta} = \frac{\vec{i}_o}{\overleftarrow{i}_o} \exp - \eta F/RT \qquad [6]$$

Since we have also defined the adsorption pseudocapacitance

---

* We give below a detailed discussion of this model, which will be referred to as the "Boudart" induced heterogeneity model".

by equation [7], viz.

$$C = \frac{dq}{d\eta} = \frac{k' d\theta}{d\eta} , \qquad [7]$$

it is clear that the adsorption pseudocapacity should be an exponential function of potential.

Frumkin and co-workers (4,22) have demonstrated that the H-adsorption pseudocapacity at platinized platinum is practically constant over a wide potential range. This experimental fact led Temkin (50) to the formulation of a new type of adsorption isotherm (referred to as the "Temkin isotherm" or the "logarithmic isotherm") which takes into account a linear dependence of the free energy of adsorption on coverage.

The original derivation given by Temkin (50) is as follows: it is assumed that the surface of the electrode is made up of small, equal sized patches, to each of which the Langmuir isotherm applies independently. By rearrangement of equation [33] we obtain the well known relationship

$$\theta = \frac{aP}{1 + aP} \qquad [35]$$

which, for each small patch of area dS on the surface will have the form

$$d\theta = \frac{aP}{1 + aP} \, dS \qquad [36]$$

It is further assumed that the free energy of adsorption

decreases (in absolute value) by equal decrements between successive patches, starting from a value ΔG_o at $\theta = 0$ and reaching a value $\Delta G_o - r$ at $\theta = 1$; the free energy of adsorption at the i'th patch will hence be

$$\Delta G_i = \Delta G_o - Sr \qquad [37]$$

where S is the area* already covered by the adsorbed intermediate, so that

$$a_i = a_o \exp -Sr/RT \qquad [38]$$

Combining equations [36] and [38] leads to

$$\theta = \int_o^1 \frac{aP}{1+aP}\, dS = \int_o^1 \frac{a_o P \exp(-Sr/RT)}{1+a_o P \exp(-Sr/RT)}\, dS$$

$$= \int_o^1 \left[\frac{1}{1+(1/a_o P)\exp(Sr/RT)}\right] dS = \left[S - \frac{RT}{r}\ln(1+1/a_o P \quad \exp rS/R\right.$$

$$= \frac{RT}{r}\left[\ln \frac{\exp(rS/RT)}{1+1/a_o P \exp(rS/RT)}\right]_o^1$$

$$= \frac{RT}{r}\left\{\ln\left[\frac{a_o P \exp(r/RT)}{a_o P \exp(r/RT)}\right] - \ln\left(\frac{a_o P}{1+a_o P}\right)\right\} \qquad [39]$$

and hence, finally,

$$\theta = \int_o^1 \frac{aP}{1+aP}\, dS = \frac{RT}{r} \ln \left[\frac{1 + a_o P}{1+a_o P \exp(-r/RT)}\right] \qquad [39a]$$

---

* The quantity S used here is a normalized or fractional surface area, and will vary between zero and unity.

For appreciable values of r (say $r/RT > 10$) we may assume

$$a_o p \exp(-r/RT) \ll 1; \qquad [40]$$

further, at appreciable values of the pressure and hence the coverage we note that

$$a_o p \gg 1 \qquad [41]$$

With these two assumptions,* we obtain the well-known simplified form of the Temkin isotherm, viz

$$r\theta = RT \ln a_o p \qquad [42]$$

It is of some interest to point out that, while the complete Temkin isotherm for dissociative chemisorption has a slightly different form, namely

$$\theta = \frac{RT}{r} \ln \left[\frac{1 + a_o p}{1 + a_o p \exp(-r/RT)}\right]^2 \qquad [39b]$$

as also found in the Langmuir case (cf. equations 33,33a), the simplified form, obtained by combining equations [39b], [40] and [41] is identical with that obtained for the case of

---

* The assumptions made in equations [40] and [41] are not contradictory, since the exponential term exp -r/RT is very small. The condition $a_o p \gg 1$ would lead, with Langmuir behaviour, to $\theta \longrightarrow 1$. This is not the case here, since, as the coverage increases, it becomes increasingly difficult to adsorb further molecules (or atoms) and a much higher pressure is required to reach a given coverage than for Langmuir conditions.

physical adsorption.

It may be argued that the supposition of the existence of surface heterogeneities having a linearly varying energy of adsorption, which is a fundamental assumption in the derivation of the Temkin isotherm, is rather unlikely. This point will be discussed in detail below and it will be shown that several other models, which are probably more sound physically, can also lead to a linear decrease of the free energy adsorption with coverage. Moreover, it must be remembered that Temkin's isotherm was derived initially to explain amongst other things, the constant capacity behaviour observed by Frumkin and co-workers (4,22) and it is in this sense correct even if the model assumed in its derivation seems physically unlikely in the general case.

(ii) Kinetic Equations for Electrode Reactions in Terms of the Langmuir and Temkin Isotherms

In this section, we shall discuss briefly the formulation of kinetic equations for electrode reactions in terms of the Langmuir isotherm and the applications of the Temkin isotherm in regard to deduction of the mechanism of electrolytic hydrogen evolution. A generalization of the latter treatment to rather more complicated electrode reactions (i.e. oxygen evolution) where several intermediates may be adsorbed simultaneously on the electrode surface to an

appreciable extent, will be discussed in a following chapter.

(a) Langmuir Isotherm Applicable

We consider, as before, the hydrogen evolution reaction proceeding through reaction [A] followed by reactions [B] or [C] which we give again below for ease of reference.

$$H_3O^+ + e + M \longrightarrow MH + H_2O \qquad [A]$$

$$H_3O^+ + e + MH \longrightarrow M + H_2O + H_2 \qquad [B]$$

$$MH + MH \longrightarrow 2M + H_2 \qquad [C]$$

If reaction [A] is rate-determining we have, at appreciable overpotential,

$$i = \overrightarrow{i_o} (1-\theta) \exp(-\beta\eta F/RT)^* \qquad [2a]$$

which, at limitingly low coverage, results in a linear Tafel relationship with a characteristic slope of

$$b_1 = d\eta/d \ln i = -RT/\beta F$$

If reaction [B] or [C] is rate-determining, the

---

* We might note here that the exact form of equation [2a] depends on whether the discharge step is followed primarily by atom-atom recombination (equation C) or by ion-atom recombination. In the latter case, the total current is twice that given by equation [2a], since for each charge transfer act in the rate-determining step, another charge transfer occurs in a following step. While the overall rate is seen to depend on the mechanism as a whole, the Tafel slope still remains characteristic of the rate-determining step.

kinetics can generally be treated by the steady state method; however, Parsons (51) has shown that under these circumstances the discharge step can usually be assumed to be practically at equilibrium and treated as though it were at complete equilibrium. Equating the rates of the forward and reverse reactions of the discharge step (equation A), we hence obtain equation [6]

$$\frac{\theta}{1-\theta} = \frac{\overrightarrow{i_o}}{\overleftarrow{i_o}} \exp(-\eta F/RT) \qquad [6]$$

which at low coverage can be written as

$$\theta = K_A \exp(-\eta F/RT) \qquad [6a]$$

where K_A is a constant at constant composition of the solution and at constant temperature.

If ion-atom recombination is rate-determining, we obtain the well-known result

$$i = \overrightarrow{i_o}\, \theta \exp(-\beta \eta F/RT) = K_B \exp[-(1+\beta)\eta F/RT] \qquad [44]$$

and

$$b_1 = -RT/(1+\beta)F$$

or at practically complete coverage, when $\theta \longrightarrow 1$ and is independent of potential

$$b_1 = -RT/\beta F.$$

Alternatively, if atom-atom recombination (reaction C) is rate-determining we have

$$i = \overrightarrow{i}_o \theta^2 = K_C \exp(-2\gamma F/RT) \qquad [45]$$

and

$$b_1 = -RT/2F$$

In this case (for Langmuir conditions) a linear Tafel relationship can only be obtained at low coverage ($1-\theta \doteq 1$) and b_1 will tend to infinity as $\theta \longrightarrow 1$.

Anodic gas evolution reactions (6,7,11) are usually more complex and proceed by more than two steps. The oxygen evolution reaction involves, for example, at least three consecutive reactions such as

$$\begin{aligned} M + OH^- &\longrightarrow MOH + e \\ MOH + OH^- &\longrightarrow MO + H_2O + e \\ MO + MO &\longrightarrow 2M + O_2 \end{aligned} \qquad \text{Scheme A}$$

or

$$\begin{aligned} M + OH^- &\longrightarrow MOH + e \\ MOH + MOH &\longrightarrow MO + H_2O + M \\ MO + MO &\longrightarrow 2M + O_2 \end{aligned} \qquad \text{Scheme B}$$

or a more complicated sequence of consecutive steps such as

$$\begin{aligned} M + OH^- &\longrightarrow MOH + e \\ MOH + OH^- &\longrightarrow MO + H_2O + e \\ MO + OH^- &\longrightarrow MHO_2 + e \\ MHO_2 + MOH &\longrightarrow 2M + H_2O + O_2 \end{aligned} \qquad \text{Scheme C}$$

where M is a site on the surface, and OH^- represents the species from which OH radicals are discharged on the surface (this may be a hydrated OH^- ion or a water molecule).

The kinetics of this reaction have been previously treated in detail (6,61) following arguments similar to those given above for the hydrogen evolution reaction and, in particular, assuming Langmuir conditions. A detailed derivation of the Tafel slopes obtained for oxygen evolution under various limiting conditions was given recently (41) and will not be reproduced here. Two general results of any treatment based on the Langmuir isotherm are relevant to the following discussion: (a) linear Tafel relationships are predicted only for limitingly low or limitingly high coverage conditions (10,13,30); (b) the Tafel slope for a given step decreases the further down it is in a reaction sequence (6,7,10). (thus considering scheme B for oxygen evolution, a Tafel slope of RT/2F is predicted if the second step is rate-determining, while a slope of RT/4F would be predicted if the third step were rate-determining, even though both steps are formally similar "atom-atom" recombination steps). It will be shown below that these are two important aspects in which the predicted behaviour based on a Langmuir isotherm differs from that based on the Temkin isotherm.

(b) Limitations of Calculations Using the Langmuir Isotherm

The inadequacy of the Langmuir isotherm in accounting for the experimentally observed behaviour in various electrode reactions has been referred to above. It may be argued, on general thermodynamic grounds, that equation [6], which is an expression for the equilibrium coverage at a given potential, represents an equilibrium constant in terms of concentrations of reactants and products

$$\frac{\theta}{1-\theta} = \frac{\vec{i}_o}{\overleftarrow{i}_o} \exp(-\eta F/RT) = K(\eta) \qquad [6b]$$

The coverage θ is proportional to the concentration of products (in this case adsorbed hydrogen atoms) and the term $(1-\theta)$ is proportional to the concentration of reactants (free surface sites); since concentrations rather than activities are used to define the constant $K(\eta)$, it will not be a true thermodynamic equilibrium constant, and will be expected to be a function of concentration, or in our case, a function of coverage and overpotential. It could then be further argued that the coverage dependence of $K(\eta)$ in equation [6b] may arise either from a variation of the activity coefficient of products with coverage (due to lateral interaction effects) or that of reactants in the sense of the sites on the metal

(due to induced heterogeneity at the surface).

The above is a rather qualitative argument introduced here only to show that a variation of free energy of adsorption with coverage is expected on general grounds, and that the Langmuir isotherm can only serve as a first approximation. The form of the variation of the free energy of adsorption with coverage can obviously not be predicted from purely thermodynamic considerations.

It was pointed out above that the constant pseudo-capacities observed at the platinum electrode for anodic dissolution of adsorbed hydrogen (4,22) could not be accounted for if the adsorbed atoms obeyed a Langmuir isotherm, and this led to the formulation of the Temkin isotherm (50) where a linear variation of free energy of adsorption with coverage was considered.

Adsorption studies involving the gas/solid interface (56) show that the heat of adsorption decreases with coverage, and in the range $0.1 < \theta < 0.9$ this decrease can be approximately represented in terms of a linear function of θ. This led Parsons (53) to assume that the free energy and the heat of adsorption vary in the same way with coverage, i.e. that the non-configurational entropy of adsorption is practically independent of coverage. The same view was adopted by Thomas (30) in relating the kinetics of hydrogen evolution to

the behaviour of hydrogen adsorbed from the gas phase on metals. A different view is held, however, by some of the German school of electrochemists (25,32,46) who claim that the free energy of adsorption of hydrogen on some noble metals electrodes is independent of coverage (and hence a Langmuir adsorption isotherm is obeyed) owing to a compensation between the changes in enthalpy and entropy with coverage.

Thomas (30) has pointed out that for hydrogen evolution a Tafel slope of less than $RT/\beta F$ can only be predicted at limitingly low coverage ($\theta < 0.1$) if the Langmuir isotherm is obeyed, while such slopes have been observed (54,55,24) at platinum and palladium where the coverage θ was found to be appreciably greater than 0.1 (56,25). A similar argument applies to oxygen evolution where low Tafel slopes have been established in the range where $\theta > 0.5$ (7,39,41). Moreover, a treatment based on the Langmuir isotherm predicts linear Tafel relationships only at extreme values of θ (below 0.1 or above 0.9) while such linear relationships are observed (55,56) for intermediate coverages.

Thomas (30) has further pointed out that in several cases Tafel slopes having a value close to 2.3 RT/F have been observed for hydrogen evolution (57,58,59). Such slopes could not be predicted for hydrogen evolution assuming Langmuir conditions (but see p. 68).

Comparison of Tafel slopes and open-circuit decay slopes constitutes another case where results cannot be accounted for by assuming the applicability of the Langmuir isotherm. It was pointed out by Conway and Bourgault (39) that the relationship

$$\frac{d\eta}{d \ln i} = - \frac{d\eta}{d \ln (1+\phi)} \qquad [46]$$

was only valid when the total capacity at the metal solution interface was sensibly constant over the potential range investigated. Under Langmuir conditions, this could only be the case as $\theta \longrightarrow 0$ or $\theta \longrightarrow 1$, when the adsorption pseudo-capacity is negligible with respect to the ionic double-layer capacity and the variation of the latter with potential may be considered relatively negligible in this case.

Butler and Armstrong (35) found that the Tafel slope and the open-circuit decay slope on platinum during hydrogen evolution were both numerically equal to 2.3 RT/2F. The mechanism indicated is fast discharge followed by slow, rate-determining, atom-atom recombination. Since the coverage of platinum electrodes at $\eta = 0$ is known to be appreciable (4,22), and as $\theta \longrightarrow 1$ the Tafel slope would tend to infinity for this mechanism, the applicability of equation [46] in this case indicates the existence of a constant adsorption pseudo-capacity over an appreciable potential range, which is in

agreement with results of Frumkin and co-workers (4,22) from direct coverage measurements, and cannot be explained assuming Langmuir conditions.

(c) Application of the Temkin Isotherm in Evaluation of Kinetic Equations for the h.e.r.

In the previous section, a short resumé of the general treatment of electrode kinetics in terms of a Langmuir adsorption isotherm was given. It was shown that, in general, the free energy of adsorption should be expected to depend on coverage and a substantial part of the experimentally observed phenomena in the study of the electrode kinetics of reactions involving adsorbed intermediates can only be accounted for if such a dependence is considered.

The Temkin isotherm (50) which, as we have shown, involves the assumption of a linear decrease in free energy of adsorption with increasing coverage, was formulated in 1941. The general kinetic equations for the electrolytic h.e.r. obtained in the range of coverage where this isotherm is applicable, were given by Frumkin and co-workers (55,62) and the consequences of assuming "Temkin" behaviour were more or less implicitly indicated in several later papers (46,63,29, 31,32).

It is perhaps surprising that the bulk of experimental data both in electrode kinetics and non-electrochemical hetero-

geneous reaction kinetics is still often interpreted in terms of a limiting Langmuir adsorption isotherm, even though the formal tools for a better approximation (i.e. the Temkin adsorption isotherm and the consequently modified rate equations) have been available for the last twenty years. Moreover, the Temkin treatment has been restricted, until very recently (8,9,10,61), to the case of the hydrogen evolution reaction. Other electrode reactions, in particular the anodic oxygen evolution, have only been previously discussed in terms of the Langmuir isotherm except in recent work by Conway and Bourgault (for oxygen evolution at the nickel oxide electrode) and by Conway and Dzieciuch (for anodic decarboxylation and the Kolbe reaction).

In order to exemplify the treatment for Temkin conditions, the general rate equations for hydrogen evolution will be given in the present section, following partly the method of presentation given by e.g. Parsons (53), Thomas (30) and Krishtalik (64).

The general rate equations for the discharge step in the h.e.r. and its reverse may be written

$$v_A = k_A (1-\theta) c_{H_3O^+} \exp-[\Delta G^{\neq}_A + \alpha r\theta + \beta VF]/RT \qquad [47]$$

$$v_{-A} = k_{-A}\, \theta \exp-[\Delta G^{\neq}_{-A} - (1-\alpha)r\theta - (1-\beta)VF]/RT \qquad [48]$$

In these and following rate equations the terms $k_n \exp \Delta G_n^{\neq}/RT$ and $k_{-n} \exp \Delta G_{-n}^{\neq}/RT$ represent the specific rate constants of the forward and reverse reaction of the n'th step, respectively, V is the metal-solution potential difference, r is a parameter* determining the rate of variation of the free energy of adsorption with coverages, α and β are symmetry factors (see p. 67) related to the form of the energy barrier for reactions at the metal solution interface and $c_{H_3O^+}$ is the concentration of H_3O^+ in the double layer.**

If a following desorption step is rate-determining, the initial discharge step may be assumed to be in quasi-equilibrium, as we have discussed above. Then putting $v_A = v_{-A}$ we hence obtain

$$\frac{\theta}{1-\theta} \exp\left(\frac{r\theta}{RT}\right) = {}^{1}K_A \exp\left(-\frac{VF}{RT}\right) \qquad [49]$$

---

* From the definition of r in equation [37] it is clear that it should take a negative sign if exoergic free energies of adsorption are to have negative values. In the present and following rate equations we shall use r to represent the absolute numerical value of this parameter to conform with our own (10) and previously published work of others (30,53).

** We shall neglect here, and in the following treatment, all double-layer effects and assume that the concentrations of reactants in the double-layer are not changed during the reaction. In some cases we shall include this constant concentration term in the relevant specific rate constant. The term $\exp(\beta\psi F/RT)$ involving the inner or outer Helmholtz layer potential ψ has also been included in the specific rate constants in all our equations, and ψ has been assumed to be essentially independent of electrode potential. This assumption has been made since we are only interested, in the present discussion, in effects involving the adsorbed intermediate and not the structure and associated potentials in the ionic double-layer.

where ${}^1K_A$ is a constant at constant temperature and composition. This result is to be compared with equation [6] obtained for the same equilibrium assuming Langmuir conditions. The term $\theta/(1-\theta)$ on the l.h.s. of equation [49] is a configurational term, and appears also in equation [6]. We shall refer to it, and to terms derived directly from it (see below), as "the Langmuir term". The exponential term in θ arises from the assumption of a free energy of activation varying linearly with coverage if the free energy of adsorption of intermediates varies linearly with coverage (Temkin isotherm) and will accordingly be referred to as the "Temkin term". At very low values of θ, the exponential term in θ approaches unity and hence equation [49] reduces to equation [6a] i.e. Langmuir behaviour is, in the limiting case, observed. Similarly, at high coverage, the Temkin term becomes practically constant and equation [49] may be rewritten as

$$\frac{\theta}{1-\theta} = {}^1K_A \exp\left(\frac{r\theta}{RT}\right) \exp\left(-\frac{VF}{RT}\right) = {}^2K_A \exp\left(-\frac{VF}{RT}\right) \qquad [49a]$$

which is again a Langmuir isotherm (cf. equation 6a) but with a different free energy of adsorption from that for zero coverage conditions.

At intermediate values of the coverage, the variation of the pre-exponential Langmuir term with θ is negligible with respect to the variation of the Temkin term (cf. 53,30), and

equation [49] then simplifies to

$$\exp\left(\frac{r\theta}{RT}\right) = K \exp\left(-\frac{VF}{RT}\right) \qquad [49b]$$

or

$$r\theta = -VF + \text{constant}$$

Under the same conditions, we may also modify the rate equations [47] and [49], neglecting the pre-exponential terms and obtain

$$v_A = k_A c_{H_3O^+} \exp - [\Delta G_A^{\neq} + \alpha r\theta + \beta VF]/RT \qquad [47a]$$

$$v_{-A} = k_{-A} \exp -[\Delta G_{-A}^{\neq} - (1-\alpha) r\theta - (1-\beta)VF/RT \qquad [48a]$$

This form of the rate equation was used in all previous discussions of electrode kinetics at intermediate coverage in the range where Temkin conditions prevail. We shall show subsequently that neglect of the pre-exponential term in $\theta/(1-\theta)$ in the rate equations is justified à priori only for electrode reactions which proceed through two steps. Moreover, in deducing the corresponding adsorption pseudocapacity behaviour, we show below that the Langmuir term can never be neglected (unless an unreasonably high value is assumed for the parameter r, say $r/RT > 30$) without introducing a substantial error in the evaluation of C as a function of potential.

If we substitute equation [49b] into [47a] and [48a]

it follows that the rates of the discharge step and its reverse are <u>independent of potential</u> so long as they can be considered at equilibrium (the latter condition is necessary for equation [49b] to be valid).

We now examine the case where the electrolytic hydrogen evolution reaction occurs through discharge followed primarily by atom-atom recombination, with the latter rate-determining. Before writing the rate equation for any desorption step we must now discuss the conditions for which activated or non-activated adsorption of hydrogen arises and how this influences the desorption kinetics. In the case of the dissociative chemisorption of molecular hydrogen to form adsorbed hydrogen atoms, the molecules first approach the surface and become physically adsorbed without dissociation. This process requires no activation energy (30,65). The physically adsorbed molecules will then undergo dissociation on the surface and become chemically adsorbed, and, depending on whether the potential energy curves for $H_2 \longrightarrow MH_2$ and $2H \longrightarrow 2MH$ cross above or below the line for zero energy (referred to that of hydrogen molecules at infinite distance from the surface), "activated" or "non-activated" adsorption, respectively, arises. The situation is represented schematically in Figs. 5a and 5b. It is obvious from these figures, that if adsorption is non-activated, any change in

Figure 5. Schematic potential energy diagrams for non-activated and activated adsorption conditions.

a) Non-activated adsorption case. Energy of desorption = activation energy for desorption.

b) Activated adsorption case; curves across above the zero energy line.

c) Intermediate activated adsorption case; curves cross above the zero energy line only at finite coverage but not at zero coverage.

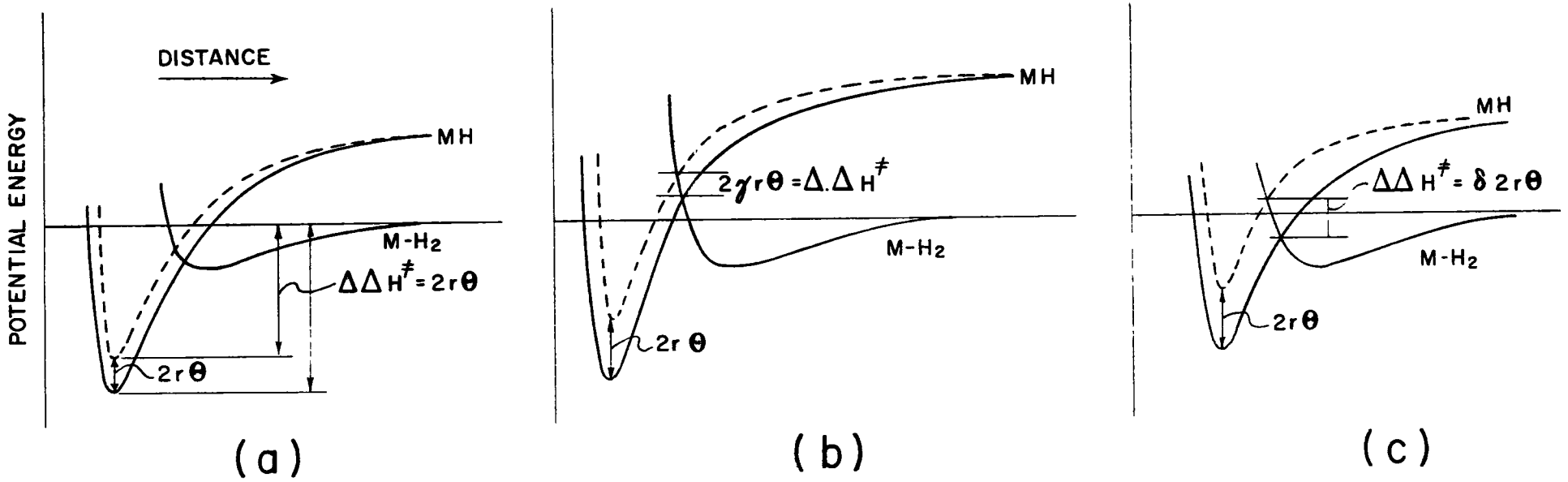
POTENTIAL ENERGY
DISTANCE
MH
M-H2
ΔΔH≠ = 2rθ
2rθ
(a)
MH
2γrθ = Δ.ΔH≠
M-H2
2rθ
(b)
MH
ΔΔH≠ = δ 2rθ
M-H2
2rθ
(c)

the free energy of adsorption ΔG of the atomic or radical intermediates (i.e. due to the dependence of ΔG on θ, as discussed above) will result in a numerically equal change in the free energy of activation for the desorption process. Conversely, if the molecular adsorption to form atoms is activated, the change in free energy of activation for the desorption process will amount to a fraction α of the total change in free energy of adsorption, where α is a symmetry factor in the usual sense used in electrode kinetics, i.e. it is related to the relative slopes of the potential energy curves for the initial and final states but is not necessarily equal to the symmetry factor β for the charge transfer step.*

The rate equation for atom-atom recombination at intermediate coverage, when the pre-exponential term in θ is negligible with respect to the exponential term, is then

---

* We shall use the symmetry factors α and β for terms involving θ and V, respectively in all our rate equations. It is well understood that a characteristic symmetry factor should be used, in principle, for each step, but in view of the lack of detailed information regarding the actual numerical values of these parameters for different steps in electrode reactions, we shall assume throughout this thesis that $\alpha = \beta = 0.5$ for all the reactions steps to be discussed. For a simple discharge step producing an intermediate, it will be generally true that $\alpha = 1-\beta$.

$$v_C = k_C \exp - [\Delta G_C^{\neq} - 2ar\theta]/RT \qquad [50]$$

when adsorption of hydrogen is activated

or

$$v_C = k_C \exp - [\Delta G_C^{\neq} - 2r\theta]/RT \qquad [51]$$

when it is non-activated. Substituting the value of $r\theta$ in terms of potential from equation [49b] and differentiating V with respect to ln i then gives

$$dV/d \ln i = -RT/2aF^{*}$$

or

$$dV/d \ln i = -RT/2F$$

for conditions of activated and non-activated adsorption of hydrogen, respectively.

Thus, activated adsorption can lead, under Temkin conditions, to a Tafel slope of about 0.058 volt (with $a \doteq 0.5$) in agreement with some experimental results (57,58,59,60). This slope, deduced by Thomas (30)** for this mechanism, is characteristic of a radical desorption step in which molecule production occurs.

Non-activated adsorption leads to a Tafel slope of $RT/2F = 0.029$ volt, which is numerically equal to that predicted

---

* Horiuti and co-workers (63,101,102) have deduced a Tafel slope of 1.5 RT/F to RT/F, for the recombination mechanism, taking into account lateral interaction effects. Their conclusions depend on a rather particular set of energy parameters, and were disregarded in most later discussions of this mechanism (cf. ref. 30,58,64).

** The same slope was, however, previously deduced for "first order recombination" (66) or slow diffusion of H atoms to recombination sites (67) under Langmuir conditions at low coverage.

for the same mechanism under Langmuir conditions. This result should, nevertheless, be considered "new" in the sense that it applies to intermediate values of the coverage which most likely arise at metals (e.g. Pt or Pd) where this slope is observed experimentally. We note also that due to the slower, linear, variation of θ with potential under Temkin conditions (cf. equation 49b), a constant Tafel slope of $RT/2F$ may be observed over a much wider range of potentials than in the Langmuir case. Anticipating some of the original numerical calculations to be given below, we find that if $\theta\ (\eta = 0) = 0.01$ the characteristic recombination slope will only be observed under Langmuir conditions over about 0.06 volt. If Temkin conditions prevail, however, at intermediate coverage values with, say, a value of $r = 5$ Kcal.g. equiv.$^{-1}$, the same slope could be observed over a range of 0.35 volts.

A similar treatment may be given for the rate-determining ion-atom recombination reaction (reaction B) at intermediate coverage; the rate equations are

$$v_B = k_B c_{H_3O^+} \exp - [\Delta G_B^{\ddagger} - \alpha r\theta + \beta VF]/RT^* \qquad [52]$$

---

* The symmetry factors α and β appearing in this equation may be quite different (unlike in most cases) since they refer to different pairs of potential energy curves, representing sections of the potential energy surface in different directions. This arises since effects of potential on the energy of the H_3O^+ ions and electrons in the initial state must originate in a different way from effects of changing adsorption energies of the adsorbed H in the initial state. We shall nevertheless take $\alpha=\beta=0.5$ in this case, as in all other cases.

for activated adsorption and

$$v_B = k_B c_{H_3O^+} \exp -[\Delta G_B^{\ddagger} - r\theta + \beta VF]/RT \qquad [53]$$

for non-activated adsorption. Upon substitution of $r\theta$ in terms of VF from equation [49b] we obtain the Tafel slopes

$$dV/d \ln i = -RT/(\alpha + \beta) F \doteq -RT/F$$

and

$$dV/d \ln i = -RT/(1 + \beta) F \doteq -(2/3)RT/F$$

for activated and non-activated adsorption, respectively.

The slope RT/F, obtained if adsorption is activated, is characteristic of radical desorption steps in which molecules are produced, as pointed out above. It is seen that the same Tafel slope is predicted for both reactions (B) or (C) if rate-determining. A similar result, namely that different mechanisms give rise, under Temkin conditions, to the same value of the Tafel slope, will be deduced in the discussion of rather more complicated anodic reaction sequences to be presented in the chapters on original calculations. In general, the Tafel slopes for reactions proceeding under Temkin conditions are less diagnostic of reaction mechanism than they can be under Langmuir conditions.

The possible variations in Tafel slopes with potential

for the mechanism discussed above (fast discharge followed by slow rate-determining ion-atom desorption) are of some interest. At very low coverage (assuming that $\theta(\eta = 0)$, is, say, less than 0.01) the Temkin term is negligible in any case and a slope of $-RT/(1+\beta)F \doteq 0.038$ volt obtained under Langmuir conditions, will be observed. As the cathodic overpotential is increased, the Temkin region can be reached (corresponding roughly to $0.2 < \theta < 0.8$) where a Tafel slope of $-RT/2\beta F \doteq 0.058$ volt may be obtained. With further increase in cathodic overpotential another Langmuir region is entered, corresponding in this case to a Tafel slope of $-RT/\beta F \doteq 0.116$ volt. On account of the relatively slow variation of θ with V in the Temkin region, we may, in principle, expect to find three long and well defined linear Tafel regions, which might ordinarily be explained in terms of three apparently different mechanisms. Such a course of current-potential behaviour does not appear to have been observed experimentally. We have introduced this example only to indicate the added difficulty in interpreting experimental results, arising from what appears to be an unavoidable necessity of introduction of the Temkin terms into the rate equations (cf. ref. 53).

We believe (contrary to the view of Thomas (30)) that conditions of non-activated adsorption, leading in this case to a Tafel slope of 0.038 volt, are as likely for the ion-atom recombination step as they are when desorption occurs

by an atom-atom recombination mechanism. The initial state for the ion-atom desorption step consists of the species, MH, H_3O^+ and the electrons in the metal. The ground state of the first entity is affected by the change in free energy of adsorption with coverage and provided that the energy of the activated state is still negative with respect to the energy of free molecular hydrogen (i.e. adsorption is non-activated), the free energy of activation for the whole desorption step will be changed by an amount numerically equal to half the change in free energy of adsorption per mole which results from an increase of surface coverage (Temkin isotherm applying). The term in potential will always contain the usual symmetry factor (whether adsorption is activated or non-activated) because only part of the potential drop across the interphase will be operative in forming the activated complex, or, in other words the electrochemical potential of the activated state will be intermediate between that of the final and initial states (51).

Only two extreme cases have been discussed by Thomas (30) when adsorption is activated or non-activated throughout the range of coverage considered. We can however consider an intermediate, and probably more general, case when at a coverage corresponding to $\eta = 0$ adsorption is non-activated, but as the potential energy curve for MH is moved upward with increasing coverage (and associated increase in cathodic potential), a point is reached when activated adsorption

sets in (see Fig. 5c). Consequently the Tafel slope will change slowly from -0.029 volts or -0.038 volt to -0.059 volt, in a manner similar to that due to a change in mechanism (16). However, while a dual mechanism leading to a non-linear Tafel relationship can normally only be effective over a short potential range, the non-linear Tafel region due to transition from non-activated to activated adsorption may extend over several hundred millivolts on the potential scale.

It may be argued that the Tafel slopes calculated for non-activated adsorption at intermediate coverage (i.e. -0.029 volt and -0.038 volt) will never be realized in practice, since under these conditions the surface will be almost completely covered. This, in fact, is found to be the case for adsorption from the gas phase. However, it was pointed out by Thomas that the extent of coverage by hydrogen atoms in solution will be reduced, compared with that in the gas phase, to an extent depending on the relative free energies of adsorption of hydrogen and water molecules in the interphase. Little quantitative information is, however, available for adsorption of water. Kemball (69) found the heat of adsorption of water at mercury from the vapour phase to be 17.6 Kcal.mole^{-1}. On more strongly adsorbing metals the figure may be expected to be even higher. The competitive adsorption of water could therefore decrease the extent of coverage θ_H of the surface by hydrogen to an appreciable extent and lead to intermediate

values of θ_H under non-activated conditions (specifically adsorbed anions in the solution may lead to a further decrease in θ_H, cf. (32)). Experimentally, these conditions of non-activated adsorption under Temkin conditions are indicated for the hydrogen evolution behaviour on Pt and on Pd, as discussed above.

(iii) <u>The Form of the Variation of Adsorption Pseudo-Capacity with Potential</u>

The Temkin isotherm in its simplified form, when the Langmuir term is altogether neglected, leads to a linear dependence of coverage on potential as we have shown above, viz.

$$r\theta = -VF + \text{constant} \qquad [49b]$$

and consequently to a <u>constant</u> adsorption pseudocapacity given by

$$C_T = -k' \, d\theta/dV = k' F/r \qquad [54]$$

where we have added the subscript T to indicate that it is a term arising under Temkin conditions in the sense defined above. The rather limited applicability of this equation will be discussed below, where we shall show that the pseudocapacity can never be considered strictly constant. The total adsorption pseudocapacity will be close to C_T only for appreciable values of r. Taking, say, r = 10 Kcal.equiv.$^{-1}$ and substituting

numerical values into equation [54] we obtain approximately

$$C_T = \frac{10^{15} \times 1.6 \times 10^{-19} \times 10^5}{4.2 \times 10^4} = 3.8 \times 10^{-4} \text{F.cm}^{-2} = 3.8 \times 10^2 \mu\text{F.cm}^{-2}$$

where the number of sites per cm^2 of real surface area is taken as 1×10^{15}*. The Temkin pseudocapacity, even for appreciable values of r can hence be about an order of magnitude higher than the ionic double-layer capacity with which it lies in parallel, and should be easily distinguishable from it. On the other hand, it is appreciably lower than the "Langmuir pseudocapacity" as we shall show below.

Sucken and Weblus have shown (46) that the adsorption pseudocapacity is a simple function of coverage, if Langmuir conditions are assumed to prevail, as follows

$$C_L = \frac{k'F}{RT}\theta(1-\theta) \qquad [55]$$

This function has a maximum value at $\theta = 0.5$ given by

$$C_L(\max) = \frac{k'F}{4RT} = \frac{1.6 \times 10^{-4} \times 10^5}{4 \times 8.3 \times 300} \times 10^6 \doteq 1.6 \times 10^3 \mu\text{F.cm}^{-2}$$

a value which is appreciably greater than that obtained for the Temkin term C_T above with the same value of k'. The potential

---

* The same value for k' will be used throughout the following general discussion of pseudocapacity. It is obvious that the exact value of k' depends on the nature (size and electrochemical valence) of adsorbed intermediates and the geometry of the adsorbent surface. The form of the C-V curves will, however, not depend on the numerical value of k'.

dependence of C_L has been previously calculated (70) and it was found that C_L would only be appreciable over a limited potential range (ca. 0.2 volt). It was also shown that from the overpotential at which the maximum in the C-η curve occurs, the coverage at the reversible potential ($\eta = 0$) could be calculated. This method is, however, limited to cases where a Langmuir isotherm is strictly obeyed at all values of the coverage.

Eucken and Weblus (46) have also given an expression for the dependence of total adsorption pseudocapacity on coverage when both a Temkin and a Langmuir term are included, viz.

$$C = \frac{k'F}{RT} \times \frac{\theta(1-\theta)}{1+(r/RT)\theta(1-\theta)} \qquad [56]$$

but they did not attempt to examine the numerical or quantitative significance of this equation. Their expression can be reduced to a form derived in a different way by Conway and Gileadi (10) (see below). It leads to a maximum value of the pseudocapacity given by

$$C(max) = \frac{k'F}{RT} \times \frac{1}{4+r/RT} \qquad [57]$$

It is seen that

$$\lim_{r \to 0} C(max) = C_L(max)$$

and

$$\lim_{r \to \infty} C(max) = C_T$$

Taking r = 10 Kcal/equiv., the numerical value of C(max) is seen to be

$$C(max) = \frac{1.6\times10^{-4}\times10^{5}}{8.3 \times 300} \times \frac{1}{4+16.7} \times 10^{6} = 3.1 \times 10^{2}\ \mu F.cm.^{-1}$$

i.e., somewhat lower than C_T obtained for the same value of r.

The H-pseudocapacity of noble metals under steady state cathodic polarization was measured by Bucken and Weblus (46) and later by Breiter (31,32) by the a.c. bridge method as a function of potential. Two maxima were observed and were interpretated by the above authors as being due to Langmuir type adsorption at two crystallographically different surfaces. The peaks were found 0.12 volt apart, corresponding to a difference of 2.8 Kcal/equivalent in the free energies of adsorption on the two kinds of surfaces exposed. The above interpretation could easily be confirmed by repeating the measurements on single crystal electrodes, where a single peak should be observed. Results of such experiments have not been published. Conway, Gileadi and Dzieciuch (8) have reported single peaks in the C-V plot for the anodic decarboxylation reaction with formate ions in formic acid at noble metal electrodes. These results will, however, be examined in more detail below.

CHAPTER II

NEW CONTRIBUTIONS TO THE THEORY OF CONSECUTIVE REACTION KINETICS AT INTERMEDIATE COVERAGES

1. THE ORIGIN OF THE VARIATION OF HEAT AND FREE ENERGY OF ADSORPTION WITH COVERAGE

It has been shown above that general thermodynamic considerations regarding the activities of components in the surface phase lead to the conclusion that the free energy of adsorption is a function of coverage so that the Langmuir isotherm can, in most cases, serve only as a first approximation. Experimental evidence from gas phase adsorption studies (52,71,72) shows that the heat of adsorption usually decreases with coverage in an approximately linear manner at intermediate values of the coverage. The behaviour of adsorbed intermediates in electrode reactions (4,7,8,22,30,39) and in particular the dependence of adsorption pseudocapacity on potential is, in a number of cases, consistent with the assumption of a linearly decreasing free energy of adsorption with coverage.

In this chapter, we shall first discuss the different models which could lead to a decrease in free energy of adsorption with increasing coverage and then examine the kinetic consequences of applying these models to electrochemical reactions

For simple electrode reactions, where a single

adsorbed intermediate is involved (e.g. in the hydrogen evolution reaction) equations [47a] and [48a] can be rewritten as

$$v_A = k_A c_{H_3O^+} \exp -[\Delta G_A^{\neq} + a f(\theta) - \beta VF/]/RT \qquad [47b]$$

$$v_{-A} = k_{-A} \exp - [\Delta G_{-A}^{\neq} - (1-a) f(\theta) + (1-\beta) VF]/RT \qquad [48b]$$

where we have written the adsorption energy term $r\theta$ of equations [47a, 48a] in a general form as $f(\theta)$, and $f(\theta)$ may now be <u>any</u> simple function of θ. Equation [49b] will then take the form

$$f(\theta) = VF + \text{const.} \qquad [49c]$$

and if the latter relationship is introduced into, say, equation [50], which now has the form

$$v_C = k_C \exp -[\Delta G_C^{\neq} - 2a f(\theta)]/RT \qquad [50a]$$

the same result is obtained as when $f(\theta)$ was taken simply as equal to $r\theta$.

It is evident, therefore, that the exact form of the variation of ΔG with θ does not affect the kinetics of simple electrode reactions when a single adsorbed intermediate is involved and this is a conclusion of some general importance. However, for complex reactions involving two or more intermediates, the results will depend slightly on the model used to account for the variation of free energy of adsorption with

coverage. We shall therefore discuss first the various possible models, and then work out the kinetic equations for a particular case, the oxygen evolution reaction, in terms of each model. This case is chosen / since the reaction involves more than two consecutive steps and more than one adsorbed intermediate. It is also relevant to previously published work from this Laboratory and to some of the experimental work to be described in Chapters IV and V.

(i) Intrinsic Heterogeneity of the Surface

This factor is the one considered in the model originally examined by Temkin (50), who assumed that the electrode catalyst surface was heterogeneous on the atomic scale, and different sites on it had intrinsically different affinities for the adsorbate. While the concept of a heterogeneous surface is physically sound and is well recognized in general theories of catalysis, and probably also accounts in most cases for at least a part of the total change in free energy of adsorption with coverage, it would seem rather fortuitous that the affinities of sites (or small groups of sites) would vary linearly* with coverage, as postulated by

---

* This is, of course, not the only distribution of adsorption energies associated with heterogeneity of the surface that has been considered. An exponential distribution has, for example, been considered by Zeldovich (83).

Temkin. It should be remembered, however, that a wide Gaussian distribution of affinities of sites may, at intermediate coverage, behave as one effectively involving an almost flat maximum (i.e. leading to the required linear relationship). Moreover since the Temkin isotherm is really applicable only at intermediate values of the coverage, the deviations from linearity in the relation between free energy of adsorption and coverage at extreme values of the coverage will not usually be significant in any case.

(11) Interaction Effects

Lateral interaction effects might seem to be the most obvious reason for the experimentally observed fall of heats of adsorption with coverage. It has been shown, however, by Boudart (72) and others (73) that two-dimensional interaction energies are generally not large enough to account for most of the changes of heats of adsorption with coverage which have been observed in various adsorbent-adsorbate systems. Moreover, ion-ion and dipole-dipole repulsions can lead to a decrease of energy of adsorption with $\theta^{1/2}$ and $\theta^{3/2}$, respectively, and the experimentally observed approximately linear relationship between the heat of adsorption and θ (at intermediate coverage) could not be explained.* At high

* Conway, Gileadi and Dzieciuch (9) have reported an experimental case consistent with a dipole-dipole repulsion effect. This model should not, therefore, be completely disregarded. Similarly, dipole repulsion effects are important in oriented monolayers of surface active molecules as shown by Mitchell (100) and by Barradas and Conway (84).

coverage, the "London" dispersion forces may become important and lead to an attraction term in θ^3 which may decrease or even reverse any long range electrostatic repulsion forces at short distances. This attractive effect would be largely operative at high coverages, where the Langmuir term is predominant in any case, and would hardly be expected to be significant experimentally.

(iii) "Induced Heterogeneity" Effects

The physical picture of "induced heterogeneity" as discussed by Boudart (72) is that the affinity of a particular surface site towards the adsorbate is changed on account of adsorption at other sites. The term "induced heterogeneity" was adopted by Boudart for this kind of long range interaction effect, since it leads to a differential free energy of adsorption gradually changing with coverage on a surface assumed to be initially intrinsically homogeneous.

The Russian workers have developed (64,74,75,76) an induced heterogeneity model, based on the assumption of a two-dimensional electron gas at the metal surface, and the theoretical treatment of this model leads to a linear decrease of heat of adsorption with coverage. The idea of induced heterogeneity (without reference to its cause) was also implicitly used by Eucken (71) to explain the kinetics of

hydrogen adsorption on nickel from the gas phase. Boudart (72) has proposed a model in which the adsorbed intermediates set up a surface potential proportional to the coverage (cf. the Helmholtz equation) which causes a change in the electronic work function of the metal. This change in work function is hence a linear function of coverage, so that the heat of chemisorption, which is normally determined in part by the work function (85) is then linearly related to the change in the latter.

The surface dipole model proposed by Boudart seems the most acceptable, since it depends on simple electrostatic considerations and is consistent with well known, experimentally measurable, changes in electronic work functions due to adsorption. The electron gas model, however, leads to the same electrochemical kinetic and capacity equations as in the case of the Boudart model.

2. FORMULATION OF KINETIC EQUATIONS FOR SYSTEMS OBEYING A LOGARITHMIC (TEMKIN) ISOTHERM, WHEN SEVERAL ADSORBED INTERMEDIATES MAY BE INVOLVED

In the previous section, we have discussed the various models leading to a coverage-dependent free energy of adsorption. We have referred to the fact that the induced heterogeneity model of Boudart (72) can offer the best account of the linear

variation of heat of adsorption with coverage, but other models may nevertheless be of some importance in certain cases. Thus, we may anticipate some contributions from all three effects (viz. induced heterogeneity, intrinsic heterogeneity and interaction effects) depending on coverage and the chemical nature of the adsorbate and adsorbent. We shall now proceed to discuss the kinetics of complex anodic reactions involving more than one adsorbed intermediate, in particular the oxygen evolution reaction, in terms of the various models, laying the main emphasis on Boudart's model.

(i) Kinetic Equations Arising for the Case of Intrinsic Heterogeneity

Here we first consider briefly the consequences of assuming that the variation of heat of adsorption with coverage is due to an intrinsic heterogeneity of the surface. If there is no specificity of surface sites for two or more adsorbed intermediates at a total coverage θ_T (which will be the case if they are chemically similar, as in the oxygen evolution reaction where OH and O species are involved), we can write, in general, for intermediates A and B

$$\Delta H_A = \Delta H_A^o - r_A\theta_T; \quad \Delta H_B = \Delta H_B^o - r_B\theta_T \qquad [58]$$

since the energy of adsorption of a given species will depend on the sites remaining just beyond the total coverage θ_T and

the r values define the distribution (assumed linear) of energies of adsorption with total coverage. It is not necessary that $r_A = r_B$, since the variation of the energy of chemisorption of the species A and B with coverage probably depends on the electronegativity difference between the sites and each of the species adsorbed. In many cases it will, however, be legitimate to regard $r_A \doteqdot r_B$ particularly where the species are chemically similar, as in the oxygen evolution case for O and OH adsorption. When there is complete specificity of sites for the two or more species, the surface behaves essentially as a mixture of two types of surfaces with independent properties for each of the species, so that

$$\Delta H_A = \Delta H_A^o - r_A\theta_A; \quad \Delta H_B = \Delta H_B^o - r_B\theta_B \qquad [59]$$

It is unlikely that this case applies to most electrochemical reactions including the oxygen evolution reaction.

We may proceed now to consider steps in the oxygen evolution reaction, which occurs through one of the now well-known (6,7,13) following schemes, as discussed above (other schemes could be devised and treated in an analogous way)*

I		M	+	OH^-	$\longrightarrow$	MOH	+	e		
II		MOH	+	OH^-	$\longrightarrow$	MO	+	H_2O	+ e	Scheme A
III		MO	+	MO	$\longrightarrow$	2M	+	O_2		

* In the oxygen evolution case considered here, the site M may be a site on the bare metal or on an oxide film formed on the metal. The nature of the sites involved will not influence our general discussion.

or

I	$M + OH^- \longrightarrow MOH + e$		
IV	$MOH + MOH \longrightarrow MO + H_2O + M$	Scheme B	
III	$MO + MO \longrightarrow 2M + O_2$		

or

I	$M + OH^- \longrightarrow MOH + e$		
II	$MOH + OH^- \longrightarrow MO + H_2O + e$		
V	$MO + OH^- \longrightarrow MHO_2 + e$	Scheme C	
VI	$MHO_2 + MOH \longrightarrow 2M + H_2O + O_2$		

Assuming that the primary discharge step I is in quasi-equilibrium, when followed by rate-determining II or IV we obtain

$$r_{OH}\,\theta_T = VF + \text{constant} \qquad [60]$$

which is the equivalent of equation [49b] for an anodic process. If step II is rate-determining, we have

$$v_2 = k_2\,\theta_{OH}\,c_{OH^-}\exp -[\Delta G_2^{\neq} - \alpha\, r_{OH}\theta_T + (1-\alpha) r_0\theta_T - \beta VF]/RT \qquad [61]$$

Taking $\alpha = \beta = 0.5$ and substituting the value of VF from equation [60] into equation [61] we obtain

$$v_2 = K_2 \exp (2r_{OH} - r_O)\,\theta_T/2RT \qquad [61a]$$

where K_2 includes all terms which do not contain θ_T or V* and the variation of the pre-exponential term in θ_T has been

---

* We shall mark all constants derived from the nth equation with the subscript n and an ordinal number superscript.

neglected for conditions of appreciable coverage - the case we wish to investigate. Using equation [60] to substitute θ in terms of potential into equation [61a], we obtain

$$v_2 = {}^1K_2 \exp\left(\frac{2r_{OH} - r_0}{r_{OH}}\right) VF/2RT \qquad [61b]$$

which gives a Tafel slope of

$$dV/d \ln i = \left(\frac{2RT}{F}\right)\left(\frac{r_{OH}}{2r_{OH}-r_0}\right)$$

Similarly, if step IV were rate-determining, we would obtain

$$v_4 = k_4 \theta_{OH}^2 \exp -[\Delta G_4^{\neq} - 2\alpha r_{OH} \theta_T + (1-\alpha) r_0 \theta_T]/RT \qquad [62]$$

which, under the same assumptions, can be written as

$$v_4 = {}^4K_4 \exp (2r_{OH}-r_0) \theta_T/2RT \qquad [62a]$$

leading obviously to the same Tafel slope as that when step II is rate-determining.

These equations give the same limiting results when $r_{OH} = r_0$ as the general treatment in terms of $f(\theta)$ for the induced heterogeneity model to be given below. It is also important to note, as with $f(\theta)$, that the exact form of the function of θ_T in equation [58] is immaterial, as it will always be eliminated when equation [60] is used to substitute for this function of θ_T in the rate equations in terms of VF. Any arbitrariness in assuming a <u>linear</u> function in θ_T in equation [60] is hence not of importance in the general deduction of

kinetic current-potential equations and Tafel slopes. We shall show, however, that the nature of this f(θ) is important in regard to the form of the potential and coverage dependence of the associated adsorption pseudocapacitance to be discussed further below.

A rate-determining terminal desorption step, such as III will lead to

$$v_3 = k_3 \theta_0^2 \exp -[\Delta G_3^{\neq} - 2\alpha r_0 \theta_T]/RT \qquad [63]$$

for activated adsorption of oxygen atoms from molecular oxygen. Substitution of θ_T in terms of potential from equation [60] and with the same approximations as in the previous cases, then leads to a Tafel slope of

$$dV/d \ln i = (\frac{RT}{F}).(\frac{r_{OH}}{r_0})$$

when reaction III is rate-determining. The results derived on the basis of à priori heterogeneity in the limiting case when the r values for various intermediates are identical will, in general, be the same as those which will be deduced below on the basis of the Boudart model. However, since the r values need not, in principle, be quite identical, the intrinsic heterogeneity model allows of the possibility of some variation of the Tafel slopes from the limiting values (viz. 2RT/F for step II or IV rate determining and RT/F for step III rate-determining, when O_2 adsorption is activated) which can be

derived if the r values are assumed equal.

(ii) Kinetic Equations Arising in the Case of Strong Lateral Interaction Effects

Here we consider two kinds of adsorbed species A and B (say the OH and O radicals in the oxygen evolution reaction) and assume that the fall of heat of adsorption with increasing coverage is entirely due to lateral interactions. Let ε_{AA}, ε_{BB} and ε_{AB} represent the lateral interaction energies between two species of the kind indicated by the subscript. The heat of adsorption of each species will be modified by terms corresponding to interactions with radicals of its own kind and with any other kind in proportion to the partial coverage by each species; thus

$$\Delta H_A = \Delta H_A^o - k(\varepsilon_{AA}\theta_A + \varepsilon_{AB}\theta_B)^* \qquad [64]$$

and

$$\Delta H_B = \Delta H_B^o - k(\varepsilon_{BB}\theta_B + \varepsilon_{AB}\theta_A) \qquad [65]$$

where k is a proportionality constant and the other terms have been defined previously. If we assume that the interactions are purely electrostatic,** we may use the approximation

---

* It would be physically more consistent with our arguments to use here a function θ^n (n=0.5 or 1.5). We have avoided this for the sake of convenience after it had been proved that the exact form of $f(\theta)$ does not affect our results.

** The only experimental evidence consistent with this model (9) indicates a dipole-dipole type interaction effect. "London" dispersion forces would not be important in any case except at high coverage, as we have already discussed above.

$$\varepsilon_{AB} = 1/2 \ (\varepsilon_{AA} + \varepsilon_{BB}) \qquad [66]$$

This can be written as

$$\varepsilon_{AB} = 1/2 \ (\varepsilon_{AA} + \gamma \varepsilon_{AA}) = (\tfrac{1+\gamma}{2}) \varepsilon_{AA} \qquad [67]$$

where γ is defined as the ratio of two ε values

$$\gamma \equiv \varepsilon_{BB} / \varepsilon_{AA}$$

Equations [64] and [65] can now be rewritten as

$$\Delta H_A = \Delta H_A^o - k[\theta_A + (\tfrac{1+\gamma}{2})\theta_B] \varepsilon_{AA} = \Delta H_A^o - f_A(\theta_T) \qquad [64a]$$

$$\Delta H_B = \Delta H_B^o - k[(\tfrac{1+\gamma}{2})\theta_A + \gamma\theta_B] \varepsilon_{AA} = \Delta H_B^o - f_B(\theta_T) \qquad [65a]$$

where $f_A(\theta_T)$ and $f_B(\theta_T)$ are functions of the coverage by <u>both</u> species, as defined by equations [64a] and [65a]. We note that γ may, in general, take any numerical value. For the oxygen evolution reaction, however, where 'A' and 'B' correspond to chemically similar species, the value of γ would be expected to be close to unity.

Consider, for example, scheme A (see p. 35) for oxygen evolution, and let the initial discharge step be in quasi-equilibrium, as has been assumed in the treatments examined above. We obtain, with the usual approximation for intermediate coverage

$$f_A(\theta_T) = VF + \text{constant} \qquad [68]$$

which can be written explicitly as

$$k[\theta_A + (\tfrac{1+\gamma}{2})\theta_B]\ \varepsilon_{AA} = VF + \text{constant} \qquad [68a]$$

where A and B represent 'OH' and 'O' radicals adsorbed at the surface, respectively. If step II is rate-determining, we have

$$v_2 = k_2\theta_A \exp -[\Delta G_2^{\neq} - \alpha f_A(\theta_T) + (1-\alpha)f_B(\theta_T) - \beta VF/RT \qquad [69]$$

or

$$v_2 = {}^2K_2 \exp [f_A(\theta_T) - f_B(\theta_T) + VF]/2RT \qquad [69a]$$

if $\beta = \alpha = 0.5$.

Substituting $f_A(\theta_T)$ and $f_B(\theta_T)$ from equations [64a] and [65a], respectively, we obtain

$$v_2 = {}^2K_2 \exp [k\ \varepsilon_{AA}(\tfrac{1-\gamma}{2})(\theta_A + \theta_B) + VF]/2RT \qquad [69b]$$

When step II is rate-determining, the surface will tend to be primarily covered with OH radicals, hence $\theta_A \gg \theta_B$ and

$$f_A(\theta_T) \doteq k\ \varepsilon_{AA}\ \theta_T = r_A\theta_T = VF + \text{constant} \qquad [70]$$

where r_A is the now familiar constant determining the rate of variation of the free energy of adsorption of species A with coverage. Substituting equation [70] into [69b] then leads to

$$v_2 = {}^3K_2 \exp [(\tfrac{1-\gamma}{2})\ VF + VF]/2RT = {}^3K_2 \exp[(3-\gamma)VF]/4RT \qquad [69c]$$

and the resulting Tafel slope is

$$dV/d \ln i = (\tfrac{2RT}{F})\ (\tfrac{2}{3-\gamma})$$

when reaction II is rate-determining.

When $\gamma = 1$, i.e. $\varepsilon_{AA} = \varepsilon_{BB}$, the Tafel slope becomes $2RT/F$ which is identical with the result obtained above for the same mechanism using the intrinsic heterogeneity model and assuming $r_A = r_B$.

The treatment becomes somewhat more complicated if the terminal desorption step III (see p. 85) is rate-determining and both steps I and II are assumed to be at quasi-equilibrium. For reaction I at quasi-equilibrium, we have as before

$$d\left[\theta_A + \left(\frac{1+\gamma}{2}\right)\theta_B\right]\varepsilon_{AA} = VF + \text{constant} \qquad [68a]$$

Equating the forward and backward rates for reaction II

$$k_2\theta_A \exp-[\Delta G^{\neq}_2 - \alpha f_A(\theta_T) + (1-\alpha)f_B(\theta_T) - \beta VF]/RT =$$

$$k_{-2}\theta_B \exp-[\Delta G^{\neq}_{-2} + (1-\alpha)f_A(\theta_T) - \alpha f_B(\theta_T) + (1-\beta)\,VF]/RT \qquad [71]$$

hence

$$\frac{\theta_A}{\theta_B} \exp\left[f_A(\theta_T)\right]/RT = {}^{4}K_2 \exp\left(-VF/RT\right) \qquad [71a]$$

Following substitution of $f_A(\theta_T)$ and $f_B(\theta_T)$ from equation [64a] and [65a], respectively, equation [71a] gives

$$\frac{\theta_A}{\theta_B} \exp[k\varepsilon_{AA}(\frac{1-\gamma}{2})\theta_T]/RT = {}^{4}K_2 \exp\left(-VF/RT\right) \qquad [71b]$$

In equation [71] it must be noted that the pre-exponential terms in θ_A and θ_B cannot be neglected (as in the previous discussion), since at equilibrium the ratio of these two

quantities may vary over several orders of magnitude as the potential is changed in a range corresponding to a relatively small variation of θ_T.

The rate of reaction III, which is assumed rate-determining in this case, is then given by

$$v_3 = k_3 \exp - [\Delta G_3^{\neq} - 2\alpha f_B(\theta_T)]/RT \qquad [72]$$

or

$$v_3 = K_3 \exp 2\alpha k \varepsilon_{AA} [(\tfrac{1+\gamma}{2})\theta_A + \gamma\theta_B]/RT^{*} \qquad [72a]$$

We substitute for k_{AA} using equation [68a]

$$k\varepsilon_{AA} = \frac{VF + \text{constant}}{\theta_A + (\frac{1+\gamma}{2})\theta_B} \qquad [68a]$$

and obtain

$$v_3 = {}^{1}K_3 \exp (\tfrac{2\alpha VF}{RT}) [\frac{(\frac{1+\gamma}{2})\theta_A + \gamma\theta_B}{\theta_A + (\frac{1+\gamma}{2})\theta_B}] =$$

$$ {}^{1}K_3 \exp (\tfrac{VF}{RT}) [\frac{(1+\gamma)\theta_A + 2\gamma\theta_B}{2\theta_A + (1+\gamma)\theta_B}] \qquad [72b]$$

which gives a Tafel slope of

$$dV/d \ln i = (\tfrac{RT}{F}) [\frac{2\theta_A + (1+\gamma)\theta_B}{(1+\gamma)\theta_A + 2\theta_B}$$

---

* We consider here only the case of activated adsorption (see p. 65). The equations for non-activated adsorption are equivalent except for the factor α which has to be omitted.

for step III rate-determining.

If we assume reasonably that $\gamma = 1$, the Tafel slope becomes simply RT/F which is identical with the result obtained using the intrinsic heterogeneity model and assuming $r_A = r_B$ (or in the Boudart model to be discussed below). If $\gamma > 1$ the Tafel slope will be slightly smaller and vice versa for $\gamma < 1$.

The r.h.s. of equation [71b] represents an electrochemical equilibrium constant. For the case of the oxygen evolution reaction we may regard the chemical part of this constant as being close to unity (since the chemical bond energies between each adsorbed species and the surface are probably of comparable magnitude) hence we may assume, approximately, that at the potential of zero charge (p.z.c.) $\theta_A \doteq \theta_B$.* Oxygen evolution usually occurs at potentials appreciably anodic to the p.z.c. of all metals, so that in most cases we can safely assume $\theta_B \gg \theta_A$ during oxygen evolution. This assumption leads to a Tafel slope of $(\frac{RT}{F})(\frac{1+\gamma}{2})$ for the terminal desorption step III, and should be close to RT/F since γ will be close to unity.

It is physically rather unlikely that $\theta_B \ll \theta_A$ during

---

* Specific adsorption of anions at the p.z.c. is assumed here to be negligible.

oxygen evolution. If, however, this did happen to be the case, then Tafel slopes numerically close to those obtained for the same mechanism assuming Langmuir conditions will be observed at low as well as at intermediate coverages. This point will be discussed further below.

We note that the two models discussed above lead to the same results if the adsorbed species are chemically similar, which is also the result obtained by considering the more general induced heterogeneity model (see below). In the latter case, however, our conclusions are independent of any assumptions about the nature and properties of the intermediates.

(iii) Kinetic Equations Arising in the Case of the Induced Heterogeneity Model

As discussed above, this is the most plausible model which can account for linearly falling free energies of adsorption with coverage (cf. 80) observed, for example, in the chemisorption of N (78) and O (79) at metals at intermediate values of the coverage. In the case of combined adsorption of N and H at iron (80), à priori heterogeneity of adsorption sites has been shown (72) to be quite incapable of explaining the observed adsorption behaviour of N in the presence of H. It may be noted that the latter work (72,80) indicates that the r values for variation of heats of adsorption of N and H

with coverage are different. This case is clearly relevant to the problem to be discussed here, where more than one electrochemical intermediate may be chemisorbed in a complex reaction sequence. We hence adopt the induced heterogeneity model (72) as the most reasonable one for considering a linear fall of heat of adsorption with coverage and apply it to the case of two (or more) chemisorbed species. The equations analogous to [64a] and [65a] for species A and B, may then be written as

$$\Delta H_A = \Delta H_A^o - r_A\theta_A - r_B\theta_B \qquad [73]$$

$$\Delta H_B = \Delta H_B^o - r_A\theta_A - r_B\theta_B \qquad [74]$$

since the variation of heat of adsorption of the species A or B will depend, to a first approximation, on the sum of two terms involving the respective dipole double-layer surface potential contributions from <u>both</u> species A and B,* i.e. the term in $r_A\theta_A$ will involve the dipole moment of A and that in $r_B\theta_B$,

---

* Siddiqi and Tompkins have shown very recently (82) that the surface potential change due to the adsorption of two different adsorbates can be calculated from the relative amounts and the individual dipole moments of each adsorbate. This is in agreement with the Boudart model (72) and the general form of the $f(\theta)$ function used below for this model (equations 73,74). Deviations from a simple additivity law were unambiguously correlated with the formation of "surface complexes" (82).

the moment of B. It is important to note that the same terms determine the variation of heat of adsorption of both A and B with coverage by A and B, and we shall represent the terms $r_A\theta_A + r_B\theta_B$ by $f(\theta)$.

We now proceed to discuss the oxygen evolution reaction again, but now for the induced heterogeneity model assuming, as in the previous cases, that the initial discharge step is at quasi-equilibrium, with one of the following steps rate-determining.

From equilibrium in the initial discharge step we obtain the previously derived equation

$$f(\theta) = VF + \text{constant} \qquad [68b]$$

This can, of course, be considered the most general form of this equation, applicable to any model, with the definition of $f(\theta)$ depending on the model.

(a) An Intermediate Step Rate-Determining

We now consider the kinetic equations which arise when step II is rate-determining; this is a radical-ion recombination with charge transfer (cf. $MH + H_3O^+ + e \longrightarrow H_2O + M + H_2$) but in distinction to the corresponding hydrogen producing process shown in the brackets, does not involve desorption of the immediate product. The rate equation for II is then

$$v_2 = k_2\, \theta_{OH}\, c_{OH^-} \exp -[\Delta G_2^{\neq} - \alpha f(\theta) + (1-\alpha)f(\theta) - \beta VF]/RT \qquad [75]$$

and, with equation [68b], taking $\alpha = \beta = 0.5$

$$v_2 = {}^5K_2 \exp \; VF/2RT \qquad [75a]$$

where ${}^5K_2$ is a constant independent of θ and V, and the variation of the pre-exponential term in θ with potential has been neglected at intermediate coverage. The corresponding Tafel slope for step II is then obviously

$$dV/d \ln i = 2RT/F$$

This result is obtained since the effects of coverage by OH and O radicals on the energy of activation for reaction II cancel out if $\alpha = 0.5$.

The Tafel slope (2RT/F) obtained is identical with that arising under limiting Langmuir conditions at $\theta_{OH} \rightarrow 1$. It will be noted that reaction II, with coverage-dependent free energy of activation, does not lead to a slope of $RT/(1 + \beta)F$ (i.e. $\frac{2}{3}RT/F$ with $\beta = 0.5$) as in the Langmuir case at <u>low</u> coverage, or in the case of a radical-ion desorption to form a gaseous product (as in the atom-ion desorption path in hydrogen evolution).

When the OH species are removed by a formal "recombination" type of process (actually an H transfer process) such as IV, not involving charge transfer, the rate equation is

$$v_4 = k_4 \theta^2_{OH} \exp -[\Delta G^{\neq}_4 - 2\alpha f(\theta) + (1-\alpha)f(\theta)]/RT \qquad [76]$$

Substituting f(θ) from equation [68b] and neglecting the pre-exponential term in θ gives

$$v_4 = {}^1K_4 \exp 2VF/RT \quad \text{and} \quad dV/d \ln i = 2RT/F \qquad [76a]$$

i.e., the same result as for II under comparable conditions. We note that a first order heterogeneous chemical step such as occurs in electrochemical decarboxylation reactions (8), e.g. the reactions

$$HCOO^{\bullet} \longrightarrow H^{\bullet} + CO_2$$

or

$$CF_3COO^{\bullet} \longrightarrow CO_2 + CF_3^{\bullet}$$

following discharge of the corresponding ions, will not involve exponential terms in f(θ) since they cancel out, so that the rate of such steps at intermediate coverages will be practically independent of potential (a slight dependence may be observed since the rate of these reactions is proportional to the surface concentration of the appropriate radical, and hence to the coverage; since the latter is a linear function of potential [according to equation 68b], the Tafel slope will tend to infinity). Under Langmuir conditions, the velocities of these reactions, when rate-controlling, will involve terms in exp VF/RT arising from quasi-equilibrium in the previous ion-discharge step, so that their Tafel slopes would be

$dV/d \ln i = RT/F$.

(b) A Terminal Desorption Step Rate-Determining

For the oxygen evolution process, at least two steps must occur prior to the final reaction producing oxygen molecules. If the final step is recombination of MO entities, and is rate-determining, both MOH and MO species can cover the surface significantly, depending on the magnitude of the chemical or electrochemical equilibrium constants for reactions IV and II, respectively.* The f(θ) can then involve significant terms in both θ_{OH} and θ_O, determined by

$$\left(\frac{\theta_O}{\theta_{OH}}\right) = {}^{6}K_2 \exp VF/RT \qquad [77]$$

for reaction II and by

$$\left(\frac{\theta_O}{\theta^2_{OH}}\right) = {}^{2}K_4 \exp f(\theta)/RT = {}^{3}K_4 \exp VF/RT \qquad [78]$$

for reaction IV. The rate equation for the final step III (e.g. in schemes A or B) is

$$v_3 = k_3 \theta^2_O \exp -[\Delta G^{\neq}_3 - 2f(\theta)]/RT \qquad [79]$$

for non-activated adsorption of O_2 (cf. reference 30) and

---

* See, however, p. 94 for a discussion of the probable values of these equilibrium constants.

$$v_3 = k_3 \theta_0^2 \exp -[\Delta G_3^{\neq} - 2\alpha f(\theta)]/RT \qquad [79a]$$

for activated adsorption of O_2. For the case when reaction III is rate-determining we can only regard the pre-exponential term in θ_0 as relatively invariant with potential compared with the term exp $2f(\theta)/RT$ if θ_0 is at least comparable with θ_{OH}, that is if the equilibrium constants in equation [77] and [78] are not very much less than unity. This is probably the case for the species involved in this reaction during steady-state oxygen evolution, as discussed above.

From equations [79] and [68b], and [79a] and [68b], the Tafel slopes for the case when reaction III is rate-determining are then obviously

$$dV/d \ln i = RT/2F \text{ or } RT/2\alpha F, \text{ respectively.}$$

The corresponding slope for the terminal step under Langmuir conditions (θ_{OH} and $\theta_0 \ll 1$) is $RT/4F$.

Under conditions for which the chemical equilibrium constants in equations [77] and [78] are much less than unity (and at low anodic potentials), θ_0 can be much less than θ_{OH}. If the total coverage (i.e. that now principally due to OH entities) is still of the order 0.5, equations [79] and [79a] still hold except that the potential dependence of θ_0 must be taken into account, i.e. equation [79] becomes

$$v_3 = {}^2K_3 \theta_{OH}^2 \exp (2VF/RT) \exp -[\Delta G_3^{\neq} - 2f(\theta)]/RT \qquad [79b]$$

and with equation [68b] and θ_{OH} of the order 0.5, the Tafel slope for reaction III is RT/4F. Similarly, using equation [79a], the slope is RT/2F(1 + α) or RT/3F if α = 0.5. The same results for the Tafel slopes follow if reaction IV is the equilibrium step preceding rate-determining III. In general, θ_O will always tend to become appreciable or predominant at higher anodic potentials and the results first deduced (equations 79 and 79a) will apply.

We have hitherto examined the kinetics for steps in a sequence of three reactions. In a scheme such as C, (see p. 86) the kinetics for I and II will be the same as we have discussed above. The kinetic equation for the case when reaction V is rate-determining will be

$$v_5 = k_5\, \theta_O\, c_{OH^-} \exp -[\Delta G^{\neq}_5 - \alpha f(\theta) + (1-\alpha) f(\theta) - \beta VF]/RT \qquad [80]$$

where f(θ) involves θ_O, θ_{OH} and θ_{HO_2}. Again the same f(θ) will be related to VF by equation [68b] with I in quasi-equilibrium giving the Tafel slope for reaction V as dV/d ln i = 2RT/F. Similarly, the recombination step VI in scheme C will give

$$v_6 = k_6\, \theta_{OH}\, \theta_{HO_2} \exp -[\Delta G^{\neq}_6 - 2\alpha f(\theta)]/RT \qquad [81]$$

or

$$v_6 = k_6\, \theta_{OH}\, \theta_{HO_2} \exp -[\Delta G^{\neq}_6 - 2 f(\theta)]/RT \qquad [81a]$$

for the cases of activated and non-activated adsorption of O_2, respectively, as in the case when reaction III is rate-determining. The Tafel slopes are then obviously RT/2αF or RT/2F as for reaction III, with the same assumptions made above [and previously (20)] about the magnitude of the pre-exponential θ terms.

(iv) Generalizations

It is clear from the above discussions of steps in the oxygen evolution reaction, that some important general conclusions may be drawn regarding the kinetic consequences of considering coverage dependent activation energies in a complex sequence of reactions. In the Langmuir case, Tafel slopes diminish down a sequence of consecutive reactions following a primary ion discharge step. Thus, for successive steps involving charge transfer the Naperian Tafel slopes will be RT/(n + β)F where n is an integer $\geqslant 0$, while formal bimolecular "chemical" recombination steps will be associated with slopes of RT/mF where m is an integer > 2 and increases down the reaction sequence, e.g. IV gives RT/2F, and III or VI give RT/4F.

In the present case, for which coverage-dependent activation energies are introduced, it is clear that normally no slopes less than RT/2F will arise and the values are less diagnostic of mechanism than are the corresponding slopes for

low coverage, Langmuir conditions. It will also be seen that the "recombination" slope of RT/2F arises only in the case of a terminal recombination step in a series of consecutive reactions, and intermediate recombination (or bimolecular rearrangement) steps are not associated with this slope or corresponding values of the form RT/mF. Also the slope RT/2F arises under Temkin conditions if the terminal step is a recombination irrespective of how many previous steps are involved, while the corresponding Langmuir slope can be RT/mF where m is an integer only equal to two for a recombination step immediately following the initial charge transfer step, as in the hydrogen evolution reaction. The conditions $\theta_O \ll \theta_{OH}$ during the steady state oxygen evolution leading to the lower slopes RT/4F or RT/3F, are unlikely in anodic oxygen evolution since, on chemical grounds, the chemical equilibrium constants in equations [77] and [78] will not be expected to be $\ll 1$ and, in addition, the potential will normally be well above the potential of zero charge for most metals at rates of oxygen evolution which can be conveniently measured (i.e. at current densities $> 10^{-7}$ a.cm.$^{-2}$) as pointed out above.

The results deduced above were shown to be independent of the exact form of $f(\theta)$ (see p. 87), since $f(\theta)$ can always be expressed in terms of VF and constants in an equation of

the form of [68b] for quasi-equilibrium in the ion-discharge step (when a subsequent step is rate-controlling), and the same f(θ) always arises in the argument of the exponential involving the free energy of activation in the rate equation for the rate-controlling step. These general conclusions only apply, of course, to intermediate coverage conditions. At very low or quite high coverage, limiting Langmuir conditions apply with the Tafel slopes as previously deduced (6,7,13,39), based on direct potential-dependence of the concentrations of all adsorbed intermediates in pre-exponential terms in the rate equations for the steps prior to the rate-determining step.

We have shown above that the model assumed to account for the variation of heat and free energy of adsorption with coverage will have no effect on the kinetic equations deduced if a single adsorbed intermediate is involved. However, if several intermediates may be adsorbed at the interphase, slightly different results are obtained for different models. With the induced heterogeneity model, the Tafel slopes derived are independent of the chemical nature of the adsorbate.*

---

* This is only the case, however, if the adsorbed species on the reactant "side" of the rate-determining step form a major part of θ_T when the relevant Faradaic process occurs at a steady state under a given set of conditions. This depends, of course, on the chemical properties of the adsorbates as well as on the position of the p.z.c. with respect to the reversible potential.

The other two models yield the same results in the limiting case when the variations of the heats of adsorption with coverage, or the energies of lateral interaction of the different adsorbed species, are equal. These models (i.e. those associated with intrinsic heterogeneity and lateral interaction effects) allow for the possibility of slightly different Tafel slopes arising, to an extent related to the chemical properties of the adsorbed species. In general, the induced heterogeneity model will lead to round values or simple fractional values of RT/F for the Tafel slopes if the symmetry factors are taken as 0.5. The other models, however will lead to such round values only as special cases for limiting relative values of the r coefficients for the various species.

Although we have made the above deductions for steps in the oxygen evolution reaction, it is clear that the conclusions are general for any electrode reaction involving several steps and more than one adsorbed intermediate; applications, for example, to decarboxylation reactions have been considered elsewhere by Conway and Dzieciuch (8) and are recorded in another thesis (27).

CHAPTER III

NEW CONTRIBUTIONS TO THE KINETIC THEORY OF ADSORPTION PSEUDOCAPACITY

1. GENERAL

The dependence of adsorption pseudocapacity on coverage and potential has been discussed by Bucken and Weblus (46) and by Bockris and Kita (70) assuming limiting Langmuir conditions, and was briefly reviewed in the Introduction (see p. 75) Bucken and Weblus have also given an equation for the total effective adsorption pseudo-capacitance (containing a "Langmuir" term as well as a "Temkin" term) in terms of coverage, which can be shown to be equivalent to the equation derived in a different way by Conway and Gileadi (10). The significance of the form of the C-θ relationship has been discussed by Conway and Bourgault (39) and by Conway and Gileadi (10). The latter authors also computed the C-V relationship numerically for a general case and discussed its relation to the parameter r determining the rate of decrease of free energy of adsorption with coverage.

Here we derive first the expressions for the adsorption pseudocapacity under Langmuir conditions, using the steady

state assumption,* in order to develop it further to general forms involving, in addition, Temkin, or "Temkin-like" terms (we use this term here to refer to cases when the free energy of adsorption is a linear function of θ^n with $n \neq 1$). We shall see below that under certain limiting conditions the steady state treatment gives results identical with those obtained from the quasi-equilibrium assumption. In certain cases, notably when the discharge step can no longer be considered at equilibrium, only the steady state treatment is applicable and leads to different results to be developed below.

2. PSEUDOCAPACITY UNDER LANGMUIR CONDITIONS

Consider a general sequence of anodic reactions

$$M + A^- \longrightarrow MA + e \qquad \text{VII}$$

$$MA + A^- \longrightarrow MB + e + C \qquad \text{VIII}$$

$$2MB \longrightarrow 2M + B_2 \qquad \text{IX}$$

---

* The normal requirement for validity of a steady state treatment for deducing concentrations of intermediates is that the concentrations of the intermediates are small and hence do not change significantly during the course of the reaction. This condition does not, however, apply to electrochemical reactions under constant current and potential conditions, since the reaction is forced to be in a steady state, irrespective of the concentrations of the various intermediates involved. The steady state treatment can hence legitimately be used for calculating the coverage by intermediates and the associated pseudocapacity.

We shall assume first that the rate constant for reaction IX is much greater than that of either of the previous steps, so that $\theta_B \ll \theta_A$ and $\theta_A \doteq \theta_T$ which we shall write for simplicity as θ. With this assumption, we proceed to calculate the steady state coverage by A radicals, determined by the condition

$$d\,\theta_A/dt = 0$$

The rates of the relevant reaction steps can be written in abbreviated form

$$v_7 = k_7 (1-\theta) \exp (V/b) = a_7 (1-\theta) \qquad [82]$$

$$v_{-7} = k_{-7}\, \theta \exp (-V/b) = a_{-7}\theta \qquad [83]$$

$$v_8 = k_8\, \theta \exp (V/b) = a_8\theta \qquad [84]$$

where k_7, k_{-7} and k_8 are the rate constants at unit concentrations in the double-layer and including the double-layer potential term (cf. p. 62) and a_7, a_{-7} and a_8 are the corresponding electrochemical rate constants (13). The parameter b is defined as $b = 2RT/F$ (assuming here that all symmetry factors are equal to 0.5).

The steady state requirement leads to

$$\frac{d\theta}{dt} = v_7 - v_{-7} - v_8 = 0 \qquad [85]$$

hence

$$a_7(1-\theta) - a_{-7}\,\theta - a_8\,\theta = 0 \qquad [86]$$

or

$$\theta = \frac{a_7}{a_7 + a_{-7} + a_8} \qquad [87]$$

differentiating with respect to V we have

$$\frac{d\theta}{dV} = \frac{(a_7+a_{-7}+a_8)a_7/b-(a_7-a_{-7}-a_8)a_7/b}{(a_7+a_{-7}+a_8)^2} = \frac{2a_{-7}a_7/b}{(a_7+a_{-7}+a_8)^2} \qquad [88]$$

The Langmuir pseudocapacity is hence given as

$$C_L = k'(d\theta/dV) = k' \frac{2a_{-7}a_7/b}{(a_7+a_{-7}+a_8)^2} \qquad [89]$$

where k' is the charge required to form a complete monolayer of adsorbed intermediates on the surface, as defined above. Substituting for the a values from equations [82-84] this gives

$$C_L = k' \frac{2k_7 k_{-7}/b}{[k_7\exp(V/b)+k_{-7}\exp(-V/b)+k_8\exp(V/b)]^2} \qquad [89a]$$

The maximum in capacity will occur at a potential where the condition $dC_L/dV = 0$ is satisfied, that is when,

$$\frac{dC_L}{dV} = \frac{2k'k_7k_{-7}}{b} \frac{d}{dV} (a_A+a_{-A}+a_B)^{-2} = 0 \qquad [90]$$

hence

$$a_7 - a_{-7} + a_8 = 0 \qquad [91]$$

so that

$$(k_7 + k_8) \exp (V_m/b) = k_{-7} \exp (-V_m/b) \qquad [91a]$$

or

$$\exp\ (2V_m/b) = k_{-7}/(k_7+k_8) \qquad [91b]$$

Equation [91b] defines the potential V_m at which C_L will reach its maximum value.

Combining equations [89], [91] and [91a], we obtain

$$C_L(\max) = \frac{k'k_7}{2bk_{-7}} \exp 2V_m/b = \frac{k'}{2b} \times \frac{k_7}{k_7+k_8} \qquad [92]$$

Substituting the value of b^* into this equation we have

$$C_L(\max) = \frac{k'F}{4RT} \times \left(\frac{k_7}{k_7+k_8}\right) \qquad [92a]$$

Equations [89a] and [92a] are the general expressions for the Langmuir adsorption pseudocapacity and its maximum value when a single intermediate is adsorbed on the surface of the electrode. If step VIII is rate-determining we have $k_7, k_{-7} \gg k_8$ and hence

$$C_L = \frac{k'F}{RT} \times \frac{k_7}{k_{-7}} \times \frac{\exp(VF/RT)}{[1+(k_7/k_{-7})\exp(VF/RT)]^2} \qquad [89b]$$

with

$$C_L(\max) = \frac{k'F}{4RT} \qquad [92b]$$

---

* In the above derivation we assumed $\beta=0.5$ and defined accordingly $b=2RT/F$. Our final results (equations 89b, 92b) do not depend on this assumption since the symmetry factor β cancels out between terms in β and $(1-\beta)$. This must be so since θ, and consequently its derivative C_L are quantities defined by (quasi)-equilibrium conditions, and cannot therefore depend on the form of the energy barrier, as discussed in the Introduction.

The constant k' has been defined above as the charge associated with formation of a monolayer of adsorbed intermediates per unit real surface area. Taking the number of sites per sq. cm. as 10^{15} (e.g. for adsorbed H), we obtain

$$k' = 1.6 \times 10^{2}\ \mu C.\ cm.^{-2} \quad C_L(max) = 1.6 \times 10^{3}\ \mu F.cm.^{-2}$$

The numerical value of k' obviously depends on both the size and "valency" of the adsorbate, and the geometry of the adsorbent surface involved. We shall arbitrarily use the value given above for our general calculations, since our discussion and conclusions do not depend on this value.

The coverage θ_M at which C_L reaches its maximum value is obtained by substituting equation [91] into equation [87] as

$$\theta_M = \frac{a_7}{a_7+a_{-7}+a_8} = \frac{a_7}{2(a_7+a_8)} = \frac{1}{2}\left(\frac{k_7}{k_7+k_8}\right) \qquad [93]$$

Assuming that step VIII is rate-determining, we have

$$\theta_M = 0.5$$

We note that our resulting equations in terms of the steady state assumption are reduced to those obtained using the quasi-equilibrium assumption (46,70) when $k_7 \gg k_8$. This is to be expected since the above inequality applies when step VIII is rate-determining, and this is also the requirement for the applicability of the quasi-equilibrium assumption.

In the following development we shall assume quasi-equilibrium in the initial discharge step. Cases for which equilibrium in steps prior to the rate-determining step is not maintained will be discussed separately.

In the limiting Langmuir case, the coverage can be expressed explicitly in terms of potential, and the adsorption pseudocapacity can hence be obtained directly as a function of potential. This procedure cannot be followed when a general adsorption isotherm is considered which involves both linear and exponential terms in θ. In the latter case, we express the potential in terms of the coverage and obtain from it the variation of pseudocapacity with coverage. Combining the data from the C-θ and the V-θ relationships, we then obtain numerically the required dependence of C on V.

We shall now derive the variation of pseudocapacity with coverage under Langmuir conditions, using the quasi-equilibrium assumption. Thus, putting $v_7 = v_{-7}$, we have

$$a_7(1-\theta) = a_{-7}\,\theta \qquad [9a]$$

hence

$$\frac{\theta}{1-\theta} = \frac{a_7}{a_{-7}} = \frac{k_7}{k_{-7}} \exp \frac{VF}{RT} = K_7 \exp \frac{VF}{RT} \qquad [9b]$$

which is another equivalent form of equation [9], written for a general anodic process. Equation [9b] can be rewritten as

$$V = \frac{RT}{F} \ln \left(\frac{\theta}{1-\theta}\right) + {}^{1}K_7 \qquad [9c]$$

where

$$^{1}K_{7} = -(RT/F)\ln K_{7}$$

Then differentiating with respect to θ, we have

$$\frac{dV}{d\theta} = \frac{RT}{F}\left[\frac{1}{\theta} + \frac{1}{1-\theta}\right] = \frac{RT}{F}\,\frac{1}{\theta(1-\theta)} \qquad [96]$$

so that

$$\frac{k'}{C_L} = \frac{RT}{F}\,\frac{1}{\theta(1-\theta)} \qquad [96a]$$

and

$$C_L = \frac{k'F}{RT}\,\theta(1-\theta)^{*} \qquad [97]$$

From the latter equation, the values of $C_L(max) = (k'F/4RT)$ and $\theta_m = 0.5$ are obtained directly. We remark again, in concluding this introductory section, that the above result has been previously derived by several authors, but the calculations have been given here to form a basis for the original calculations which follow for the more general case where Langmuir conditions do not obtain, and when some degree of non-equilibrium in the discharge step is involved.

---

* The same result can obviously be obtained from the steady state treatment by substituting the value of θ from equation [87] into equation [89] and neglecting a_B with respect to c_A and a_{-A}.

3. THE TOTAL EFFECTIVE ADSORPTION PSEUDOCAPACITY

(1) Pseudocapacity Associated with a Single Adsorbed Intermediate

We now proceed to derive the equations for a general anodic reaction (steps VII to IX) in which the surface coverage is due predominantly to species A (e.g. as would be the case when step VIII is rate-determining, and the final product B_2 is not in equilibrium with (B). The treatment here will be in terms of the Boudart induced heterogeneity model (72) but it follows, however, that any other model giving rise to a linear variation of the free energy of adsorption with coverage will lead to the same result, provided that only a single intermediate is adsorbed on the surface, as already discussed above. The general function $f(\theta)$ in this case takes the simple form $f(\theta) = r_A\theta_A$ which we shall write as $r\theta$ for brevity. For quasi-equilibrium in the initial discharge step we have

$$k_7\,(1-\theta)\,\exp -[\Delta G_7^{\ddagger} + ar\theta - \beta VF]/RT$$

$$= k_{-7}\,\theta\,\exp -[\Delta G_{-7}^{\ddagger} - (1-a)\,r\theta + (1-\beta)VF]/RT \qquad [98]$$

which has been written for convenience at unit concentration of reactants in the double-layer. Hence

$$\left(\frac{\theta}{1-\theta}\right)\,\exp\left(\frac{r\theta}{RT}\right) = K_7\,\exp\left(\frac{VF}{RT}\right) \qquad [99]$$

$$V = \frac{RT}{F}\ln\left[\theta/(1-\theta)\right] + \frac{r\theta}{F} + {}^{1}K_7 \qquad [100]$$

where K_7 and ${}^1K_7$ are constants independent of coverage and potential. Equation [99] is obviously equivalent to equation [49] above, written here for an anodic process. The pseudocapacity for species A at the metal is then given by

$$\frac{k'}{C} = \frac{dV}{d\theta} = \frac{RT}{F}\,\frac{d \ln [\theta/(1-\theta)]}{d\theta} + r/F \qquad [101]$$

which involves a "Langmuir" term in $\theta/(1-\theta)$ in addition to a "Temkin" term in r.*

Comparison with the equations

$$\frac{k'}{C_L} = \frac{RT}{F}\,\frac{1}{\theta(1-\theta)} \qquad [96a]$$

and

$$\frac{k'}{C_T} = \frac{r}{F} \qquad [54]$$

defined previously for limiting Langmuir and Temkin conditions, respectively, shows that equation [101] can be written in the form

$$\frac{1}{C} = \frac{1}{C_T} + \frac{1}{C_L} \qquad [102]$$

i.e.

$$C = \frac{C_T C_L}{C_T + C_L} \qquad [103]$$

---

* It is important to note here that, while in the rate equations terms in θ and $1-\theta$ can be legitimately neglected when $0.2 < \theta < 0.$ and an exponential term in $f(\theta)$ is important, in the pseudocapacit equation [101] the term $d \ln [\theta/1-\theta]/d\theta$ can normally not be neglected in comparison with r/F.

The fact that we can write the overall pseudocapacity C in terms of limiting contributions from a "Langmuir term" C_L and a "Temkin term" C_T is an important conclusion since it implies that the two pseudocapacity contribution combine effectively <u>in series</u> to determine the overall pseudocapacity, i.e. when one is much larger than the other, the <u>smaller</u> capacity will determine the overall capacity. In terms of potential-dependent coverage, this implies that when two terms involve the coverage as in equation [100], the actual coverage will be determined by the term predicting the lower coverage at a given potential.

The potential dependence of C for various values of r may be evaluated by calculating C as a function of θ and θ as a function of V using equations [100] and [101]. We note that $K_7 \ll 1$, otherwise θ_A will be near unity even at low anodic overpotentials. We take $\log K_7 = -2$ as an example* and r having values of 0, 5, 10 and 20 Kcal. $mole^{-1}$ (these figures are chosen to be approximately within the observed range of mean dependence of heats of adsorption of various species upon coverage when approximately linear relations between θ and heat of adsorption arise for $0.1 < \theta < 0.9$).

---

* Choice of other values of K_7 will only shift the scale of values of V and will not change the form of the dependence of θ or C on V (70).

The calculated values* of C as a function of θ and V are shown in Figures 6 and 7, respectively, and the Langmuir case, corresponding to r = 0, is shown for comparison. These cases will apply to <u>any</u> univalent species predominantly covering the surface for the values of k' and r chosen. It will be noted that for the Langmuir case: (a) C is never potential-independent, except as it tends to zero and (b) the pseudo-capacitance will only have measurable values, in comparison with the ionic double-layer capacity, over a narrow potential range of some 240 mV. Introduction of a finite value of r produces a range of C values which are less potential-dependent than in the Langmuir case but never strictly potential-independent However, when r = 10 or 20 Kcal. $mole^{-1}$., C is sensibly constant over 350 and 700 mV, respectively, as has been previously deduced qualitatively by a quasi-thermodynamic argument in the paper by Conway and Bourgault (39). This is the kind of behaviour that is observed experimentally in some cases (7,39) but potential-dependent pseudocapacity is found under other conditions e.g.

---

* In these calculations, the same constants are used for the evaluation of k' as discussed above. Their exact values are not of importance here as we are only interested in the relative <u>variation</u> of C with θ or V. Comparison with experimental data will require an assignment of the surface concentration corresponding to θ = 1 and the charge transferred per radical adsorbed as well as the real/apparent area ratio for the electrode surface.

Figure 6. Variation of the overall adsorption pseudo-capacity with coverage θ.

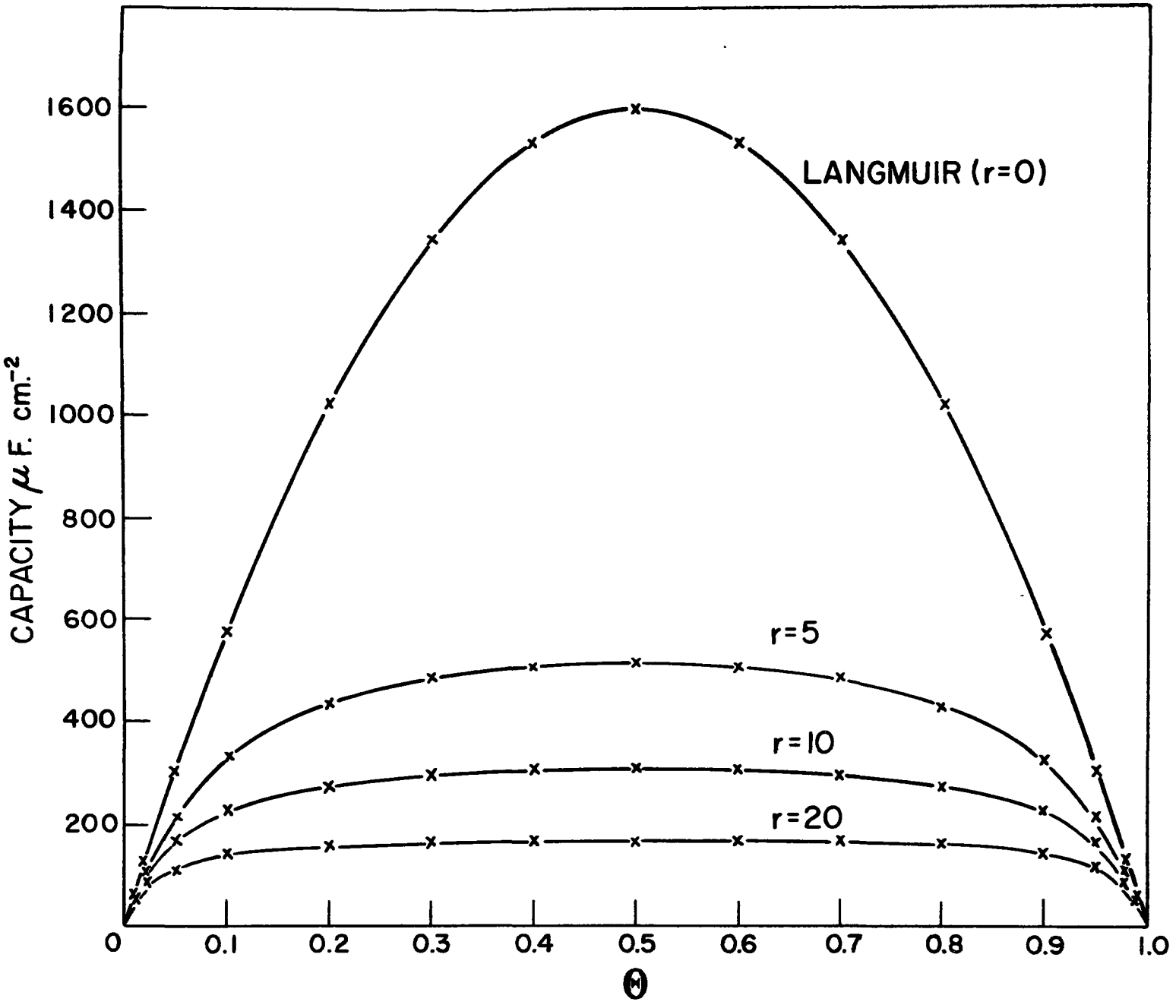
1600
1400
1200
1000
800
600
400
200
CAPACITY μF. cm.⁻²
LANGMUIR (r=0)
r=5
r=10
r=20
0
0.1
0.2
0.3
0.4
0.5
0.6
0.7
0.8
0.9
1.0
θ

Figure 7. Variation of the overall pseudocapacity with potential V.

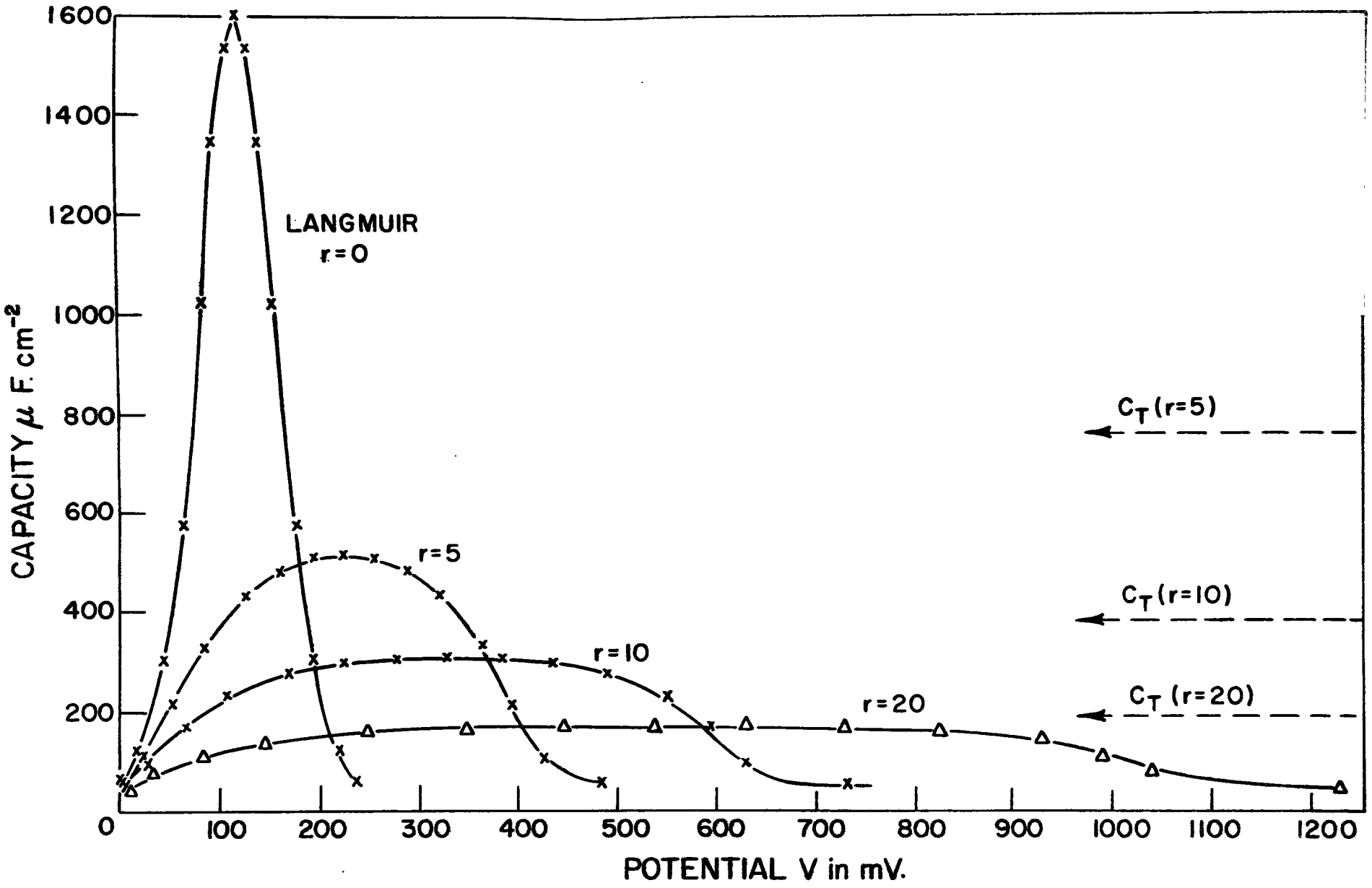
1600
1400
1200
1000
800
600
400
200
0
CAPACITY μ F. cm⁻²
LANGMUIR
r = 0
r = 5
r = 10
r = 20
C_T (r=5)
C_T (r=10)
C_T (r=20)
100
200
300
400
500
600
700
800
900
1000
1100
1200
POTENTIAL V in mV.

for the hydrogen evolution reaction at nickel in alkaline solution (12), and with the nickel oxide electrode (7,39).

When a potential independent pseudocapacity contribution is involved ("Temkin" conditions; r finite) it will be noted that the maximum pseudocapacity is substantially lower than the C_{max} calculated (1.6×10^3 μF. cm^{-2}) for the "Langmuir" case. However, for values of r even as high as 20 Kcal. $mole^{-1}$, the maximum capacity should be readily distinguishable, over a wide range of potential or coverage, from the ionic double-layer capacity, which normally does not exceed about 100 μF. cm^{-2} at potentials anodic to the potential of zero charge (17). In all cases at very high potentials $C \longrightarrow C_{d.l.}$, i.e. the measured capacity will tend to the ionic double-layer capacity. The "Langmuir" case (equation [97]) is evidently a special case of equation [100] and in most cases will not correspond to experimental conditions, since heats of adsorption are rarely independent of coverage. Even if r is as low as 1 Kcal. $mole^{-1}$, C(max) will be significantly less (actually about 1.1×10^3 μF. cm^{-2}) than 1.6×10^3 μF.cm^{-2} and the range of the potential dependence of C will be substantially larger than that for the "Langmuir" case. Some values of C(max) and C_T as a function of r have been plotted in Figure 8; C_T can have values greater than C_L,(max) for low r, but combined with C_L (equation 102) must lead to values of

Figure 8. Variation of the maximum pseudocapacity and the "Temkin" contribution with values of r.

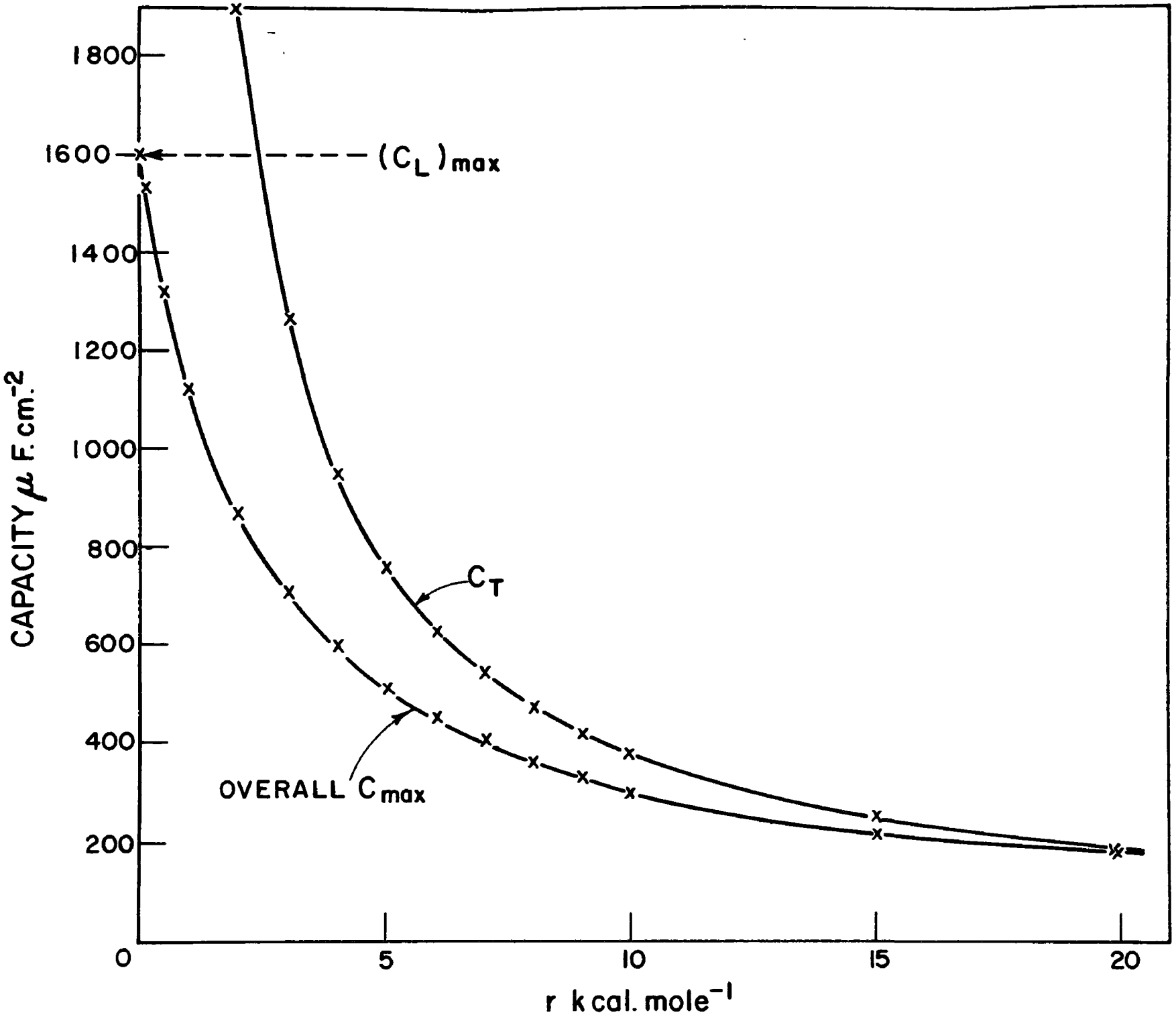
1800
1600
1400
1200
1000
800
600
400
200
0
5
10
15
20
$(C_L)_{max}$
C_T
OVERALL C_{max}
CAPACITY μ F. cm.$^{-2}$
r k cal. mole^{-1}

overall C(max) less than C_L(max). The above conclusions are general and will refer to any single adsorbed species which arises from a Faradaic process in an electrochemical reaction, using the appropriate value of r. We now examine a more general case for more than one adsorbed species at the surface.

(ii) Pseudocapacity Associated with More than One Adsorbed Species

The reaction scheme

M + A^-	⟶	MA + e	(fast)		VII
MA	⟶	MB	(fast)		X
2MB	⟶	B_2	(slow)		IX

is considered with IX rate-controlling so that θ_A and θ_B may both be significant. The heats of adsorption of A and B are assumed to be given by equations [73] and [74] involving f(θ). For VII and X at equilibrium (cf. equation 68b)

$$f(\theta) = VF + K_7 \qquad [104]$$

and

$$\theta_B/\theta_A = k_{10}/k_{-10} = K_{10} \qquad [105]$$

The latter ratio is independent of total coverage and potential, so that

$$f(\theta) = r_A\theta_A + r_B\theta_B = r_A\theta_A + K_{10}\, r_B\theta_A = {}^1K_{10}\theta_A \qquad [106]$$

where $^{1}K_{10} = r_A + K_{10}r_B$

Now

$$C = k' \frac{d\theta_T}{dV} = k' d [\theta_A + \theta_B]/dV \qquad [107]$$

but

$$\theta_A + \theta_B = \theta_A + K_{10}\,\theta_A = (1 + K_{10})\theta_A \qquad [108]$$

Now from equations [106] and [68b]

$$d\theta_A/dV = F/[r_A + K_{10}r_B] \qquad [109]$$

so that, from equations [107] and [108]

$$C = k'(1 + K_{10})\, d\theta_A/dV = k'\left(\frac{1 + K_{10}}{r_A + K_{10}r_B}\right)F = k'F/r' \qquad [110]$$

where we have defined

$$r' = (r_A + K_{10}\, r_B)/(1 + K_{10}).$$

It is thus seen that when more than one intermediate is adsorbed, a constant pseudocapacity contribution is still obtained and, moreover, the apparent value of the rate of change of free energy/adsorption with coverage is simply a weighted average of the values for the two individual species.

Normally the ratio θ_B/θ_A will depend on potential, either: (a) due to a change in the number of adsorbed species caused by an act of the given step (e.g. in a case such as 2 MA $\longrightarrow$ MB, viz. 2 MOH $\longrightarrow$ MO + H_2O [reaction IV]) with the previous charge transfer step in quasi-equilibrium; or (b)

when there is a direct potential-dependence of the equilibrium constant for X (i.e. for a reaction such as MA + A^- ⟶ e + MB + C (cf. reaction VIII). In either case, θ_A and θ_B will only be comparable* over a small range of electrode potentials (which may or may not be accessible practically in an experiment) so that we can treat the problem generally by assuming $\theta_A \gg \theta_B$ or $\theta_A \ll \theta_B$ which implies that $f(\theta) \doteq r_A\theta_A$ or $r_B\theta_B$.

The total Temkin pseudocapacity contribution given by equation [110] will combine with the Langmuir term as in equations [101] and [102] to give the overall pseudocapacity which will then have a potential dependence similar to that deduced above depending now on the value of r' in equation [110].

4. ELECTRODE POTENTIAL AND COVERAGE

It is of some interest to evaluate the form of the variation of surface coverage with potential under various conditions. In the limiting Langmuir case (r = 0) this variation is given by equation [9b] or [95], while the general relationship is obtained from equation [100].

---

* Thus if step X was replaced by VIII, the following equation would result: $\theta_P/\theta_A = K_\theta \exp VF/RT$ (cf. equation 77). If θ_A is equal to θ_B at a *given* value of V, then we shall find $\theta_A \ll \theta_B$ or $\theta_B \ll \theta_A$ if the potential is changed by plus or minus 0.06 V or more, respectively, so that in practice the total coverage will be largely determined by that of one species or the other over a wide potential range. The same conclusions would follow if step X were of the form 2 MA ⟶ MB + C.

In the Langmuir case (r = 0), θ varies with potential as shown in Figure 9. An approximately linear region occurs over a range of about 60 mV. As r increases, the linear region of θ *vs* V is extended, but at high or low potentials a short non-linear region always arises from the linear term in θ in the rate equations. The coverage is essentially linear with V over 400 mV. when r is 10 Kcal. mole^{-1}. The dotted lines in Fig. 9 show what the θ-V behaviour would be if only the Temkin term (i.e. the linear term in θ in equation [100]) determined the dependence of θ on V. Obviously this must lead to a completely linear dependence of θ on V as shown. This is a fictitious case, since in reality at very low or very high θ, the $\theta/(1-\theta)$ term will always be important and give the curving-off region of the lines at each extremity.

It is of interest, however, that in the range where θ is linear with V (for appreciable values of r), the actual values of θ at any given potential are significantly different from those calculated from the exponential (Temkin) term in θ alone. For example, when r = 10 Kcal., the pre-exponential term in θ never becomes negligible compared with the exponential one, so far as the relationship between θ and V is concerned. Nevertheless, a linear variation of θ with V (constant capacity) is still obtained, since the deviation of the pre-exponential term from a linear θ-V relationship is negligible with respect

Figure 9. Variation of coverage θ with potential V for Langmuir (r = 0) and Langmuir + Temkin conditions (indicated r values).

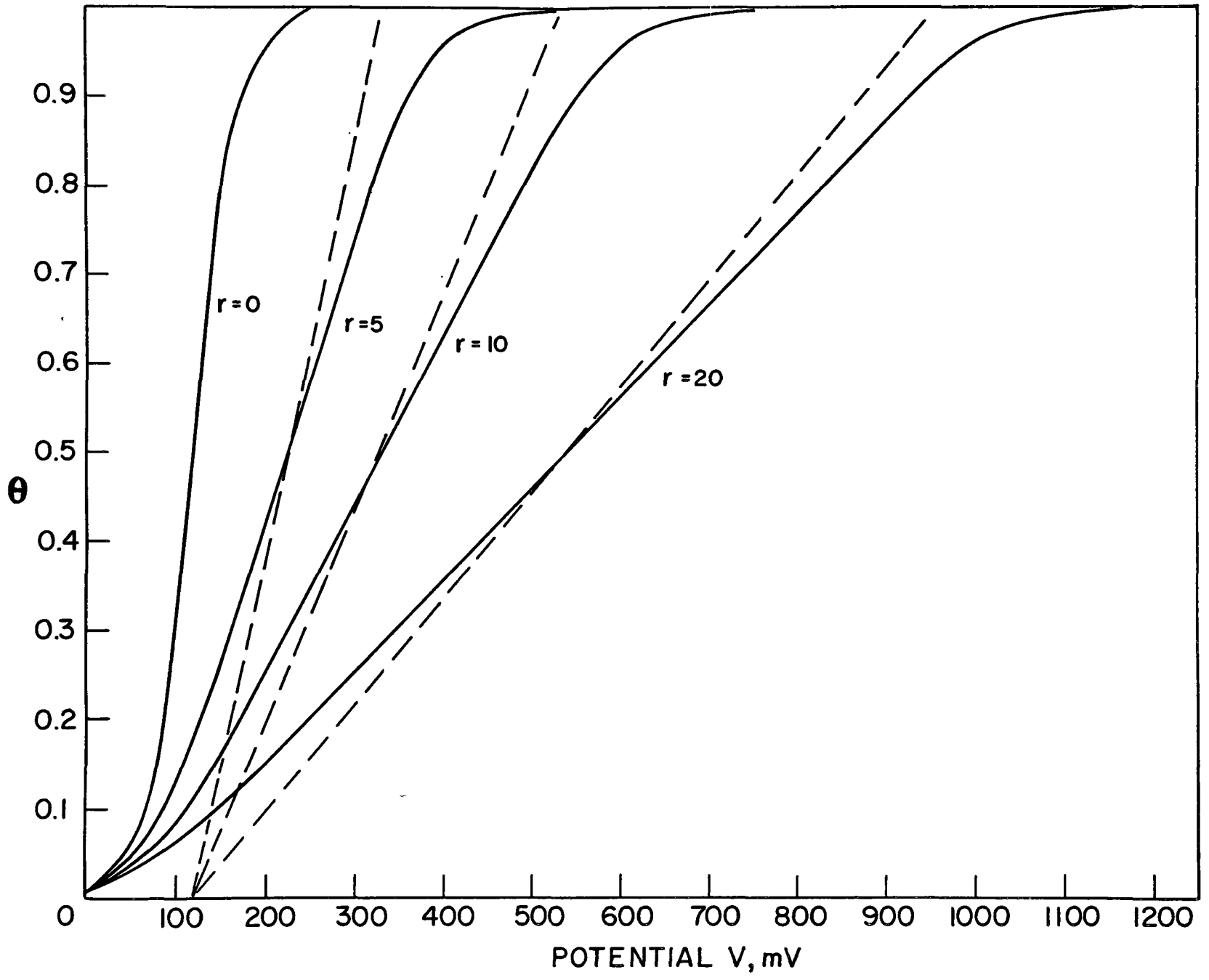
θ
0.9
0.8
0.7
0.6
0.5
0.4
0.3
0.2
0.1
0
r = 0
r = 5
r = 10
r = 20
100
200
300
400
500
600
700
800
900
1000
1100
1200
POTENTIAL V, mV

to the value of θ arising from the exponential term, except at very high or very low θ.

5. THE FORM OF THE C-V RELATIONSHIP WHEN THE FREE ENERGY VARIES WITH θ^n ($n \neq 1$)

In the previous sections, we derived the form of the dependence of the total effective adsorption pseudocapacitance on coverage and potential assuming that the free energy of adsorption decreased linearly with increasing coverage. Here we wish to treat the case for which the free energy of adsorption has the form

$$\Delta G_\theta = \Delta G_o - r\theta^n \qquad [111]$$

with n having values other than unity. More specifically, we shall discuss cases in which n = 0.5 and 1.5, corresponding to a model involving electrostatic repulsions in the two-dimensional surface phase where the decrease in free energy of adsorption is due to ion-ion or dipole-dipole repulsions, respectively. As pointed out above, it is unlikely that this model accounts for the variation of the free energy of adsorption with coverage in most cases over the whole coverage range, but it may become significant at higher values of θ (72). Some of our own results are consistent with a dipole-dipole interaction effect (see Conway, Gileadi and Dzieciuch (9) and also below) and it is therefore relevant to discuss the effect of

assuming n ≠ 1 in equation [111] on the form of the C-V plot.

If n = 0.5 (ion-ion repulsion model) and we assume, as before, that quasi-equilibrium is maintained in the initial discharge step, we obtain

$$k_1(1-\theta)\exp -[\Delta G_1^{\neq} + \alpha r\theta^{1/2} - \beta VF]/RT =$$

$$= k_{-1}\theta \exp -[\Delta G_{-1}^{\neq} - (1-\alpha)r\theta^{1/2} + (1-\beta)\,VF]/RT \qquad [112]$$

when the surface is mainly covered by one species, and the equations have been written for simplicity again at unit concentration of reactants in the double-layer (see p. 62). Neglecting the pre-exponential terms in θ for intermediate values of the coverage, we obtain

$$V = \frac{r\theta^{1/2}}{F} + K_1 \qquad [113]$$

where K_1 is a constant independent of θ and V. The Temkin pseudocapacity* is hence obtained as

$$\frac{k'}{C_T} = \frac{r}{2F\theta^{1/2}}\ ;\ C_T = \frac{2k'F}{r}\,\theta^{1/2} \qquad [114]$$

or, in terms of potential,

$$\theta = \left(\frac{VF-K_1}{r}\right)^2\ ;\ C_T = \frac{2k'F}{r} \times \left(\frac{VF-K_1}{r}\right) \qquad [115]$$

---

* When the free energy of adsorption is not a linear function of θ, we should strictly no longer refer to "Temkin behaviour" and a "Temkin pseudocapacity". We shall retain the term, however, for convenience.

Similarly, if n in equation [111] is taken equal to 1.5 (corresponding to a dipole-dipole repulsion effect) we obtain

$$V = \frac{r\theta^{3/2}}{F} + {}^{1}K_{1} \qquad [113a]$$

and corresponding to equations [114] and [115]

$$\frac{k'}{C_T} = \frac{3}{2}\frac{r\theta^{1/2}}{F}\,; \quad C_T = \frac{k'F}{r}\cdot\frac{2}{3}\,\theta^{-1/2} \qquad [114a]$$

or

$$\theta = \left(\frac{V-{}^{1}K_{1}}{r}\right)^{2/3} \text{ and } C_T = \frac{k'F}{r}\cdot\frac{2}{3}\left(\frac{V-{}^{1}K_{1}}{r}\right)^{-1/3} \qquad [115a]$$

The overall effective adsorption pseudocapacity will be determined by a series combination of the Langmuir and Temkin terms (equations 102,103) but owing to the dependence of C_T on coverage and potential when $n \neq 1$, the resulting C-V and C-θ plots will have an appreciable degree of skewness, as shown in Fig. 10 and Fig. 11, where the case for $n = 1$ is given for comparison. It is seen that the shape of the pseudocapacity-potential relationship can indicate, by the degree of skewness, the approximate form of the function of θ relating the free energy of adsorption at intermediate coverage to its value at $\theta = 0$. In particular, it would be qualitatively easy to distinguish cases for which $n < 1$ from those for which $n > 1$ (cf. equation 111), since a <u>different direction</u> of skewness along the potential or coverage axis results. Thus, a dipole-

Figure 10. The dependence of adsorption pseudo-capacitance on potential when the free energy of adsorption decreases with θ^n and $n \neq 1$.

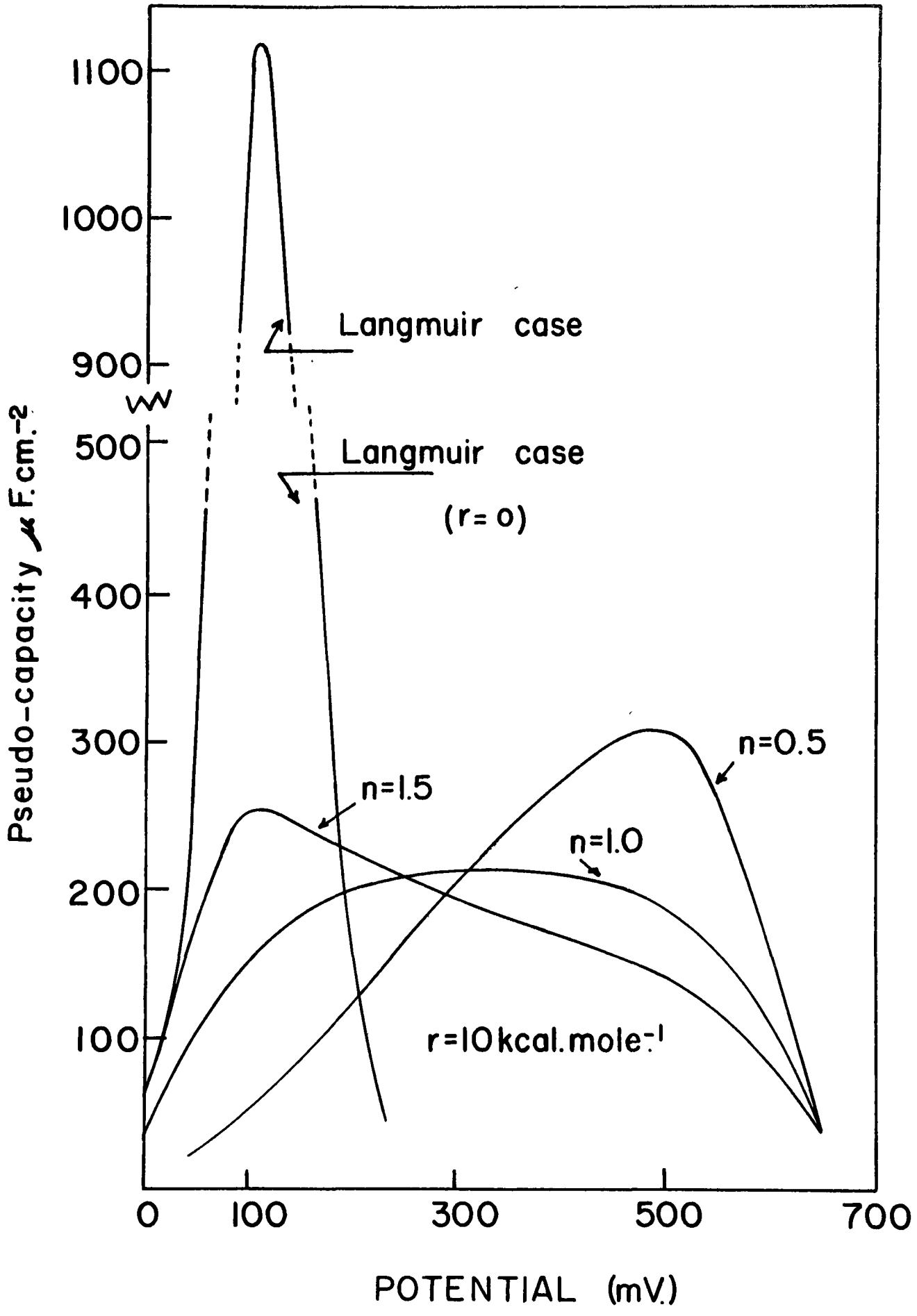
1100
1000
900
500
400
300
200
100
Pseudo-capacity μF.cm.⁻²
Langmuir case
Langmuir case
(r= 0)
n=0.5
n=1.5
n=1.0
r=10 kcal.mole⁻¹
0
100
300
500
700
POTENTIAL (mV.)

Figure 11. The dependence of adsorption pseudo-capacitance on coverage when the free energy of adsorption decreases with θ^n and $n \neq 1$.

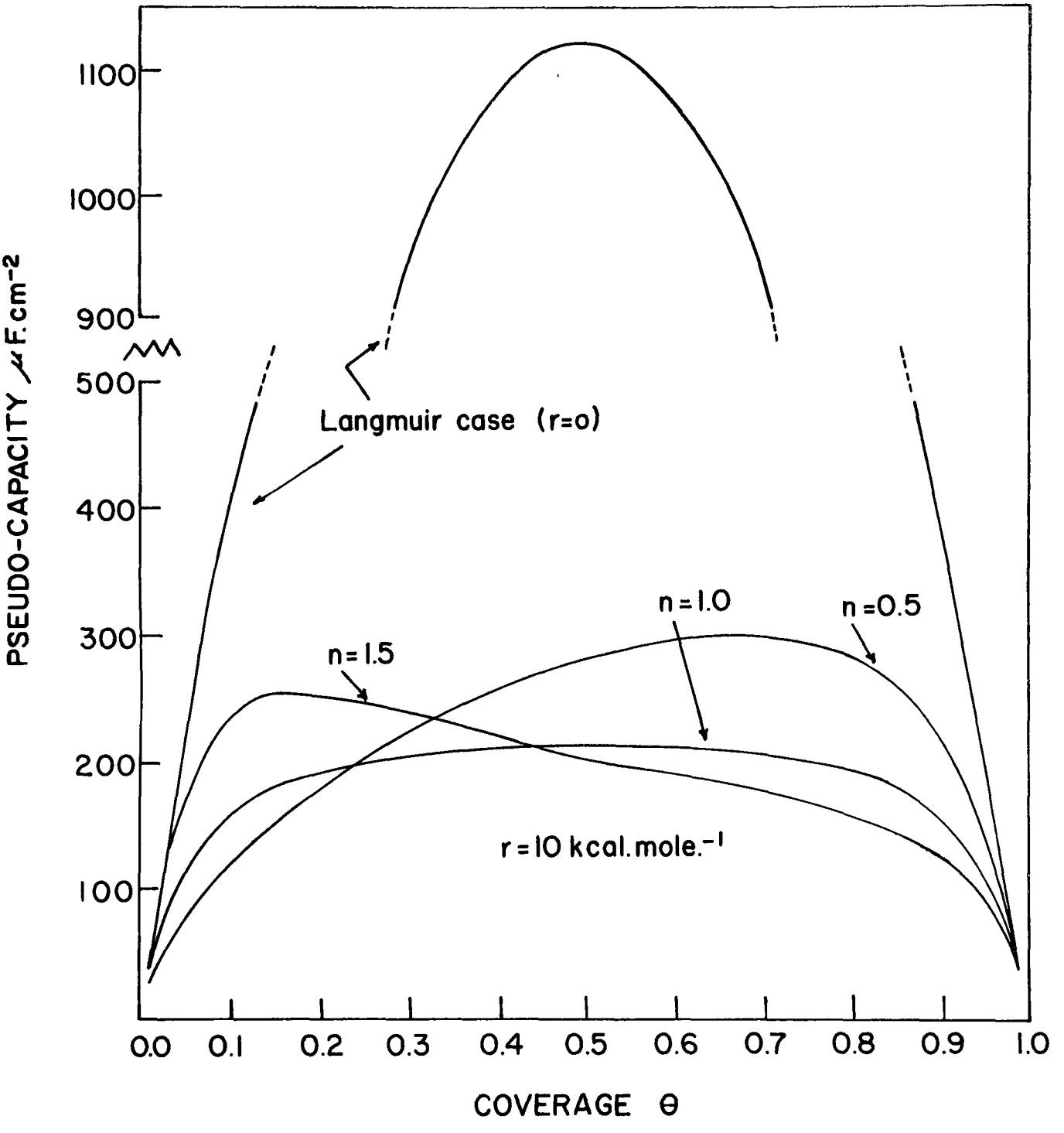
PSEUDO-CAPACITY / μF.cm⁻²
1100
1000
900
500
400
300
200
100
Langmuir case (r=o)
n=1.0
n=0.5
n=1.5
r=10 kcal.mole.⁻¹
0.0
0.1
0.2
0.3
0.4
0.5
0.6
0.7
0.8
0.9
1.0
COVERAGE θ

dipole repulsion effect will lead to a C-V plot skewed towards lower potentials, while an ion-ion repulsion term will tend to cause a skewness towards higher values of V.

We maintain that the most satisfactory model for the variation of the free energy of adsorption with coverage is that involving induced heterogeneity in the sense defined by Boudart and discussed above, so that any significant lateral interaction effects should be detectable from the skewness of the C-V plot. It must be pointed out, however, that this only applies if the adsorbed species on the surface are at least partially hindered with respect to lateral motion. If no such hindrance exists, the adsorbate on the surface can be considered as a two-dimensional, non-ideal gas.* Applying an equation of state such as the Reichsanstalt (81) equation, the first order correction term for non-ideality due to lateral interactions (i.e. the second virial coefficient) will be linear in θ, and the contribution of terms in higher powers of θ will probably be negligible. It does <u>not</u> seem probable, however, that in most electrochemical reactions (but the hydrogen evolution reaction may be an exception here) the adsorbed radicals can, in fact, move freely on the surface,

---

* We are indebted to Dr. R. Parsons for bringing this additional possibility to our attention during discussion of this work at the American Chemical Society meeting, 1962.

and consequently be treated as a free two-dimensional gas.

6. PSEUDOCAPACITY BEHAVIOUR IN CASES FOR WHICH THE ASSUMPTION OF QUASI-EQUILIBRIUM IN THE INITIAL DISCHARGE STEP IS NOT APPLICABLE

Here we consider briefly the form of the C-V relationship for a case in which the usual assumption of quasi-equilibrium in the pre rate-determining discharge step is not valid. We recall that when the standard free energy of activation of a given step in a consecutive reaction sequence is much larger than that of any other step, i.e. its specific rate constant is much smaller, the rate of the overall reaction will be governed by the rate of the slowest step, and all other steps prior to the rate-controlling step will effectively be in equilibrium. The fundamental requirement for the applicability of the quasi-equilibrium assumption is, hence, that a rate-determining step will unambiguously exist. The rates of electrochemical reactions may, in general, depend on potential in different ways, so that, as the potential is changed, conditions may change from those where the quasi-equilibrium assumption is applicable to those where it is not.

For the purpose of discussing the kinetics of electrode reactions, we can usually assume that a rate-determining step exists over most of the range of potentials studied since (a) a relatively small difference in the standard

free energies of activation of the various steps will generally be sufficient to make one of them rate-determining (thus if $\Delta G^{\#}$ for one step is 2.8 Kcal.mole^{-1} larger than that for another, the ratio of specific rate constants will be 10^2) and (b) the electrochemical rate constants for different steps will usually depend on potential to different extents (i.e. the Tafel slopes associated with these steps will be different) and the region of potential over which two steps can have comparable rates is strictly limited as shown by Parsons (68); Parsons's arguments apply, however, only to limiting Langmuir conditions, and we have shown above that when a Temkin type isotherm is applicable, several mechanisms may correspond to the same Tafel slope, i.e. the rates of different steps may vary with potential in the same way. Moreover, we shall show below that, while for the purpose of discussion of electrode kinetics, a step may be considered rate-determining if its rate constant is, say, two orders of magnitude smaller than that of any other consecutive step, the ideal shape of the C-V curve may not be observed under certain circumstances (in particular when the free energy of activation varies excessively with coverage i.e. $r/RT \gg 1$) unless the rate constant of the rate-determining step is <u>five to ten</u> orders of magnitude smaller than that of any other consecutive step in a given reaction sequence.

We shall proceed below to discuss a general anodic reaction occurring through an initial discharge step followed

by an ion-atom recombination step, with a possible final desorption step which is very fast, and not at equilibrium with its products (cf. reactions VII to IX). The form of the dependence of pseudocapacity and coverage on potential will be evaluated first (for non-equilibrium in the discharge step) assuming limiting Langmuir conditions, and then using a general adsorption isotherm (including both Temkin and Langmuir Terms) for various ratios of the specific rate constants of the initial discharge step and the following ion-atom recombination step. It is clear that a somewhat different set of equations will be obtained if a different sequence of consecutive electrochemical steps is considered. However, our method of treating the problem, as given below, will be applicable in general, and the present case serves both to exemplify this method and to demonstrate the rather more limited range of applicability of the quasi-equilibrium assumption when calculation of C and θ, and their dependence of potential, are considered.

(i) Limiting Langmuir Conditions

The equations for the adsorption pseudocapacity in terms of potential for the Langmuir case have already been derived above using the steady state treatment. There we obtained (see p. 111)

$$C_L = \frac{k'F}{RT} \cdot \frac{k_7 k_{-7}}{[(k_7+k_8)\exp(V/b) + k_{-7}\exp(V/b)]^2} = \frac{k'F}{RT} \cdot \frac{(k_7/k_{-7})\exp(VF/RT)}{[1+(\frac{k_7+k_8}{k_{-7}})\exp(VF/RT)]^2} \qquad [89c]$$

The maximum in the C-V plot was shown to occur at a potential given by

$$V_m = (RT/F) \ln (k_{-7}/(k_7 + k_8)) \qquad [91c]$$

where the value of C_L is

$$C_L(max) = \frac{k'F}{4RT} \cdot \left(\frac{k_7}{k_7 + k_8}\right) \qquad [92a]$$

We have used equation [89c] to calculate C_L as a function of V taking three values for the ratio k_8/k_7, which determines the "extent" of non-equilibrium in the discharge step. Results of these calculations are shown in Fig. 12. The quasi-equilibrium assumption obviously corresponds in the limiting case to $k_8/k_7 = 0$. As this ratio is increased, the pseudocapacity corresponding to any potential decreases, and the maximum is shifted towards less anodic potentials (or, in general, to lower values of the overpotential). The shapes of the curves remain, however, unchanged. This can be demonstrated by normalizing the curves in Fig. 12 so that they all have the same maximum (this is done by multiplying each capacity value by a factor of $(k_7 + k_8)/k_7$ and shifting the curves parallel along the potential axis so that all maxima will occur arbitrarily at the same potential). The capacity curves normalized in this manner then become all identical.

Figure 12. The adsorption pseudocapacity under limiting Langmuir conditions as a function of pptential under non-equilibrium conditions when the specific rate constants for the initial discharge step (k_7) and the following ion-atom desorption step (k_8) are of comparable magnitude.

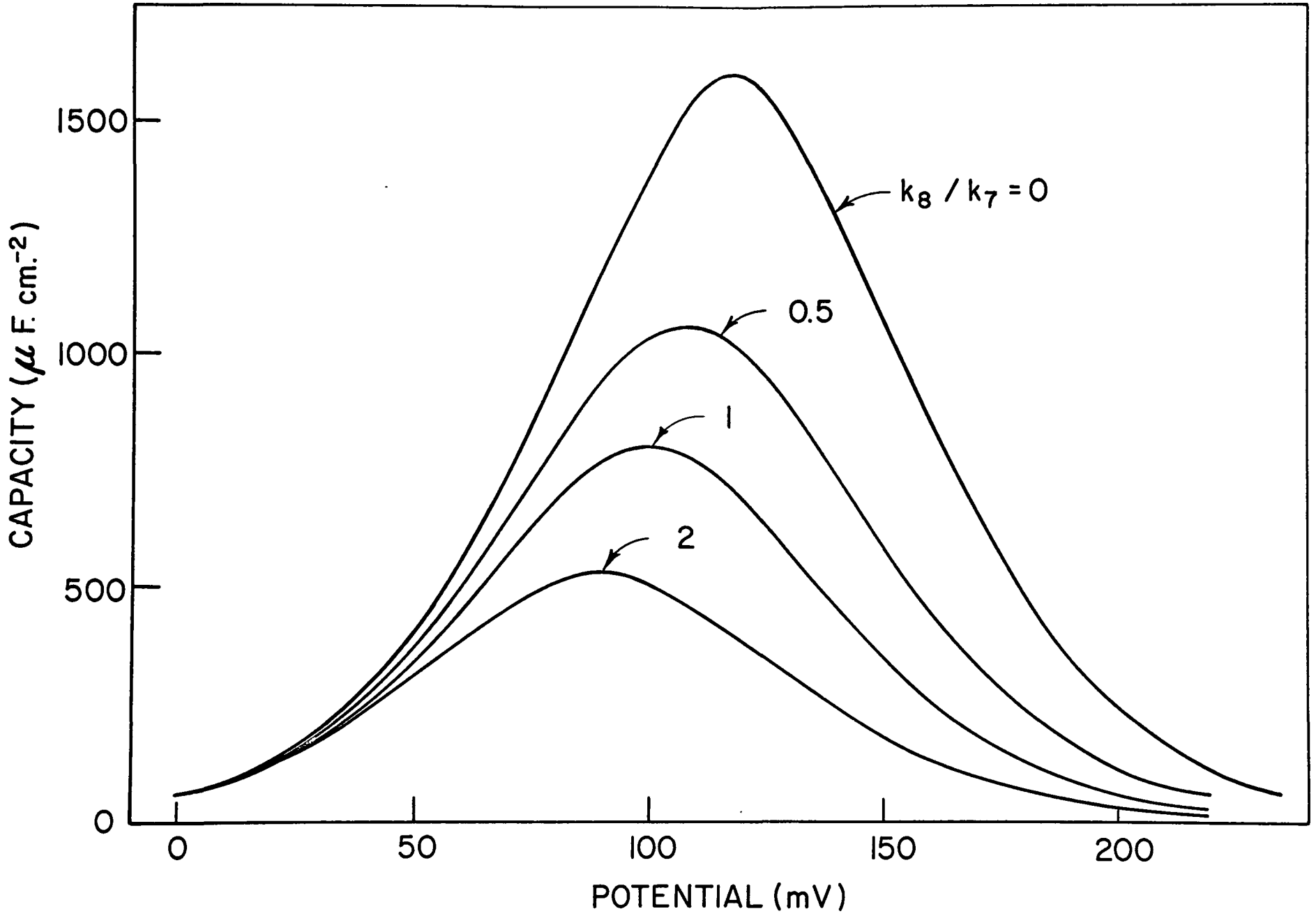
1500
1000
500
0
CAPACITY (μ F. cm.⁻²)
0
50
100
150
200
POTENTIAL (mV)
k8 / k7 = 0
0.5
1
2

In this case, when limiting Langmuir conditions are assumed to prevail, we note that conditions for a given step to be rate-controlling are similar to those required in the discussion of the electrode kinetics. Thus for $k_7/k_8 = 10^{-2}$ (i.e. for the discharge step to be rate-determining) we have $C_L(max) = 0.01\ (k'F/4RT)$ which is of the order of magnitude of the ionic double-layer capacity, and in addition C_L will go from practically zero to its maximum and back to zero in a range of about 6mV (cf. equation 91c and our argument above about the symmetrical form of the C-V curve for any value of k_8/k_7). Hence, when $k_7/k_8 = 10^{-2}$ (i.e. when the discharge step is rate-determining) practically no adsorption pseudocapacity will be observed, a conclusion previously reached (13) for this mechanism. Taking the other extreme case, when $k_7/k_8 = 10^2$, $C_L(max)$ becomes equal to 0.99 $(k'F/4RT)$ and the maximum occurs at a potential $V_m = 115$ mV if we take $k_{-7}/k_7 = 10^2$ (i.e. the equilibrium constant for the discharge step) as in the previous calculations (cf. p. 117). The maximum capacity thus obtained is 99% of the value deduced assuming complete quasi-equilibrium, and the potential range over which the pseudocapacity is appreciable is only some 6 mV less than in the complete equilibrium case. Thus, when $k_7/k_8 = 10^2$, the quasi-equilibrium assumption may be considered valid for most practical purposes. It is important

to emphasize, however, that these conclusions will only apply under limiting Langmuir conditions, as we now show below.

(ii) A General Case (Combined Langmuir and Temkin Isotherm Under Non-Equilibrium Conditions)

We proceed now to calculate the total effective adsorption pseudocapacitance, using the steady state treatment, i.e. without any limiting assumption regarding quasi-equilibrium. We write the rate equations for reactions VII and VIII as

$$v_7 = k_7 (1-\theta)\exp(-\alpha r\theta/RT) \exp(\beta VF/RT) \qquad [116]$$

$$v_{-7} = k_{-7}\, \theta \exp[(1-\alpha)r\theta/RT] \exp[-(1-\beta)VF/RT] \qquad [117]$$

$$v_8 = k_8\, \theta \exp(\alpha r\theta/RT) \exp(\beta VF/RT) \qquad [118]$$

In the steady state $v_7 = v_{-7} + v_8$, hence

$$k_7 (1-\theta) \exp(-r\theta/2RT) \exp(VF/2RT) = k_{-7}\, \theta \exp(r\theta/2RT)$$

$$\exp[-VF/2RT) + k_8\, \theta \exp(r\theta/2RT) \exp(VF/2RT) \qquad [119]$$

where all symmetry factors have been taken equal to 0.5. This equation can be rearranged to have the form

$$k_7 \left(\frac{1-\theta}{\theta}\right) \exp(-r\theta/RT) = \left[\frac{k_{-7}\exp(-VF/2RT) + k_8\exp(VF/2RT)}{\exp(VF/2RT)}\right]$$

$$= k_8 + k_{-7} \exp(-VF/RT) \qquad [120]$$

so that

$$\left[k_7 \left(\frac{1-\theta}{\theta}\right) \exp(-r\theta/RT) - k_8\right]/k_{-7} = \exp(-VF/RT) \qquad [120a]$$

and

$$V = \frac{RT}{F} \ln \left[\frac{k_{-7}}{k_7\left(\frac{1-\theta}{\theta}\right)\exp(-r\theta/RT)-k_8}\right] \qquad [121]$$

The total effective adsorption pseudocapacity will be obtained by differentiating the above equation; thus

$$\frac{k'}{C} = \frac{dV}{d\theta} = -\frac{RT}{F}\frac{d}{d\theta}\ln\left[k_7\left(\frac{1-\theta}{\theta}\right)\exp(-r\theta/RT)-k_8\right] \qquad [122]$$

or

$$\frac{k'}{C} = \left[\frac{(1-\theta)\theta r+RT}{F\theta^2}\right] \times \left[\frac{k_7\exp(-r\theta/RT)}{k_7\left(\frac{1-\theta}{\theta}\right)\exp(-r\theta/RT)-k_8}\right] =$$

$$= \left[\frac{(1-\theta)\theta r+RT}{F\theta^2}\right] \times \left[\frac{1}{(1-\theta)/\theta-(k_8/k_7)\exp(r\theta/RT)}\right] \qquad [122a]$$

This equation obviously has the correct form, since if we assume $k_8/k_7 = 0$, i.e. when the discharge step is at quasi-equilibrium in the limiting case, the above relation takes the simple form

$$\frac{k'}{C} = \frac{r}{F} + \frac{RT}{F}\cdot\frac{1}{\theta(1-\theta)} \qquad [101]$$

which is the expression obtained previously (cf. page 116) in a very simple manner, using the quasi-equilibrium assumption. The total adsorption pseudocapacitance is hence related to the coverage in the most general case (subject only to the assumption that the free energy of adsorption decreases linearly with coverage) by the equation

$$C = (k'F/RT)\left[\frac{\theta^2}{(1-\theta)\theta r/RT+1}\right]\left[(1-\theta)/\theta-(k_8/k_7)\exp(r\theta/RT)\right] \qquad [123]$$

We cannot split this expression into terms which can be recognised as "Langmuir" and "Temkin" contributions as in the quasi-equilibrium case (cf. p. 73). We may, however, usefully discuss some limiting conditions, viz. $r = 0$ (Langmuir case) or $r/RT \gg 1$ and $\theta/(1-\theta) \doteq 1$ (Temkin case).

When we substitute $r = 0$ into equation [123] above, we obtain

$$C_L = (k'F/RT)[(1-\theta)\theta - \theta^2 k_8/k_7] \qquad [124]$$

The first term in the square bracket is the usual quantity obtained using the quasi-equilibrium assumption ($k_8/k_7=0$). When we take, say, $k_8 = k_7$, the pseudocapacity becomes

$$C_L = 2(k'F/RT)[(0.5 - \theta)\theta]$$

This corresponds to a pseudocapacity varying symmetrically with coverage between $\theta = 0$ and $\underline{\theta = 0.5}$ with $C_L(\max) = k'F/8RT$, i.e. half the quasi-equilibrium value. This result is to be expected since when $k_8 = k_7$ it is evident that the coverage cannot rise above 0.5, and the value of $C_L(\max)$ is exactly half the value obtained for the case when $k_8/k_7 = 0$ as derived above (cf. equation 92a).

Our second limiting case, when $r/RT \gg 1$ and $\theta/(1-\theta) \doteq 1$, leads to the expression

$$C_T = \frac{k'F}{r}[1-(k_8/k_7)\exp(r\theta/RT)] \qquad [125]$$

This equation is applicable only if

$$1 > k_8/k_7 \exp r\theta/RT$$

since if the r.h.s. of this inequality becomes larger than unity, the calculated pseudocapacity has a negative value, which has no physical significance in this case. In fact the equation

$$1 = k_8/k_7 \exp (r\theta/RT)$$

defines the limiting value of the coverage which can be reached for a given ratio of the rate constants and some assumed value of r/RT as

$$\theta = (RT/r) \ln (k_7/k_8) \qquad [126]$$

Were the pre-exponential terms in θ in equation [123] entirely negligible, we would then have $\theta = 0$ for $k_7 = k_8$, i.e. the adsorption of intermediates would be impossible.* Equation [125] can hence only be discussed in relation to cases where $k_8/k_7 < 1$. At low coverage, when $(k_8/k_7) \exp (r\theta/RT) \ll 1$, it leads to a practically constant pseudocapacity, which at high coverage $(k_8/k_7)\exp (r\theta/RT) \gg 1$) decreases exponentially with coverage. In the Langmuir case we found (cf. p. 139) that C_L reached 99%

---

* This is, however, a completely hypothetical case since, for any value of r/RT, when θ becomes very small, the assumptions leading to equation [125] are no longer valid, i.e. the pre-exponential terms in θ cannot be neglected.

of its value calculated using the quasi-equilibrium assumption when $k_7/k_8 = 10^2$. For C_T in equation [125] to approach its quasi-equilibrium value $k'F/r$ to the same extent, we must have

$$(k_8/k_7) \exp (r\theta/RT) = 10^{-2}$$

From this we can calculate the required ratio of k_7/k_8 for any chosen value of r/RT and θ. Taking for example r/RT = 20 and θ=0.5, we have $k_7/k_8 \doteq 3 \times 10^8$. For r/RT = 10 and θ = 0.5 we would require $k_7/k_8 = 10^5$. It is thus seen that under limiting Temkin conditions the applicability of the quasi-equilibrium assumption may be limited to cases for which the rate constant of the rate-determining step is smaller, by at least several orders of magnitude, than that of the initial discharge step.

Equation [125] need not be discussed in any further detail, since, as we have observed above, the pre-exponential terms in θ are never completely negligible with respect to the exponential terms in equations relating the pseudo-capacity to coverage; equation [125] does not therefore represent a real physical case. We hence now proceed to discuss the general case (equation 123) where both "Langmuir" and "Temkin" terms are included.

Equation [123] relating the total effective adsorption pseudocapacity to coverage can obviously be applied only over

the range of coverage for which the resulting pseudocapacity is not negative. This correspond to

$$\frac{1-\theta}{\theta} > k_8/k_7 \exp(r\theta/RT)$$

Hence the highest attainable coverage for given values of k_7/k_8 and r/RT is defined by the equation

$$\frac{\theta}{1-\theta} \cdot \exp(r\theta/RT) = k_7/k_8 \qquad [127]$$

The function on the l.h.s. of equation [127] is plotted in Fig. 13 against θ, for values of r/RT equal to 0, 10 and 20. The values of θ obtained from this graph constitute the limiting coverages approached at very high overpotentials for given values of the parameters k_7, k_8 and r. As r/RT is increased, the ratio of k_7/k_8 required for the limiting coverage to reach a given value increases rapidly, i.e. it becomes harder to realize a state of quasi-equilibrium (which obviously corresponds to a θ value approaching unity at sufficiently high overpotentials). Thus for the limiting value of the coverage to be 0.9, with $r/RT = 20$, we require $k_7/k_8 = 6 \times 10^8$ corresponding to a difference of about 12 Kcal. mole^{-1} in the standard free energies of activation of the two consecutive steps. It is obvious that in many cases complete quasi-equilibrium may, without serious error, be assumed for the purpose of discussion of the <u>kinetics</u> of the reactions; however, the corresponding

Figure 13. The highest limiting coverage attainable under non-equilibrium conditions for a given value of the ratio of specific rate constants of the initial discharge step (k_7) and the following desorption step (k_8). $k_7/k_8 = \theta/(1-\theta) \exp(r\theta/RT)$.

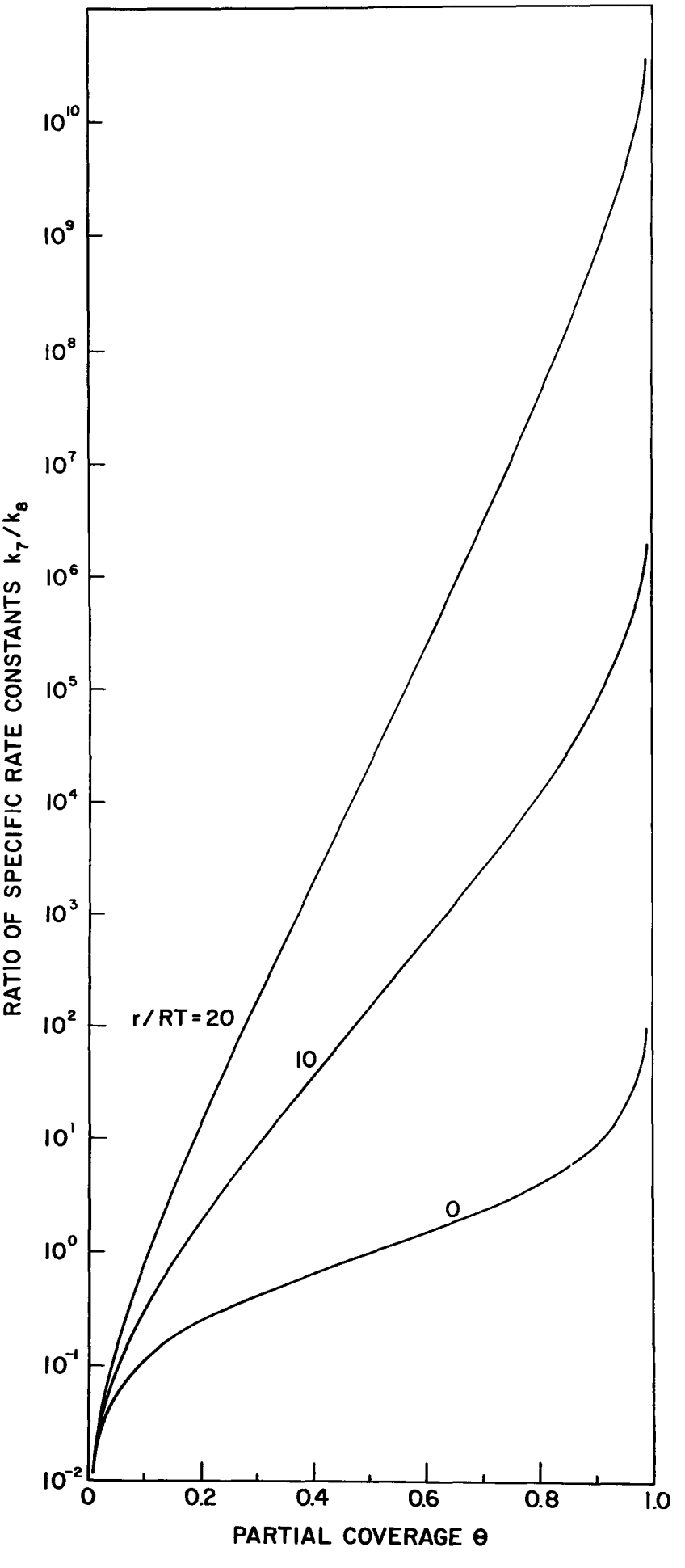
RATIO OF SPECIFIC RATE CONSTANTS k_7/k_8
10^{10}
10^{9}
10^{8}
10^{7}
10^{6}
10^{5}
10^{4}
10^{3}
10^{2}
10^{1}
10^{0}
10^{-1}
10^{-2}
r/RT=20
10
0
0
0.2
0.4
0.6
0.8
1.0
PARTIAL COVERAGE θ

C-V behaviour will be appreciably different from that arising under quasi-equilibrium conditions for the same steps, and is therefore a more sensitive indication of the kinetic behaviour in a sequence of consecutive reactions.

We have used equation [123] to calculate the adsorption pseudocapacity as a function of coverage for different rate-constant ratios k_8/k_7 and two values of r/RT equal to 10 and 20. These results are shown in Figs. 14 a, b. On the low coverage branch the curves are almost identical with the one obtained for $k_8/k_7 = 0$ (the limiting quasi-equilibrium case), while on the high coverage side they deviate markedly from the quasi-equilibrium curve to an extent dependent on the values of r/RT and the ratio k_7/k_8.

The corresponding variation of coverage with potential was calculated for the same values of r/RT and k_7/k_8, using equation [121], and is plotted in Figs. 15 a,b.* Combining equations [121] and [123], we obtain numerically the dependence of pseudocapacity on potential, as shown in Figs. 16 a,b. It is seen that for intermediate values of k_7/k_8 large enough

---

* We have assumed here, as previously, that $k_{-7}/k_7 = 10^2$. Choice of other values for this ratio will only shift the C-V and θ-V plots in a parallel manner along the potential axis and will not affect their forms.

Figure 14. The total effective adsorption pseudo-capacity as a function of coverage under non-equilibrium conditions, for different values of the ratio of specific rate constants for the initial discharge step (k_7) and the following ion-atom desorption step (k_8).

a. $r/RT = 10$,

b. $r/RT = 20$.

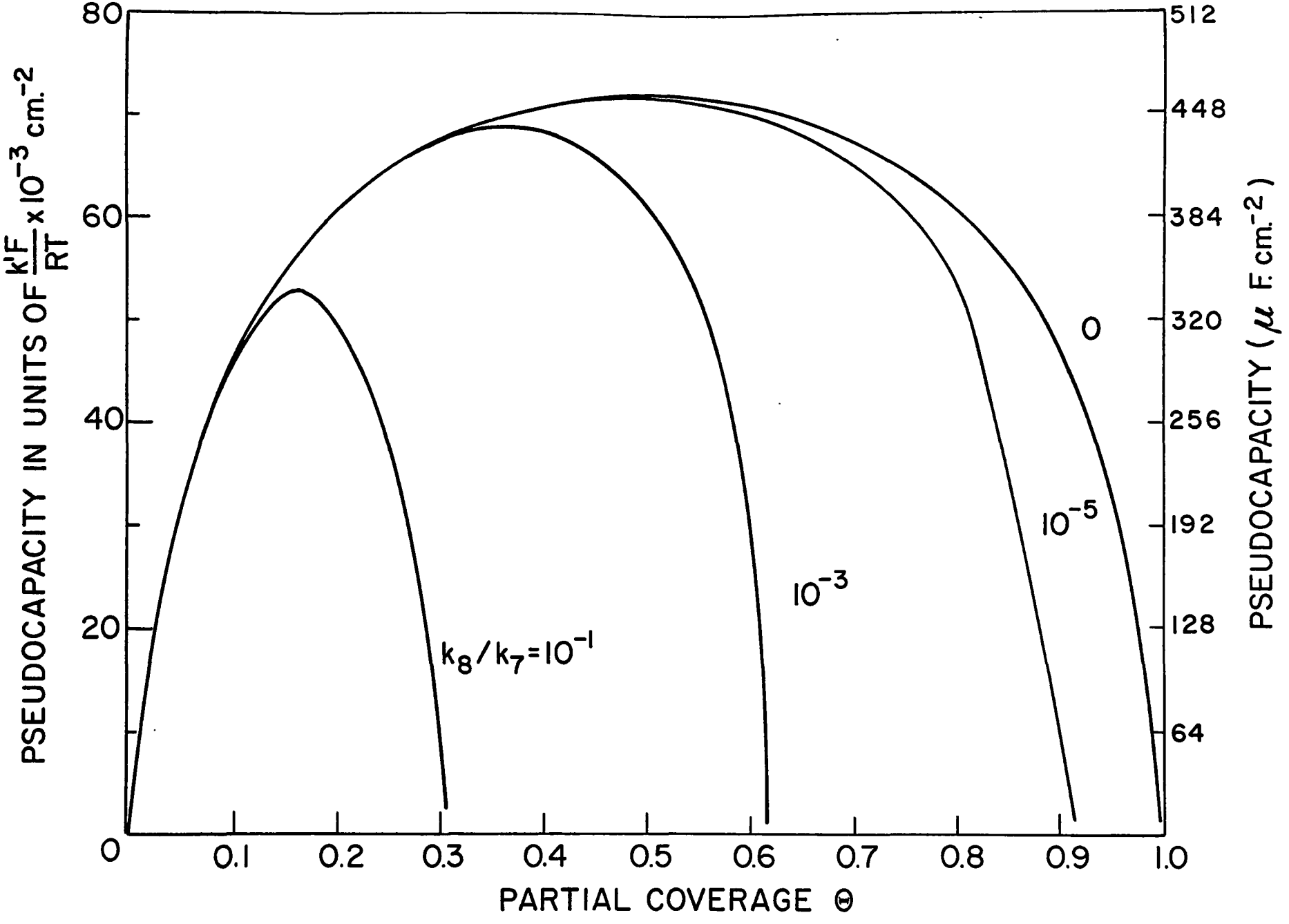
80
60
40
20
0
512
448
384
320
256
192
128
64
0.1
0.2
0.3
0.4
0.5
0.6
0.7
0.8
0.9
1.0
PSEUDOCAPACITY IN UNITS OF $\frac{k'F}{RT} \times 10^{-3}$ cm.$^{-2}$
PSEUDOCAPACITY (μ F. cm.$^{-2}$)
PARTIAL COVERAGE Θ
$k_8/k_7 = 10^{-1}$
10^{-3}
10^{-5}
0

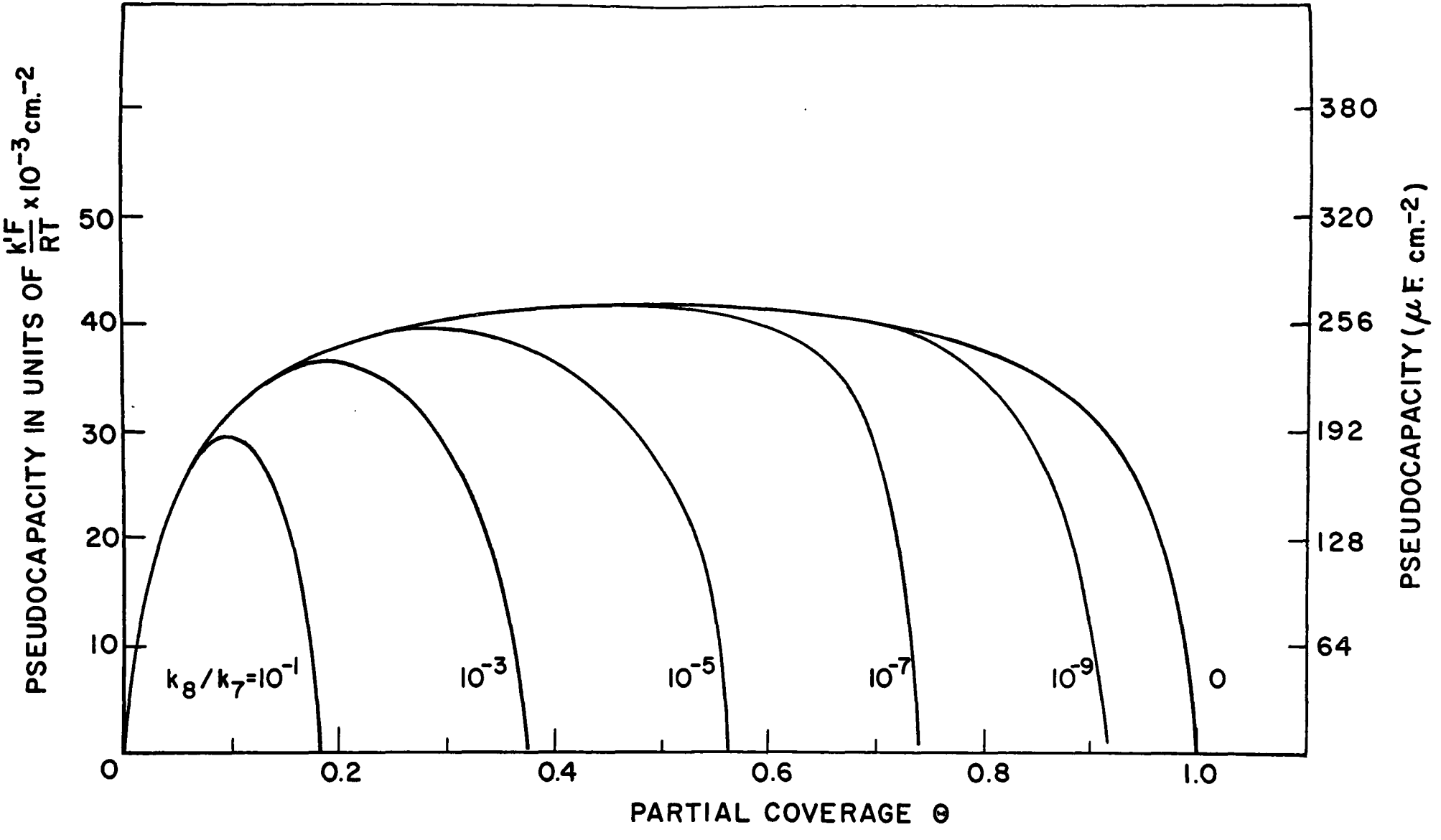
PSEUDOCAPACITY IN UNITS OF $\frac{k'F}{RT} \times 10^{-3} cm.^{-2}$
PSEUDOCAPACITY (μF. cm.$^{-2}$)
PARTIAL COVERAGE θ
0
10
20
30
40
50
64
128
192
256
320
380
0.2
0.4
0.6
0.8
1.0
$k_8/k_7 = 10^{-1}$
10^{-3}
10^{-5}
10^{-7}
10^{-9}
0

Figure 15. The coverage as a function of potential under non-equilibrium conditions, for different values of the ratio of specific rate constants for the initial discharge step (k_7) and the following ion-atom desorption step (k_8)

a. $r/RT = 10$,

b. $r/RT = 20$.

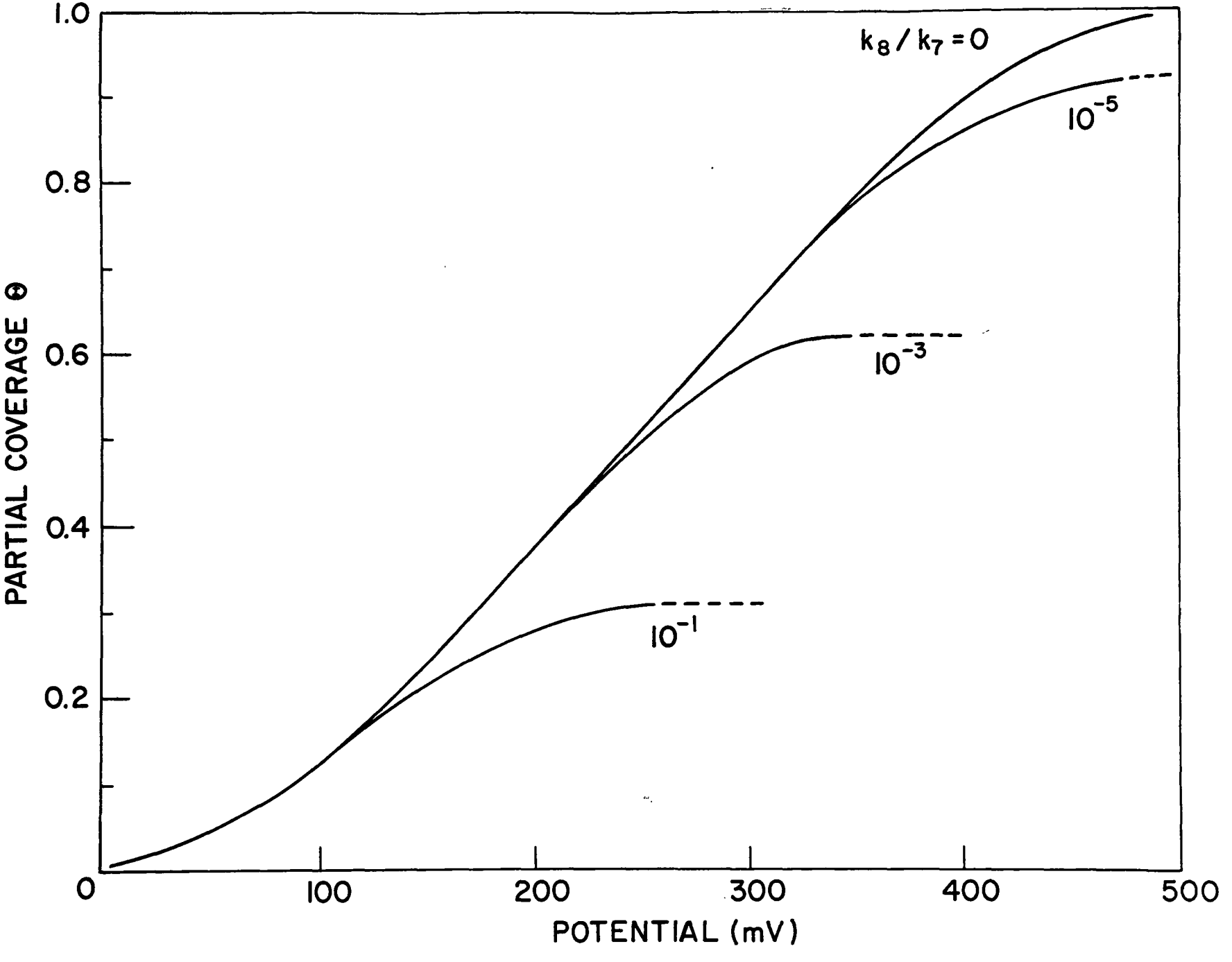
1.0
0.8
0.6
0.4
0.2
0
PARTIAL COVERAGE θ
100
200
300
400
500
POTENTIAL (mV)
$k_8 / k_7 = 0$
10^{-5}
10^{-3}
10^{-1}

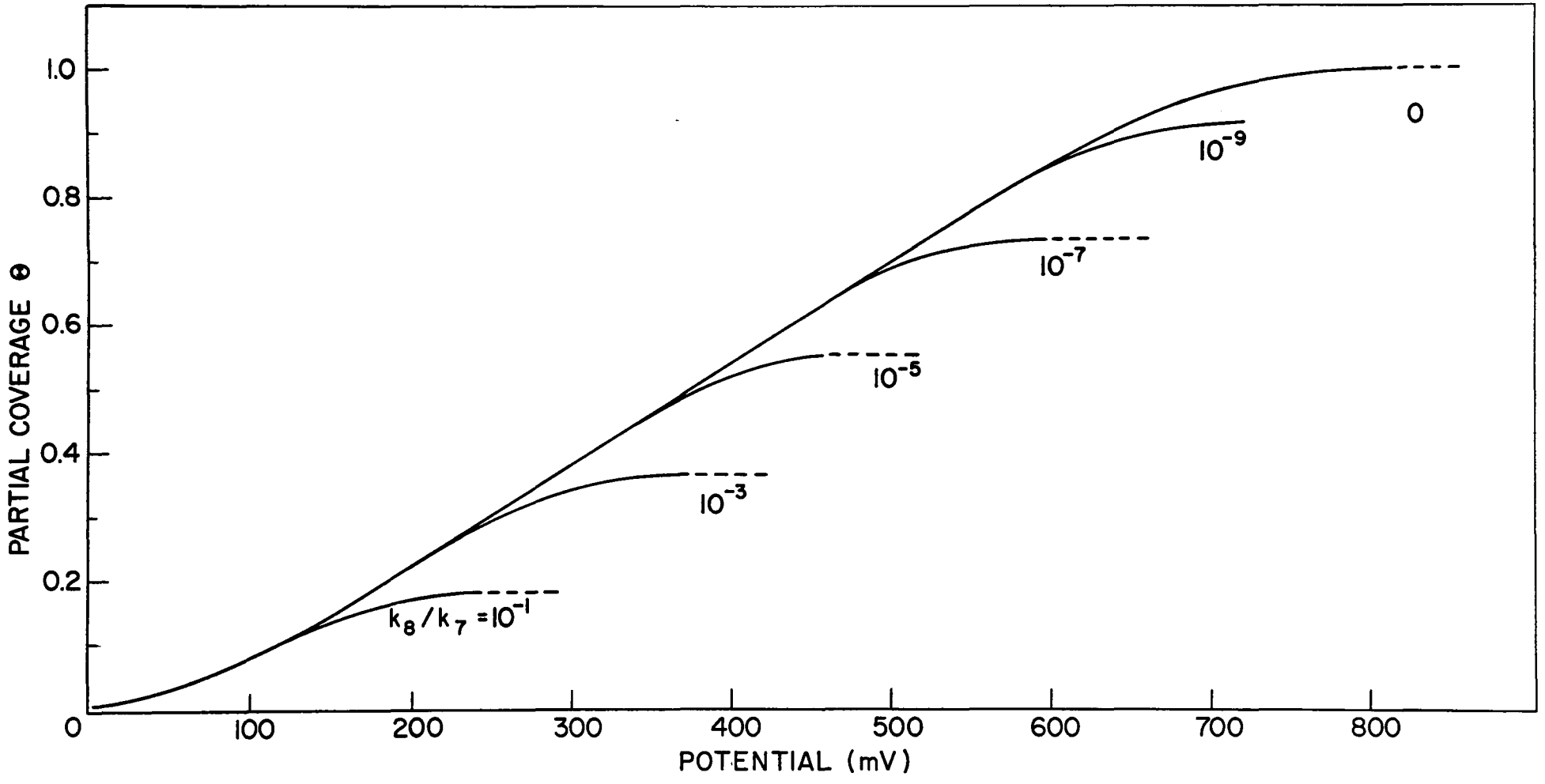
1.0
0.8
0.6
0.4
0.2
0
PARTIAL COVERAGE θ
100
200
300
400
500
600
700
800
POTENTIAL (mV)
0
10^-9
10^-7
10^-5
10^-3
k8 / k7 = 10^-1

Figure 16. The total effective adsorption pseudocapacity as a function of potential under non-equilibrium conditions for different values of the ratio of specific rate constants for the initial discharge step (k_7) and the following ion-atom desorption step (k_8)

a. r/RT = 10,

b. r/RT = 20.

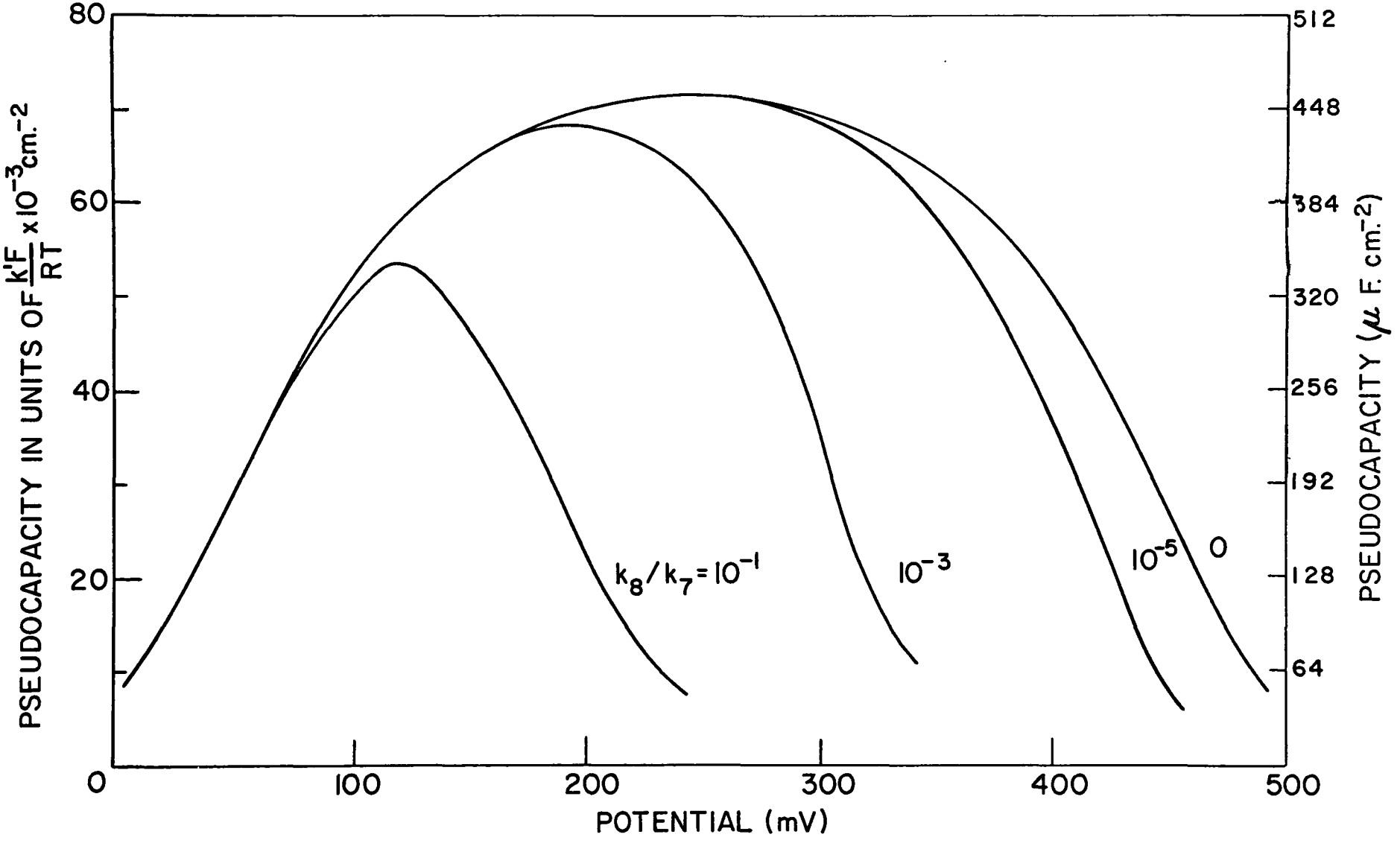
80
60
40
20
0
100
200
300
400
500
512
448
384
320
256
192
128
64
PSEUDOCAPACITY IN UNITS OF $\frac{k'F}{RT} \times 10^{-3} cm.^{-2}$
PSEUDOCAPACITY (μ F. cm.$^{-2}$)
POTENTIAL (mV)
$k_8/k_7 = 10^{-1}$
10^{-3}
10^{-5}
0

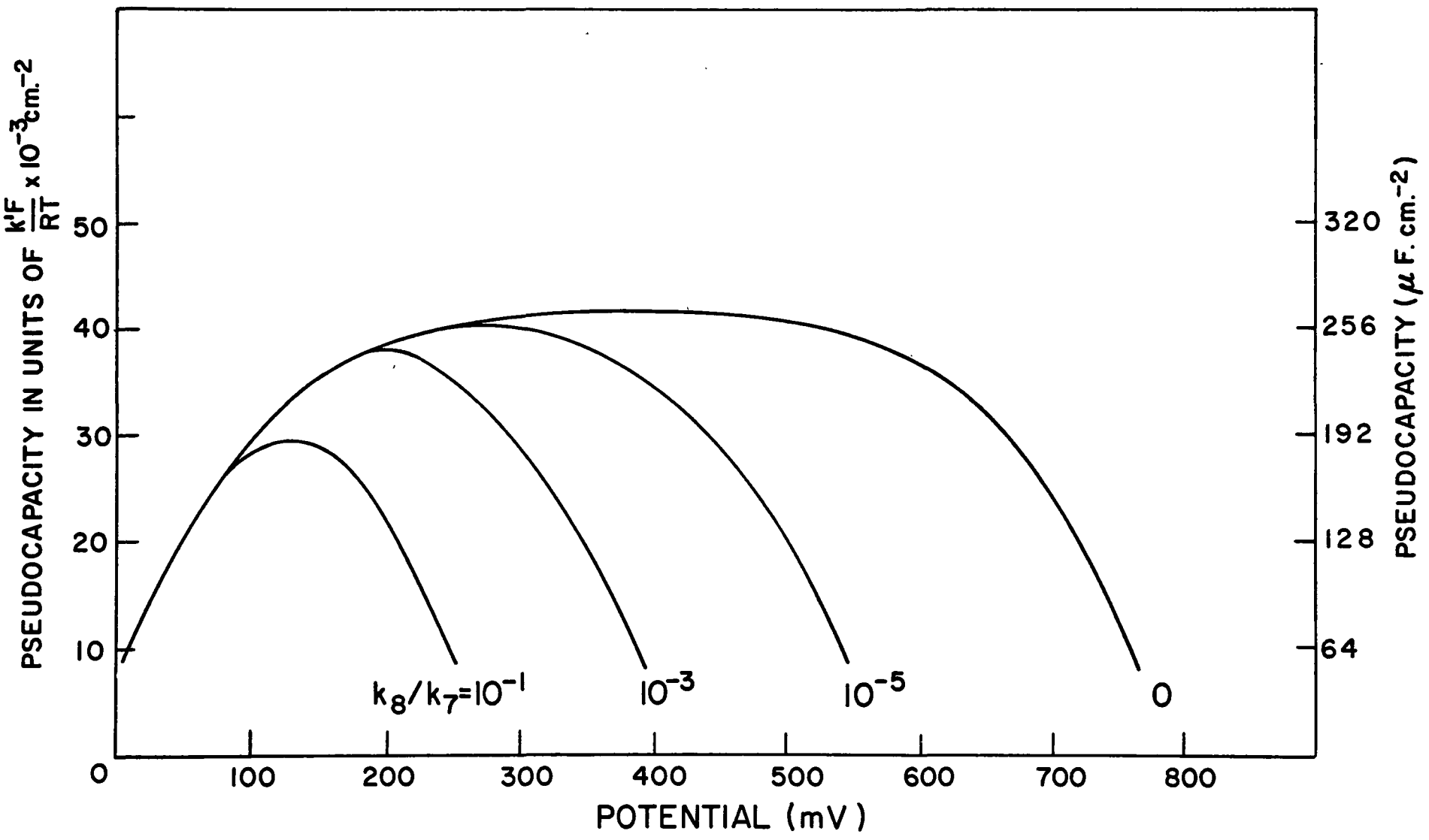
PSEUDOCAPACITY IN UNITS OF $\frac{k'F}{RT} \times 10^{-3} cm.^{-2}$
PSEUDOCAPACITY (μ F. cm.$^{-2}$)
POTENTIAL (mV)
0
10
20
30
40
50
64
128
192
256
320
100
200
300
400
500
600
700
800
$k_8/k_7=10^{-1}$
10^{-3}
10^{-5}
0

for the discharge step to be considered practically at quasi-equilibrium for the purpose of discussing the kinetics of the reaction, the pseudocapacity will reach a maximum value close to that obtained for complete quasi-equilibrium, but the potential range over which the pseudocapacity will be appreciable will be greatly decreased. This effect may lead to low apparent values of the parameter 'r' and the roughness factor 'f', which can be obtained from an analysis of the shape of the C-V curve by a method to be discussed in the following Chapter.

(iii) Conclusions

We may conclude that the pseudocapacity function appears to be much more sensitive to the various assumptions made in deriving the rate equations than the resulting overall current-potential behaviour. Thus we observed that while the pre-exponential terms in θ can be neglected with respect to the exponential terms when the current-potential relationship is considered at intermediate coverage, this is hardly ever justified for the purpose of calculating the total effective adsorption pseudocapacity and its dependence on θ and V. Further, the kinetic behaviour was shown to be independent of the form of the function $f(\theta)$ determining the variation of free energy of adsorption with coverage (cf. equations 58, 64, 73

while the form of the C-V relationship strongly depends on it (see Figs. 10, 11). Finally, if a primary charge transfer step exists which, without serious error, could be considered kinetically at quasi-equilibrium, it may nevertheless have to be considered significantly removed from a state of equilibrium when considerations of its pseudocapacity behaviour are involved.

CHAPTER IV

APPLICATIONS OF PSEUDOCAPACITY CALCULATIONS TO CERTAIN ELECTROCHEMICAL REACTIONS

The contents of this Chapter is largely based on a paper by Conway, Gileadi and Dziechuch (9) now in press in Electrochimica Acta. The experimental results which will be examined from a theoretical point of view concern the formate decarboxylation reaction, and were reported in detail in a previous thesis (27) and in several papers by Conway and Dziechuch now in press in the Canadian Journal of Chemistry.

1. THEORETICAL BASIS OF METHODS USED

(i) Determination of Pseudocapacity and Coverage

The various available methods for the determination of pseudocapacity and coverage have been critically reviewed in the Introduction. The adsorption pseudocapacity arising in the formate decarboxylation reaction was evaluated by combining the current-potential relationship obtained during steady state galvanostatic polarization, with open-circuit decay measurements, as discussed in the Introduction. Thus, at any potential, the self-discharge current density is in general $i_o \exp \eta_t/b_1$, where η_t is the overpotential at a time t after cessation of polarization and b_1 is the relevant Naperian

Tafel slope. This current density is also given in terms of capacitance as C $d\eta_t/dt$ at any time t during the e.m.f. decay when the overpotential has fallen to η_t. It follows that the capacity at any potential during the e.m.f. decay is given by

$$C = - \frac{i_o \exp(\eta_t/b_1)}{d\eta_t/dt} \qquad [128]$$

It is necessary to assume here that whatever process is rate-determining during steady state polarization at any potential is also rate-determining in the self discharge process at the same potential on open-circuit decay. This is usually implicit in most previous discussions (36,37,39) of the mechanism of e.m.f. decay on open-circuit at non-ideally polarizable electrodes, as discussed above. In fact, the commonly used method of determining the capacity from the steady state polarizing current density and the initial rate of decay of potential with time immediately following cessation of polarization can be shown to be a special case of our present method since, if we substitute t = 0 in equation [128] above, we obtain

$$C = \frac{i_o \exp(\eta_{in}/b_1)}{(d\eta/dt)_{t=0}} = - \frac{i_{in}}{(d\eta/dt)_{t=0}} \qquad [129]$$

where i_{in} and η_{in} are the values of the initial current density and overpotential, respectively, in the steady state

prior to cessation of polarization, and $(d\eta/dt)_{t=0}$ is the initial limiting decay slope at $t \rightarrow 0$. A further assumption which is required is that the pre rate-determining step involving the entities associated with the adsorption pseudo-capacity remains effectively at equilibrium throughout the e.m.f. decay. This is a satisfactory assumption, since the relative rates of the different consecutive steps in a reaction sequence depend on potential in the same way on open-circuit as during steady state polarization. If, therefore, it is justified to assume, for example, that the primary ionic discharge step is at quasi-equilibrium during polarization over a given range of potentials (when a subsequent step is rate-determining) the same assumption will continue to be valid for open-circuit decay in the same potential range. If conditions are such that quasi-equilibrium cannot be assumed to exist during steady-state polarization, our method of measuring the capacity will still be valid, since the deviation from a state of quasi-equilibrium at a given potential will be the same during open-circuit decay as during steady state polarization. Our discussion of the theoretical significance of the resulting C-V relationship will then have to be modified, however, as discussed in the previous chapter.

Past and Jofa (37) have compared, rather qualitatively, the capacity values obtained from initial decay slopes and

from analysis of the whole of the open-circuit decay curves in the case of the hydrogen evolution reaction on iron and nickel, and found that results from the two methods were in general agreement. Evidence of a more quantitative nature to the same effect is given in the following section for the case of oxygen evolution on a charged nickel oxide electrode at relatively high overpotential. We may note that equation [128] should not be taken as implying that knowledge of the Tafel slope b_1 is required for this method to be applicable. Moreover, it is not even required that a linear Tafel relationship exists in the range of potentials where the capacity is to be measured. In fact, the present method is best suited to cases where a transition region (in which the potential varies very rapidly with current density) is observed, as is the case in the formate decarboxylation reaction in pure formic acid (8,9,27) or during anodic passivation of metals (86). In general, the capacity is calculated from

$$C = - i_\eta / (d\eta_t/dt) \qquad [129a]$$

where i_η is the current density measured during steady state polarization at an overpotential η, and $d\eta_t/dt$ is the potential decay slope at a time t, when the overpotential has reached the same value η. In the formate decarboxylation reaction in pure anhydrous formic acid (the case examined here), there is very little hysteresis in the current-potential

relationship in the transition region, i.e. results obtained when the current density is gradually increased are almost identical with those obtained during gradual decrease of the current density. In other cases, when such hysteresis is found to occur e.g. in the formate decarboxylation in aqueous solutions (8), it is obvious that the i_η values used in equation [129a] should be those obtained during measurements at successively <u>decreasing</u> current densities.

Another way of determining the capacity at the metal solution interface from open-circuit decay behaviour was described in the Introduction and in previous papers (7,41). It was shown that the capacity was given by

$$C = \frac{i_{in}}{b_1} \cdot \phi \qquad [32]$$

where ϕ was a parameter (having the dimensions of time) which could be described as the time required for the potential to decay from a value corresponding to an infinite polarizing current density, to that corresponding to i_{in}. The parameter ϕ is determined experimentally as the quantity required to make a plot of η versus $\log (t+\phi)$ linear for all values of t down to $t \rightarrow 0$. It has been pointed out by Morley and Wetmore (36) and by Conway and Bourgault (61) that open-circuit decay lines commenced from different overpotentials plotted logarithmically in $(t+\phi)$ should all be superimposable if the

correct value of β has been used. We shall show below that this is, in fact, observed experimentally and values of the capacity obtained from equation [32] are in agreement with those obtained from equations [128] and [129] above.

(11) Determination of the Parameter r

The maximum value of the Langmuir pseudocapacity was shown above, and previously (10,46,70), to be

$$C_L(max) = \frac{k'F}{4RT} \qquad [92b]$$

where k' is the charge associated with the formation of a monolayer of adsorbed radicals on 1 $cm.^2$ of real surface of the electrode. It is evident, therefore, that if the maximum value of the total pseudocapacity per unit real surface area is experimentally available (e.g. if C can be measured as a function of V over a range where it passes through the maximum) and if k' can be estimated, it is possible to obtain C_T from equation [103]

$$C = \frac{C_T C_L}{C_T + C_L} \qquad [103]$$

and since $C_T = F/r$, the parameter r, determining the rate of decrease of free energy of adsorption with coverage, can be obtained. Normally, this procedure cannot be used, since the real to apparent surface area ratio (i.e. the roughness factor f) is not known accurately.

In the previous chapter we have derived equations for the relations between the total adsorption pseudocapacitance and coverage (equation [101]) and the coverage and potential (equation [100]); by combining these equations, we have numerically evaluated the total effective pseudocapacity associated with univalent radicals produced in an ion discharge step (when the subsequent step is rate-determining) as a function of electrode potential (see Fig. 6,7). From these calculations it was qualitatively evident that the width (along the potential axis) of the C-V curves, at a capacity corresponding to a given fraction of the maximum capacity, was a simple, approximately linear function of r. We shall now derive analytically the relation between the width of the C-V curve and the parameter r and propose a method by which both r and the roughness factor f can be obtained by means of a quantitative analysis of the curve.

From equation [101], namely

$$\frac{k'}{C} = \frac{RT}{F} \frac{d \ln \theta/(1-\theta)}{d\theta} + \frac{r}{F} \qquad [101]$$

we have

$$\frac{k'}{C} = \frac{1}{F} \left[\frac{RT}{\theta(1-\theta)} + r\right] \qquad [101a]$$

hence

$$C = k'F \left[\frac{\theta(1-\theta)}{RT + \theta(1-\theta)r}\right] \qquad [56a]$$

We then differentiate with respect to θ and make the differential coefficient equal to zero to obtain C(max). Thus

$$\frac{dC}{d\theta} = \frac{RT}{[RT+\theta(1-\theta)r]^2} (1-2\theta) = 0; \qquad [130]$$

the maximum hence occurs at $\theta = 0.5$, as in the limiting Langmuir case, and its value is given by substituting this value of the coverage into equation [56a] as

$$C(max) = \frac{k'F}{4RT + r} \qquad [57a]$$

We now calculate the two values of coverage at which the pseudocapacity equals a given fraction μ of the maximum value C(max), where

$$\mu = C_\mu/C(max) \qquad [131]$$

Combining equations [56a, 57a and 131] we obtain

$$\mu = k'F \left[\frac{\theta(1-\theta)}{RT+\theta(1-\theta)r}\right]/\left[\frac{k'F}{4RT+r}\right] = \frac{(4RT+r)\theta(1-\theta)}{RT+\theta(1-\theta)r} \qquad [132]$$

which is a quadratic equation in θ, namely

$$\theta^2 [4RT+r(1-\mu)] - \theta [4RT+4(1-\mu)] + \mu RT = 0 \qquad [132a]$$

the solution of which is

$$\theta_\mu = \frac{1}{2} \pm \frac{1}{2} \left\{(1-\mu) \left[\frac{4RT+r}{4RT+r(-\mu)}\right]\right\}^{1/2} \qquad [133]$$

where θ_μ is now the value of the coverage at which the pseudocapacity is the fraction μ of its maximum value C(max), as defined by equation [131]. The two solutions of the quadratic

equation [132a] represent two points on the C-θ diagram, symmetrically situated about C(max), where the capacity has a value defined by equation [131].

For the limiting Langmuir case (r = 0), equation [133] becomes

$$\theta_\mu = 0.5 \pm 0.5\,(1-\mu)^{1/2} \qquad [133a]$$

We next calculate the potentials corresponding to each of the two values of θ_μ calculated above (equation 133) and their difference ΔV_μ, which is obviously the quantity sought in the present calculation, i.e. the distance along the potential axis between two points corresponding to the same value of the pseudocapacity C_μ defined by equation [131] on the C-V diagram.

For the limiting Langmuir case we obtain by combining equations [100] and [133a]

$$V_2 = \frac{RT}{F} \ln\left\{\frac{0.5 + 0.5\,(1-\mu)^{1/2}}{1-[0.5+0.5(1-\mu)^{1/2}]}\right\} + {}^1K_7$$

$$= \frac{RT}{F} \ln\left[\frac{1 + (1-\mu)^{1/2}}{1 - (1-\mu)^{1/2}}\right] + {}^1K_7 \qquad [134]$$

$$V_1 = \frac{RT}{F} \ln\left\{\frac{0.5-0.5\,(1-\mu)^{1/2}}{1-[0.5-0.5(1-\mu)^{1/2}]}\right\} + {}^1K_7$$

$$= \frac{RT}{F} \ln\left[\frac{1-(1-\mu)^{1/2}}{1+(1-\mu)^{1/2}}\right] + {}^1K_7 \qquad [134a]$$

hence

$$\Delta V_\mu = V_2 - V_1 = \frac{2RT}{F} \ln \left[\frac{1 + (1-\mu)^{1/2}}{1 - (1-\mu)^{1/2}}\right] \qquad [135]$$

when r = 0. We may now consider the more general case when r can assume any value. Equation [133] is rewritten for convenience as

$$\theta_\mu = 1/2 \pm a \qquad [133b]$$

where a is defined by

$$a = 1/2 \left\{(1-\mu) \left[\frac{4RT + r}{4RT + r(1-\mu)}\right]\right\}^{1/2} \qquad [136]$$

When the two resulting values of θ_μ are now substituted into equation [100], we obtain

$$V_2 = \frac{RT}{F} \ln \left[\frac{0.5+a}{1-(0.5+a)}\right] + \frac{r}{F}(0.5 + a) + {}^1K_7 \qquad [137]$$

$$V_1 = \frac{RT}{F} \ln \left[\frac{0.5-a}{1-(0.5-a)}\right] + \frac{r}{F}(0.5 - a) + {}^1K_7 \qquad [137a]$$

hence

$$\Delta V_\mu = V_2 - V_1 = \frac{2RT}{F} \ln \left(\frac{0.5+a}{0.5-a}\right) + \frac{2ra}{F} \qquad [138]$$

From equation [138], we can calculate values of ΔV_μ for any value of μ and plot them numerically as a function of r with the quantity a calculated from equation [136]. The value of r can then be determined from the experimentally measured potential "width" ΔV_μ at any position up an experimental (symmetrical) C-V curve defined by a value of μ.

We may note that ΔV_μ in equation [138] is comprised of two terms, which we denote by

$$\Delta V_\alpha = \frac{2RT}{F} \ln \left(\frac{0.5+a}{0.5-a}\right) \quad \text{and} \quad \Delta V_\beta = \frac{2ra}{F} \qquad [139]$$

Since a varies rather slowly with r (at intermediate values of μ, say $0.3 < \mu < 0.7$) we can regard ΔV_α as almost independent of r and ΔV_β as linear function of r. Thus equation [138] becomes

$$\Delta V_\mu = K_\alpha + K_\beta r \qquad [140]$$

where K_α and K_β are, to a first approximation, independent of r. In Fig. 17 is shown the variation of ΔV_μ, ΔV_α and ΔV_β with r. It is clear then that over a wide range of values of r, the quantity ΔV_μ is almost a linear function of r. The deviations of the slope of the ΔV_μ-r plot at each extreme (r/RT = 0 to r/RT = 40) from the mean slope at r/RT = 20 is less than 3%, so that the error arising from the use of equation [140] is negligible with respect to errors involved in the determination of ΔV_μ, as will be discussed below. The scope of this method is obviously not limited by the approximate nature of equation [140]. Were ΔV_μ obtainable experimentally with a high degree of accuracy, equation [138] could be used instead to evaluate r with an accuracy corresponding to that of ΔV_μ. Such a calculation would be justified if the assumptions leading to equation [138], in particular that regarding the

Figure 17. The width ΔV_μ (and its components ΔV_α and ΔV_β) of the C-V plot at a capacity $C_\mu = \mu\, C(max)$ along the V axis (cf. equation 140) as a function of the parameter r.

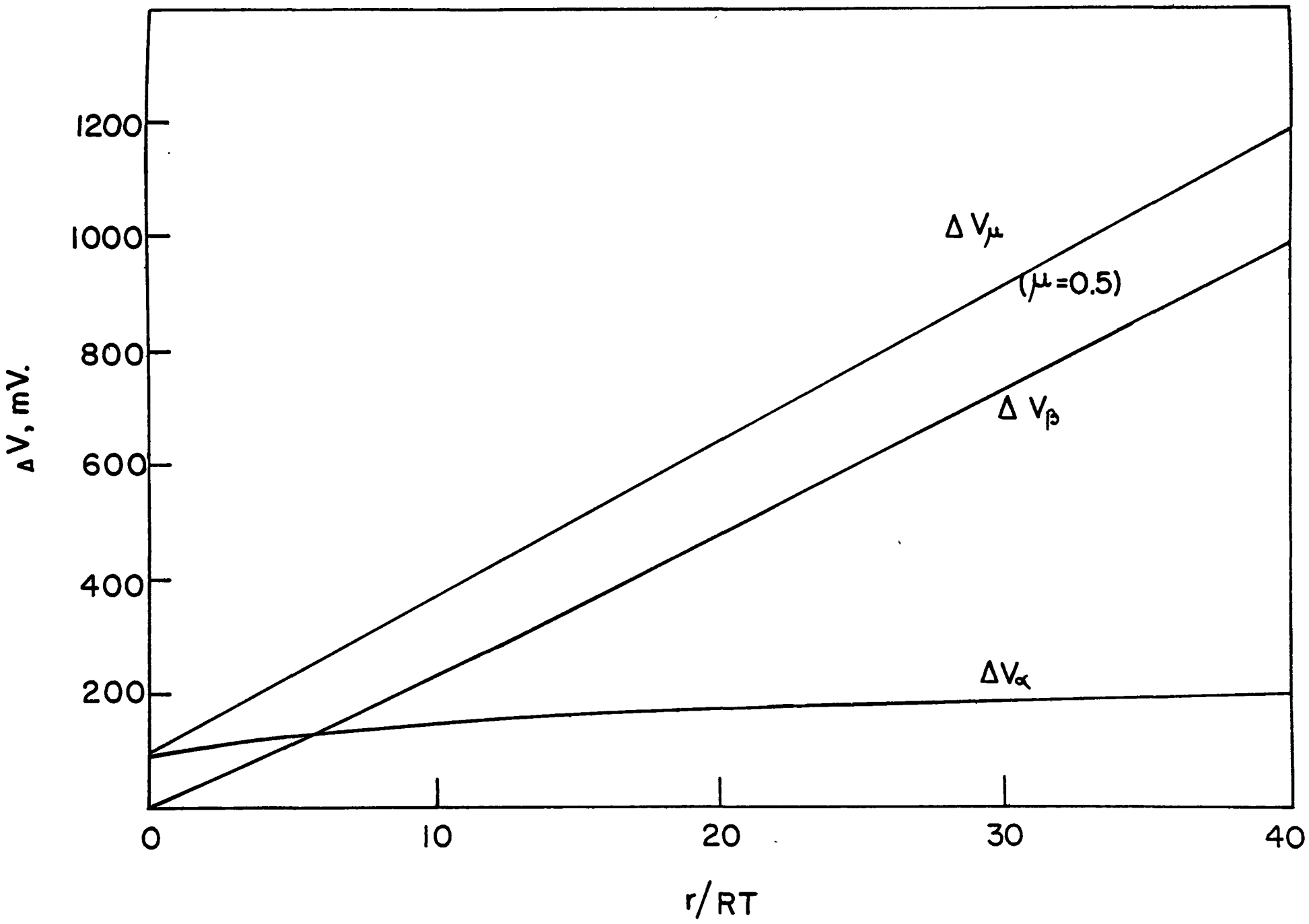
1200
1000
800
600
400
200
ΔV, mV.
ΔVμ
(μ=0.5)
ΔVβ
ΔVα
0
10
20
30
40
r/RT

existence of a rate-determining step with the previous ion discharge step at quasi-equilibrium, were valid.

Numerically equation [140] is

$$\Delta V_{0.5} = 90 + r/90.3 \times 10^3$$

for μ taken as equal to 0.5, with $\Delta V_{0.5}$ expressed in mV and r in J. equivalent^{-1}. Similar, almost linear expressions can be obtained for ΔV_{μ} as a function of r for other intermediate values of μ. It is obvious that the r value calculated from a given experimental C-V curve should be independent of the fraction μ at which it is determined and this requirement can, in fact, serve as a criterion for testing whether the experimentally obtained C-V curve has the theoretically predicted shape.

The fundamental advantage of the method just described for the determination of r is that it depends only on relative values of the measured capacity, and is therefore completely free from errors due to rather arbitrarily assigned values of the roughness factor. Moreover, determination of r by the method described above enables us to estimate the roughness factor, as we now proceed to show.

The parameter r can, however, only be determined by this method when the adsorption pseudocapacity is known over a potential region where it passes through a maximum and the shape of the C-V curve is symmetrical with respect to this

maximum. It is also required that the initial discharge step be at quasi-equilibrium with a following step rate-determining, as discussed above.

(iii) Determination of the Roughness Factor of Electrodes from Adsorption Pseudocapacity Data

The rates of heterogeneous reactions are usually proportional to the area of the interface and specific rate constants must hence be defined per unit surface area. In electrode kinetics the overpotential is related in an unambiguous manner to the current density, defined in terms of the current passing across the metal-solution interface per unit real area of the interface. It has been realised early in the study of electrode kinetics that the geometrical apparent surface area is not equal to the real surface area available for electrochemical reactions even on highly polished, apparently smooth electrodes; thus a method by which the roughness factor f (i.e. the real to apparent surface area ratio) could be estimated, is required. Frumkin and co-workers (4) have estimated the real surface area of solid electrodes by measuring the capacity associated with charging of the ionic double-layer, and comparing it with the ionic double-layer capacity at mercury (where obviously f = 1) at a

comparable rational potential,* preferably somewhat negative to the potential of zero charge. This method has since been used in numerous electrochemical studies and it probably yields the right order of magnitude of the roughness factor. However, since the double-layer capacity behaviour at solid electrodes is not usually well known, and the position of the potential of zero charge usually cannot be determined accurately, the quantitative comparison of ionic double-layer capacities at solid electrodes with that at mercury must remain somewhat dubious.

Breiter, Knorr and Volkl (25) have attempted to estimate the real surface area of electrodes by measuring the charge required to form an oxide monolayer during anodic charging at a constant current density. It has been pointed out by Bockris and Devanathan (21) that this method could not be regarded as satisfactory, since the oxide film formed could hardly be expected to be stoichiometric, particularly on the noble metals, the oxides of which are known to be non-stoichiometric even when produced in the bulk phase;

---

* The term "rational potential" was first introduced by Grahame, (17) and refers to the potential relative to the p.z.c.

alternatively oxides in different and unknown valency states could be formed.

Recently (7,48) the B.E.T. method has been used with krypton to determine the real surface area of porous electrodes. This method involves drying the electrode material and measuring the extent of adsorption of the inert gas. The B.E.T. method can be expected to yield results of the right order of magnitude only, since the structure of the porous electrode may be altered to a significant extent during the drying process and, moreover, the surface available for gas adsorption may not be equal to that available for electrochemical reactions, particularly at porous electrodes which may have an intricate fine structure.

Here we propose a new method for the determination of the roughness factor, developed by Conway, Gileadi and Dzieciuch (9) and apply it to the measurement of real surface areas of Pt and Pd electrodes used in the studies of electrochemical decarboxylation of formate in pure anhydrous formic acid solutions.

The maximum value of the adsorption pseudocapacity has been given above as

$$C(max) = \frac{k'F}{4RT + r} \qquad [57a]$$

We have shown in the previous section how the parameter r, determining the rate of decrease of the free energy of adsorption

with increasing coverage, could be determined by a method which does not require a knowledge of the real surface area of the electrode. Hence, if the experimentally determined value of the maximum pseudocapacity per unit apparent (geometrical) surface area is divided by the quantity calculated from equation [57a], the roughness factor is obtained. In order to apply this method experimentally, we have to know k', which involves assigning a value to the number of adsorption sites per $cm.^2$ on the electrode surface. This is generally achieved by estimating the number of sites e.g. on Pt and Ni electrodes (12,21,28) from the lattice parameters for the metals, assuming for example that one hydrogen atom is required per metal atom on the surface to form a complete monolayer. In examining the formate decarboxylation reaction, Conway and Dzieciuch (8), have used Courtauld space filling models to estimate the number of formate radicals per unit real surface area, and took this number as the reciprocal of the projected surface area of a single radical. Both methods are probably rather approximate, but it must be remembered that the uncertainty in the value of k' causes a non-random error which is inherent in the calculation of the fractional coverage θ from the surface concentration even if the real surface area were known very accurately. The proposed method of determining the roughness factor f is hence not limited practically by the error involved in k'.

A second method may, under certain conditions, be employed for the determination of the roughness factor. It depends on the fact that the maximum in the C-V curve will always occur at $\theta = 0.5$, provided that the assumptions leading to the general equation [56a] for the pseudocapacity are valid. The charge required to cover half the surface can be obtained from the equation

$$\Delta q = \int_{V_1}^{V_2} C dV \qquad [141]$$

where Δq is the charge required to change the potential of the electrode from a value V_1 to V_2. The lower potential V_1 is chosen such that the coverage corresponding to it is negligible, and V_2 is taken as the potential at which C is a maximum. The integral in equation [141] can then be evaluated numerically, using the experimentally determined C-V relationship. Since Δq calculated in this manner corresponds to $\theta = 0.5$, the real surface area can be determined once k' has been estimated, as discussed above. This method would be most satisfactorily applicable to systems for which r was rather small and the position of the maximum in the C-V plot could be determined accurately.

The two methods of determining the roughness factor from capacity measurements described above offer obvious

advantages over the B.E.T. method, since they measure the electrochemically accessible area of the electrode under working conditions; thus whatever surface area is available for adsorption of reaction intermediates is obviously available also for the relevant electrochemical process as a whole. The pseudocapacity methods are to be preferred to the method depending on measurement of the ionic double-layer capacity, since they do not depend on the rather dubious extrapolation from one system to another (i.e., from a liquid mercury electrode to solid metal electrodes).

The same limitations apply here as in the case of the method for the determination of the parameter r, discussed above; namely, that the pseudocapacity must be known experimentally as a function of potential over a range where it passes through its maximum. The form of the C-V curves must be symmetrical (confirming that the free energy of adsorption decreases <u>linearly</u> with coverage), and the initial discharge step must be at equilibrium with a following step rate-determining, as discussed above.

2. APPLICATION TO THE FORMATE DECARBOXYLATION REACTION*

We now apply the above analysis to e.m.f. decay and

---

* The experimental basis of the work discussed in this section has been reported in a recently presented thesis in this Department (27), in a series of papers by Conway and Dzieciuch (8) and in a joint theoretical paper by Conway, Gileadi and Dzieciuch (9).

polarization curves obtained in a previous study (8) in this laboratory, of the mechanism of decarboxylation of formate ions in 100% formic acid examined as a model reaction for studies of the Kolbe synthesis. In this reaction, a sharp transition in the current-potential curve is observed (8) which is analogous to that found when anodic passivation of metals occurs. The transition behaviour is not associated with a diffusion-controlled limiting current and must be ascribed to some change of condition of the surface at a critical current density. The results obtained by analysis of the e.m.f. decay and polarization data for this transition region enable an evaluation to be made of the pseudocapacity changes which occur in this region. Examination of the capacity-potential curve then allows calculation of surface coverage by the reaction intermediates and estimation of the parameter r relating the free energy of adsorption of the intermediates to surface coverage in a Temkin type adsorption isotherm (10,30,50,53).

(1) Experimental

(a) General

Current-potential curves, obtained from constant current anodic polarization runs, were used with complementary e.m.f. decay measurements, to examine the dependence of coverage and pseudocapacity on potential. The current potential curves are in course of publication elsewhere (8) in a paper on the

kinetics of formate decarboxylation (and have been presented in the thesis mentioned above, 27) and only a typical plot will be reproduced here (Fig. 18). Similarly, only a single typical e.m.f. decay curve (Fig. 19) is given which illustrates the arrest of potential normally observed in this system on open-circuit decay, and associated with an appreciable adsorption pseudocapacity. When time-variation of the electrode potential occurred near the observed transition current region during polarisation (Fig. 18), the steady values obtained after waiting 5-10 minutes were taken. In the linear Tafel regions above and below the limiting current-density for transition in the current-potential behaviour, little time-variation of potential was encountered.

Decay of e.m.f. was followed by interrupting the polarizing current by means of a fast (2-3 μsec.) mercury-wetted vacuum relay, after a steady potential had been reached. The e.m.f. measured with respect to either of a pair of hydrogen electrodes in the same solution, was fed to a calibrated Hewlett-Packard oscilloscope through a Keithley electrometer (input impedance 10^{14} ohms). The decay curves were photographed and enlarged some ten times for quantitative measurement. Slopes $d\eta/dt$ were obtained by the prism and set-square method to ± 2%.

Figure 1). Current-potential curves showing typical transition behaviour for anodic polarization of Pd, Pt and Au in 100% formic acid + 1M potassium formate at 5°C. A typical population of points for several electrodes in the case of Au is shown. The Tafel lines for Pd and Pt are the mean lines for eight electrodes in two solutions.

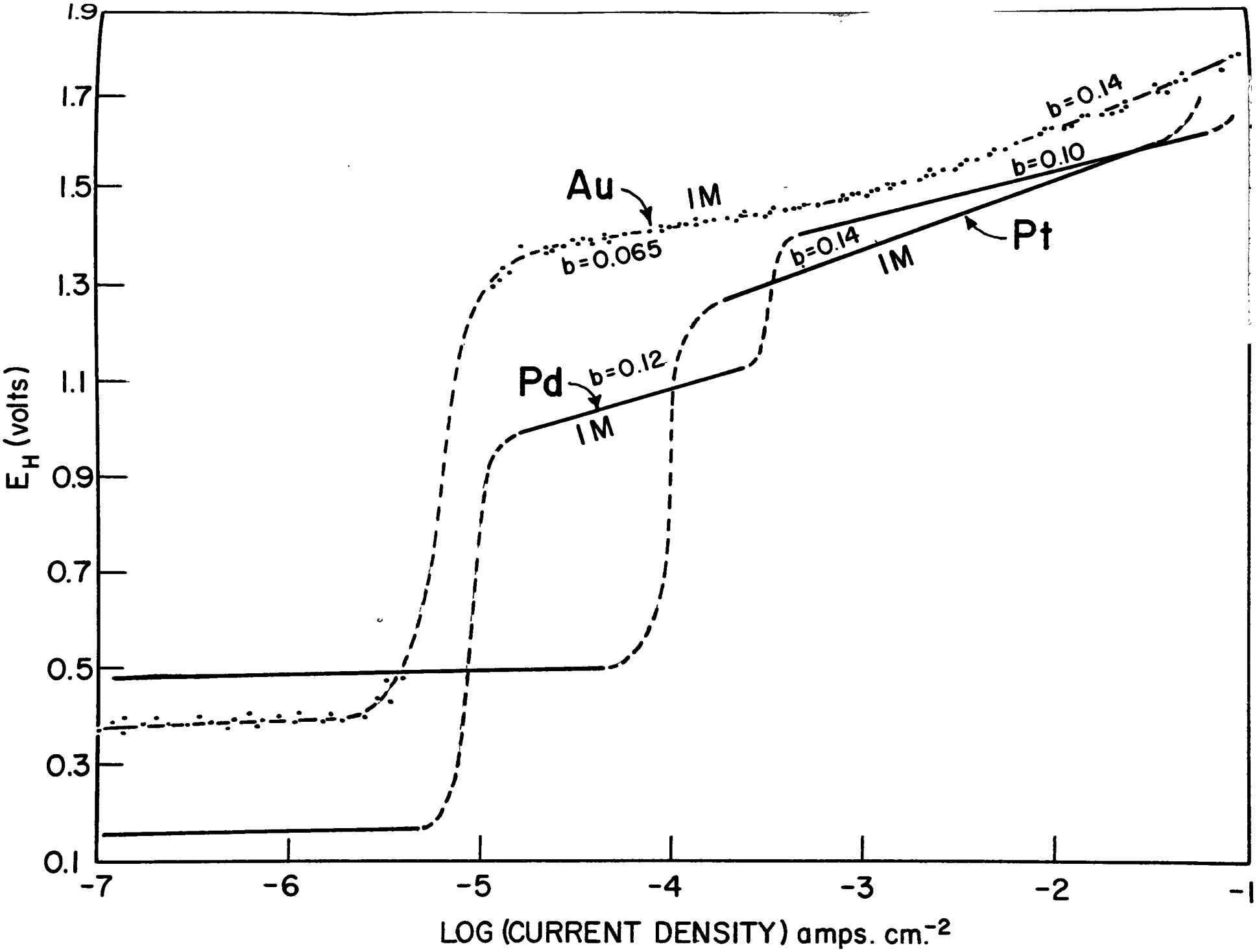
1.9
1.7
1.5
1.3
1.1
0.9
0.7
0.5
0.3
0.1
E_H (volts)
-7
-6
-5
-4
-3
-2
-1
LOG (CURRENT DENSITY) amps. cm.$^{-2}$
Au
1M
b=0.065
b=0.14
b=0.10
Pt
b=0.14
1M
Pd
b=0.12
1M

Figure 19. Typical e.m.f. decay curve following anodic polarization to the transpassive region in formate decarboxylation in pure anhydrous formic acid at a Pt electrode.

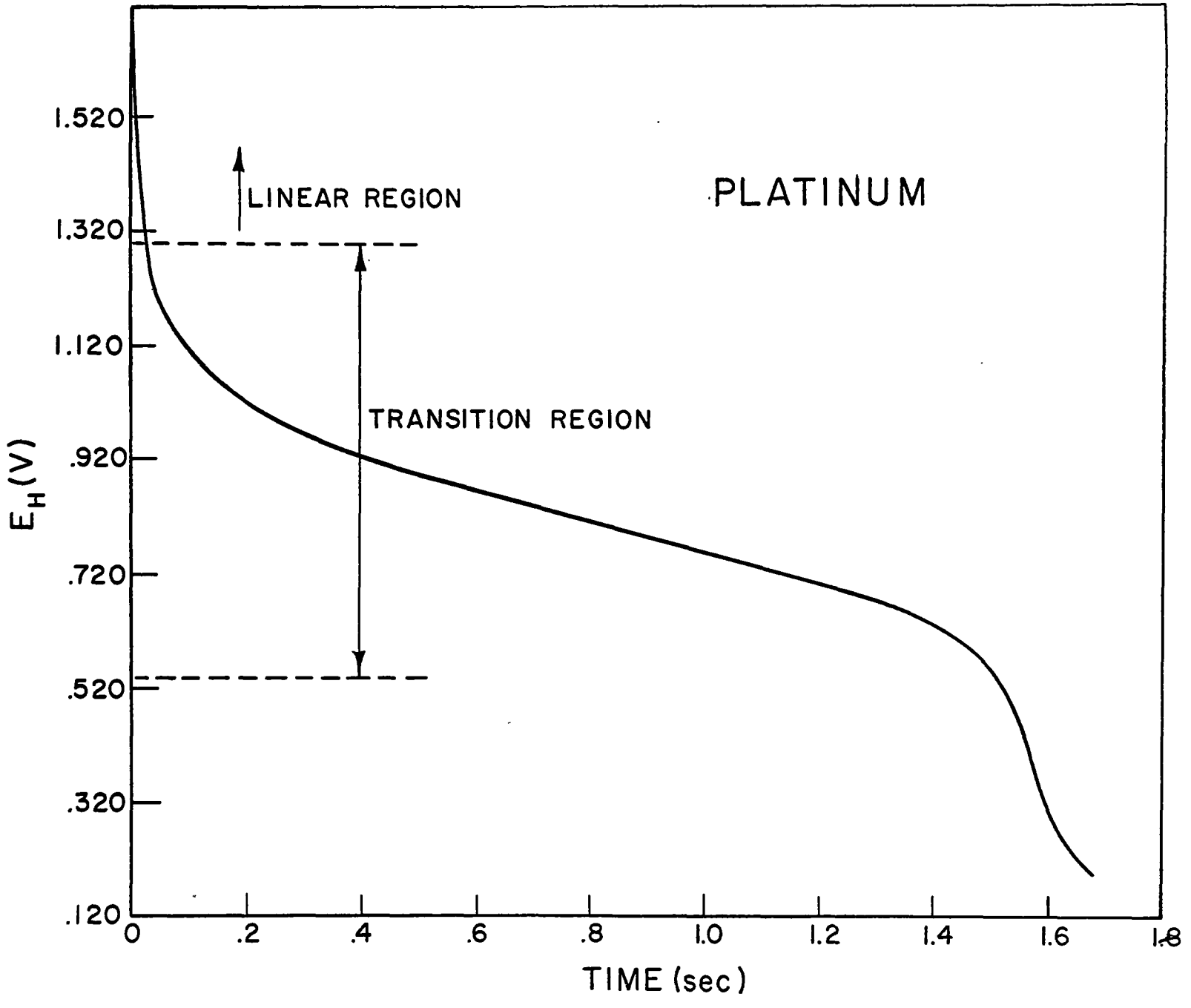
1.520
1.320
1.120
.920
.720
.520
.320
.120
E_H (V)
LINEAR REGION
PLATINUM
TRANSITION REGION
0
.2
.4
.6
.8
1.0
1.2
1.4
1.6
1.8
TIME (sec)

(b) Preparation of Electrodes and Solutions; Instrumentation

High purity methods were used as described previously (87). All solutions were pre-electrolysed (24h.; 10^{-2}Amp.cm.$^{-2}$) and electrodes were prepared in protective glass bulbs (83) and maintained thus in the solution during electrolytic purification of the electrolyte. Electrode metals were Johnson Matthey spectroscopically pure gold, palladium and high purity platinum.

Details of solution preparation, electrical circuit and instrumentation have been described in detail previously (8,27). Pure formic acid was prepared by dehydrating the reagent grade material over anhydrous boric oxide and anhydrous copper sulphate followed by distillation in vacuo. One molar solutions of anhydrous potassium formate as the electrolyte were made up in the 100% formic acid. Purified medical grade carbon dioxide was bubbled through the solutions during the pre-electrolysis and initial polarisation; purified hydrogen (87) was bubbled through the separate reference electrode compartment at the time of the run.

All runs were conducted at 5^{o}C in order to minimise anodic attack of the palladium electrodes which occurs significantly at room temperature in this system.

(ii) Results

(a) General

Typical steady-state current-potential curves are shown in Fig. 18 for Pd, Au and Pt. It is seen that at Pt and Au, two Tafel regions are well defined and separated by a transition region associated with an activation-controlled limiting current. The transition behaviour is not associated with a diffusion-controlled oxidation of impurities since it remains unchanged even in the most rigorously purified formate/formic acid solutions. Qualitatively similar behaviour is observed in the trifluoroacetate decarboxylation (8) and in the aqueous formate decarboxylation reactions.

At Pd two transition regions are observed with an intermediate linear Tafel region which is, however, less reproducible. The significance of the two transition regions observed will be discussed below. In general, the behaviour in the linear Tafel regions above and below the transition region are quite reproducible and the data shown are based on runs conducted with ten electrodes of each metal in at least two separately prepared solutions. The potentials in the transition region, at a given current density, vary with time and cannot, therefore, be determined quite as accurately as in the linear Tafel regions (more precise results can be obtained in

this region potentiostatically). However, as we have shown above, we require only the current-density which is approximately constant in this transition region, so that the capacity is mainly determined by $d\eta/dt$ (equation 129a), which is the principal variable over this range of potential. The significant uncertainty in the potential as a function of current density in the transition region hence does not seriously limit the accuracy of the capacities calculated for this region. Below and above the transition region, where the current varies more with potential than in the middle region, the current-potential relation can be defined experimentally with normal precision; hence the capacities can be evaluated again with satisfactory accuracy.

In the present anhydrous formic acid system, there is little hysteresis in the current-potential relationship for increasing and decreasing current densities; the observed current-potential relationship for steady d.c. polarization at successively increasing constant current densities may hence be used in conjunction with the open-circuit decay curves for the calculation of the pseudocapacity as a function of potential. When hysteresis is observed (e.g. during formate decarboxylation in aqueous solutions (8)) the current-potential relation for decreasing current-densities would have to be used, as discussed above.

A typical e.m.f. decay curve for the anodic decarboxylation of formate (1M HCOOK) in 100% formic acid at 5°C is shown in Fig. 19 for the palladium electrode.

(b) Intermediates Involved in the Formate Decarboxylation Reaction

A general discussion of the mechanism of decarboxylation of formate in formic acid has been given by Conway and Dzieciuch (3). It has been shown that the reaction is

$$HCOO^- \longrightarrow H^+ + CO_2 + 2e \qquad XI$$

[or $HCOOH \longrightarrow 2H^+ + CO_2 + 2e$]

and that the intermediate steps at a site M on the metal surface are probably

$$HCOO^- + M \longrightarrow MHCOO + e \qquad XII$$

$$MHCOO \longrightarrow MH + CO_2 \qquad XIII$$

$$MH \longrightarrow M + H^+ + e \qquad XIV$$

or

$$MHCOO \longrightarrow M + CO_2 + H^+ + e \qquad XV$$

Reaction XIV will be very fast at the high anodic potentials involved ($E_H > + 1.5$ V) so that significant coverage by H* is unlikely. The ionisation steps XIV or XV are thus preferred to H recombination to give H_2, a step which is not observed (8). This is presumably why a "Kolbe" reaction (to give H_2) does

not occur in formate decarboxylation. Any pseudocapacity will hence be mainly associated with adsorbed HCOO in XII and XIII and the coverage will be appreciable if the rate constants for the forward and backward directions of XII tend to be much greater than those for XIII or XV.

(c) Evaluation of Pseudocapacity in the Transition Region

The electrode capacity is evaluated using equation [128] in which the self-discharge current $i_o \exp \eta_t/b$ passing at the potential η_t on the e.m.f. decay plot, is identified with the actual current passing at the same potential determined from the steady-state current-potential relations (Fig. 18). In the transition region itself, which is of special interest here, the current (which we denote by i_T) is almost independent of electrode potential over about 0.5 - 1.0 V. Hence, at any point in the e.m.f. decay curve over this range of potential, the self-discharge current passing will be approximately constant and equal to i_T and its exact dependence on η will not be of critical importance in the evaluation of C.

The values of C as a function of overpotential* for

---

* Here we have used the overpotential referred to a theoretical potential, with respect to the hydrogen electrode in the same solution, for the reaction $HCOOH \rightarrow CO_2 + H_2$ at 25°C. An estimate of the standard entropy change (89) for this reaction indicates that the reversible potential will be approximately 17 mV. different at 5°C. This will not significantly change the calculated values of capacity or surface coverage deduced below for the transition region but will only shift the potential scale for the potential dependence of these quantities.

the reaction (based on a theoretical reversible potential (8) for XI of E_H = -0.230 V [European convention] standard state unit mole fraction of HCOOH, 25°C) are shown in Figures 20, 21 and 22. It is evident that the values of C are much larger than those (ca. 40-100 μF. cm.$^{-2}$) corresponding to an anodic ion double-layer capacity (17) and hence must be identified with an adsorption pseudocapacity . The curves of C as a function of η also have the correct (10,70) form, viz. a maximum with C decreasing towards zero at potentials appreciably higher or lower than that of the maximum. We suggest that this pseudocapacity is associated with production of HCOO• radicals at the surface, since the steady state concentration of H• will tend to be very small under the conditions of high anodic polarisation.

In the case of Pd, a region of appreciable pseudocapacity arises at the first transition region (Fig. 18) and is then succeeded by another pseudocapacity region at a higher potential. The magnitude and range of potential dependence of this second pseudocapacity (Fig. 22) indicates that it approaches ideal Langmuir behaviour the most closely in the present series of results. An ideal Langmuir pseudocapacity (10,30) will have a maximum value of $k'F/4RT$ F.cm.$^{-2}$ where k' is the charge associated with formation of a monolayer of adsorbed radicals on one cm.^{2} real surface area. For HCOO•,

Figure 20. The variation of capacity with overpotential in the transition region for the formate decarboxylation reaction at a Pt anode in pure anhydrous formic acid. The capacity was obtained from open-circuit decay and steady-state polarization measurements.

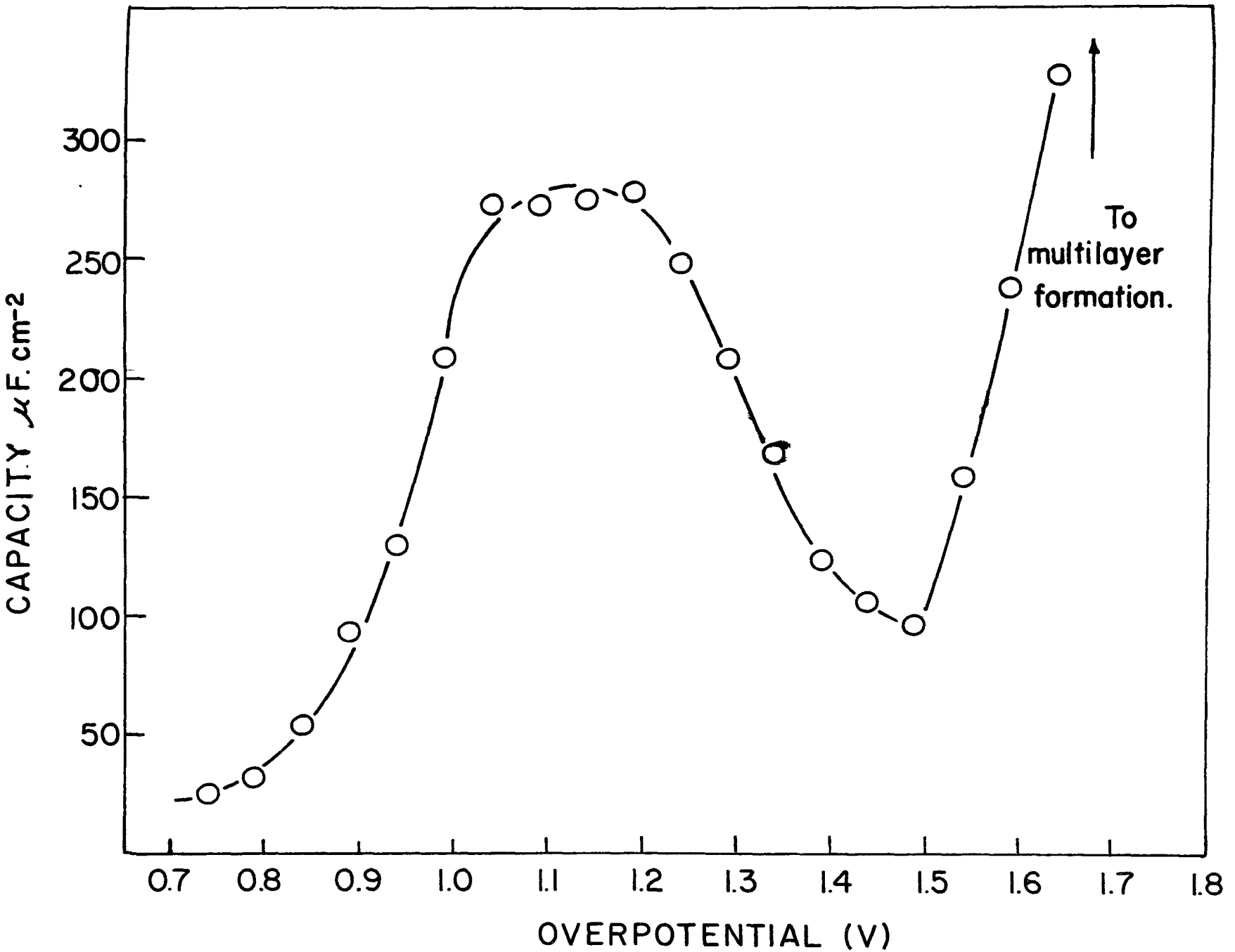
CAPACITY μF.cm⁻²
300
250
200
150
100
50
0.7
0.8
0.9
1.0
1.1
1.2
1.3
1.4
1.5
1.6
1.7
1.8
OVERPOTENTIAL (V)
To multilayer formation.

Figure 21. The variation of capacity with overpotential in the transition region for the formate decarboxylation reaction on a gold anode in pure anhydrous formic acid. The capacity was obtained from open-circuit decay and steady-state polarization measurements.

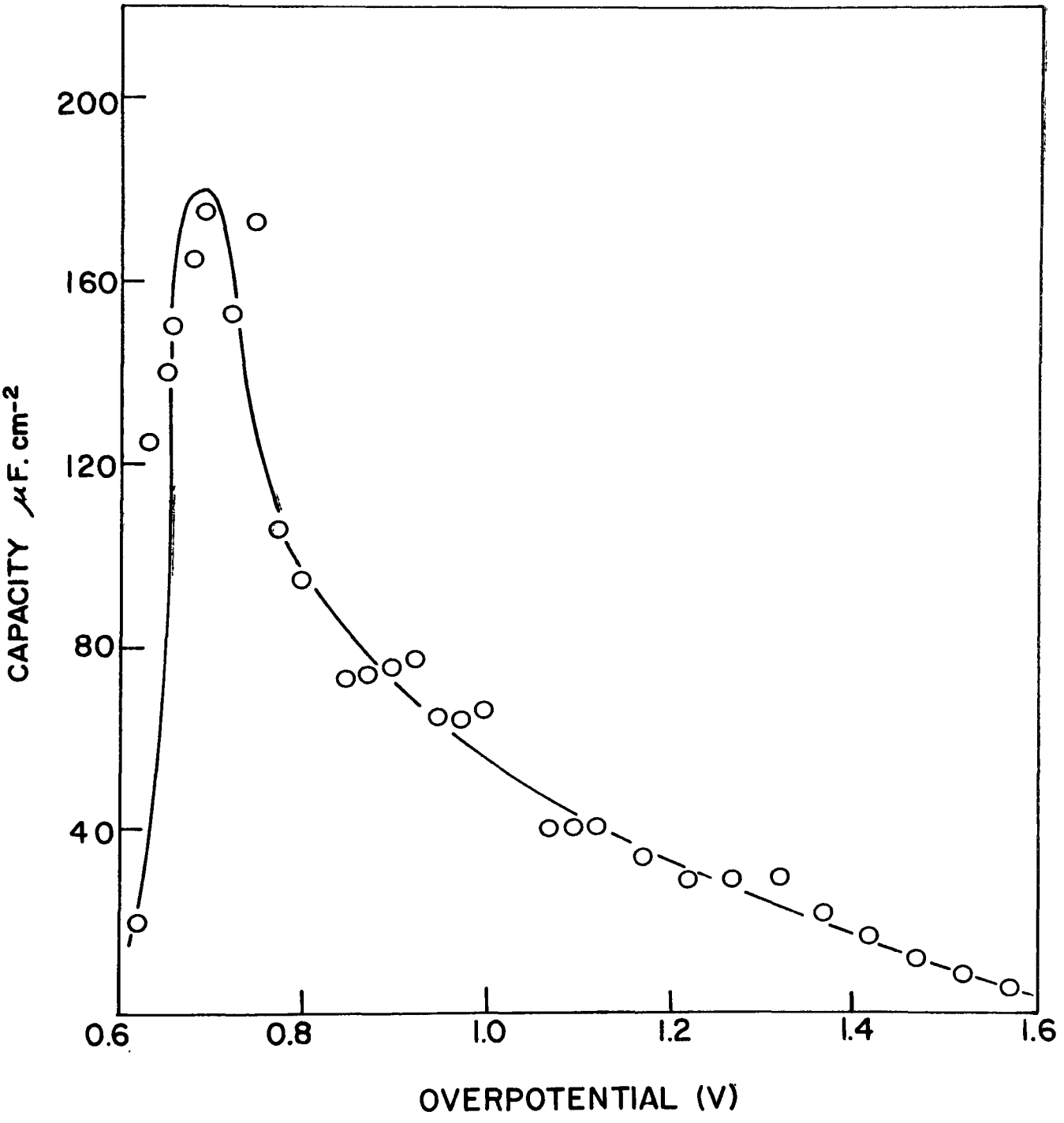
200
160
120
80
40
CAPACITY μF. cm⁻²
0.6
0.8
1.0
1.2
1.4
1.6
OVERPOTENTIAL (V)

Figure 22. The variation of capacity with overpotential in the transition region for the formate decarboxylation reaction at a Pd anode in pure anhydrous formic acid. The capacity was obtained from open-circuit decay and steady-state polarization measurements.

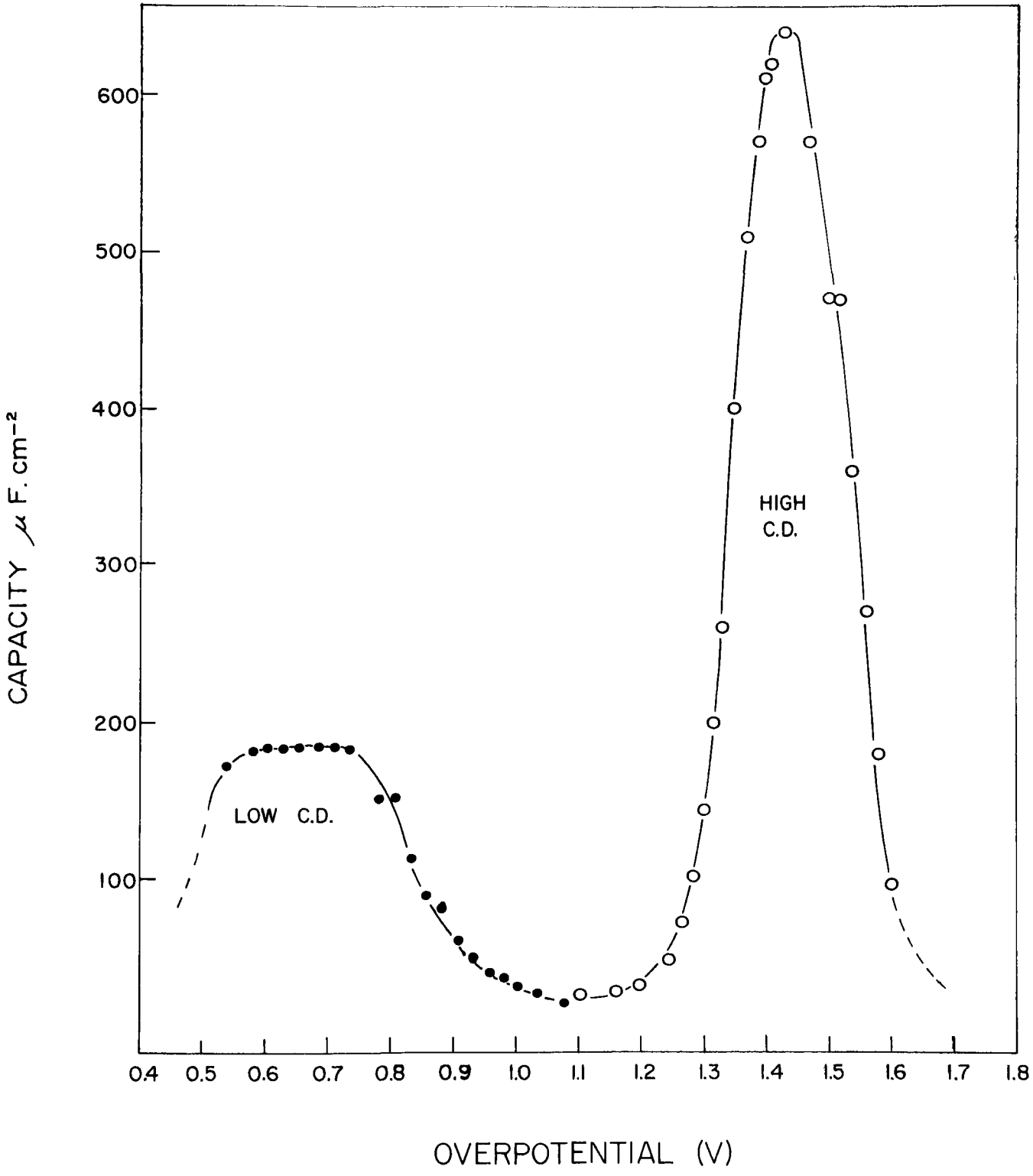
CAPACITY μ F. cm⁻²
600
500
400
300
200
100
LOW C.D.
HIGH
C.D.
0.4
0.5
0.6
0.7
0.8
0.9
1.0
1.1
1.2
1.3
1.4
1.5
1.6
1.7
1.8
OVERPOTENTIAL (V)

the molecular area is approximately 14 $\AA^2$ (from space-filling Courtauld models) so that k' is 113 $\mu c.\ cm.^{-2}$ and the maximum Langmuir pseudocapacity will be $1.1 \times 10^3\ \mu F.cm^{-2}$. The pseudocapacity found at Pt and Au, and at lower current densities at Pd, is less dependent on potential and has lower values. This is as expected theoretically, as we have shown above and elsewhere (10), since the more the overall pseudocapacity originates from a Temkin term involving a linear dependence of coverage upon potential (corresponding to a constant Temkin pseudocapacity contribution) the lower will be the maximum value of the overall capacity and the wider will be its range of potential dependence.

(d) Determination of the Parameters r and f at Pt and Pd Electrodes in the Formate Decarboxylation Reaction

The method described above and previously (9) was used to determine r for $HCOO^*$ adsorption in the formate decarboxylation reaction in pure anhydrous formic acid on Pt and Pd electrodes. The calculations were based on an equation such as [140]. Data were also available for gold electrodes (8) but the resulting experimental C-V curve was skewed and the analysis developed above could not, therefore, be applied. This case will, however, be discussed further below. From the known value of r and the experimental value of the maximum

pseudocapacity, the roughness factor was calculated using a value of $k' = 113\ \mu c/cm^2$ for the charge required to form a monolayer of formate radicals on the electrode surface. These results are summarised in Table 1 below. The r values obtained are appreciable (though considerably less than those obtained in the intermediate coverage region in chemisorption of species such as H; O; N from the gas phase (80)) and indicate significant deviations from Langmuir behaviour.

At current densities appreciably above the critical current at the transition region, anodic films thicker than a monolayer are eventually built up during extended periods of anodic electrolysis (8), particularly at palladium. Under such conditions, the analysis discussed above will be inapplicable. However, it is important to note that the electrode passes from an active to a passive region as a monolayer of adsorbed intermediates is formed on the surface and further formation of a thicker layer is to be considered a secondary effect, not fundamental in reaching an initial passive state.

(iii) Discussion of the Capacity Calculations

(a) Experimental Error in the Calculation of C,q,r and f

In this section we shall discuss the sources and approximate magnitudes of errors involved in the experimentally

Table 1

Values of the parameters r and f in the formate decarboxylation reaction at Pt and Pd

Electrode material	r Kcal. g. equiv.$^{-1}$ (see note 4)	Apparent roughness factor[4]
Pd[1]	7.3	1.5
Pd[2]	2.6	0.9
Pd[2]	1.8	0.3
Pd[2]	2.8	3.9
Pt[3]	5.9	1.0
Pt[3]	7.2	1.0
Pt[3]	5.5	1.8

Notes on Table 1

1. Data given here are for the first transition region observed in the current potential curve (cf. reference 8).
2. Data given here are for the second transition region observed at higher current densities (cf. reference 8).
3. Only one transition region is observed at Pt.
4. The data given in each case are for several runs on separate electrodes.

determined quantities (i.e. in C,q,r, and f).

The pseudocapacity is obtained from a current measured to ± 0.5% (8) and a rate of decay of potential (equation 128) estimated to ± 2%, hence C itself can be obtained to approximately ± 2%. The capacity per unit apparent surface area can, however, only be obtained to ± 5%, with small wire electrodes, owing to the usual uncertainties of determining the exposed length of wire originally sealed in a bulb.

The charge q is obtained by integration of the capacity-potential relationship. The potentials are reproducible to ± 10 mV. in the upper and lower Tafel regions and determined to ± 20 mV. in the transition region. This constitutes an error of 5% - 10% over the range of potentials measured. The error Δq in q is of the order of the sum of the errors in C and V; more accurately

$$\frac{\Delta q}{q} = \left[\left(\frac{\Delta C}{C}\right)^2 + \left(\frac{\Delta V}{V}\right)^2\right]^{1/2}$$

so that the error in the total charge will be ± <u>ca</u>. 10% and the error in the charge per unit apparent surface area will be ± <u>ca</u>. 15%.

The error in r depends on:

(α) The accuracy in the values of C and V which are used to plot the C-V curve;

(β) possible deviations of this curve from the <u>form</u> which can be predicted according to equations [100] and [101].

Empirical graphical estimates of the error in r arising in (a) lead to a value of ± 20-30% which is consistent with the observed deviations between results obtained in "identical" duplicate runs. In this estimate we are only involved with the 2% error in the actual value of C (and not that per unit area) since only relative values of C (e.g. $C_{0.5}/C_{max}$) are used in determining r.

Deviations of the C-V plot from the theoretical form (equation 101) are obvious if the curve is not symmetrical. Nevertheless, such a curve may be symmetrical, yet different in shape from that expected theoretically. This is revealed by an apparent dependence of r on the value of the parameter μ at which ΔV_μ is measured (cf. equation [140]). This effect was observed in one or two cases but the variation of r with μ for a given C-V curve was rather small and well within the estimated limits of error given above.

The error in the roughness factor f depends on the measured maximum capacity (per unit apparent surface area), the calculated value of r and the numerical value assigned to k', the charge per unit real surface area required to form a monolayer. The maximum pseudocapacity can be measured to about ± 5% and calculated (from equation [57a]) with a relative error of the order of magnitude of the sum of the relative errors in k' and r. However, since the error in k' is a

systematic one (the same value of k' being used throughout) we may disregard it and conclude that the roughness factor can be calculated to about ± 30%, with a possible bias due to the uncertainty in k'.

Experimentally much larger fluctuations in f are observed (cf. Table 1), and we believe this corresponds to significant variations in the real surface area of different electrodes used in otherwise identical runs, rather than to random errors in the measurement of these areas and f factors.

(b) The Quasi-Equilibrium Assumption

It is clear, as we have pointed out above, that our calculations of r and f are only correct if the pseudocapacity depends on potential in the theoretical way predicted by equations [100] and [101], which were derived assuming (a) a linear decrease of free energy of adsorption with coverage and (b) that a rate-determining step exists with a previous discharge step effectively in equilibrium. We have shown above that a non-linear relationship between the free energy of adsorption and coverage should be easily detectable experimentally from the skewness in the C-V relationships (Fig. 10); the assumption of quasi-equilibrium, however, requires further consideration. It can be appreciated that, since the formate decarboxylation reaction involves steps other than those

to which our discussion of non-equilibrium conditions refers, a different relationship between potential and coverage results. Moreover, it can be easily shown* that in the present case (i.e. formate decarboxylation) we cannot derive an explicit analytical relationship to express the pseudocapacity as a function of either potential or coverage under non-equilibrium conditions, and the quantities θ and C can only be calculated numerically as a function of V. The general conclusions in our previous discussion of cases for which quasi-equilibrium cannot be assumed to exist are nevertheless probably valid, and in particular it must be borne in mind that the pseudo-capacity behaviour may be much more sensitive to slight deviations from equilibrium conditions in the initial discharge step than other kinetic parameters (e.g. Tafel slopes). This may limit the usefulness of our methods of determining r and f, described in the previous section, unless the ratio of specific rate constants of the initial discharge step and the following step is known to be very large. This effect is expected to be particularly manifest at high values of r (say, $r/RT > 20$). Since, however, relatively small values of r were observed

---

* A detailed discussion by Conway and Gileadi of the pseudo-capacity behaviour under steady state conditions for different reaction mechanisms is now in course of publication, and is based in part on the calculations presented in Chapter III.

in the present case, (cf. Table 1) the quasi-equilibrium assumption can probably be considered an adequate approximation here.

(c) The Significance of the Two Pseudocapacity Regions at Pd

The current-potential plot in Fig. 18 shows two transition regions in the case of Pd (while only one such region is observed at Pt and Au electrodes), and correspondingly two regions of appreciable pseudocapacity are observed in the C-V plot (Fig. 22). Formally this behaviour could arise for one of several reasons: (a) by Faradaic deposition of another entity on a surface already occupied by a first intermediate; (b) on account of the existence of two separate populations of sites at the surface having different and non-overlapping ranges of adsorption energies for a given single intermediate [this is possibly the case for adsorption of H at some metals (31,46)]; (c) by oxidation, to a higher valence state, of the species already adsorbed more or less to the extent of a complete monolayer. If the potentials associated with a z-electron oxidation of a previously deposited species obey a Nernst relation with respect to the activities of oxidised and reduced forms of the ad-species, or if the oxidised and reduced species behave ideally we can write

$$E = E^{o} + \frac{RT}{zF} \ln \left[\frac{c_o}{c_m - c_o}\right] \qquad [142]$$

where c_o and c_m are the surface concentrations of oxidised species at any degree of oxidation, and at complete oxidation, respectively ($c_m - c_o$ is then the concentration of the species in the reduced form). Since the formation of the oxidised species from the reduced will be associated with a Faradaic process at the surface, the c_o and c_m can be expressed in terms of corresponding charge q_o and q_m so that a pseudo-capacity C given by

$$C = \frac{zF}{RT} (q_m - q_o) \; q_o/q_m \qquad [143]$$

will arise (39) and has a maximum when $q_o = 0.5\, q_m = q_{reduced}$, given by

$$C_{max.} = \frac{zF}{4RT} \cdot q_m$$

i.e. a result exactly similar to that for the normal maximum adsorption pseudocapacitance for Langmuir conditions (cf. equation 92b). It is of interest to note that the maximum pseudocapacity in this case will occur at the standard potential for the surface redox process.

In the present case for Pd, it is difficult to envisage for (a), above, any radicals which are different from $HCOO^{\bullet}$ which could be deposited, although deposition of a second layer of the same species is feasible; for (b), the

behaviour observed is neither found for the other metals studied, nor for Pd when 5M HCOOK solutions are used, and is therefore probably not associated with a general property of the metals; explanation (c) is hence most plausible and would tend to give a more ideal Langmuir type pseudocapacity relation, since the specific coverage effects, involving an appreciable r value at the metal have already been effective in determining the potential variation of the pseudocapacity in the lower current density region as θ_{HCOO^-} increased and tended to its initial maximum value. Some confirmation of this supposition is afforded by comparison of the value of r for the lower transition region at Pd with that for the single transition region at Pt (Table 1); the two values are quite comparable but appreciably greater than that for the upper transition region at Pd.

3. APPLICATION TO THE OXYGEN EVOLUTION REACTION AT A CHARGED NICKEL OXIDE ELECTRODE

(1) General

The electrochemistry of the nickel oxide electrode and the mechanism of oxygen evolution on a fully charged nickel oxide electrode have been extensively studied in this laboratory. A detailed account of techniques used and experimental results, as well as a discussion of these results

have been given in a previous thesis (41) and in several papers by Conway and Bourgault (7,39,47,61). This work is closely related to the discussion of the role of adsorbed intermediates in electrode kinetics presented in the previous chapters since much of the experimental data can best be interpreted in terms of the theories proposed here and, in fact, the need for a proper explanation for these results initiated partially the theoretical work presented in this thesis.

In this section we shall discuss some results obtained for the oxygen evolution reaction at a fully charged nickel oxide electrode at relatively high current densities (up to 2 Amp.gm^{-1}*) in relation to the comparison of three different methods for the determination of the adsorption pseudocapacity. In the next chapter, a study of the reversible potential for the Ni^{II} - Ni^{III} system as a function of degree of charge of the electrode will be presented, where again surface effects are shown to be of importance in determining the thermodynamic behaviour.

---

* It has been found (7) most convenient to express the current densities at these electrodes per unit weight of active material ($Ni(OH)_2$) rather than per unit surface area, since the latter can only be estimated from B.E.T. measurements on the dry material and may not be equal to the real surface areas available for electrochemical reaction, as discussed above. The area measured by the B.E.T. method was 4×10^5 cm^2 gm^{-1} for the fully charged electrode.

(ii) Experimental

Nickel hydroxide electrodes were prepared in sintered nickel plaques as described previously (7,90). Each electrode was charged and discharged three times before use at approximately a five hour charging rate in order to stabilise its electrochemical behaviour (7,39). All solutions were prepared as described previously* (7,41). Relatively small electrodes were used in this series of experiments (the apparent surface area was about 9 $cm.^2$ as compared to about 40 $cm.^2$ in previous work (7,39,41) and in the study of reversible potentials discussed in the next chapter) and the electrodes were impregnated only once, so that the amount of electrochemically active material (i.e. $Ni(OH)_2$) in each electrode was only about 10% of that in previous studies. This enabled the measurements to be extended to higher current densities and potentials than those used previously (up to about 2×10^3 mA per gram of active material, calculated as the gain in weight of the electrode upon impregnation). A fast recorder (Brush, Mark II) operated from the output of a high impedence Keithly electrometer was used with a maximum chart speed of 125 $mm.sec.^{-1}$ The change of potential with time on open-circuit could be

---

* High purity techniques are not required here owing to the large real surface area of the electrodes (about 4×10^5 $cm.^2 gm.^{-1}$ of $Ni(OH)_2$ as discussed previously (41)).

observed from about 0.01 sec. after cessation of polarization. The actual potentials were measured on a Radiometer type M4 high stability electronic potentiometer (input impedence 10^{12} ohms) and results obtained on the fast recorder were checked against a high impedence Philips recorder, type PR2212-A/00, whenever the rate of change of potential was such that it could be measured on both instruments (the maximum speed of the Philips recorder [1.2 mm.sec.$^{-1}$] was almost equal to the lowest speed [1 mm.sec.$^{-1}$] available on the fast recorder).

The steady state current-potential behaviour was studied over 2-3 orders of magnitude of the current densities, and open-circuit decay was followed after the steady state has been reached at each current density.

(iii) Results

We have shown in the Introduction (cf. page 41, equations [28] to [32]) that the adsorption pseudocapacity* can be obtained from the equation

$$C = \frac{i_{in}}{b_1}\phi \qquad [32]$$

where i_{in} is the steady state polarizing current density passing at an overpotential η_{in}, b_1 is the Naperian Tafel

---

* That is, when the adsorption pseudocapacity is large compared with the ionic double-layer capacity, as previously discussed.

slope for the relevant electrochemical process, ϕ is an experimental parameter obtained empirically from a plot of V against log $(t + \phi)$, where ϕ is chosen such that the above relationship will remain linear down to $t = 0$ (see. p. 41).

We have used equation [32] to determine C as a function of potential, by determining ϕ for different values of i_{in}. Results are given in Fig. 23 a and b (for 1N and 10N KOH solutions, respectively), where we have included also the pseudocapacity values obtained from initial decay slopes $(dV/dt)_{t=0}$ and in Fig. 23a also from slopes in continuous decay runs (v. equations 128,129). The agreement between the various methods used to determine the capacity is seen to be satisfactory. Since the fast recorder used in most of these experiments was not rectilineal, the initial decay slopes could not be determined directly from the recorder trace, and values had to be replotted on squared graph paper. As a result, the estimates of $(dV/dt)_{t=0}$ tend to be somewhat <u>too small</u>, leading to values for the calculated pseudocapacity (cf. equation 128) which are rather too high. This, we believe, can account for the somewhat higher values of C obtained from initial decay measurements shown in Fig. 23a and b than from the other methods. We note, however, that the pseudocapacity

Figure 23. The variation of capacity with potential during oxygen evolution at a nickel oxide electrode in the "overcharged" state.

Capacity calculated from

XXX initial decay slopes

000 decay slopes and Tafel parameters

ΔΔΔ from the parameter ϕ in $dV/d \log(t+\phi)$

a. 1N solution of KOH

b. 10N solution of KOH.

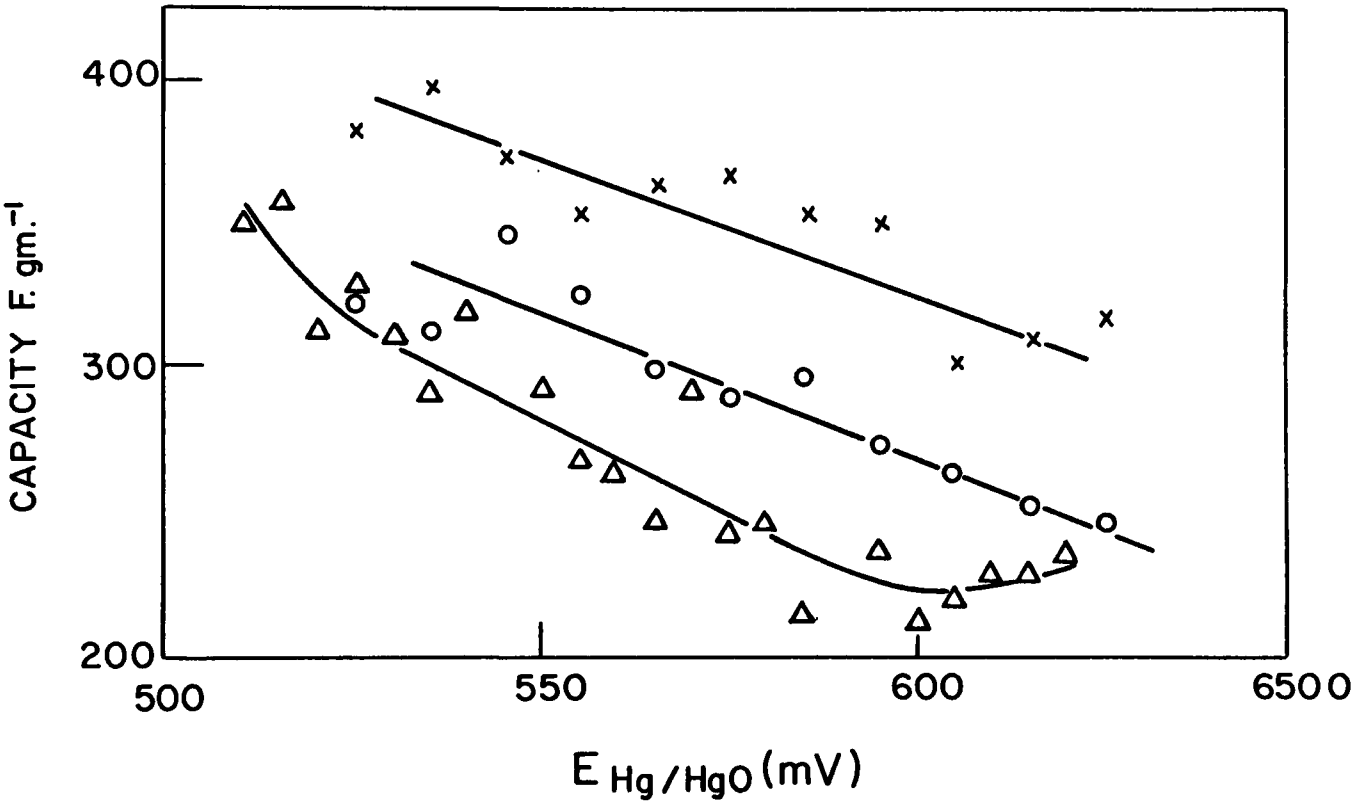
400
300
200
CAPACITY F.gm.⁻¹
500
550
600
6500
E Hg/HgO (mV)

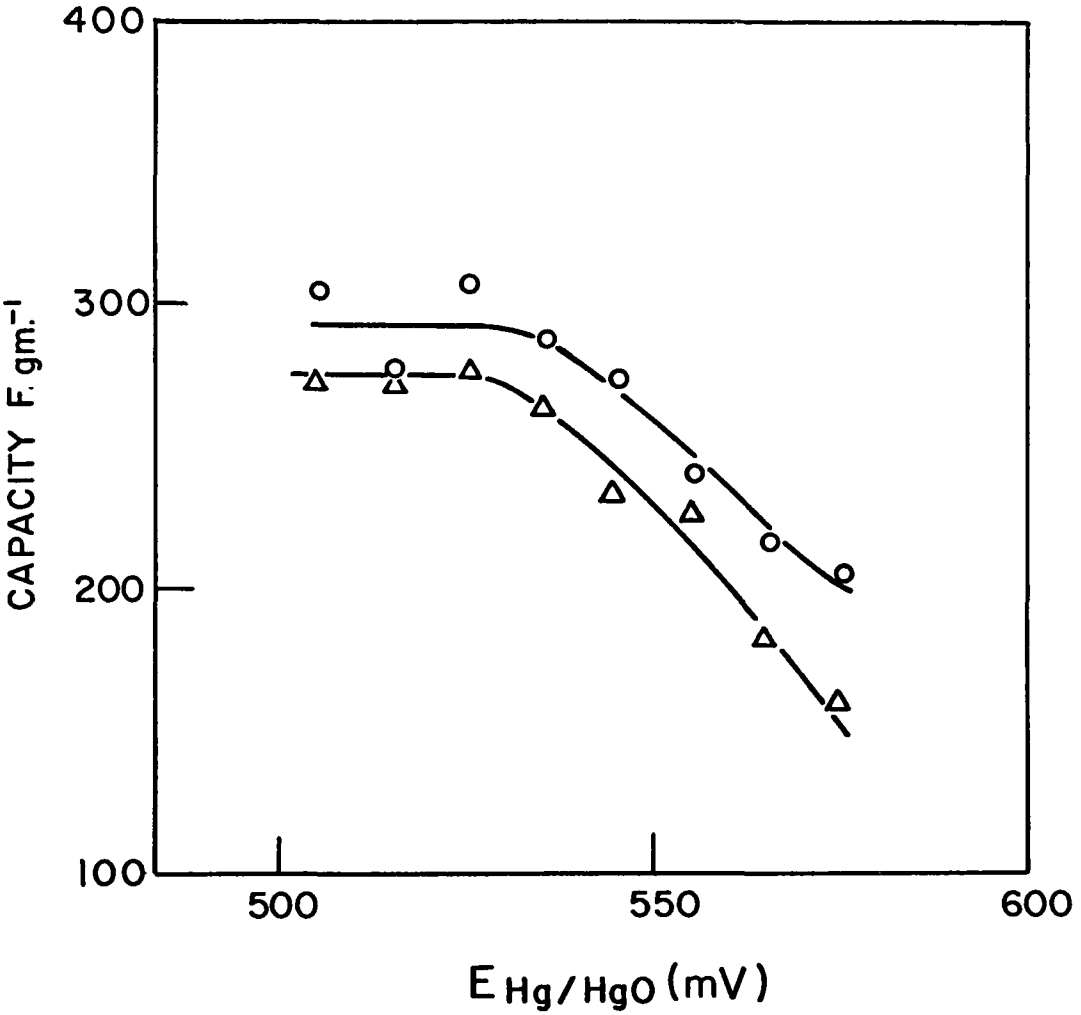
400
300
200
100
CAPACITY F.gm.-1
500
550
600
E Hg/HgO (mV)

calculated by all three methods depends on potential in the same way and, in fact, the difference between values of C obtained by different methods at various given potentials is a constant, within experimental error.

It was pointed out by Morley and Wetmore (36) that it is possible to superimpose open-circuit e.m.f. decay lines plotted logarithmically in $(t + \phi)$ and initiated at different overpotential values, if the correct value of ϕ is used. Conway and Bourgault (41,61) have given some experimental evidence to this effect, and have also shown that a plot of ϕ against $1/i$ is a straight line passing through the origin, as predicted from equation [32] if the capacity were constant. Their conclusions were, however, based on rather few experimental results, and we accordingly present here further experimental evidence that open-circuit decay plots taken after polarisation to widely different current densities can be superimposed (Fig. 24) and the plot of ϕ over a range of values of $1/i$ is linear, as expected (Fig. 25), thus validating the method of evaluating the capacity C.

(iv) Discussion of the Capacity Measurements at the Nickel Oxide Electrode

We have given direct experimental proof that the three methods (ie. from initial values of dV/dt; from

Figure 24. A plot of V as a function of log $(t+\theta)$ for open-circuit decay following steady-state oxygen evolution at an "overcharged" nickel oxide electrode in 10N KOH solution. Results of twelve experiments on the same electrode are given (the steady-state current prior to cessation of polarization ranging from 6.6 $mA.gm.^{-1}$ to $1.97 \times 10^{3} mA.gm.^{-1}$). The lines in the actual experiments are based on 15-25 points, but are represented here by three points only for clarity, since the points form indistinguishable populations.

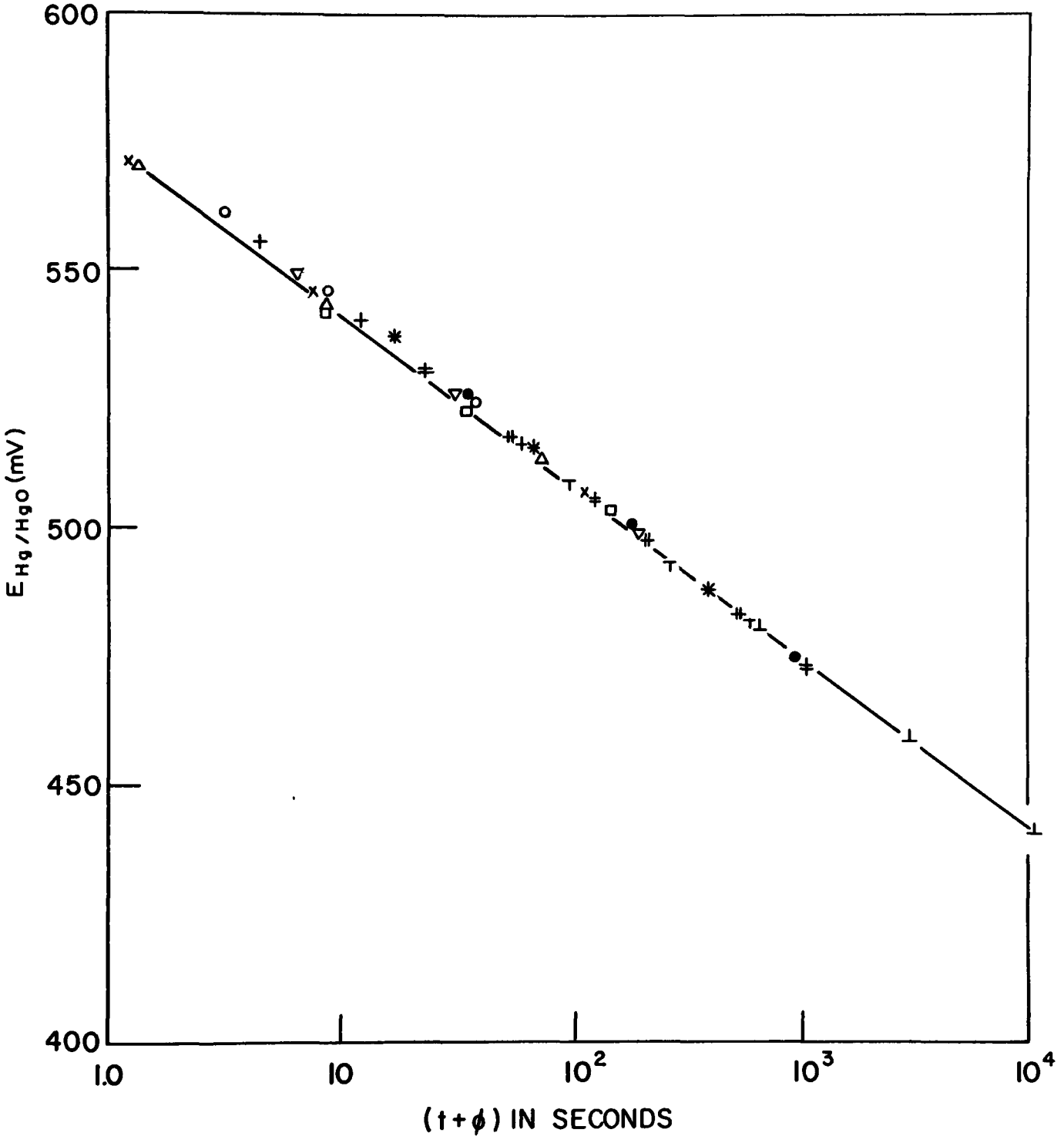
600
550
500
450
400
$E_{Hg/HgO}$ (mV)
1.0
10
10^2
10^3
10^4
$(t+\phi)$ IN SECONDS

Figure 25. A plot of the parameter ø against 1/i for oxygen evolution on an "overcharged" nickel oxide electrode in 1N KOH solution.

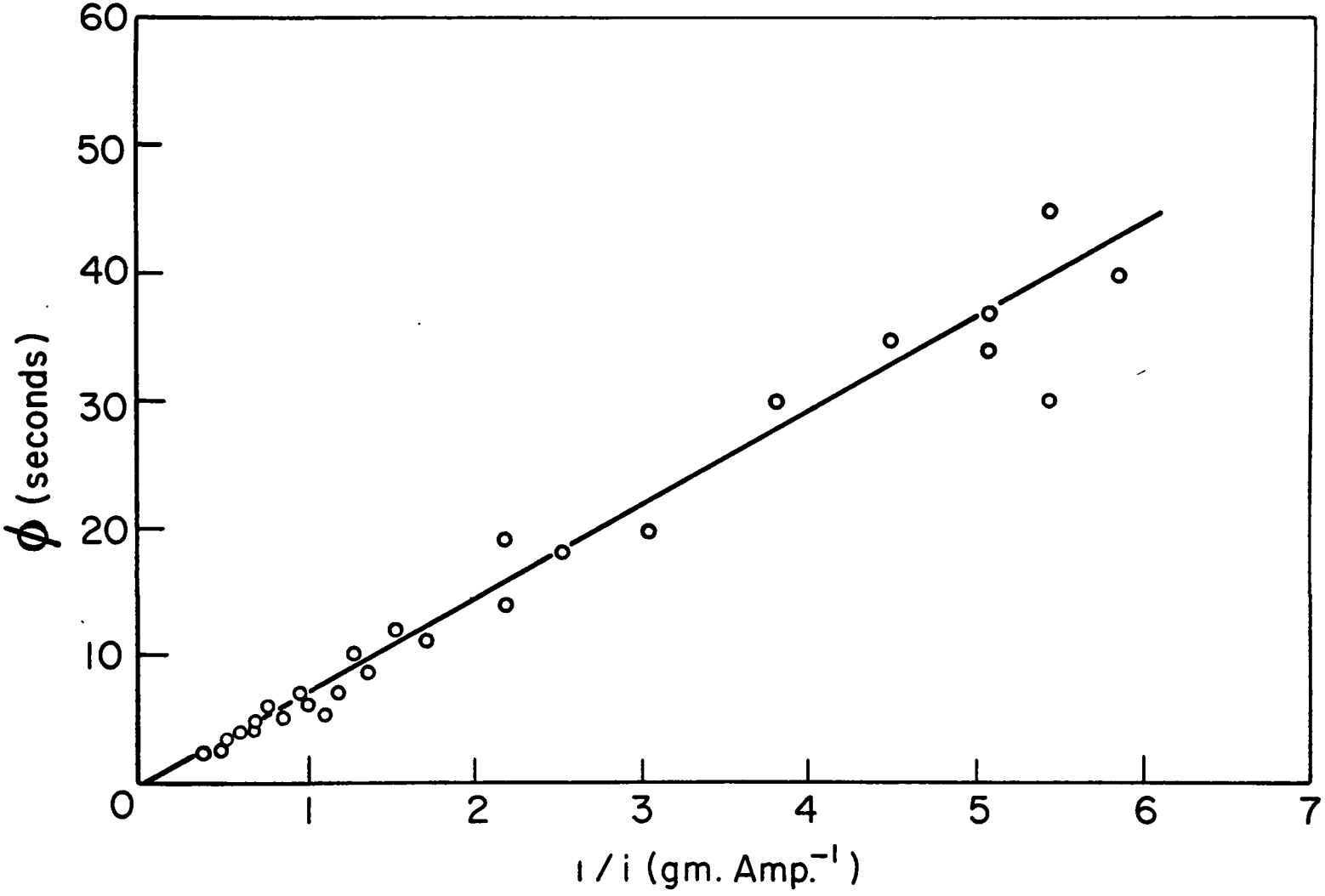
60
50
40
30
20
10
0
1
2
3
4
5
6
7
ϕ (seconds)
1 / i (gm. Amp.$^{-1}$)

analysis of the whole of the decay curve combined with the known steady state V - i relationship and from the parameter ϕ in semi-logarithmic decay curves) discussed in the Introduction and used in our experimental work all give values of C in agreement, within experimental error. The values of ϕ are obtained by a trial and error method which may not seem accurate enough; however, since all decay curves are seen to be almost identical (Fig. 24) when the values of ϕ used to calculate the pseudocapacity are also used in plotting V against log $(t + \phi)$, the ϕ values should be considered reliable. Experimentally we estimate the error in ϕ to be within $\pm$ 10% in these series of experiments.

The "overcharged" nickel oxide electrode is seen to be rather unsuitable for the study of pseudocapacity behaviour, compared with the "formate" electrode. A relatively low Tafel slope is observed and since at low current densities a steady state is reached extremely slowly (for i = 10 $mA.cm^{-1}$ or less it may be more than several hours before a steady state is reached), the electrode reaction can only be studied over a rather limited range of potentials (about 0.12 volts); as a result only a small portion of the C-V curve can be obtained. As pointed out above, the discussion regarding the pseudo-capacity-potential behaviour of electrochemical systems can

best be tested in cases where a sharp transition region is observed (3,86); that is, where the current-potential relationship, as well as the open-circuit decay behaviour, can be studied over a large potential range of the order of 0.5 - 1.0 volt.

Work is now in progress in our laboratory to study further, from the point of view of pseudocapacity behaviour, several other systems where a transition region in the i-V relationship is observed and is associated with transition phenomena such as the filling up of the surface with adsorbed radicals formed in a prior discharge step.

The main purpose of the work which has been described in this thesis has been to provide a theoretical basis for such studies and to discuss applications of the theory to two systems for which experimental data could be obtained.

CHAPTER V

THE ROLE OF SURFACE EFFECTS IN DETERMINING THE REVERSIBLE POTENTIAL OF THE Ni^{II} - Ni^{III} SYSTEM

1. INTRODUCTION

In the previous chapters we have discussed in detail the importance of adsorbed intermediates in determining the mechanism and kinetics of electrode reactions. Here we describe some work on the behaviour of the nickel oxide electrode during charging and discharging and with regard to the dependence of the reversible potential for the Ni^{II} - Ni^{III} system on the degree of charge of the electrode. This work forms a logical continuation of previous studies of the chemistry of the nickel oxide electrode carried out in this department (7, 41,61) in particular, the study of the reversible potential of the Ni^{II} - Ni^{III} couple at a constant state of oxidation of the electrode, as a function of KOH activity in the solution. The work described in this chapter is related to our discussion of surface effects in the previous chapters in that it will be shown that the composition of the surface phase can play a major role in determining the thermodynamic as well as the kinetic behaviour of the nickel oxide electrode.

The real reversible potential of the nickel oxide (Ni^{II} - Ni^{III}) electrode has been the subject of controversy for some years and previously reported values are misleading since they have not been based on well-defined equilibrium conditions or a well-defined state of the system. Determination of the reversible potential is complicated by the self-discharge processes which occur at the electrode in the oxidised form and also because the electrode may exist in a range of chemical states corresponding to the extent of conversion of Ni^{II} to Ni^{III} (and possibly Ni^{IV} under certain conditions) in the hydrated oxide.

The true reversible potential of partially charged nickel oxide electrodes at a single controlled state of oxidation "$NiO_{1.25}$" was examined (by Conway and Bourgault,7) as a function of potassium hydroxide and water activities in aqueous alkali solutions, and distinguished from the mixed potential assumed erroneously in previous work (91,95,96) to be the reversible potential. A polarization decay method was employed, in which the reversible potential was approached both from the anodic and the cathodic directions and has been described and discussed in detail previously (7,39,41).

In the part of the work to be described in the present chapter, the same method has now been applied to the study of the potential of partially charged nickel oxide electrodes as

a function of the degree of charge, at constant electrolyte composition. This method was found to be applicable only over a limited range of degree of oxidation of the electrode ("$NiO_{1.10}$" -"$NiO_{1.30}$") owing to problems of extrapolation to the reversible potential to be discussed below. Stationary potentials taken at very long times on open-circuit, were therefore also measured as a function of the degree of charge over a much wider range of degree of oxidation ("$NiO_{1.025}$" - "$NiO_{1.50}$").

The role of the surface and bulk phases in determining the measured potential was deduced. It will be shown that three well defined regions in the charging process can be distinguished experimentally. In the first, the surface phase alone is being charged; in the intermediate region, the Faradaic current is used to charge both phases, until the surface phase is fully charged, after which oxidation of the bulk is the main Faradaic process. (Most of the charging process occurs at a potential anodic to the reversible oxygen electrode, so that oxygen evolution must occur to a certain extent as a parallel process in all three regions described above. It does not, however, become appreciable until most of the bulk material has been charged)

2. EXPERIMENTAL

(i) General

Nickel hydroxide electrodes were prepared by impregnating sintered nickel plaques with recrystallised $Ni(NO_3)_2$ followed by conversion to $Ni(OH)_2$ by cathodic polarization in 20% KOH, as described previously (7,90). Each electrode was charged and discharged three times before use at a five-hour charging rate in order to stabilise its electrochemical behaviour (7,39,41). Electrodes were used at least one week after preparation in order to minimize changes in behaviour due to aging effects (98,99) during the experiments.

All solutions were prepared from reagent grade (see footnote on p. 197) materials as described previously (7,41). Most experiments were carried out in 1N KOH at 25°C. Some comparative runs were also performed in 7.2M KOH.

(ii) Reversible Potentials

The reversible potential of the Ni^{II} - Ni^{III} system was obtained by extrapolating anodic and cathodic e.m.f. decay lines, plotted logarithmically in time, to the potential of their intersection, as described previously by Conway and Bourgault (7,41).

The "discharged" electrodes still contained a small amount of the higher oxide of nickel, which, at the apparent

end of discharging is evidently inaccessible, probably due to insulation by the less conducting $Ni(OH)_2$ (92). The electrodes were reduced completely by prolonged cathodic polarisation until a total of 3F. equiv.$^{-1}$ had been passed. The electrodes were then transferred to another cell containing freshly prepared electrolyte and reference electrodes, and left on open-circuit overnight with purified oxygen bubbling through the cell.

The following sequence of operations was then performed at a current corresponding to a two-hour charging rate i.e. at 143 ma. g.$^{-1}$ of active material calculated as $Ni(OH)_2$.

a. The electrode was charged for 24 min. to an extent of oxidation of 20% ($NiO_{1.10}$) based on the oxidation change $Ni^{II} \longrightarrow Ni^{III}$ in the oxide. The current was then interrupted and open-circuit decay of potential followed for about an hour.

b. Charging was continued for 24 min., followed immediately by discharge for the same length of time. The current was then interrupted and build-up (i.e. recovery of potential on open-circuit to more anodic values) was followed for an hour, the degree of charge again being 20% as in (a). Anodic and cathodic open-circuit decay and recovery of potential were followed in a similar manner at the 40%, 60% and 80%

charged electrodes corresponding to formal degrees of oxidation of $NiO_{1.20}$, $NiO_{1.30}$, $NiO_{1.40}$ respectively. Charging and discharging curves for one of these experiments are shown in Fig. 26. Similar charging and discharging cycles were carried out to obtain data for electrodes in 25%, 50% and 75% degrees of oxidation (see Table 2).

(iii) Stationary Potentials

In this series of experiments, the electrodes were charged to a given degree of oxidation and decay of e.m.f. on open-circuit was followed by means of a high impedance recorder for about a week, at which time the e.m.f. varied at a rate of 1mV per day or less.

(iv) Sparingly Charged Electrodes

A series of experiments was conducted on electrodes charged to a very small extent (0.33% to 5% of their total charge capacity). In this part of the work, only open-circuit decay measurements following anodic polarization could be studied.

3. RESULTS

Plots of decay of e.m.f. after anodic and cathodic polarization *vs.* log $(t + \emptyset)$ are shown in Fig. 27. The significance of this type of plot, of e.m.f. decay slopes and of the

Figure 26. Anodic and cathodic polarization curves for the nickel oxide electrode in 1N KOH, 2 hour charging rate. Vertical broken lines correspond to open-circuit e.m.f. decay or recovery. Solid lines correspond to changes of potential associated with changes of degree of charge between successive open-circuit measurements.

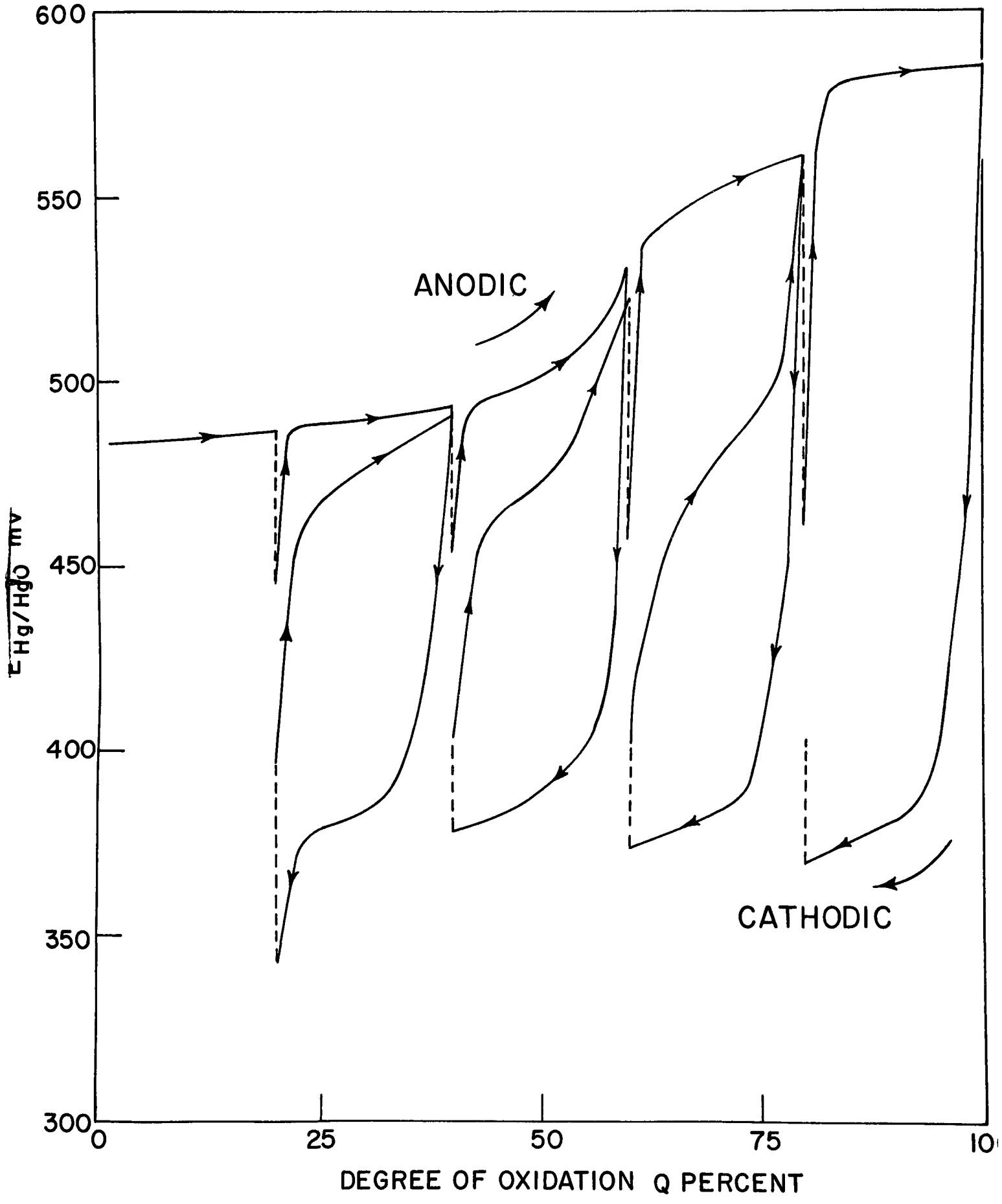
600
550
500
450
400
350
300
$E_{Hg/HgO}$ mv
ANODIC
CATHODIC
0
25
50
75
10
DEGREE OF OXIDATION Q PERCENT

Table 2

Reversible potential for the Ni^{II}-Ni^{III} system as a function of the degree of charge of the electrode; and open circuit decay and build-up slopes

Degree of charge	KOH concentration	Anodic decay slope: Initial b_1(mV.)	Anodic decay slope: Lower b_2(mV.)	Cathodic build-up slope b_3(mV.)	**$E_{rev.}$ (mV.)	Number of experiments
20%	1 N	-12.8	-18.2	+11.0	423	1
25%	1 N	-9.5±0.6	-18.3±3.5	+13.1±2.1	424±4	5
40%	1 N	-12.0	-15.2	+9.0	427	1
50%	1 N	-10.8±1.5	-19.8±5.0	+10.9±1.6	423±5	9
60%	1 N	-35.3	-17.8	+11.4	*	1
75%	1 N	-32±13	-22±2.3	+9.4±1.2	*	5
90%	1 N	-60	-21.0	+14.3	*	1
"over-charge"	1 N	-45±2.6	-	-	*	6

* See comment in text with regard to these degrees of oxidation.

** The reversible potentials are given vs. that of a Hg/HgO reference electrode in the same solution.

Figure 27. Decay and recovery of e.m.f. of the nickel-oxide electrode in log [time] at various degrees of charge after anodic and cathodic polarization, respectively (Data for 1N KOH); compare ref. 7.

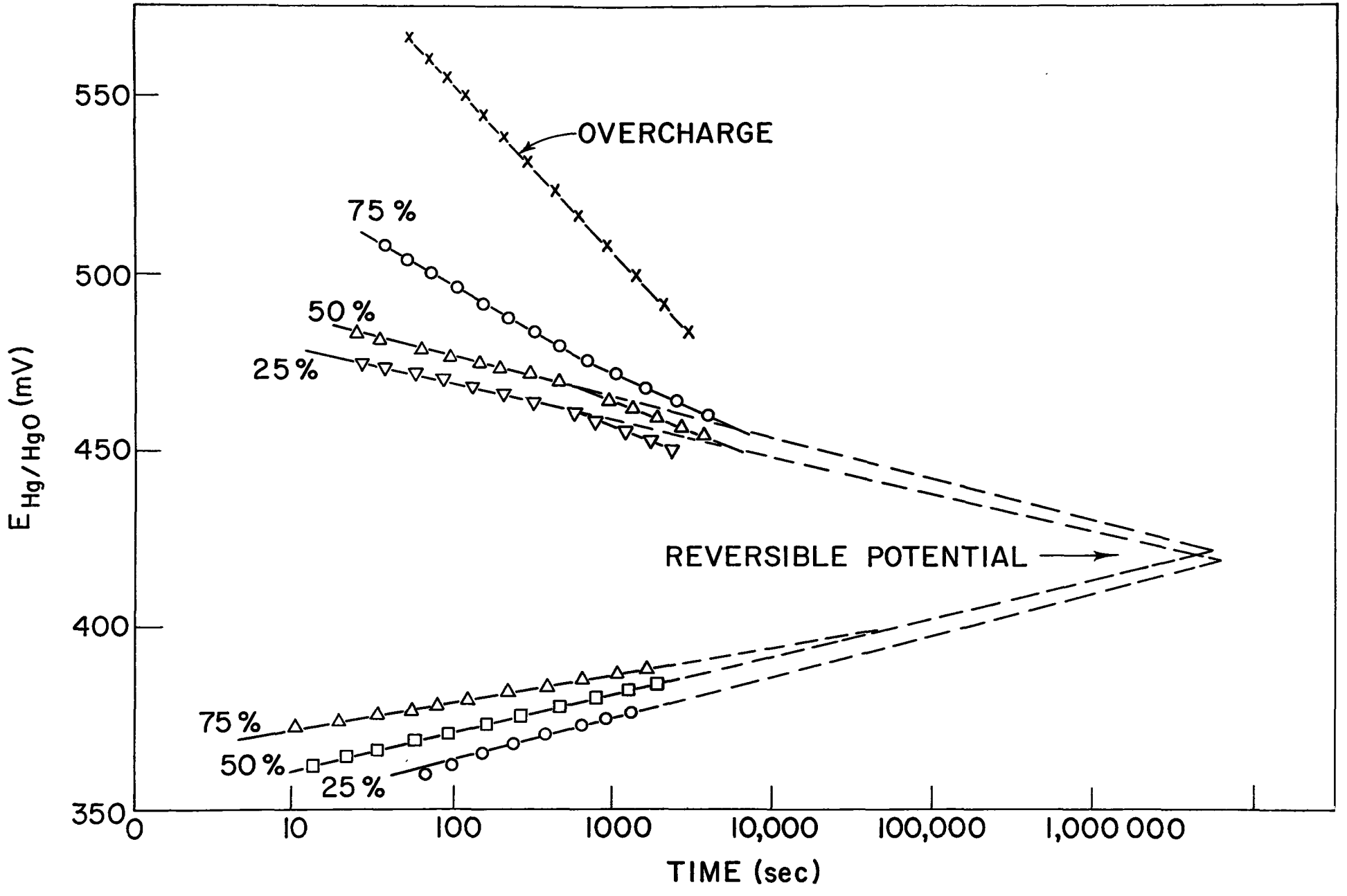
550
500
450
400
350
$E_{Hg/HgO}$ (mV)
OVERCHARGE
75 %
50 %
25 %
REVERSIBLE POTENTIAL
75 %
50 %
25 %
0
10
100
1000
10,000
100,000
1,000 000
TIME (sec)

parameter ϕ have been discussed above (cf. p. 41) and previously (7,35,36,39).

All e.m.f. decay lines from anodic polarization are seen to have two distinct regions. For electrodes charged to 50% ("$NiO_{1.25}$") or less, an initial low slope (about -10mV) is followed by a higher slope (about -20mV). When the electrode is charged to 75%, a high initial slope (about -32mV) is followed by the same slope (-20mV) mentioned above in the lower potential region. E.m.f. recovery lines from cathodic polarization have a slope of about +11 mV, independent of degree of charge. Results for a typical individual experiment are given in Fig. 27. Some slight increase of recovery slope is apparent as the charge is reduced; however, this trend does not appear to be very significant statistically (e.g. see Table

In Table 2, the reversible potentials for the Ni^{II} - Ni^{III} system, obtained by extrapolating cathodic and (initial) anodic e.m.f. decay lines (7) are given for different degrees of charge (between 20% and 50% formal degree of oxidation) of the electrode at 25°C, together with other kineti parameters. An important result obtained here is that the reversible potential is seen to be <u>independent</u> of formal degree of charge over the above range of charge. Similar conclusions were arrived at from two comparative runs in 7.2 N KOH.

For reasons to be discussed, it is not possible to obtain the true reversible potentials by extrapolation of cathodic and anodic e.m.f. decay lines above degrees of oxidation of about 50%. In order, however, further to study the potentials of the nickel oxide electrode, the "stationary" potentials were examined at higher states of oxidation.

In Table 3, the "stationary" potentials measured after 4×10^5 sec. and 6×10^5 sec. on open-circuit are given for various degrees of charge of the electrode between 5% and 100% ("overcharged" electrode). These results were obtained by reducing the electrode completely, polarizing it anodically to the appropriate degree of charge, and then leaving it on open-circuit for 6×10^5 sec. or longer. It is seen that the "stationary potential" measured after a long period of standing on open-circuit is still independent of the degree of charge above 10% extent of oxidation ("$NiO_{1.05}$"), and in this respect exhibits a behaviour similar to that of the true reversible potentials.

Results of experiments on sparingly charged electrodes (0.33% to 5% degree of oxidation) are shown in Fig. 28, where the e.m.f. - time relation is plotted for decay on open-circuit after anodic charging for various degrees of charge. It is seen that the decay process changes qualitatively once quite low degrees of charge are reached. These results can, for the

Table 3

Stationary potentials of the nickel oxide electrode in 1N KOH, 25°C.

Degree of charge	Potential reached after 4×10^5 sec. (mV. Hg/HgO)	Potential reached aft 6×10^5 sec. (mV. Hg/HgO)
"overcharge"	426.5	422.6
50%	426.5	424.0
20%	420.4	417.2
10%	422.6	419.9
7%	406.0	404.8
5%	401.5	399.3

Figures 28. Plots of e.m.f. decay at sparingly charged electrodes, for various degrees of charge.

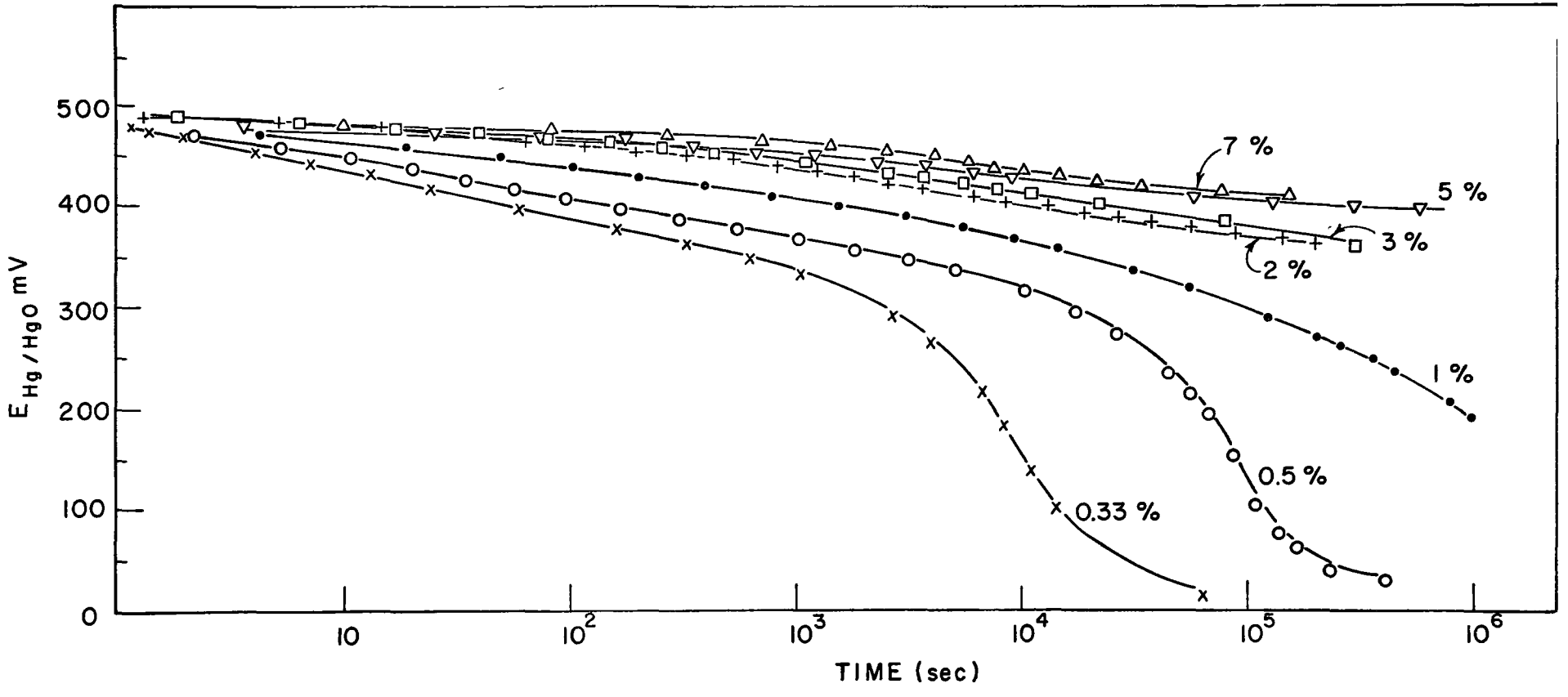
500
400
300
200
100
0
$E_{Hg/HgO}$ mV
10
10^2
10^3
10^4
10^5
10^6
TIME (sec)
7 %
5 %
3 %
2 %
1 %
0.5 %
0.33 %

purpose of interpretation, be best represented graphically as plots of the degree of charge, Q, held by the electrode *vs.* the time required for the electrode potential to decay to a given value (Fig. 29) or in terms of the charge held *vs.* the potential reached after a given time (Fig. 30). These plots are equivalent to taking cuts at a given value of the abscissa or ordinate in Fig. 28.

It is seen from both these derived plots that two linear regions are observed for each of the two families of lines, which intersect at a degree of charge of 1.5 ± 0.1%. This observation leads to the important conclusion that electrodes charged to 1.5% or less are in a fundamentally different state than electrodes charged to a greater extent. This point is further demonstrated by examining the decay slopes listed in Table 4 below. It was shown previously (7) that the initial low slope (*ca.* -10 mV) is characteristic of the oxidation of the bulk nickel oxide. In the present work, this slope was only observed for electrodes charged to 2% or more. Below the latter extent of charge, no oxidation of the bulk material appears to occur, and the potential on open-circuit drops much more rapidly.

4. DISCUSSION

The reversible potential for the Ni^{II} - Ni^{III} system in the electrochemically formed nickel oxide has been shown to

Figure 29. The length of time necessary for the electrode to reach a certain potential on open-circuit, *vs.* the degree of charge of the electrode. (Lines show inflection at common degree of charge Q = 1.6 ± 0.1%).

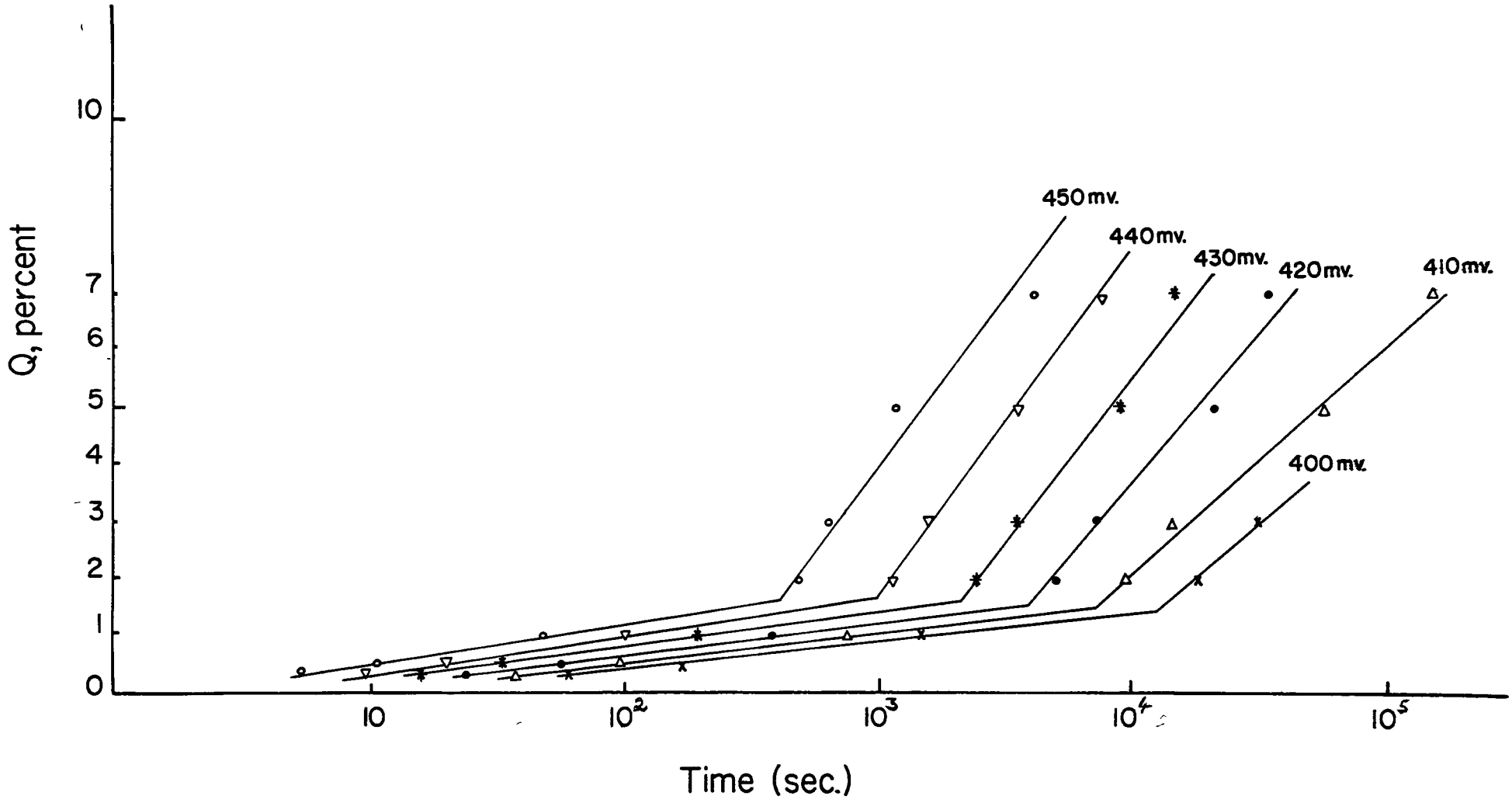
Q, percent
10
7
6
5
4
3
2
1
0
450mv.
440mv.
430mv.
420mv.
410mv.
400mv.
10
10^2
10^3
10^4
10^5
Time (sec.)

Figure 30. The potential reached after a given length of time on open-circuit, *vs.* the degree of charge (lines show inflection at common degree of charge of $Q = 1.35 \pm 0.1\%$).

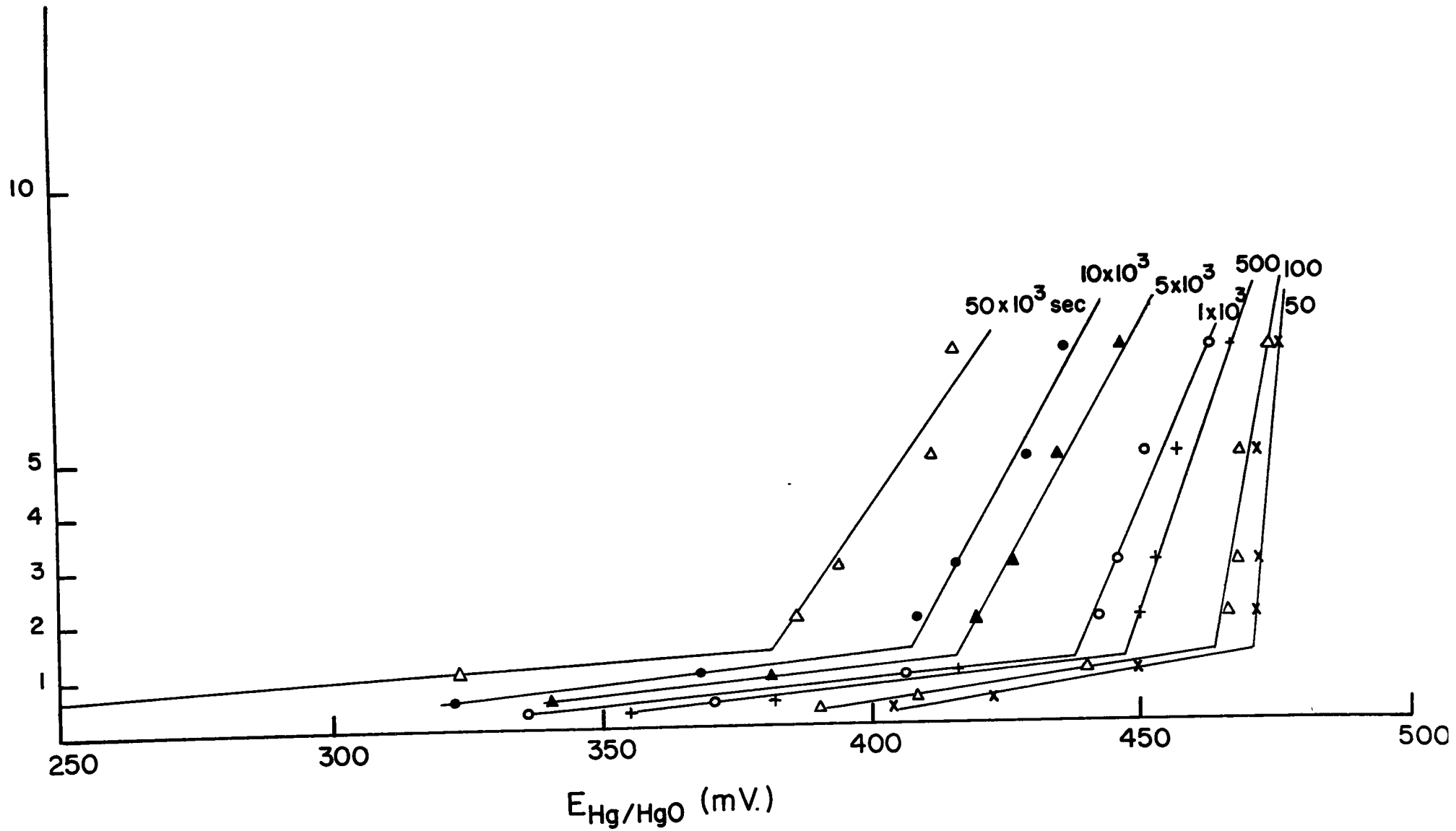
10
5
4
3
2
1
50 x 10^3 sec
10x10^3
5x10^3
1x10^3
500
100
50
250
300
350
400
450
500
E Hg/HgO (mV.)

Table 4

E.m.f. and e.m.f. - decay behaviour at sparingly charged nickel oxide electrodes.

Degree of Charge	Decay slopes b_1(mV.), b_2(mV.) (as in Table 1)		E.m.f.* (mV.) at time of last measurement	Time of last measurement, (sec.) after cessation of polarization	$\Delta V/\Delta t$ for the last day, $mV.day^{-1}$
7%	-	-	404.8	6×10^5	0.2
5%	-12.3	-23.2	398.3	7×10^5	0.8
3%	-15.5	-34.1	366.5	2.8×10^5	5
2%	-12.6	-34.2	356.1	6×10^5	2
1%	-34.3	$>\|100\|$	188.6	9.5×10^5	8
1/2%	-40	$>\|100\|$	41	4.1×10^5	1
1/3%	-48	$>\|300\|$	18	0.7×10^5	1

* Measured against the Hg/HgO electrode in the same solution.

be independent of the degree of charge of the electrode over an appreciable range of degrees of oxidation. Between 20% and 50% degree of charge, it was measured by extrapolating anodic and cathodic e.m.f. decay lines, plotted logarithmically in time, as described and discussed earlier (7). Values of the reversible potential could only be obtained over a limited range of degrees of oxidation (20% - 50% of total charge) since at a higher degree of charge the initial low anodic slope, characteristic of the oxidation of the bulk material, was not observed (see Fig. 27) and at a very low degree of charge, cathodic e.m.f. recovery lines were irregular and difficult to reproduce.

It is of interest to discuss why the reversible potential cannot be obtained by extrapolation of anodic and cathodic polarization decay lines above a degree of charge of about 50%. In Fig. 27 it is evident that the e.m.f. decay line, e.g. for 75% degree of charge shows two linear regions in "concave" relationship to one another as also found for the "overcharged" electrode (7), whereas at lower degrees of charge, a "convex" relation is observed between two linear regions. It has been shown previously (68,7,16) how such relations arise from two processes in an overall mechanism which are consecutive or alternative (i.e. in parallel) respectively. Above 50% degree of charge (for example, with the 75% charged

electrode), it is clear that the former type of process is operative, as it is in oxygen evolution at overcharged nickel oxide electrodes (7); moreover, the Tafel slopes are similar to those obtained for the oxygen evolution process at the overcharged electrode. We cannot hence identify the initial process as involving the Ni^{II} - Ni^{III} oxidation reaction as has been done for the 50% charged electrode and so cannot obtain the true reversible potential by the extrapolation procedure under these conditions. We can have, in effect, two pathways for the anodic reaction which could be written, for example, as

$$M + OH^- \longrightarrow MOH + e \qquad I$$

$$MOH + OH^- \longrightarrow MO + H_2O + e \qquad II$$

A ← MO → B

A: oxide oxidation in bulk of material.

B: O_2 evolution by further steps (see p. 85)

e.g.

$$MO + MOH \longrightarrow MHO_2 \qquad XII$$

$$MHO_2 + MOH \longrightarrow O_2 + H_2O + 2M \qquad VI$$

or

$$MO + OH^- \longrightarrow MHO_2 + e \qquad V$$

$$MHO_2 + MOH \longrightarrow O_2 + H_2O + 2M \qquad VI$$

or

$$2MO \longrightarrow O_2 + 2M \qquad III$$

At the higher degrees of charge (> ca. 50%), the pathway is evidently one involving <u>consecutive</u> rate-determining

steps and is therefore probably associated with the scheme I, II with pathway B to oxygen evolution with, for example, II or III (cf. 61) rate-determining.

At low degrees of charge, 50% or less, the course of the e.m.f. decay corresponds to alternative reactions, one or the other of which becomes predominant as the potential changes, as shown previously (7). The pathway is thus probably I, II and A at short times after decay (higher anodic potentials) and I, II and B to oxygen evolution at longer times when the pathway which is faster at lower anodic potentials dominates the kinetics of the decay process.

The above discussion is intended only as a qualitative, plausible explanation of the effects associated with the e.m.f. decay behaviour as a function of charge. The evidence for assignment of some of the mechanisms involved in the oxygen evolution process in the scheme shown above has been discussed in detail by Conway and Bourgault (7,41,61).

In order to supplement the above data on true reversible potentials, steady or "stationary" potentials were measured over a wider range of degrees of oxidation (5% - 100%). The significance of these potentials as kinetically determined mixed potentials has been discussed previously (7). They cannot be related directly to the reversible potential of the system at different degrees of charge, since the exchange

current for the $Ni^{II} \rightarrow Ni^{III}$ oxidation process may strictly depend on the degree of charge. Nevertheless, the constancy of these potentials over a large range of formal degree of oxidation of the electrode ("$NiO_{1.05}$" to "$NiO_{1.50}$"), combined with the fact that the true reversible potential has been shown above to be independent of degree of charge in the range where it is directly accessible, makes it most probable that the reversible potential is, in fact, constant over the whole range of degrees of oxidation where the steady potential is found to be constant. This is contrary to conclusions reported by Lukovtsev and Temerin (33) who claimed that the apparent reversible potential of this system follows a Nernst type equation with a slope of 0.050 volt. The observed variation of actual potential during charging and discharging on which the latter conclusion was based is probably due to a concentratio polarization in the solid phase (33,92) or a change in effective current density due to a change in available surface area, and not due to a variation of the true reversible potential of the system, as claimed by Lukovtsev and Temerin.

Our present findings are not in conflict with the equation

$$E = a + b_2' \log \left(\frac{q_{ox} - q_{red}}{q_{red}}\right)$$

discussed by Lukovtsev and Temerin and examined and evaluated

by Conway and Bourgault (39,41) since that equation refers to the variation of electrode potential with degree of oxidation of the surface phase in the overcharge region, and in fact the potential of the electrode was shown (7) to involve a term corresponding to uptake of adsorbed KOH.

For electrodes charged to less than 10%, the open-circuit steady potential was found to depend on the degree of charge to a large extent. Electrodes charged to 1% or less behaved quite differently from those charged to a greater extent. The results suggest that up to a degree of charge Q = 1.5 ± 0.1% (i.e., the average value of Q at the points of interaction of the lines in Fig. 29 and Fig. 30) only a surface phase is being charged. Above that, and up to a degree of oxidation of about 10% both surface and bulk phases are being charged. When the electrode has been charged to 10% of its total charge capacity, it appears that the surface phase is completely charged, and any further charging can then only affect the bulk material.

The variation of the observed true reversible and stationary or quasi-equilibrium potentials as a function of charge in 1M KOH is shown in Fig. 31. The electrochemical behaviour of the electrode is evidently determined by the surface phase, since the reversible (or steady) potential is independent of the degree of charge so long as the surface phase is apparently completely charged, i.e., above 10% formal

Figure 31. True reversible potentials and "stationary" potentials of the nickel oxide as a function of degree of oxidation. One-electron theoretical Nernst slope is shown for comparison.

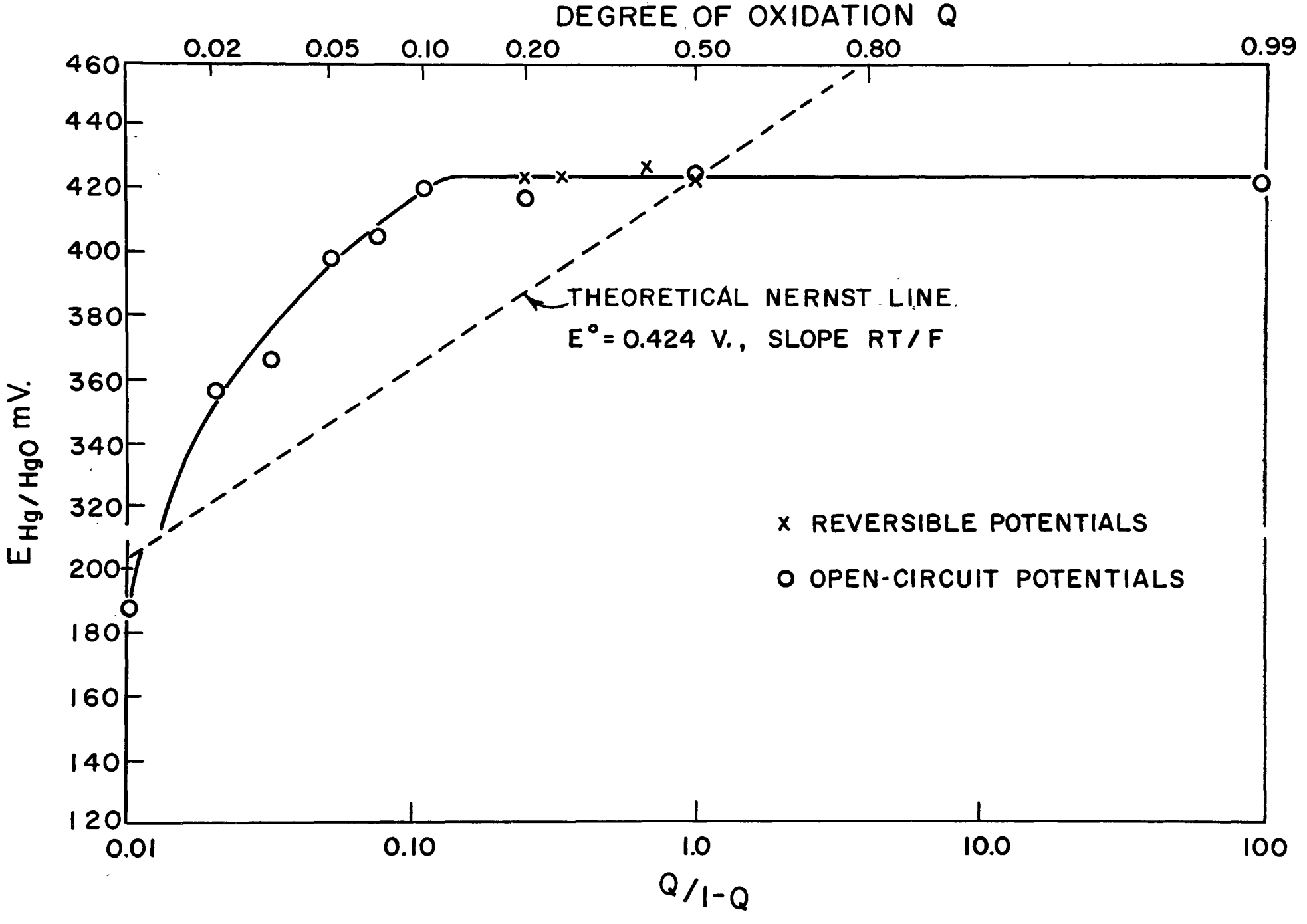
DEGREE OF OXIDATION Q
0.02
0.05
0.10
0.20
0.50
0.80
0.99
460
440
420
400
380
360
340
320
200
180
160
140
120
E Hg/HgO mV.
THEORETICAL NERNST LINE
E° = 0.424 V., SLOPE RT/F
x REVERSIBLE POTENTIALS
O OPEN-CIRCUIT POTENTIALS
0.01
0.10
1.0
10.0
100
Q/1-Q

degree of oxidation. The theoretical Nernst plot for a one-electron transfer process (in terms of formal degree of charge) which would be observed for ideal solid-solution behaviour with the bulk material potential-determining is shown in Fig. 31 for comparison.

The independence of reversible (or steady) potential demonstrated above a degree of oxidation of 10% could formally arise for either of the following reasons: (a) If the electrode were a two-phase mixture of lower and higher oxide, the potential would be independent of apparent degree of oxidation so long as both oxides were present; (b) If the potential were determined by a surface phase of constant composition, superimposed on a bulk-phase of varying degree of oxidation but not potential-determining, the observed potential would be independent of composition of the bulk.

The latter situation (b) is consistent with previous kinetic conclusions (7) on the mechanism of charging of the bulk material via a surface phase, and the observation of a large adsorption pseudocapacity associated with the (over-charged) nickel-oxide electrode. The former possibility (a) is rendered unlikely by the X-ray diffraction pattern of nickel-oxide at various degrees of charge (93,94) where it was shown that there was a continuous variation of the pattern consistent with a complete range of solid solutions of Ni II and III oxide

states. The observed variation of potential between 2% and 10% degree of oxidation confirms that a two-phase mixture cannot be present and potential-determining since such a mixture should give a constant potential except at a state of complete oxidation or complete reduction. We must conclude that the surface-phase is potential-determining and above a degree of oxidation of 10% of the whole material in the oxide electrode, a more or less constant potential is reached.

We may conclude by summarising the reasons why previous assignments of reversible potentials (91,95,96) are of limited validity:

a) in most cases, kinetically determined mixed potentials were involved which differ from the true reversible values by 0 - 30 mV. depending on concentration of KOH.

b) the species e.g. "NiO_2", (97) to which the potentials were assumed to refer have not been identified or characterised and their existence is doubtful (such species probably correspond only to the surface phase at the overcharged electrode).

c) the phase to which the potentials refer is evidently not the bulk phase oxide but the electrochemically active surface phase.

d) potentials attained during charging or discharging of the electrode differ substantially and neither can be identified with a thermodynamically significant reversible potential.

CLAIMS TO ORIGINAL RESEARCH

1. The role of coverage-dependent free energies of adsorption ΔG_{ads} of intermediates in electrochemical reactions has been examined particularly for reactions involving more than two consecutive steps and hence several simultaneously adsorbed intermediates. Models which can lead to a linear dependence of ΔG_{ads} on coverage (Temkin isotherm) have been discussed for cases of adsorption both of single and several species at the surface. It has been concluded that Boudart's postulate of an "induced heterogeneity" effect is the most appropriate for examination of coverage effects on ΔG_{ads} and hence on electrochemical free-energies of activation.

2. Kinetic equations have been derived for reactions involving more than two steps and Tafel slopes have been deduced for various conditions of coverage by adsorbed intermediates; cases for which adsorption of the product gases is either activated or non-activated have been distinguished. Generalisations regarding the electrochemical kinetic behaviour have been proposed for conditions of intermediate coverage, and the results are distinguished from those which arise under limiting Langmuir conditions.

3. The adsorption pseudocapacity behaviour associated with the potential-dependence of coverage by intermediates has been

deduced in the general case where significant coverage arises and the adsorption isotherm passes from a Langmuir type to a Temkin type and back to a Langmuir type as the coverage θ goes from zero to unity. The calculations show that the overall pseudocapacity can be expressed as a series combination of two capacity terms, one associated with pre-exponential terms (Langmuir) and the other with exponential terms (Temkin) in θ in the rate equations.

4. The potential and coverage dependence of the pseudocapacity has been evaluated explicitly for various values of the parameter r which determines the variation of free energy of adsorption with coverage. Values of pseudocapacity which are constant with potential are only predicted with rather unreasonably high values of r.

5. When the free energy of adsorption varies with coverage on account of lateral interaction effects and hence depends on $\theta^{1/2}$ or $\theta^{3/2}$ (rather than on a linear function of θ as postulated by Temkin) characteristic, non-symmetrical relationships between pseudocapacity and coverage or potential have been shown to result.

6. The pseudocapacity behaviour is shown to be determined to an important extent by the degree of equilibrium existing in the primary ion discharge step (in which the adsorbed intermediate is formed). This effect becomes more pronounced the

larger is the value of the parameter r. It is shown in general that cases may arise for which the initial discharge step can legitimately be considered at equilibrium for the purpose of discussing the kinetics of the reaction sequence, while the pseudocapacity behaviour is significantly different from that obtained assuming complete equilibrium in the initial discharge step.

7. Under non-equilibrium conditions in the initial discharge step, limiting values of the coverage, less than unity, are predicted at high overpotentials and have been evaluated for various ratios of the rate constants for the primary discharge step and an assumed potential dependent radical-ion desorption step. The limiting values of θ are also dependent on the value of r involved for the intermediate concerned. These conclusions depend, however, on the mechanism assumed.

8. A method has been developed which allows the parameter r to be evaluated from the width of the observed pseudocapacity-potential curves when they are symmetrical. It is also shown how the surface roughness factor can be deduced under conditions which are specifically relevant to the electrode process occurring. Applications have been made to the pseudo-capacity behaviour associated with the anodic formate decarboxylation reaction.

9. Experimental studies on the nickel oxide electrode have enabled the pseudocapacity associated with adsorbed O-containing species to be evaluated over a small range of potentials. Several methods of determination of the capacity have been shown to lead to consistent results.

10. Studies on the reversible potential of nickel oxide electrodes have demonstrated that this potential is independent of the degree of charge held by the bulk oxide except below ca. 10% degree of charge. These observations indicate the important result that for this electrode system, the reversible potential is determined largely by processes at the surface.

11. The charging characteristics of a completely discharged nickel oxide electrode have been evaluated. Three regions are distinguished, corresponding to the charging of the surface phase alone, then both surface and bulk phases and finally the bulk phase alone.

REFERENCES

1. J. Tafel, Z. Phys. Chem., 50, 641 (1905).
2. M. Volmer and H. Wick, Z. Phys. Chem., 172, 429 (1935).
3. J. Horiuti and M. Ikusima, Proc. Imp. Acad. Tokyo, 15, 39 (1939).
4. A. Slygin and A.N. Frumkin, Acta Physicochim. U.R.S.S., 3, 791 (1935); A. Slygin and B.V. Ershler, ibid, 11, 45 (1939).
5. J.O'M. Bockris and B.E. Conway, Proc. Roy. Soc. London A240, 394 (1958).
6. J.O'M. Bockris, J. Chem. Phys., 24, 817 (1956).
7. B.E. Conway and P.L. Bourgault, Can. J. Chem., 37, 292 (1959); ibid., 38, 1557 (1960).
8. B.E. Conway and M. Dzieciuch, Can. J. Chem., in course of publication.
9. B.E. Conway, E. Gileadi and M. Dzieciuch, Electrochim. Acta., in course of publication.
10. B.E. Conway and E. Gileadi, Trans. Faraday Soc., 58, 2493 (1962).
11. H.G. Oswin and M. Salomon, Can. J. Chem., in course of publication.
12. M.A.V. Devanathan and M. Selvaratnan, Trans. Faraday Soc., 56, 1020 (1960).

13. J.O'M. Bockris, Modern Aspects of Electrochemistry, Butterworths Publ., Chapter IV, 193 (1954).

14. S.B. Baars, Gen. Naturw. Marburg, 63, 213 (1928).

15. F.P. Bowden and E.K. Rideal, Proc. Roy. Soc., 120A, 59, 80 (1928).

16. B.E. Conway, Trans. Roy. Soc. Can., 54, 19 (1960).

17. D.C. Grahame, Chem. Rev., 41, 441 (1947).

18. R. Parsons, Modern Aspects of Electrochemistry, Part I, Butterworths Publ., Chapter III, 103 (1954).

19. D.C. Grahame, J. Electrochem. Soc., 99, 3706 (1952).

20. B.V. Ershler, J. Phys. Chem., U.R.S.S., 22, 683 (1948).

21. J.O'M. Bockris and M.A.V. Devanathan, Office of Naval Research. Report No. ONR 551(22), 1957.

22. A. Slygin and A.N. Frumkin, Acta Physicochim., U.R.S.S., 4, 991 (1936); ibid., 5, 819 (1936).

23. F.P. Bowden, Proc. Roy. Soc., 125A, 440 (1929).

24. J.O. Pearson and J.A.V. Butler, Trans. Faraday Soc., 34, 1163 (1938).

25. M. Breiter, C.A. Knorr and W. Völkl, Z. Electrochem., 59, 681 (1955).

26. A. Hickling, Trans. Faraday Soc., 41, 333 (1945).

27. M. Dziecluch, Ph.D. Thesis, Ottawa (1962).

28. M.A.V. Devanathan, J.O'M. Bockris and W. Mehl, J. Electroanalytical Chem., 1, 143 (1959/60).

29. H. Gerischer and W. Mehl, Z. Electrochem., 59, 1049 (1955).

30. J.G.N. Thomas, Trans. Faraday Soc., 57, 1603 (1961).

31. M. Breiter, Trans. Symposium on Electrode Processes Ed. E. Yeager, John Wiley and Sons, 307 (1959).

32. M. Breiter, Electrochim. Acta, 7, 25 (1962).

33. P.D. Lukovtsev and I. Temerin, Trudy Akad. Nauk., S.S.S.R. Otdel Khim. Nauk., 494 (1953).

34. T.M. Barkley and J.A.V. Butler, Trans. Faraday Soc., 36, 128 (1940).

35. G. Armstrong and J.A.V. Butler, Trans. Faraday Soc., 29, 1261 (1933).

36. H.B. Morley and F.E.W. Wetmore, Can. J. Chem., 34, 359 (1956).

37. V.E. Past and Z.A. Jofa, J. Phys. Chem., U.R.S.S., 33, 913, 1230 (1959).

38. P.C. Milner, J. Electrochem. Soc., 107, 343 (1960).

39. B.E. Conway and P.L. Bourgault, Trans. Faraday Soc., 58, 593 (1962).

40. P.D. Lukovtsev and [illegible].D. Lev'na, J. Phys. Chem., U.R.S.S., 21, 599 (1947).

41. P.L. Bourgault, Ph.D. Thesis, Ottawa, (1962).

42. J.O'M. Bockris and E. [illegible] Potter, J. Electrochem. Soc., 99, 169 (1952).

43. F. Krüger, Z. Physikal. Chem., 45, 1 (1903); Z. Electrochem 19, 620 (1913).

44. M. Proskurnin and A.N. Frumkin, Trans. Faraday Soc., 31, 110 (1935).

45. T. Borissowa and M. Proskurnin, Acta Physicochim., U.R.S.S. 4, 819 (1936).

46. A. Eucken and B. Weblus, Z. Electrochem., 55, 114 (1951).

47. P.L. Bourgault and B.E. Conway, J. Electroanal. Chem., 1, 8 (1959/60).

48. P. Rüetschi, J.B. Ockerman and R. Amlie, J. Electrochem. Soc., 107, 325 (1960); ibid., 108, 377 (1961).

49. T. Langmuir, J. Am. Chem. Soc., 40, 1361; 1403 (1918); ibid., 54, 2798 (1932).

50. M.T. Temkin, Zhur. Fiz. Khim., 15, 296 (1941).

51. R. Parsons, Trans. Faraday Soc., 47, 1332 (1951).

52. J.H. de Boer, Chemisorption, Butterworths, (1956).

53. R. Parsons, Trans. Faraday Soc., 54, 1053 (1958).

54. J.O'M. Bockris and A.M. Azzam, Trans. Faraday Soc., 48, 145 (1952).

55. A.N. Frumkin and N. Aladjalova, Acta physicochim., U.R.S.S., 19, 1 (1944).

56. B.V. Ershler and A.N. Frumkin, Trans. Faraday Soc., 35, 464 (1939).

57. J.P. Hoare and S. Schuldiner, J. Electrochem. Soc., 102, 485 (1955).

58. A.W. Carson, T.B. Flanagan and F.A. Lewis, Trans. Faraday Soc., 50, 371 (1960).

59. J.O'M. Bockris, T.A. Ammar and A.K.M.S. Huq, J. Phys. Chem., 61, 879 (1957).

60. A.A. Antoniou and F.E.W. Wetmore, Can. J. Chem., 37, 292 (1959).

61. B.E. Conway and P.L. Bourgault, Can. J. Chem., 40, 1690 (1962).

62. A.N. Frumkin, P. Dolin and B.V. Ershler, Acta Physicochim., U.R.S.S., 3, 791 (1949).

63. J. Horiuti, Trans. Symposium on Electrode Processes, Ed. E. Yeager, John Wiley and Sons, 17 (1959).

64. L.T. Krishtalik, R.J. Phys. Chem., 33, 600 (1959).

65. S. Glasstone, K.J. Laidler and H. Eyring, The Theory of Rate Processes, McGraw-Hill, 340 (1941).

66. K.J. Laidler, J. Phys. Coll. Chem., 53, 712 (1949).

67. J.O'M. Bockris, N. Pentland and E. Sheldon, J. Electrochem. Soc., 104, 182 (1957).

68. R. Parsons, J. Chim. Phys., 49, c82 (1952).

69. C. Kemball, Proc. Roy. Soc., 190A (1947).

70. J.O'M. Bockris and H. Kita, J. Electrochem. Soc., 108, 676 (1961).

71. A. Bucken, Z. Electrochim., 53, 285 (1949).

72. M. Boudart, J. Am. Chem. Soc., 72, 3556 (1952).

73. G.D. Halsey and H.S. Taylor, J. Chem. Phys., 15, 624 (1947).

74. A.Kh. Breger and A.A. Zhukkovitskii, Zhur. Fiz. Khim., 21, 423 (1947).

75. F.F. Vol'kenshtein, ibid., 24, 1068 (1950); 27, 159; 167 (1953); 28, 1219; 1682 (1954).

76. M.T. Temkin, Problems of Chemical Kinetics, Catalysis and Reactivity. Izd. Akad. Nauk. S.S.S.R., (1955).

77. F.P. Bowden, J. Chem. Soc., 242 (1950).

78. R.C.L. Bosworth, Trans. Roy. Soc., N.S.W., 79, 53; 166 (1946).

79. R.C.L. Bosworth and E.K. Rideal, Physica. 4, 925 (1937).

80. J.H. de Boer, Electron Emission and Adsorption Phenomena. Cambridge (1935).

81. E.A. Moelwyn-Hughes, Physical Chemistry, p. 589, Pergamon Press, London (1961).

82. M.M. Siddiqi and F.C. Tompkins, Proc. Roy. Soc., 268A, 452 (1962).

83. J. Zeldovitch, Acta Physicochim. U.S.S.R., 1, 961 (1935).

84. B.E. Conway and R.G. Barradas, Electrochim. Acta, 5, 319 (1961).

85. D.A. Bowden, J. Chem. Soc., 242 (1950).

86. T.P. Hoare, Modern Aspects of Electrochemistry, Butterworths Publ., Part II, Chapter IV, 204 (1958).

87. A.M. Azzam, J.O'M. Bockris, B.E. Conway and H. Rosenberg, Trans. Faraday Soc., 46, 918 (1950).

88. J.O'M. Bockris, B.E. Conway and W. Mehl, J. Sci. Inst., 33, 400 (1956).

89. F.D. Rossini, D.D. Wagman, W.H. Evans, S. Levine, I. Joffe, Circular 500, National Bureau of Standards, U.S.A., (1952).

90. E.J. Casey, P.L. Bourgault and P.C. Lake, Can. J. Technol., 34, 95 (1956).

91. F. Kornfeil, Proc. 127th U.S. Army Battery Research and Development Conference (1958).

92. B.V. Ershler and E.M. Kuchinskii, Zh. Fiz. Kim., 20, 539 (1946).

93. O. Glemser and J. Einerhand, Z. Anorg. Chem., 261, 26 (1950); Z. Electrochem., 54, 302 (1950); (see also G.W.D. Briggs and W.F.K. Wynne-Jones, Trans. Faraday Soc., 52, 1272 (1956).

94. W. Feitknecht, H.R. Christen and H. Studer, Z. Anorg. u. Allgem. Chem., 283, 88 (1956).

95. F. Foerster, Z. Electrochem., 13, 414 (1907); ibid., 14, 285 (1908).

96. J. Zedner, Z. Electrochem., 11, 809 (1905); ibid., 12, 463 (1906); ibid., 13, 752 (1907).

97. W.M. Latimer, Oxidation Potentials, 2nd Ed., Prentice Hall (1952).

98. G.W.D. Briggs and W.F.K. Wynne-Jones, Electrochim. Acta, 7, 241 (1962).

99. G.W.D. Briggs, F.W. Stott and W.F.K. Wynne-Jones, Electrochim. Acta, 7, 249 (1962).

100. J.S. Mitchell, Trans. Faraday Soc., 31, 980 (1935).

101. G. Okamoto, J. Horiuti and K. Hirota, Sci. Papers Inst. Phys. Chem. Res. Tokio, 29, 229 (1936).

102. J. Horiuti, J. Res. Inst. Catal. Hokkaido University, 4, 55 (1956).